TIMING AND TECTONIC SETTING OF VOLCANOGENIC MASSIVE SULPHIDE DEPOSITS IN BRITISH COLUMBIA: CONSTRAINTS FROM U-Pb GEOCHRONOLOGY, RADIOGENIC ISOTOPES, AND GEOCHEMISTRY

by

FIONA CHRISTINA CHILDE

B.Sc., McGill University, 1989
M.Sc., McGill University, 1992

A THESIS SUBMITTED IN PARTIAL FULFILLMENT OF
THE REQUIREMENTS FOR THE DEGREE OF
DOCTOR OF PHILOSOPHY
in
THE FACULTY OF GRADUATE STUDIES
(Department of Earth and Ocean Sciences)

We accept this thesis as conforming
to the required standard

THE UNIVERSITY OF BRITISH COLUMBIA
April 1997

In presenting this thesis in partial fulfillment of the requirements for an advanced degree at the University of British Columbia, I agree that the Library shall make it freely available for reference and study. I further agree that permission for extensive copying of this thesis for scholarly purposes may be granted by the head of my department or his or her representatives. It is understood that copying or publication of this thesis for financial gain shall not be allowed without my written permission.

Department of Earth and Ocean Sciences
The University of British Columbia
Vancouver, Canada

April 28, 1997

ABSTRACT

Volcanogenic massive sulphide (VMS) deposits occur within several of the allochthonous terranes of the North American Cordillera in British Columbia. In this study, the age of mineralization was determined for a number of these deposits. The radiogenic isotopic and geochemical signatures of host rocks and the mineralization were used to constrain the tectonic settings in which these deposits formed.

The radiogenic isotopic signatures and geochemical affinities of three of these deposits in Stikinia, the Middle Jurassic Au-Ag-rich Eskay Creek deposit, the Late Triassic Cu-rich Granduc deposit, and the Late Mississippian polymetallic Tulsequah Chief deposit, assist in defining the evolution of this complex terrane. Rhyolite, which hosts and underlies mineralization at Eskay Creek has a primitive radiogenic isotopic and chemical character which is distinct from that of rhyolites of the same age within the region. Similarly, basalt which structurally underlies mineralization at Granduc is isotopically and chemically primitive relative to basalt which occurs within the same group regionally, and indicates formation within a back arc basin or immature island arc. The Tulsequah Chief deposit in northern Stikinia exhibits isotopic and geochemical features indicative of a more evolved island arc setting, which may reflect a variation in the basement to this terrane.

The Cu-Zn-rich Kutcho Creek VMS deposit is hosted within felsic-dominated strata of the Kutcho Assemblage. Permo-Triassic to earliest Triassic ages are established for volcanic rocks which host mineralization. These ages, along with primitive radiogenic isotopic and geochemical signatures, indicate that these rocks and their contained mineralization formed in a primitive arc or fore-arc setting built on oceanic basement. Uranium-Pb dating and isotopic and geochemical studies of volcanic and intrusive rocks in fault-bounded slices further south in the Cordillera indicate that this Permo-Triassic magmatic event was widespread, and possibly define a new terrane.

Age, isotopic and geochemical information was also obtained for igneous rocks within pendants and belts enclosed within the Coast Plutonic Complex which host VMS mineralization. New data for intrusive rocks from the Scotia-Quaal Belt and Anyox pendant are permissive of formation of these units within Stikinia.

TABLE OF CONTENTS

LIST OF TABLES

LIST OF FIGURES

LIST OF PLATES

FOREWORD

This thesis presents geological research with academic and economic applications, produced within a university, in collaboration with both industry and government. This study has benefited from the expertise of many scientists. To recognize the specific input of individuals who contributed to the publications that were produced during the course of this dissertation, and in accordance with guidelines of The University of British Columbia and the doctoral committee, this thesis is presented as a series of research papers. Five papers, which constitute chapters two and four have been submitted for publication in refereed professional and government journals, the names of co-authors, and their specific contributions to these manuscripts are outlined below. Chapters three, five, six and seven represent future contributions to referred publications. Finally, four British Columbia Geological Fieldwork papers which were produced during the course of this thesis are presented in Appendix 3.

The paper which comprises chapter two has been published in *Economic Geology* as a sole authored contribution. Critical reviews by Drs. J.F.H. Thompson and J.K. Mortensen, thesis directors, and Directors of the Mineral Deposit Research Unit (MDRU), and Geochronology Laboratory in the Department of Earth and Ocean Sciences, respectively, Dr. T.J. Barrett, MDRU Project Coordinator, and Drs. T. Barrie and F. Corfu, journal reviewers, greatly improved the manuscript.

Chapter four is composed of four individual papers. The first three parts detail the geology, age, radiogenic isotopic systematics and geochemistry of three fault bounded regions within the Cordillera; the final part represents a tectonic synthesis for these regions, based on the data presented in the first three sections. The first part is co-authored by Dr. J.F.H. Thompson, and reflects his contribution to the interpretation of data, assistance in the field and editorial supervision. Part two is co-authored by Mr. P. Schiarizza of the British Columbia Geological Survey, who is currently conducting a mapping project of the region discussed in this section, and contributed his knowledge of the local geology. Part three is co-authored by Dr. J.F.H. Thompson, as well as Drs. R.M. Friedman and J.K. Mortensen, both of the Geochronology Laboratory and MDRU, in the Department of Earth and Ocean Sciences, and reflect their

contributions in the field and laboratory, as well as with editorial assistance. Part four, the tectonic synthesis of the chapter is co-authored by all of those people who contributed to parts one through three, as well as K. Bellefontaine of the British Columbia Geological Survey, and J.M. Marr of Agate Bay Resources Ltd. The latter two people contributed ideas which assisted in the initiation of this aspect of my research. I am grateful to all of my co-authors for their assistance.

All of the research and ideas not specifically mentioned above was performed by Fiona Childe, in accordance with the guidelines of The University of British Columbia. The papers which comprise chapters two and four are as follows:

CHAPTER 2

Childe, F.C. 1996. U-Pb Geochronology and Nd and Pb Isotopic Characteristics of the Au-Ag-Rich Eskay Creek VMS Deposit. Economic Geology, v. 91, pp. 1209-1224.

CHAPTER 4

Childe, F.C., and Thompson, J.F.H. *accepted.* Geological Setting, U-Pb Geochronology, and Radiogenic Isotopic Systematics of the Permo-Triassic Kutcho Assemblage, North-Central British Columbia. Canadian Journal of Earth Sciences.

Childe, F.C., Schiarizza, P. 1997. U-Pb Geochronology, Geochemistry and Nd Isotopic Systematics of the Sitlika Assemblage, Central British Columbia. *In* Geological Fieldwork 1996, *Edited by* D.V. Lefebure, W.J. McMillan, and J.G. McArthur, British Columbia Ministry of Employment and Investment, Paper 1997-1, p. 69-78.

Childe, F.C., Friedman, R.M., Mortensen, J.K., and Thompson, J.F.H. 1997. Evidence for Early Triassic Felsic Magmatism in the Ashcroft Map Area, British Columbia. *In* Geological Fieldwork 1996, *Edited by* D.V. Lefebure, W.J. McMillan, and J.G.

McArthur, British Columbia Ministry of Employment and Investment, Paper 1997-1, p.117-124.

Childe, F.C., Thompson, J.F.H., Mortensen, J.K., Friedman, R.M., Schiarizza, P., Bellefontaine, K., and Marr, J.M. *submitted.* Primitive Permo-Triassic Volcanism in the Canadian Cordillera: Tectonic and Metallogenic Implications. Economic Geology.

APPENDIX 3

Childe, F., and Mihalynuk, M.G. 1995. U-Pb geochronology of the Mount Stapler Quartz Monzonite: Evidence for Early Jurassic magmatism in the Tulsequah Glacier area, Northwest British Columbia (104K/13). *In* Geological Fieldwork 1994, *Edited by* B. Grant and G.M. Newell, British Columbia Ministry of Energy, Mines and Petroleum Resources, Paper 1995-1, pp. 521-527.

Sherlock, R.L., Childe, F., Barrett, T.J., Mortensen, J.K., Lewis, P.D., Chandler, T., McGuigan, P., Dawson, G.L., and Allen, R. 1994. Geological investigations of the Tulsequah Chief massive sulphide deposit, Northwestern British Columbia (104K/12). *In* Geological Fieldwork 1993, *Edited by* B. Grant and G.M. Newell, British Columbia Ministry of Energy, Mines and Petroleum Resources, Paper 1995-1, pp. 373-379.

Sherlock, R.L., Barrett, T.J., Roth, T., Childe, F., Thompson, J.F.H., Kuran, D., Marsden, H., and Allen, R. 1994. Geological investigations of the 21B deposit, Eskay Creek, Northwestern British Columbia (104B/9W). *In* Geological Fieldwork 1993, *Edited by* B. Grant and G.M. Newell, British Columbia Ministry of Energy, Mines and Petroleum Resources, Paper 1995-1, pp. 357-372.

Mihalynuk, M.G., McMillan, W.J., Mortensen, J.K., Childe, F.C., and Orchard, M.J. 1996. Age of host strata versus mineralization at Erickson-Ashby: A skarn deposit. *In* Geological Fieldwork 1994, *Edited by* B. Grant and G.M. Newell, British Columbia Ministry of Energy, Mines and Petroleum Resources, Paper 1995-1, pp. 521-527.

ACKNOWLEDGMENTS

This thesis has benefited from the assistance and expertise of many people. First and foremost, I wish to thank my doctoral supervisors John Thompson and Jim Mortensen for their guidance in the field and laboratory, as well as the countless hours they spent editing this thesis and the publications that were produced during the course of it. I also wish to thank the staff of the Geochronology Laboratory for their assistance, in particular my office mate Richard Friedman. Mary Lou Bevier is thanked for allowing access to unpublished data and procedures. The assistance of MDRU staff Sonya Tietjen and Arne Toma is greatly appreciated.

This work benefited greatly from input by members of the British Columbia Geological Survey Branch, in particular Mitch Mihalynuk, Dani Alldrick, Bill McMillan, Paul Schiarizza, and Jim Logan, whose contributions ranged from stimulating geological discussions to digging samples out of the basement for me to analyze.

This thesis was funded through the Mineral Deposit Research Unit Volcanogenic Massive Sulphide Deposits of the Cordillera Project, funded by the Natural Science and Engineering Research Council of Canada (NSERC), the Science Council of British Columbia and eleven member mining companies, namely Garanges Inc., Homestake Canada Inc., Inco Ltd., Inmet Mining Corp. (formerly Metall Inc. and Minova Inc.), Kennecott Canada Inc., Lac Minerals, Placer Dome Ltd., Teck Corp., TVI Pacific Inc., Westmin Resources Ltd., and WMC International Ltd. The author was supported in part by a NSERC doctoral scholarship.

Ron Britten, Henry Marsden, and Andrew Kaip (all formerly of Homestake Canada Inc.), and Dave Kuran and Tina Roth (Homestake Canada Inc.) are thanked for sharing their wealth of knowledge on the Eskay Creek deposit, and for allowing the author access to company reports, maps, drill logs and core from both the Eskay Creek and Kutcho Creek deposits. Terry Chandler (Redfern Resources Ltd.) is thanked for allowing the author access to similar material for the Tulsequah Chief and Big Bull deposits. Paul McGuigan (Cambria Resources Ltd.) is thanked for sharing his knowledge of the Granduc deposit. Atna Resources Ltd. is thanked for allowing the author access to samples from the Ecstall property.

Determining ages of volcanic rocks by U-Pb methods is a challenging and labour intensive endeavor. A significant number of U-Pb age determinations are presented in this thesis. The average weight of these samples was 20-30 kg, they were always the most massive, hardest rock, and the best samples always seemed to be found on the highest mountain tops, lowest valleys or furthest distance from camp. The author wishes to very gratefully acknowledge the assistance of the following people, who assisted collecting these samples and hauling them back to camps across northern and central British Columbia: Tim Barrett, Bob Beck, Dennis Bohme, Ron Britten, Kate Bull, Chris Downie, Andrew Kaip, Jeff Lewis, Peter Lewis, Julia Matsubara, Tanya Mauthner, Rob Macdonald, Paul McGuigan, Mitch Mihalynuk, Jim Mortensen, Matt Phillips, Tina Roth, Paul Schiarizza, Ross Sherlock, John Thompson, and Sarah Vance.

And last, but never least, I wish to express my sincere gratitude to Andrew Kaip. Thank you for your unwavering support through these past years.

CHAPTER 1

INTRODUCTION

The North American Cordillera of British Columbia, the Yukon Territory, and Alaska is host to a number of volcanogenic massive sulphide (VMS) deposits (Fig. 1.1). In British Columbia, VMS deposits have both current and historical economic significance, ranging from the past producing Britannia deposit, which in the early part of the twentieth century was the largest single producer of copper in the British Empire, to the currently mined, unusually Au-Ag-rich Eskay Creek deposit, which in 1997 is one of the highest grade gold and silver deposits in North America (Armstrong 1990; Prime Resources Annual Report 1996).

Rocks within the Canadian portion of the North American Cordillera can be divided into five morphogeological belts, from east to west these are the Foreland, Omineca, Intermontane, Coast, and Insular Belts; each belt is composed of a collage of tectonostratigraphic terranes of different affinities, bounded by faults (Gabrielse et al. 1991). In the current study, VMS mineralization which formed in the Intermontane Belt, as well as in pendants and belts which now lie within the Coast Belt are examined. These include the Eskay Creek, Granduc, Tulsequah Chief, Big Bull, and Anyox deposits, and the Kutcho Creek and Ecstall prospects. The Intermontane Belt is comprised of the Stikine, Quesnel, Cache Creek and Slide Mountain terranes, the former two consisting of Paleozoic and Mesozoic island arc assemblages, and the latter two of Paleozoic to Mesozoic oceanic assemblages (Gabrielse et al. 1991). These, and other allochthonous terranes of the Cordillera are believed to have accreted on to the margin of Ancestral North America in Mesozoic time (Monger et al. 1982). The Insular Belt is also host to several significant VMS deposits, including the giant Windy Craggy deposit. A recent doctoral thesis by Peter (1992) focused on the geology, geochemistry and alteration of the Windy Craggy deposit.

The Eskay Creek, Granduc, Tulsequah Chief, and Big Bull deposits formed within Stikinia. Kutcho Creek lies within a fault-bounded allochthon of unknown terrane affinity to the east of Stikinia, and Anyox and Ecstall are hosted within pendants and belts which now lie within

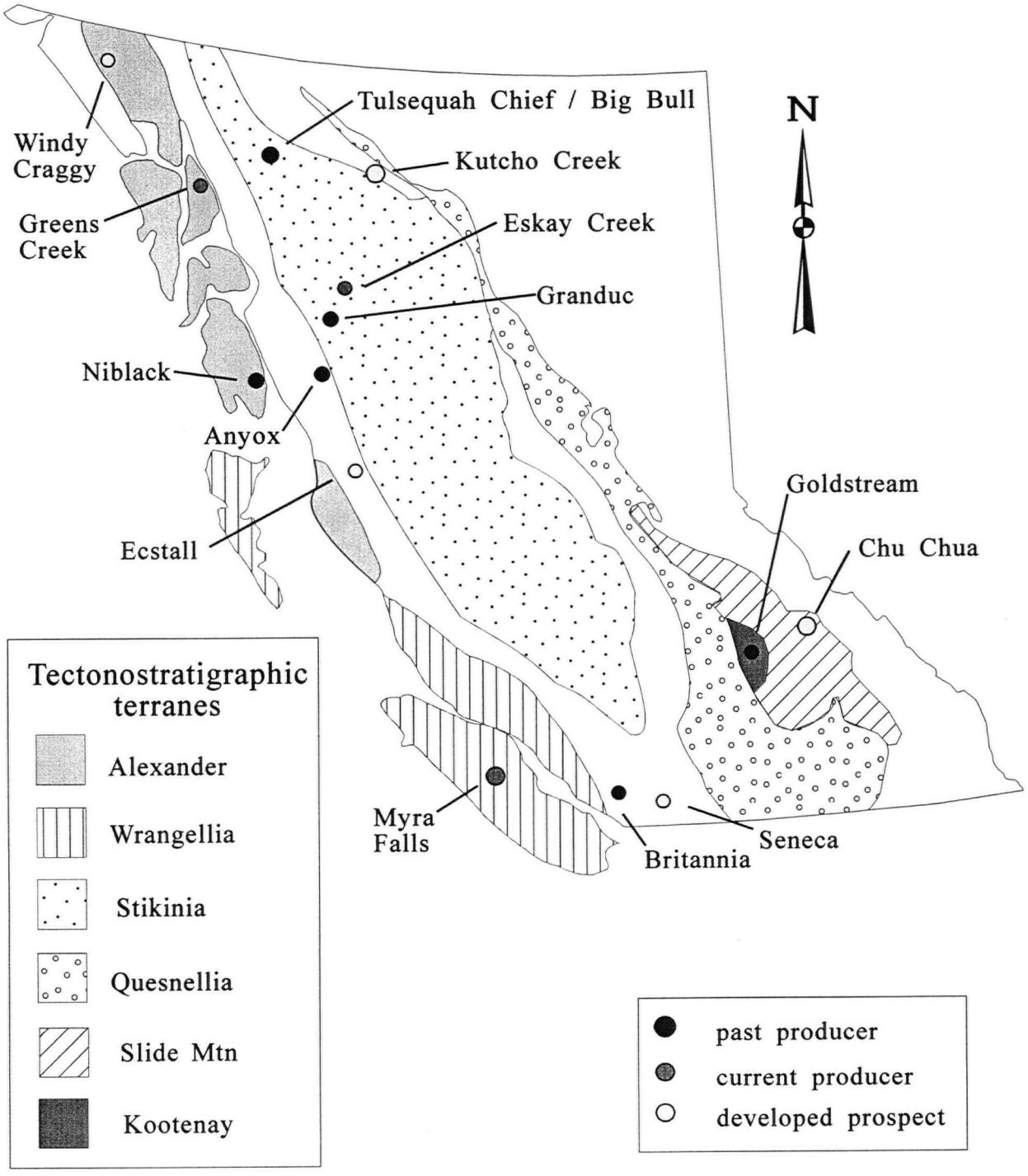

Figure 1. 1 Past and presently producing VMS deposits and developed prospects in British Columbia and southeastern Alaska, North American Cordillera.

metamorphic and plutonic rocks of the Coast Plutonic Complex, in the Coast Belt (Fig. 1.1). In this study the mineralization and host rocks of these deposits and prospects are examined at both the deposit and regional scale. The regional geology and tectonic setting of each deposit is discussed in the chapter pertaining to that deposit. The following section presents an overview of the principal characteristics of VMS deposits and recognized VMS deposit types.

VMS deposits

Volcanogenic massive sulphide deposits encompass a wide range of styles and compositions of mineralization. However, a number common features to these deposits can be discerned. These include formation in subaqueous environments at or near the seafloor, an association with volcanic +/- sedimentary rocks, and formation near convergent and divergent plate margins (Sawkins 1990; Franklin 1996). Characteristics which may be observed within well preserved VMS deposits include the presence of concordant lenses of massive sulphides overlying discordant stockwork and/or alteration zones, well developed footwall alteration zones, with little alteration extending into the hangingwall to mineralization, a metal zonation from Cu-rich bases to Pb- and Zn-rich tops within lenses in which Fe-rich sulphides (principally pyrite) dominate, exhalitive silica or sulphate horizons which may extend for a greater lateral extent than massive sulphide mineralization, and synvolcanic faults which may have served as conduits for metal-bearing hydrothermal fluids (Sawkins 1976; Höy 1991; Franklin 1996). For a detailed review of the morphology and general characteristics of VMS deposits the reader is referred to Sawkins (1976), Höy (1991), and Franklin (1996).

A threefold classification scheme for massive sulphide deposits associated with volcanic rocks was first proposed by Sawkins (1976). Sawkins (1976) suggested that VMS deposits could be divided into three broad deposit types, based on the tectonic setting and the host lithologies to mineralization; these are Kuroko-, Besshi-, and Cyprus-type deposits. Kuroko-type deposits are characterized by the presence of polymetallic (Zn-Pb-Cu$\pm$Au$\pm$Ag) sulphide lenses, hosted within the felsic portion of compositionally bimodal, calc-alkaline volcanic sequences. These deposits are thought to form within island arc and arc-related rift settings. Besshi-type deposits are characterized by the presence of Cu$\pm$Zn sulphide lenses, hosted within clastic sedimentary rocks

and mafic volcanic rocks of calc-alkaline affinity; Besshi-type deposits are considered to form within marginal and back arc settings, commonly in proximity to sources of terrigenous sediments . The third category, Cyprus-type deposits consist of Cu±Zn sulphide lenses, hosted within basaltic volcanic rocks of tholeiitic magmatic affinity. These deposits form within mid-ocean ridge settings.

Worldwide, VMS deposits are commonly concentrated within regions, such as the Hokuroko district in Japan, and the Bathurst and Noranda Camps in Eastern Canada (Ohmoto and Skinner 1983; Lydon 1988; Franklin 1996). Generally, VMS deposits within these regions are concentrated along particular horizons, perhaps in response to a change in the tectonic environment (Ohmoto and Skinner 1983, and references therein; Urabe 1987). Identification of these favourable horizons at an existing deposit, based on age, or lithological, isotopic, or geochemical characteristics is a significant exploration parameter in the search for additional VMS mineralization. On a regional scale, studying the characteristics of VMS mineralization and their host rocks can assist in determining the tectonic setting in which the deposits formed, and therefore yield additional information on the tectonic history of their host terranes.

Objectives

This thesis focuses on determination of the age, degree of evolution of radiogenic isotopes, and lithogeochemical affinity of several VMS deposits and prospects which formed in allochthonous island arc terranes of the Canadian Cordillera. As described above, VMS mineralization examined in this study is either hosted within Stikinia (Eskay Creek, Granduc, Tulsequah Chief, and Big Bull), or lies within pendants, metamorphic belts, or fault-bounded blocks of uncertain terrane affinity, which may have formed as part of Stikinia or possibly adjacent terranes (Anyox, Ecstall, and Kutcho Creek). The age, radiogenic isotopic signatures, and lithogeochemical affinity of those deposits in the former group can be contrasted with other rocks within the same group or assemblage, to further define the tectonic history of the terrane, whereas in the latter group these properties can be used to suggest whether these deposits and their host rocks could have formed as part of Stikinia.

The principal objectives of the current study were to better constrain the age and tectonic setting of a number of VMS deposits and prospects which formed in allochthonous terranes of the Canadian Cordillera in British Columbia. These objectives were achieved through geological mapping and drill core logging, as well as isotopic dating of igneous rocks using U-Pb methods, lithogeochemical and Nd isotopic analysis of igneous rocks, and Pb isotopic analysis of sulphides and igneous rocks.

In addition to the deposit specific studies, the regional context of the Kutcho Assemblage, which hosts the Kutcho Creek deposit, was examined. Using the methods outlined above, rocks of the Sitlika Assemblage and Venables Valley areas were examined to determine if they could represent temporal and tectonic equivalents of the Kutcho Assemblage.

Methods

U-Pb geochronology

Age determinations were achieved through U-Pb isotopic dating of zircon ($ZrSiO_4$). These analyses were carried out by the author at the Geochronology Laboratory of the University of British Columbia; analytical procedures are outlined Appendix 1. At some deposits U-Pb age determinations provide a refinement of existing radiometric or biochronological constraints, whereas at others they provided new and unexpected ages for VMS mineralization in the North American Cordillera.

Pb isotopic data

The Pb isotopic signature of mineralization reflects the degree of evolution of Pb, and by analogy other metals occurring in mineralization (Gulson 1986). Therefore the Pb isotopic signatures of sulphides and sulphosalts from deposits and prospects examined in this study were determined to assess the degree of evolution of the metallogenic sources to mineralization. This portion of the study built on the framework established by Alldrick (1991), who determined that mineralization of Early Jurassic and Tertiary age, in the Stewart Mining Camp of the Stikine terrane had distinct Pb isotopic compositions. Analysis of sulphides, sulphosalts, and feldspars

were carried out by the author at the Geochronology Laboratory of the University of British Columbia; analytical procedures are outlined Appendix 1.

Nd isotopic data

The Nd isotopic signatures of igneous rocks associated with several of the VMS deposits studied here were determined to establish the degree of contamination by older, evolved crustal components. Neodymium isotopic characterization of igneous rocks from each of the groups and assemblages which comprise Stikinia was interpreted by Samson et al. (1989) to indicate that these rocks have an island arc affinity, and are the products of mantle-derived continental crust. Data presented in this study are contrasted with the results of Samson et al. (1989) and other relevant studies. Rocks to be analyzed were selected by the author, and analyzed by Reg Theriault, at the Geochronology Laboratory at the Geological Survey of Canada in Ottawa. Analytical procedures follow those outlined in Theriault (1990).

Lithogeochemistry

Major, trace and rare earth element compositions were determined for volcanic and plutonic rocks at both the deposit and regional scale. The purpose of this portion of the study was to determine the chemical composition and magmatic affinity of these rocks, and compare this data with regional data sets, and detailed data acquired at some of the deposits by other researchers in the MDRU VMS Project. Whole rocks samples were analyzed for major and trace element compositions by X-ray fluorescence at McGill University in Montreal, Quebec, using glass beads for major elements and pressed pellets for trace elements; a subset of samples was analyzed by instrumental neutron activation analysis for rare earth element compositions at Activation Laboratories in Ancaster, Ontario.

Presentation

As outlined in the foreword, this thesis is presented as a series of discrete chapters, each focusing on a particular region, mineral deposit or assemblage. Five papers, based on two chapters have been accepted or submitted for publication in refereed professional and government journals. The benefits of clarity and continuity for the reader, and the facilitation of publication of

portions of this thesis warrant the style adopted here. Efforts have been made to minimize repetition of background material, methodology and references. However, a certain amount of repetition is unavoidable. The subject of each chapter is outlined below.

Chapter two discusses the geology, U-Pb geochronology and radiogenic isotopic systematics of the Eskay Creek deposit, a Au- and Ag-rich VMS deposit in the Iskut River area of Northwestern British Columbia (Fig. 1.1). The isotopic age of rocks which comprise the immediate footwall to mineralization is established, and the chemistry and Nd isotopic signature of this unit is contrasted with those of rocks of identical age which are not known to be associated with mineralization. Based on the Pb isotopic signature of mineralization at the deposit, potential metallogenic sources to mineralization are discussed. In addition, possible modern-day analogies to the Eskay Creek deposit are discussed.

The third chapter focuses on the Cu-rich Granduc VMS deposit, in the Stewart Mining Camp of Northwestern British Columbia (Fig. 1.1). In this chapter the U-Pb age of magmatic rocks and the Pb isotopic signature of mineralization are used to establish a Late Triassic age for massive sulphide mineralization in this strongly deformed deposit. Determination of this age allows for a regional comparison between the geochemical and Nd isotopic signatures of rocks which host mineralization at Granduc and unmineralized rocks of the Upper Triassic Stuhini Group, as well as a deposit comparison with Windy Craggy, a VMS deposit of comparable age and mineralogy to Granduc, occurring in the Alexander terrane. In addition, it is suggested that the Pb isotopic signature of mineralization determined in this study can now be used in a comparative way to determine if other mineralization in the region is of comparable age to Granduc.

Chapter four is presented in four sections. In the first part of the chapter the age, radiogenic isotopic characteristics, and geochemistry of the fault-bounded Kutcho Assemblage in North Central British Columbia is documented (Fig. 1.1). The Kutcho Assemblage is host to the Cu-Zn-rich Kutcho Creek VMS deposit. Data presented here indicate that the Kutcho Assemblage has an uncommon age and primitive character, both of which are distinct from other bimodal island arc sequences in the Cordillera. It is suggested that these rocks are unlike other

previously well-documented strata in the Cordillera and as such may represent a formerly unrecognized Cordilleran terrane. In the following two parts of the chapter, fault-bounded rocks of similar lithology, age, and isotopic and geochemical characteristics as rocks of the Kutcho Assemblage are documented. In the final part of the chapter, data for the three regions are compared, and the hypothesis that the rocks within the these assemblages formed in the same time period and tectonic environment is put forward.

Chapter five focuses on the age and isotopic characteristics of the Tulsequah Chief and Big Bull polymetallic VMS deposits, in Northwestern British Columbia, as well as volcanic strata of similar age in the region (Fig. 1.1). The isotopic signatures of mineralization and host rocks are contrasted with those of rocks of comparable age which occur further south within Stikinia. The data presented here have implications for both the nature of the basement to this terrane and VMS exploration in the region.

Chapter six is written in three parts, and discusses the age and Pb isotopic systematics of pendants or belts encompassed by the Coast Plutonic Complex. Part one discusses the Anyox pendant, which hosts the Anyox deposit, and part two discusses the Scotia-Quaal Belt, which hosts the Ecstall prospect (Fig. 1.1). Part three discusses the possibility of a tectonic link between these pendants and the Stikine terrane, based in part on new U-Pb age data presented in the previous parts of this chapter.

Chapter seven classifies VMS deposits in allochthonous terranes of the North American Cordillera in British Columbia based on host lithology, as was first proposed by Thompson et al. (1994). The currently interpreted tectonic setting, age and terrane affinity of several of these deposits are discussed, and this information is contrasted with the radiogenic isotopic signatures of mineralization and host rocks at each deposit.

References

Alldrick, D.J. 1991. Geology and ore deposits of the Stewart Mining Camp. Ph.D. thesis, The University of British Columbia, 417 p.

Armstrong, J.E. 1990. Vancouver Geology. *Edited by* C. Roots and C. Staargaard, Geological Association of Canada, Vancouver, 128 p.

Franklin, J.M. 1996. Volcanic-associated massive sulphide base metals. *In* Geology of Canadian Mineral Deposit Types, *Edited by* O.R Eckstrand, W.D. Sinclair, and R.I. Thorpe, Geological Survey of Canada, Geology of Canada no. 8, pp. 158-183.

Gabrielse, H., Monger, J.W.H., Wheeler, J.O., and Yorath, C.J. 1991. Morphological belts, tectonic assemblages and terranes. *In* Upper Devonian to Middle Jurassic Assemblages, Part A of Chapter 1 of Geology of the Cordilleran Orogen in Canada, *Edited by* H. Gabrielse, and C.J. Yorath, Geological Survey of Canada, Geology of Canada, no. 4, pp. 15-28.

Gulson, B.L. 1986. Lead isotopic in mineral exploration. Developments in Economic Geology, 23, Elsevier, 244p.

Höy, T. 1991. Volcanogenic massive sulphide deposits in British Columbia. *In* Ore deposits, tectonics and metallogeny in the Canadian Cordillera, British Columbia Ministry of Energy, Mines and Petroleum Resources, Paper 1991-4, 276 pages.

Lydon, J.M. 1988. Volcanogenic massive sulphide deposits, Part 1: A descriptive model. *In* Ore Deposit Models, *Edited by* R.G. Roberts and P.A. Sheahan, Geoscience Canada Reprint Series 3, pp. 145-154.

Monger, J.W.H., Price, R.A., and Templeman-Kluit, D.J., 1982. Tectonic accretion and the origin of the two major metamorphic and plutonic welts in the Canadian Cordillera. Geology, **10**: 70-75.

Ohmoto, H., and Skinner, B.J. 1983. The Kuroko and related volcanogenic massive sulphide deposits: Introduction and summary of new findings. Economic Geology Monograph 5: The Kuroko and Related Volcanogenic Massive Sulphide Deposits, pp. 1-8.

Peter, J.M. 1992. Comparative geochemical studies of the Upper Triassic Windy Craggy and modern Guaymus Basin deposits: A contribution to the understanding of massive sulfide formation in volcano-sedimentary environments. Ph.D. thesis, University of Toronto, Toronto.

Samson, S.D., McClelland, W.C., Patchett, P.J., Gehrels, G.E., and Anderson, R.G. 1989. Evidence from neodymium isotopes for mantle contributions to Phanerozoic crustal genesis in the Canadian Cordillera: Nature, **337**: 705-709.

Sawkins, F.J. 1976. Massive sulphide deposits in relation to geotectonics. Geological Association of Canada, Special Paper **14**: 221-240.

Sawkins, F.J. 1990. Metal deposits in relation to plate tectonics. Second Edition, Springer-Verlag, 461 pages.

Thériault, R., J. 1990. Methods for Rb-Sr and Sm-Nd isotopic analyses at the geochronology laboratory, Geological Survey of Canada. *in* Radiogenic Age and Isotopic Studies: Report 2, Geological Survey of Canada, Paper 89-2, p. 3-6.

Urabe, T. 1987. Kuroko deposit modeling based on magmatic hydrothermal theory. Mining Geology, **37**: 159-176.

CHAPTER 2:

U-Pb GEOCHRONOLOGY AND Nd AND Pb ISOTOPIC CHARACTERISTICS OF THE Au-Ag-RICH ESKAY CREEK VMS DEPOSIT, BRITISH COLUMBIA

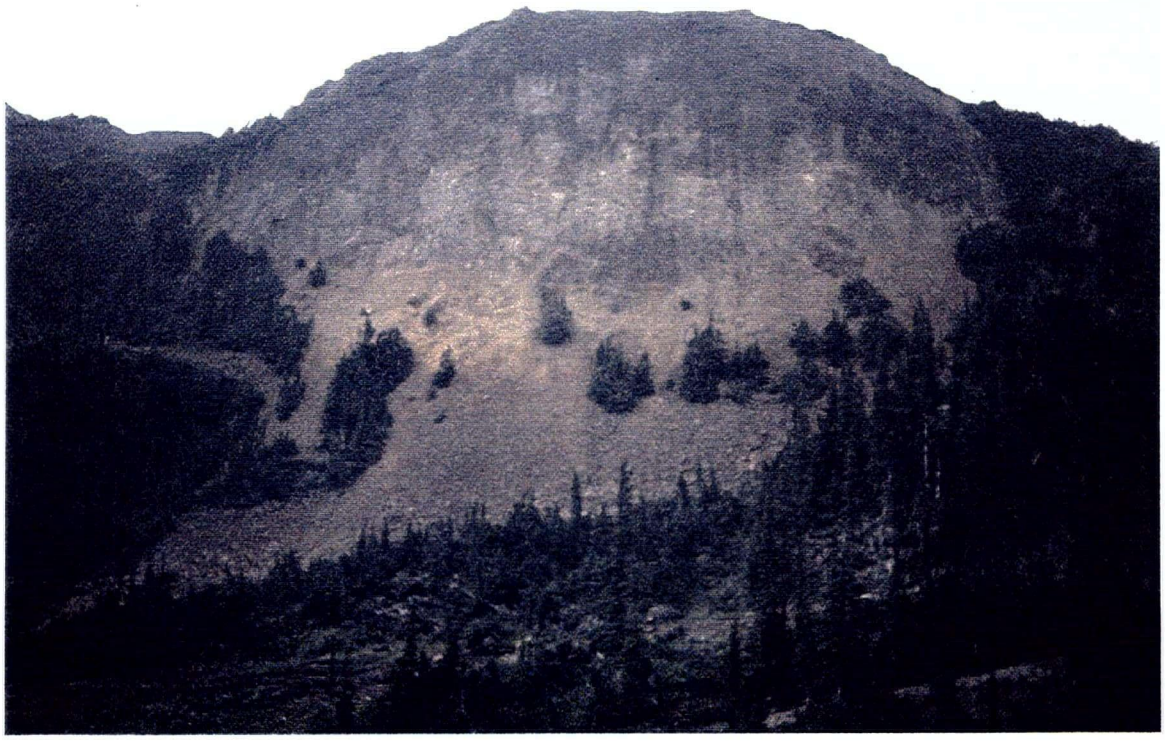

Plate 2.1. Gossanous felsite bluff, south of the Eskay Creek deposit.

Abstract

The Eskay Creek deposit is a Au-Ag-rich volcanogenic massive sulfide deposit located within the Iskut River area of northwestern British Columbia. At Eskay Creek beds of Au-Ag-rich clastic sulfides and sulfosalts hosted within the 'contact' argillite are underlain by the variably altered Eskay rhyolite, which hosts stockwork mineralization, and overlain by the barren hangingwall basalt. The Eskay rhyolite has yielded a Middle Jurassic U-Pb zircon age of 175 +/-2 Ma. Interaction textures between the Eskay rhyolite and 'contact' argillite, which imply emplacement of the rhyolite prior to lithification of the argillite, along with probable local derivation of bedded sulfide clasts indicate a Middle Jurassic age for mineralization, some 7-16 Ma younger than intrusion-related Lower Jurassic mineralization within the region. The data presented in this study demonstrate that there is a second, and significant period of Jurassic mineralization within the Iskut River area.

Initial ε_{Nd} values of +5.5 to +6.9 for the Eskay rhyolite and hangingwall basalt lie within the field for uncontaminated island-arc volcanic rocks and are consistent with formation in a subduction-related environment. Ratios of immobile elements and REE patterns for the Eskay rhyolite suggest a tholeiitic magmatic affinity, whereas unmineralized rhyolite of the same age (174 +2/-1 Ma; U-Pb zircon) is characterized by a slightly less primitive Nd isotopic signature (+4.3) and a transitional to calc-alkaline affinity.

Sulfides and sulfosalts from clastic and rhyolite-hosted mineralization in and along strike from the deposit exhibit a homogeneous Pb isotopic signature. The Pb isotopic composition of Eskay Creek sulfides and sulfosalts is inconsistent with leaching of lead from Paleozoic to Mesozoic arc assemblages which may occur at depth below the Eskay Creek deposit, but is consistent with derivation from a Lower or Middle Jurassic source.

Introduction

The Eskay Creek deposit is located in the Iskut River area (NTS 104B) of northwestern British Columbia. Within this region, Paleozoic to Mesozoic island arc assemblages of the

allochthonous Stikine terrane are overlain by marine sedimentary rocks of the Middle to Upper Jurassic Bowser Lake Group and intruded by plutons of the Tertiary Coast Plutonic Complex. A wide range of styles of base and precious metal-rich deposits occur in the Mesozoic arc complexes and Tertiary plutons of the Iskut River area. These include copper-rich volcanogenic massive sulfide (VMS), porphyry copper-gold, gold±silver vein, silver-zinc-lead vein, and gold-silver skarn deposits (Macdonald et al., 1996). The Eskay Creek deposit (Fig. 2.1) is a Au-Ag-rich VMS deposit hosted within a bimodal volcanic sequence, and is distinct in both style and mineralogy from any other known deposits in the Iskut River area. Mineralization consists of stockwork zones hosted within rhyolite, overlain by argillite and siltstone which host clastic sulfide and sulfosalt mineralization, mainly in the 21B zone (Blackwell, 1989; Britton et al., 1989; Roth, 1995). The rhyolite and sedimentary units are in turn overlain by barren pillowed to massive basalt. The 21B zone contains 1.08 million tonnes grading 65.5 grams per tonne gold, 2930 grams per tonne silver, 5.6% zinc and 0.77% copper (Homestake Canada Inc. Feasibility Report August, 1993); mining of the 21B zone began in January, 1995.

This paper summarizes the results of a multi-isotope study which (1) precisely determines the age of the Eskay Creek deposit, using U-Pb zircon geochronology; (2) uses the Nd and trace element geochemical signatures of the Eskay rhyolite and hangingwall basalt to better characterize the tectonic environment in which the deposit and host magmas formed; (3) compares the chemical and isotopic characteristics of the Eskay rhyolite to unmineralized rhyolite of the same age within the Eskay anticline; and (4) characterizes the Pb isotopic signature of the different styles of mineralization in, and along strike from, the deposit.

Regional Geology

The Eskay Creek deposit is located within Stikinia, an allochthonous terrane of the Canadian Cordillera. Anderson (1989) divided the Stikine terrane in the Iskut River area into four unconformity-bounded, tectonostratigraphic elements: (1) Paleozoic island-arc rocks of the Stikine Assemblage; (2) Mesozoic island-arc assemblages composed of the Upper Triassic Stuhini Group and the Lower to Middle Jurassic Hazelton Group; (3) Middle to Upper Jurassic sedimentary rocks of the Bowser Lake Group, an overlap assemblage occurring on Stikinia and

the adjacent Cache Creek terrane; and (4) Tertiary igneous and metamorphic rocks of the Coast Plutonic Complex (Fig. 2.1).

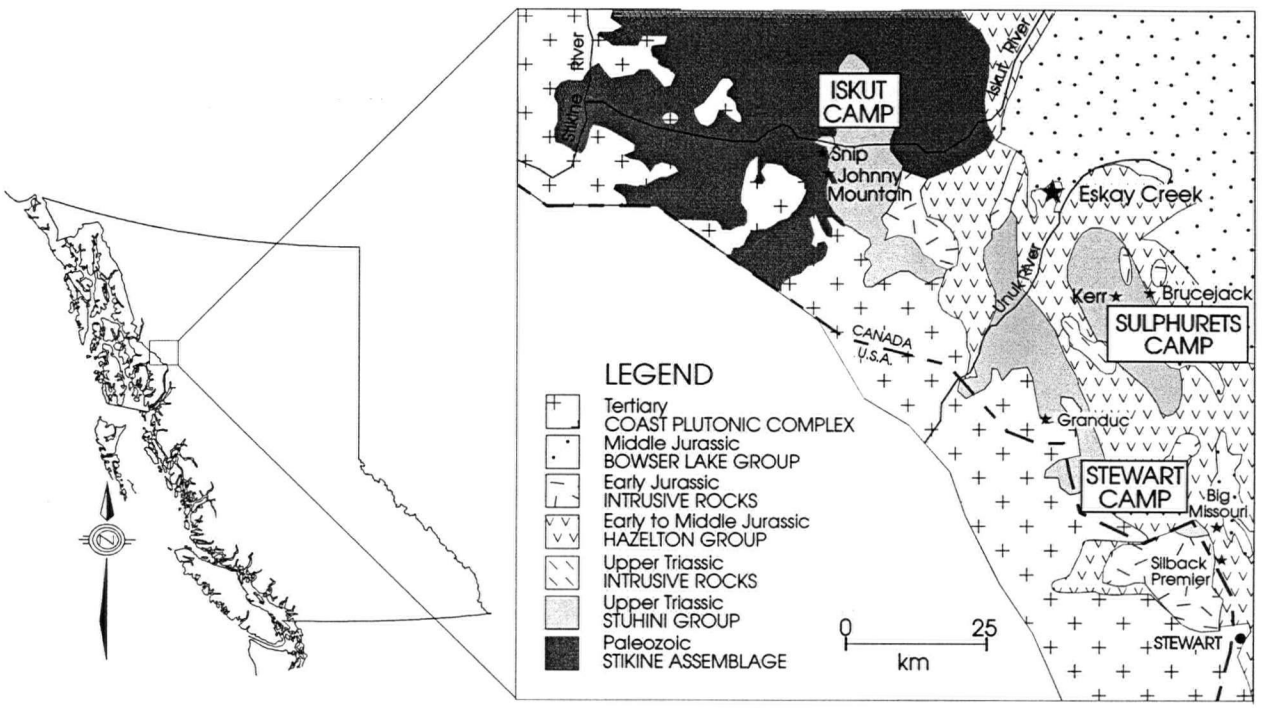

Figure 2. 1 Location map of the Eskay Creek deposit, Iskut River area, northwestern British Columbia showing the major stratigraphic units, mining camps, deposits and occurrences (after Macdonald et al., 1996).

The Iskut River area is host to various styles of mineralization. In addition to Eskay Creek, copper-rich VMS deposits (e.g. Granduc; Childe et al., 1994), porphyry deposits (e.g. Kerr and Sulphurets; Macdonald et al., 1996; Kirkham and Margolis, 1995) and Au±Ag-rich vein deposits (e.g. Snip and Brucejack Lake; Macdonald et al., 1996; Davies et al., 1994) are of economic interest. Known ages of mineralization range from Late Triassic to Eocene, with the majority of mineralization having formed in the Early Jurassic (Childe et al., 1994; Kirkham and Margolis, 1995; Macdonald et al., 1996).

The Lower to Middle Jurassic Hazelton Group, which hosts the Eskay Creek deposit, comprises subaqueous to locally subaerial, mafic to felsic volcanic and volcaniclastic rocks and their intrusive equivalents, and conglomeratic to argillaceous, and calcareous sedimentary rocks. Rocks of the Hazelton Group have been regionally metamorphosed to lower greenschist to sub-greenschist facies. Abrupt facies changes, a complex structural history, and limited age

determinations have hindered the understanding of the stratigraphic history of the Hazelton Group. Stratigraphic sections based on regional mapping by Grove (1986), Anderson and Thorkelson (1990), and Alldrick (1991) divide the Hazelton Group into four formations; from oldest to youngest these are the Unuk River, Betty Creek, Mt. Dilworth and Salmon River Formations. However, recent biochronological (Nadaradju, 1993) and geochronological (Macdonald et al., 1996; this study) information has provided new constraints that require modifications of the existing stratigraphic divisions. Lewis and Anderson (pers. comms., 1995) divided the Hazelton Group into three formations, which are used in this paper. The basal Jack Formation, first defined by Henderson et al. (1992), is composed of pebble to boulder conglomerate and fossiliferous calcareous siltstone, contains Hettangian to Sinemurian fossils, and lies unconformably on rocks of the Upper Triassic Stuhini Group. The second formation is the Betty Creek Formation, composed of andesitic to rhyolitic volcanic and epiclastic rocks, as well as argillite, sandstone, conglomerate and calcareous sedimentary rocks which may be as old as Sinemurian, and in at least one locality as young as Upper Aalenian. The third formation is the Salmon River Formation, and is composed primarily of bimodal volcanic and tuffaceous rocks, as well as locally calcareous argillite to siltstone of Aalenian to Lower Bajocian age. Rocks of the Salmon River Formation record the final stages of arc volcanism in the Stikine terrane, and are overlain by marine sedimentary rocks of the Bowser Lake Group.

Plutons coeval with both the Betty Creek and Salmon River Formations are present in the Iskut River area. Those related to Early Jurassic magmatism, including the 197 to 184 Ma Texas Creek Plutonic and Premier Porphyry Suites (Alldrick et al., 1986; Macdonald et al., 1992; Lewis and Mortensen, unpublished data), are associated with significant base and precious metal mineralization (for example Anderson, 1989; Alldrick, 1991; Macdonald et al., 1996). Plutons related to the Middle Jurassic magmatic event, including 181 to 176 Ma quartz diorite to monzodiorite intrusions (M.L. Bevier and R.G. Anderson, pers comm., 1994; J.K. Mortensen, pers. comm. 1995), contain no known mineralization.

Geology of the Eskay Creek area

Hazelton Group rocks in the Eskay Creek area are folded around the gently northeasterly-plunging Eskay anticline. Strata in the hinge region, in the vicinity of the deposit, are

dismembered by several north-northeast trending faults (Fig. 2.2). The core of the Eskay anticline is occupied by sedimentary rocks of the Jack Formation. Overlying strata of the Betty Creek Formation include undated andesite breccias overlain by Upper Pliensbachian sedimentary rocks (Nadaradju, 1993) (Figs. 2.2 and 2.3). The basal footwall volcanic unit of the Salmon River Formation consists of intermediate composition volcanic tuff and breccia, and aphanitic amygdaloidal andesite flows or sills (Roth, 1993). Overlying the footwall volcanic unit, within the Salmon River Formation, are at least two chemically distinct rhyolites, shown on Figure 2.3 as the Eskay rhyolite and the east limb rhyolite (Rye, 1992). The Eskay rhyolite occurs along the west limb and through the fold closure of the Eskay anticline, hosts stringer-style discordant mineralization and is the immediate footwall to stratiform mineralization.

West Limb

The Eskay rhyolite is characterized by aphanitic massive to flow-banded and auto-brecciated flows and associated tuffs, interpreted by Bartsch (1993) on the basis of facies variations to represent a linear flow dome complex. In proximity to stockwork mineralization, the rhyolite shows moderate to extreme alteration ranging from quartz-sericite-pyrite to chlorite-rich assemblages. A series of north-northeast trending rhyolite masses, termed felsite, which are slightly discordant to stratigraphy, occur along the length of the west limb (Fig. 2.2). Felsite is chemically indistinguishable from the Eskay rhyolite (Rye, 1992; Bartsch, 1993; Roth, 1993) and is interpreted to represent sub-volcanic portions of the Eskay rhyolite (Bartsch, 1993; Edmunds et al., 1994). Along most of the west limb, the Eskay rhyolite grades into a black matrix breccia, which in turn grades into carbonaceous black siltstone and argillite, termed the contact argillite. Black matrix breccia is composed of matrix-supported angular to sub-rounded, shattered, glassy and flow-banded rhyolitic fragments in a black siliceous matrix (Plate 2.2). This texture is interpreted to have formed as a result of intrusion of hot rhyolite into unlithified argillaceous sedimentary rocks, implying that emplacement of the Eskay rhyolite occurred prior to lithification of the contact argillite. Argillite is overlain by pillowed to massive basalt flows and sills which form the hangingwall to mineralization (Figures 2.2 and 2.3 and Plate 2.3). Peperitic textures at the contact between basalt and argillite indicate emplacement of the hangingwall basalt prior to lithification of the contact argillite. The field relationships therefore imply that the Eskay rhyolite

and hangingwall basalt were emplaced within a relatively short time span, during accumulation, and prior to lithification of the contact argillite.

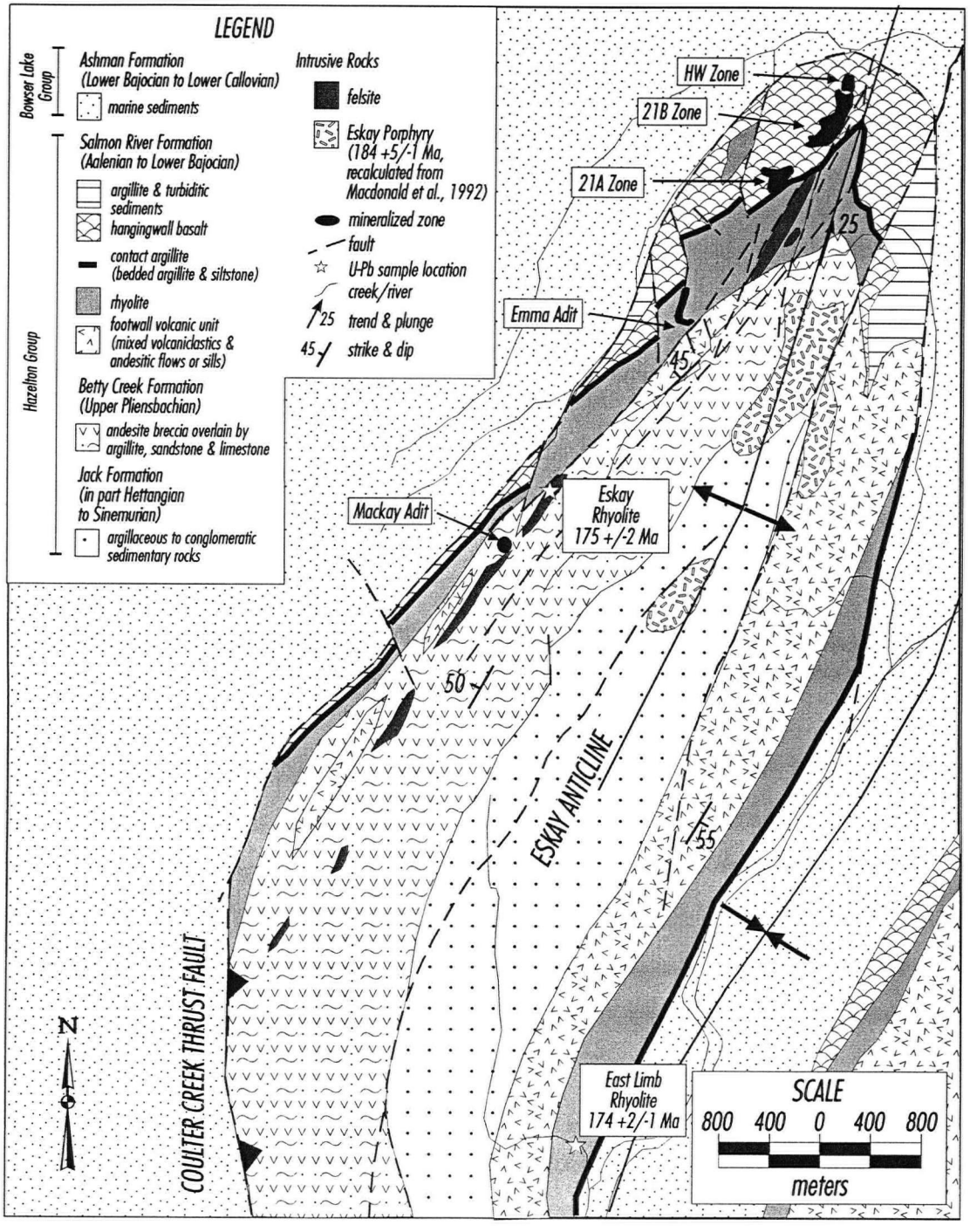

Figure 2. 2 Geology of the Prout Plateau, showing locations of selected mineralized zones projected to surface (after Edmunds and Kuran, 1991; Bartsch, 1993 and P. Lewis, pers comm., 1996).

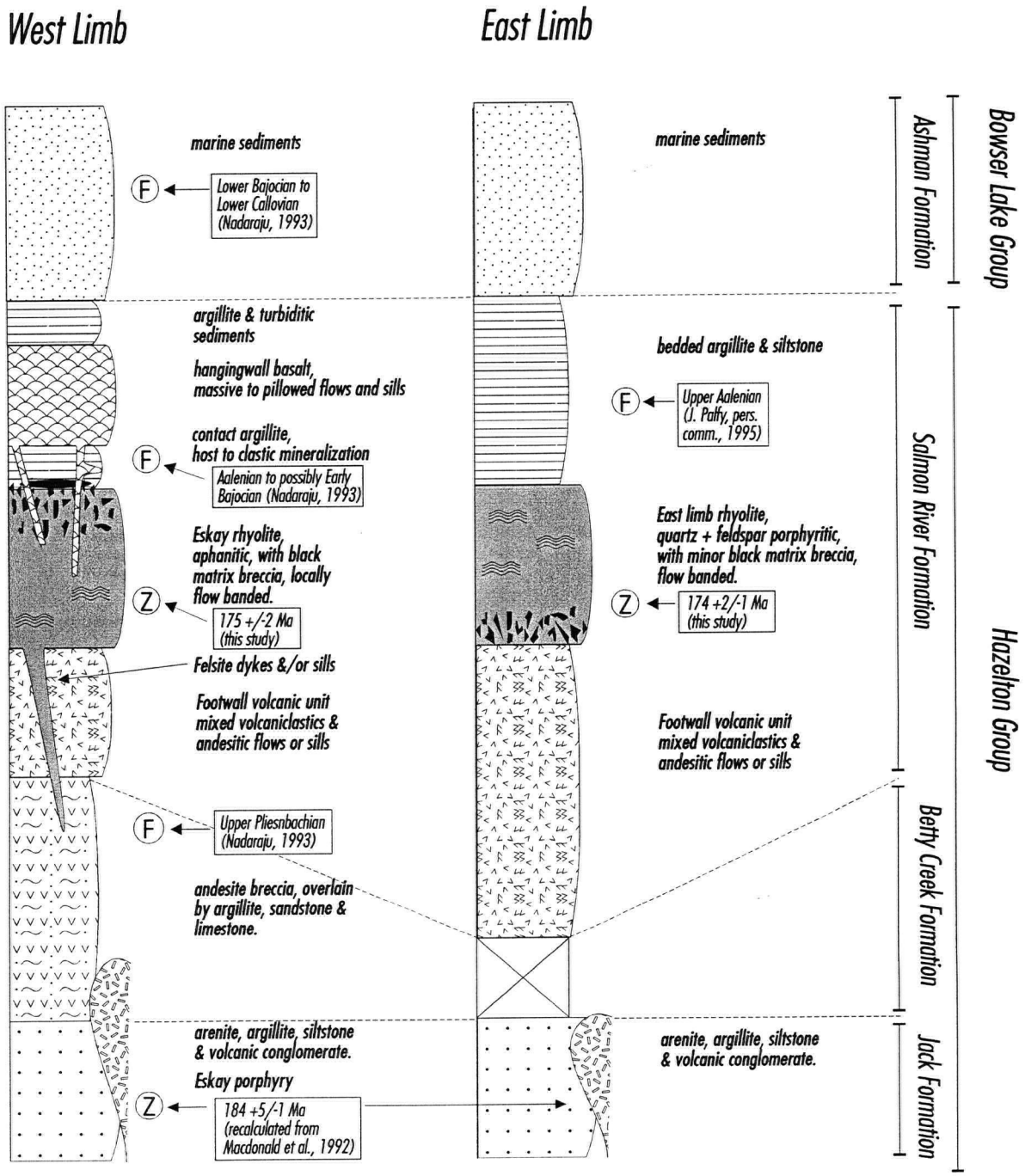

Figure 2. 3 Schematic stratigraphic sections for the east and west limbs of the Eskay anticline, F = fossil locality, Z = U-Pb zircon sample locality.

East Limb

The east limb rhyolite has a black aphanitic matrix, well preserved flow-banding and sparse 1-2 mm quartz and potassium feldspar phenocrysts (Plate 2.4). The presence of black matrix breccia along the lower margin of this rhyolite indicates emplacement into unlithified sedimentary rocks. Rhyolite is overlain by argillite which is interpreted to be the stratigraphic equivalent of the contact argillite. Mafic rocks analogous to the hangingwall basalt have not been observed on the east limb.

Eskay Porphyry

The Eskay porphyry (Figs. 2.2 and 2.3), located within the core of the Eskay anticline, is an orthoclase porphyritic to megacrystic monzodioritic intrusion within sedimentary rocks of the Jack Formation and andesitic volcanic rocks of the Betty Creek Formation. The Eskay porphyry has been dated by U-Pb zircon geochronology at 184 +5/-1 Ma (recalculated from Macdonald et al., 1992) and is contemporaneous with intrusion-related Lower Jurassic mineralization in the Iskut River and Stewart areas.

Mineralization

Mineralization at Eskay Creek can be broadly divided into two main styles, stratiform and discordant. Stratiform mineralization occurs as beds of clastic sulfides and sulfosalts within the contact argillite in the 21A, B, and C, hangingwall, and northeast extension zones. Discordant, rhyolite-hosted vein mineralization, which may in part represent feeder zones to clastic mineralization, occurs below the stratiform mineralization in the 109, Pumphouse and Pathfinder zones, and along strike at the Emma and Mackay Adits (Fig. 2.2).

At present, the 21B zone is the focus of mining at Eskay Creek. It is an elongate zone, approximately 900 meters long, 60 to 200 meters wide and 1 to 15 meters thick, composed of well-bedded fragmental sulfides, sulfosalts, argillite, altered rhyolite and barite hosted within the contact argillite (Britton et al., 1989; Roth, 1995) (Plate 2.5). The main ore minerals are sphalerite and tetrahedrite, with lesser friebergite, galena, pyrite, boulangerite, and other sulfosalts

(Roth, 1995). Well-preserved features such as graded sulfide beds with sharply defined bases, soft-sediment deformation of the sulfide beds and channel structures attest to the clastic nature of the ore within a high-energy, channel-like environment (Roth, 1995). The proximity of stockwork zones to clastic mineralization and the presence of altered rhyolite fragments interbedded with sulphide fragments suggest local derivation of clastic sulfides and sulfosalts (Macdonald et al., 1996). The distribution and mineralogy of the mineralized zones are outlined in Figure 2.4; detailed descriptions are provided by Britton et al. (1989), Roth (1993), Edmunds et al. (1994), and Roth (1995).

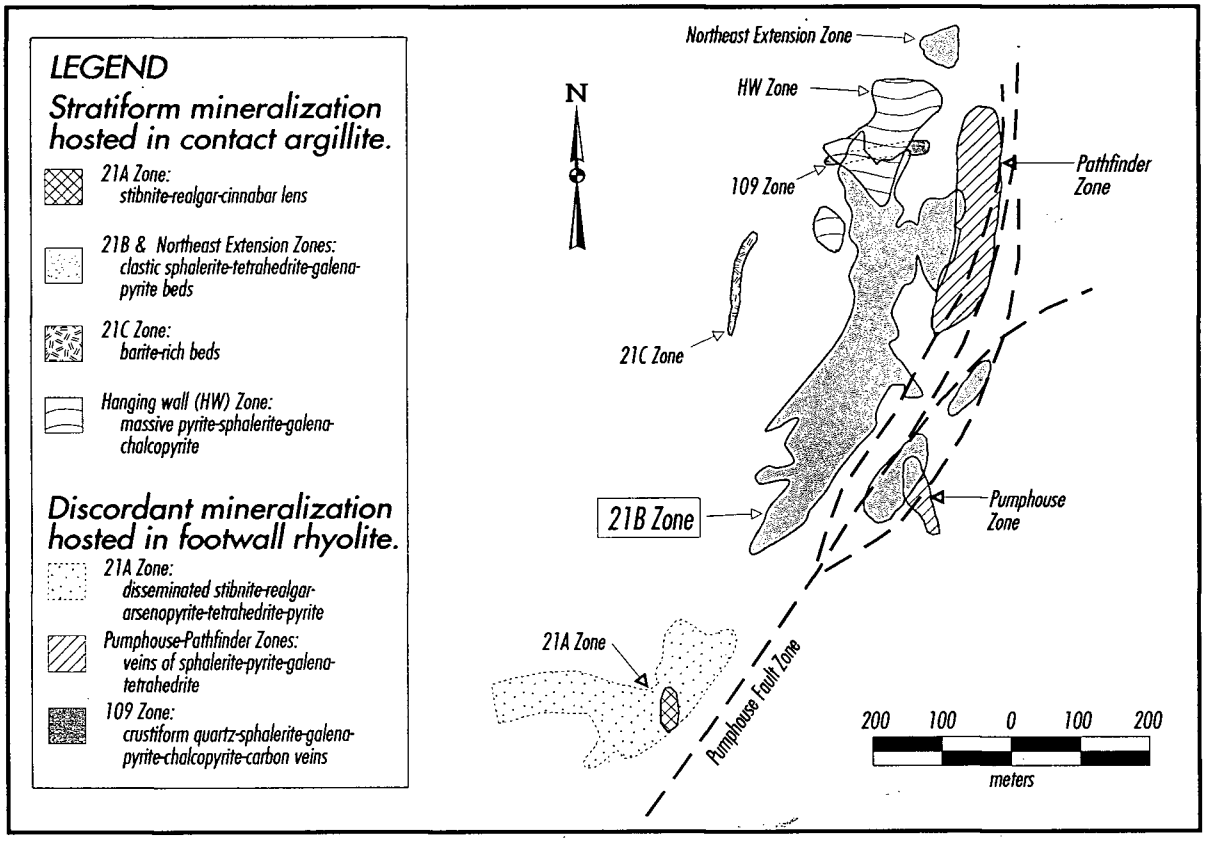

Figure 2. 4 Projection to surface of mineralized zones at the Eskay Creek deposit (courtesy of Homestake Canada Inc.).

U-Pb Geochronology

Zircon was recovered from both the Eskay and east limb rhyolites; heavy mineral extraction procedures and U-Pb zircon analytical procedures follow those of Mortensen et al. (1995). Isotopic ratios were measured using a modified single collector VG-54R thermal

ionization mass spectrometer equipped with a Daly photomultiplier. Uranium and Pb analytical blanks were in the range of 1-3 and 8-15 picograms, respectively. Concordia intercept ages and associated errors were calculated using a modified York-II regression model (York, 1969), and ages were calculated using the decay constants recommended by Steiger and Jäger (1977). Age assignments follow the time scale of Harland et al. (1990). Analytical results are given in Table 2.1 and Figure 2.5.

Table 2. 1 U-Pb zircon analytical data for Eskay and east limb rhyolites.

Fraction[1]	Wt.	U	Pb[2]	$^{206}Pb/^{204}Pb$[3]	Pb[4]	^{208}Pb[5]	Isotopic ratios($\pm1\sigma$,%)[6]			Isotopic dates(Ma,$\pm2\sigma$)[6]		
	mg	ppm	ppm		pg	%	$^{206}Pb/^{238}U$	$^{207}Pb/^{235}U$	$^{207}Pb/^{206}Pb$	$^{238}U/^{206}Pb$	$^{207}Pb/^{235}U$	$^{207}Pb/^{206}Pb$
Eskay rhyolite (EC-GC-11)												
A,f,M5,eq	0.045	2858	71	975	216	8.5	0.02525±0.13	0.1726±0.32	0.04957±0.22	160.8±0.4	161.7±0.9	174.8±10.3
D,f,M5,eq	0.034	3071	77	4388	39	7.9	0.02573±0.11	0.1757±0.22	0.04954±0.13	163.8±0.3	164.4±0.7	173.5±6.1
E,f,M5,eq	0.052	3198	84	2317	118	8.2	0.02663±0.11	0.1821±0.14	0.04959±0.07	169.4±0.4	169.8±0.4	175.8±3.1
F,f,M5,eq	0.034	3608	77	4388	39	7.9	0.02554±0.10	0.1745±0.27	0.04955±0.18	163.8±0.3	163.3±0.8	173.5±6.1
G,m,M5,eq	0.010	6790	173	2450	45	8.1	0.02589±0.14	0.1770±0.27	0.04959±0.18	164.8±0.4	165.5±0.8	176.0±8.5
East limb rhyolite (EC-GC-03)												
Morphology 1: subhedral, equant to prismatic												
A,m,N1,eq	0.062	444	112	1446	33	11.5	0.02743±0.10	0.1885±0.25	0.04984±0.17	174.5±0.3	175.4±0.8	187.8±8.0
B,f,N1,eq	0.115	426	12	3390	25	11.0	0.02729±0.10	0.1869±0.22	0.04968±0.15	173.6±0.3	174.0±0.7	180.2±6.8
C,m,M1,eq	0.115	434	12	4312	20	11.3	0.02728±0.10	0.1864±0.21	0.04954±0.12	173.5±0.4	173.5±0.6	173.6±5.6
D,f,M2,eq	0.104	405	11	4143	18	11.0	0.02749±0.10	0.1881±0.20	0.04963±0.19	174.8±0.3	175.0±0.7	177.9±5.5
L,f,N1,eq	0.123	313	9	5693	12	11.5	0.02736±0.11	0.1881±0.20	0.04987±0.12	174.0±0.4	175.0±0.6	188.7±5.7
Morphology 2: euhedral, needles												
I,f,M5,e*	0.134	1725	46	2947	118	18.4	0.02384±0.11	0.1628±0.13	0.04952±0.07	151.9±0.3	153.2±0.4	172.7±3.0
J,f,M5,e*	0.080	5710	155	2520	281	18.2	0.02461±0.13	0.1683±0.16	0.04989±0.07	156.7±0.4	157.9±0.5	175.8±3.4
K,f,M5,e	0.025	2448	67	1172	82	18.4	0.02477±0.08	0.1693±0.17	0.04956±0.13	157.8±0.2	158.8±0.5	174.5±6.0

[1]All fractions air abraded unless marked by an *; Grain size, intermediate dimension: m=<134μm and >74μm, f=<74μm; Magnetic codes: Franz magnetic separator sideslope at which grains are nonmagnetic; e.g., N1=nonmagnetic at 1°; Field strength for all fractions =1.8A; Front slope for all fractions=20°; Grain character codes: e=elongate, eq=equant to prismatic.

[2]Radiogenic Pb

[3]Measured ratio corrected for spike and Pb fractionation of 0.0043/amu ±20% (Daly collector)

[4]Total common Pb in analysis based on blank isotopic composition

[5]Radiogenic Pb

[6]Corrected for blank Pb, U and common Pb (Stacey-Kramers model Pb composition at the $^{207}Pb/^{206}Pb$ date of fraction, or age of sample)

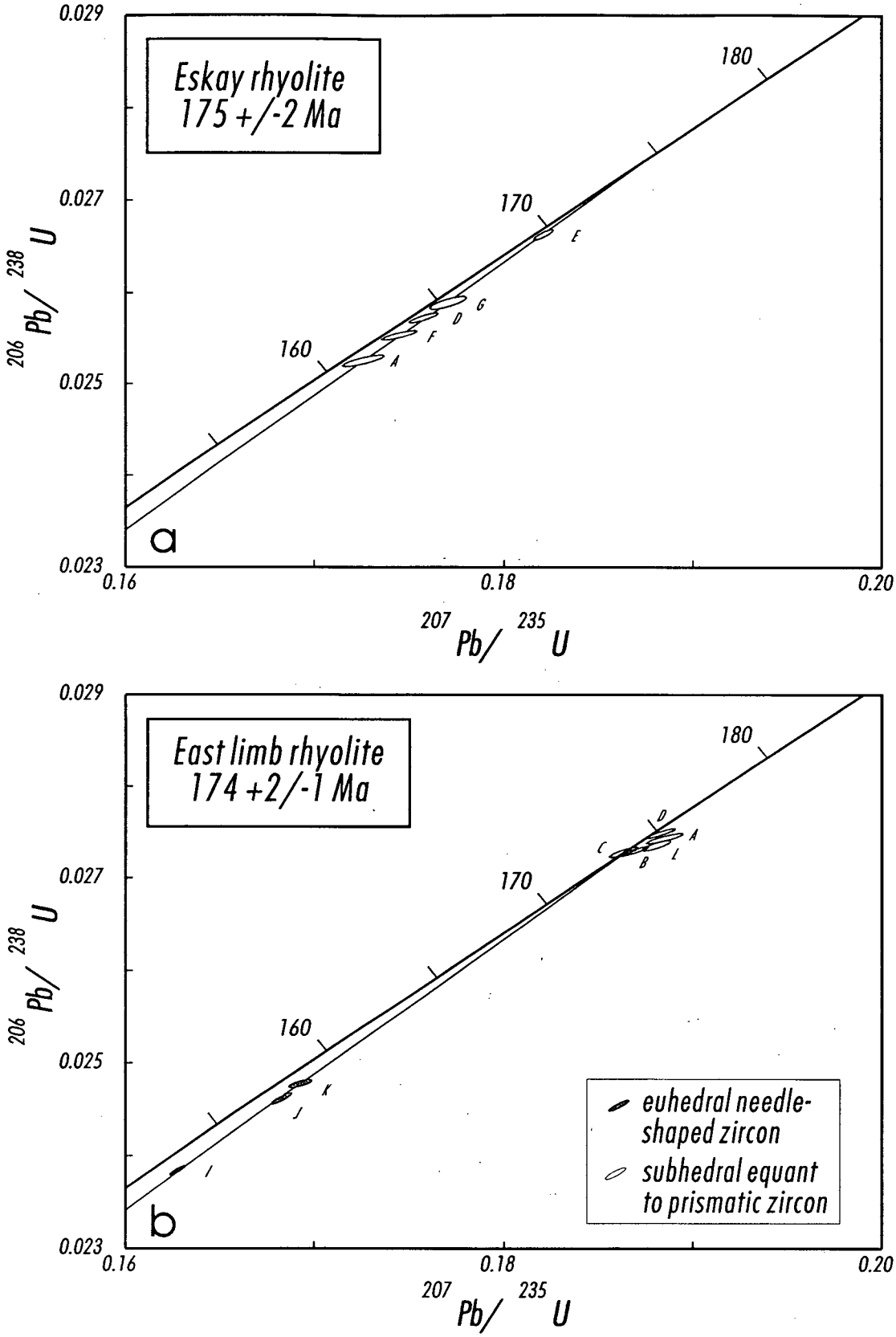

Figure 2. 5 U-Pb zircon concordia diagrams for Salmon River Formation rhyolites from the Eskay anticline a) Eskay rhyolite (EC-GC-11), showing weighted mean regression line for all fractions; b) East limb rhyolite, showing weighted mean regression line for morphology 2, euhedral needle-shaped zircon.

Eskay rhyolite

A small quantity of prismatic zircons, with relatively high magnetic susceptibility, and typical length to width ratios of 3:1, were recovered from the Eskay rhyolite (Fig. 2.2). Zircons were pale to dark brown in color, contained numerous colorless to opaque inclusions, and had poor clarity and cloudy patches. SEM analysis revealed that pyrite and potassium feldspar were present as inclusions within some of the grains (Plate 2.6). These two minerals can contain up to several hundred parts per million lead within their crystal lattice, and therefore their presence can significantly contribute to the common lead concentration in a zircon analysis. All of the zircon recovered from this rock was picked, and divided into 5 fractions. Despite strong abrasion of the zircons, all analyses are discordant. Zircon from this rock contain high concentrations of uranium (2858-6790 ppm). Cloudy portions within the zircons, combined with high uranium concentrations, suggest that sections of some grains may have become metamict, and therefore susceptible to lead-loss. It is therefore likely that high uranium concentrations and the possible resulting metamictization of these zircon contributed to their discordance.

The $^{207}Pb/^{206}Pb$ ages of zircon fractions from this rock range from 173.5 to 176.0 Ma. A best fit line through all fractions yields an upper intercept age of 177 +33/-5 Ma and a lower intercept age of 36 +101/-125 Ma. A $^{207}Pb/^{206}Pb$ weighted mean age for all fractions yields an age of 175 +/-2 Ma. The lack of any visible cores using either binocular microscope or SEM backscatter imaging, combined with a restricted range of $^{207}Pb/^{206}Pb$ ages, suggests that these zircon do not contain an inherited component. Therefore the weighted mean age of 175 +/-2 Ma is considered to be the best estimate of the age of crystallization of this rock.

East limb rhyolite

Two populations of zircon were recovered from a sample of the east limb rhyolite (Fig. 2.2 and Plate 2.4). The first population was relatively non-magnetic and consisted of colorless, subhedral, slightly resorbed equant to prismatic grains, 50 to 100 microns in width, with length to width ratios of 1:1 to 2.5:1. Zircons from this population were characterized by colorless rod- and bubble-shaped inclusions, moderate clarity and occasional turbid cores. Zircons from the second population consisted of relatively high magnetic susceptibility, elongate, colorless, doubly-

terminated needles, typically missing one or both terminations, probably broken during the mineral separation process. These zircons had widths of 25 to 50 microns, length to width ratios of 5:1 to 10:1, were very clear, and commonly contained funnel-shaped tubes aligned parallel to the c-axis of the grains. These tubes were usually filled with a dark colored, opaque substance. As the zircon was of excellent quality, the opaque material is a likely source of the high magnetic susceptibility of this zircon population. SEM analysis of the opaque material revealed quartz, a phylosillicate (muscovite?), a heavy rare earth yttrium phosphate (xenotime?), and possibly volcanic glass. The presence of rock-forming minerals, in particular micas, is consistent with the magnetic susceptibility of these grains being higher than is characteristic for pure zircon (Hutchison, 1974).

Five fractions of the equant to prismatic zircon (A, B, C, D, and L) were analyzed, following strong abrasion. The $^{207}Pb/^{206}Pb$ ages of these five fractions range from 173.6 to 188.7 Ma; fraction C is concordant at 173.6 Ma. Turbid cores, observed within some of the zircons in this population not selected for analysis, along with older $^{207}Pb/^{206}Pb$ ages than fraction C indicate that the non-concordant fractions contain an inherited component; possible sources to this inherited component include the underlying Paleozoic to Mesozoic arc assemblages. An interpreted age of 174 +6/-1 Ma is obtained from this population of zircon based on the $^{207}Pb/^{206}Pb$ age and associated $^{206}Pb/^{238}U$ and $^{207}Pb/^{206}Pb$ errors of concordant fraction C.

Three fractions of zircon with the needle-like morphology (I, J, and K) were also analyzed. Due to the high length to width ratio of the needles, the abrasion process is generally not effective. Fractions I and J were not abraded and fraction K was lightly abraded prior to analysis. All three fractions are discordant; this feature is attributed to lead-loss, which may have been enhanced by the high uranium concentrations and high surface to volume ratio of these grains. The $^{207}Pb/^{206}Pb$ ages for the three fractions range from 172.7 to 175.8 Ma, with a weighted mean of 174 +/-2 Ma. The restricted range of $^{207}Pb/^{206}Pb$ ages and the needle morphology suggest that there is no inherited component within this zircon population, and that the weighted mean age is a valid estimate of the age of crystallization of this population of zircon. The interpreted age of this rhyolite is 174 +2/-1 Ma, reflecting the $^{207}Pb/^{206}Pb$ age of concordant

fraction C, and errors calculated from the minimum $^{206}Pb/^{238}U$ age of this fraction and the maximum weighted mean age of zircon with the needle morphology.

Geochemistry

Major and Trace Elements

Major, trace and rare-earth element analyses were conducted for typical samples of the Eskay and east limb rhyolites and the hangingwall basalt (Table 2.2). In the immediate vicinity of the Eskay Creek deposit, the Eskay rhyolite is highly altered to quartz-sericite-pyrite and chlorite; the intensity of alteration decreases with distance away from zones of mineralization (Bartsch, 1993). Although major element concentrations are strongly affected in altered rocks associated with VMS deposits, ratios of immobile elements such as Ti, Al, Zr and Y remain essentially unchanged (for example: MacLean and Kranidotis, 1987; Barrett and MacLean, 1994). The samples analyzed in this study, therefore, are compared in terms of immobile element ratios with more extensive geochemical databases for the Eskay and east limb rhyolites (Bartsch, 1993; Barrett and Sherlock, 1996) (Fig. 2.6).

In a plot of Zr vs. TiO_2, the Eskay and east limb rhyolites have distinctly different trends, with the Eskay rhyolite having significantly lower TiO_2 concentrations and TiO_2/Zr ratios (Fig. 2.6a). The wide range of Zr and TiO_2 concentrations observed within the Eskay rhyolite appears to be the result of alteration. Mass change effects have produced a dispersion of points towards and away from the origin along the Eskay rhyolite trend (Barrett and Sherlock, 1996). Silicification produces mass gain, which dilutes Zr and TiO_2 concentrations, whereas sericitization and chloritization produce mass loss, which residually concentrates Zr and TiO_2 (Barrett and MacLean, 1994).

A Zr vs. Y diagram is used to characterize the magmatic affinity of the Eskay and east limb rhyolites. Using the divisions suggested by Barrett and MacLean (1994), the Eskay rhyolite, with Zr/Y ratios of 2 to 4.5, is mainly of tholeiitic magmatic affinity, whereas rhyolites on the east limb, with Zr/Y ratios of 4.5 to 8, are of transitional to mildly calc-alkaline affinity (Fig. 2.6b). Regionally, rhyolite from the Salmon River Formation in the Iskut River area ranges from a calc-

Table 2. 2. Major, trace and rare earth element, and Nd isotopic data for samples from the Eskay anticline.

Location:	surface	surface: EC-94-07	C91-707, 181m	U-58, 15.2m	CA90-527, 54m	detection
U-Pb Sample Number:	EC-GC-03		EC-GC-11			limit
Lithology:	east limb rhyolite	east limb rhyolite	Eskay rhyolite	Eskay rhyolite	hangingwall basalt	
x-ray flouresence						
SiO_2 (wt.%)	69.89	77.32	76.38	80.81	46.70	0.006
Al_2O_3	15.74	12.15	13.30	10.77	17.61	0.0120
TiO_2	0.27	0.21	0.07	0.07	1.94	0.0035
Fe_2O_3	1.06	1.10	1.31	1.28	9.63	0.003
MnO	0.02	0.02	0.01	0.01	0.14	0.003
MgO	0.19	bdl	0.93	0.83	13.06	0.0095
CaO	0.39	bdl.	0.09	0.01	0.78	0.0015
Na_2O	4.08	3.46	0.00	0.09	2.47	0.0075
K_2O	6.84	4.75	6.16	3.35	0.82	0.0025
P_2O_5	0.02	0.03	0.01	0.04	0.34	0.0035
BaO	0.25	bdl	0.05	0.12	0.13	0.0017
LOI	1.00	0.71	2.20	2.84	6.92	
Cu (ppm)	55	9	20	43	75	2
Zn	32	56	55	16	129	2
Co	28	34	39	28	47	10
Ni	12	bdl	0	2	66	3
Cr	157	bdl	5	bdl	397	15
V	19	bdl	7	18	360	10
Zr	325	321	162	152	92	1
Y	69	46	92	61	30	1
Rb	100	76	188	109	12	1
Sr	59	47	32	9	62	1
neutron activation						
La (ppm)	36.3			18.1	4.9	0.1
Ce	71			56	13	1
Nd	28			34	9	1
Sm	6.71			8.58	3.12	0.01
Eu	1.13			bdl	0.89	0.05
Tb	1.5			1.8	0.7	0.1
Yb	7.26			7.41	3.18	0.05
Lu	0.89			1.01	0.43	0.01
Th	7.5			13.1	0.3	0.1
U	2.6			8.9	bdl	0.1
Au	bdl			263	9	2
Ag	bdl			4	bdl	2
As	1			121	bdl	1
Co	22			31	89	0.1
Cs	1.1			2.4	2.7	0.2
Hf	8.2			5.4	1.7	0.2
Sb	1.4			52.6	4.5	0.1
Sc	1.9			1.1	45.8	0.1
Ta	1.5			2.6	bdl	0.3
mass spectrometry						
Sm (ppm)	6.28			8.60	3.62	
Nd	27.26			30.39	10.88	
$^{147}Sm/^{144}Nd$	0.1394			0.1712	0.2011	
$^{143}Nd/^{144}Nd$ (meas.)	$0.512791\pm4x10^{-6}$			$0.512888\pm11x10^{-6}$	$0.512997\pm7x10^{-6}$	
$\varepsilon_{Nd\,(174\,Ma)}$	+4.3			+5.5	+6.9	
T_{DM} (Ma)	542			-	634	

bdl = below detection limit.

alkaline to tholeiitic affinity (A. Kaip, pers comm., 1995). The Eskay porphyry, with Zr/Y ratios of 6 to 13, has a transitional to calc-alkaline affinity (Bartsch, 1993).

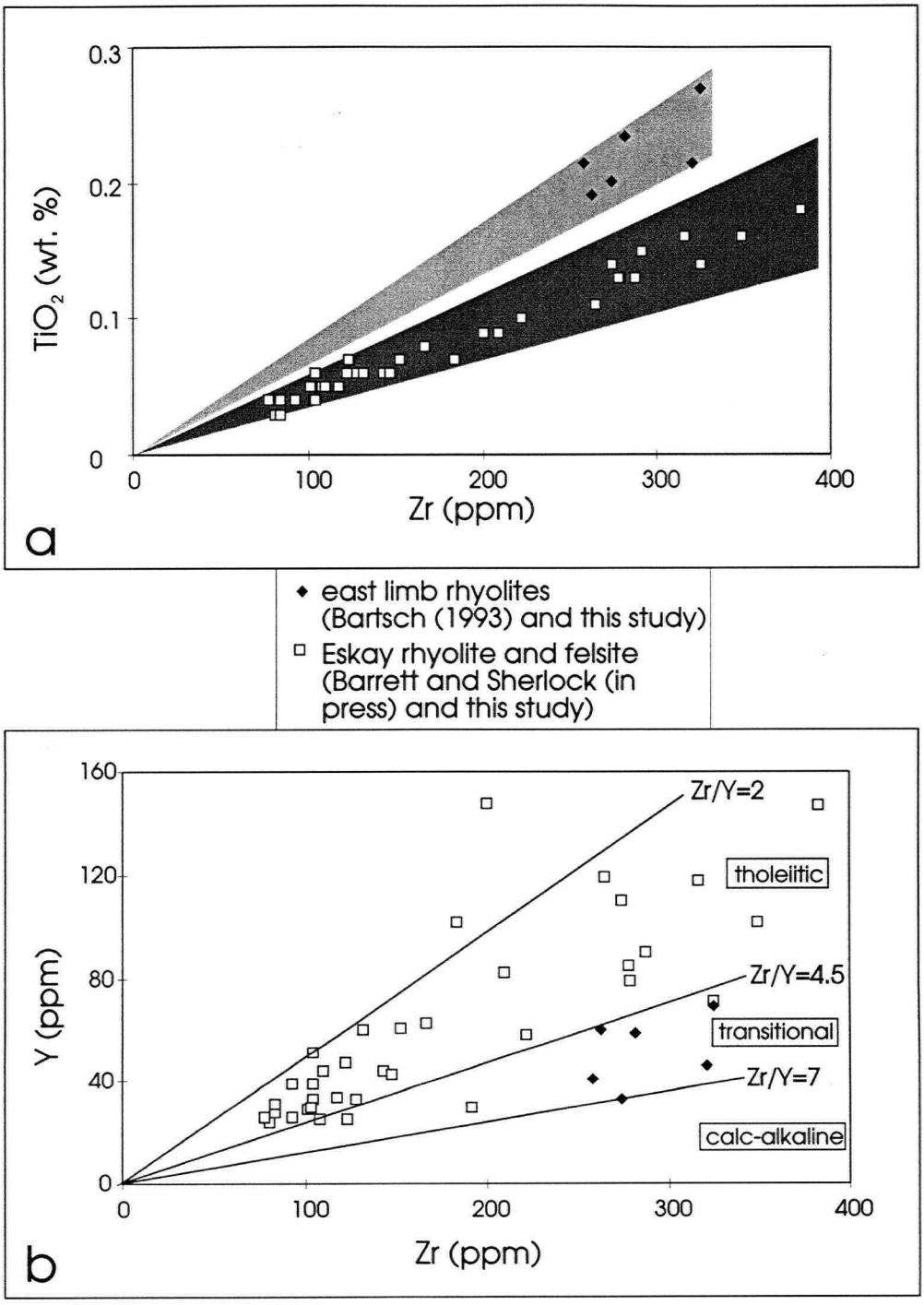

Figure 2. 6 Trace element plots for Eskay and east limb rhyolites, a) Zr vs. TiO_2, b) Zr vs. Y.

Rare Earth Elements

Rare earth element (REE) concentrations are presented in Table 2.2 and compared with the range of REE concentrations determined for these lithologies and the Eskay porphyry by Bartsch (1993) (Figs. 2.7a, b and c). The Eskay rhyolite exhibits a slight enrichment in the light REE (LREE) but a near-flat pattern for the heavy REE (HREE), and a negative europium anomaly; rhyolite from the east limb sampled in this study exhibits a similar REE pattern (Fig. 2.7a). These relatively flat REE patterns suggest that both rhyolites are the products of primitive tholeiitic magmas, either as a result of partial melting of sialic crust or fractional crystallization of basaltic magma. An inherited component to the zircon in the East limb rhyolite indicates that this rhyolite contains some component of partial melting. Although characterized by similar major and trace element chemistry, rhyolite from the southern portion of the east limb sampled in this study has a markedly more tholeiitic REE pattern than the samples reported by Bartsch (1993), suggesting the presence of a second, chemically distinct rhyolite, along the east limb of the anticline (Fig. 2.7b). A steeper REE pattern for the Eskay porphyry indicates a more evolved magmatic affinity than the Eskay and east limb rhyolites (Fig. 2.7c).

Samples of the hangingwall basalt analyzed in this study and others (Bartsch, 1993; Barrett and Sherlock, 1996) yield Zr/Y ratios between 2 and 4, consistent with a tholeitic magmatic affinity. High MgO, Cr and Ni contents indicate derivation from relatively unfractionated mantle melts (Barrett and Sherlock, 1996). However, the essentially flat REE pattern for the hangingwall basalt displays enrichment in LREE relative to N-MORB, and is comparable to that of T-MORB (Sun and McDonough, 1989) (Fig. 2.7c). These data suggest minor enrichment of the basalts relative to N-MORB.

Nd Isotopic Data

The Nd isotopic ratios of the Eskay and east limb rhyolites and the hangingwall basalt were determined to further constrain the characteristics of the magmas and their potential source regions. Isotopic analyses were conducted by R. Thériault at the Geochronology Laboratory of the Geological Survey of Canada. Analytical procedures are described by Thériault (1990). Abundances of Sm and Nd determined by isotope dilution have an uncertainty of 1% or less.

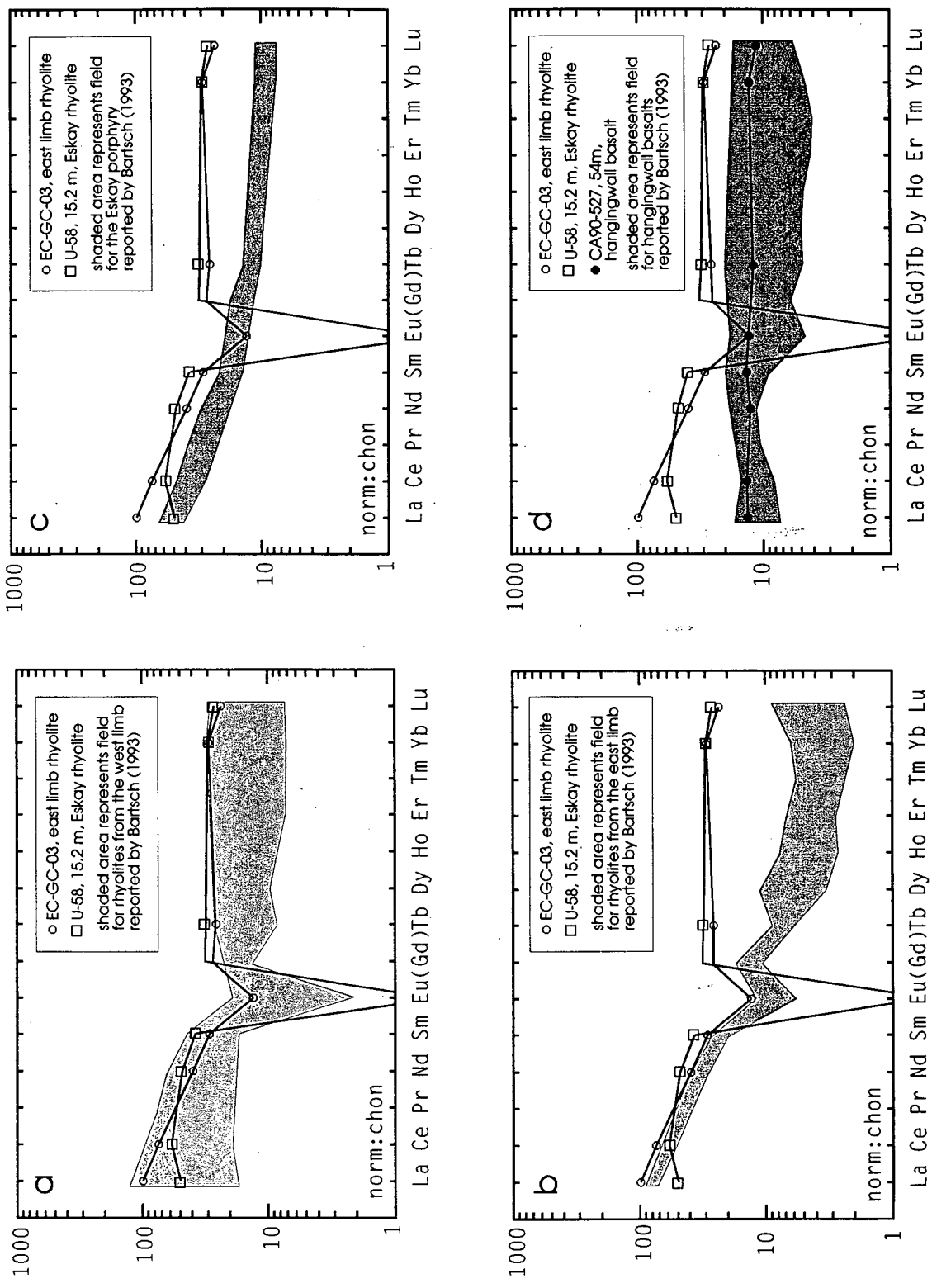

Figure 2. 7 Chondorite-normalized REE diagrams showing Eskay and east limb rhyolites and hangingwall basalt, compared with data fields for samples reported by Bartsch (1993).

Uncertainty for calculated ε_{Nd} values is ± 0.5 ε_{Nd} units. Initial ε_{Nd} values for the Eskay and east limb rhyolites are +5.5 and +4.3, respectively, whereas the hangingwall basalt has a value of +6.9 (Table 2.2).

The range of initial ε_{Nd} values determined for MORB is about +8 to +12 (DePaolo, 1988). Lavas produced within modern island arcs formed on oceanic crust, with no evidence for continental contamination such as the Isu, New Britain and Mariana arcs, yield initial ε_{Nd} values of +2 to +10 (DePaolo and Wasserburg, 1977; Nohda and Wasserburg, 1981; Hawkesworth et al., 1993). The shift to slightly more evolved (lower) ε_{Nd} values for island-arc magmas relative to MORB appears to be the result of contamination from components derived from the downgoing slab and/or the volcano-sedimentary pile, thus reflecting the subduction process (DePaolo, 1988). In contrast, lavas produced within continental margin volcanic arcs have lower initial ε_{Nd} values, reflecting contamination from more evolved continental basement (Faure, 1986 and references therein).

Initial ε_{Nd} values of +4.3 to +6.9 for Salmon River Formation rhyolite and basalt in the Eskay anticline indicate derivation from juvenile source regions, and are consistent with formation in a subduction-related environment (Fig. 2.8). A slightly more evolved signature for the East limb rhyolite, relative to the Eskay rhyolite may be reflecting a greater component of contamination by subduction-related sediments or partial melting of sialic crustal than in the Eskay rhyolite. Initial ε_{Nd} values determined in this study fall within the range of known values for Lower Jurassic felsic volcanic rocks of the Hazelton Group and Lower to Middle Jurassic felsic to intermediate intrusive rocks (Samson et al., 1989; Jackson, 1990; M. L. Bevier and R. G. Anderson, pers. comms., 1994) (Fig. 2.8); there is no comparable published database for mafic rocks or Middle Jurassic felsic volcanic rocks of the Hazelton Group.

Pb Isotopic Data

Lead isotopic compositions were determined for 21 sulfide and sulfosalt samples from the 21B, HW, 109, NEX, and Pathfinder zones, the Emma and Mackay Adits, and stockwork mineralization within the footwall volcanic unit, from directly below the deposit. The Eskay

rhyolite is too pervasively altered to yield reliable whole rock lead isotopic data. Minerals analyzed in this study included galena, boulangerite, sphalerite, chalcopyrite and pyrite (Table 3). Analytical procedures for sulfide and sulfosalt trace lead analyses are given in Childe (*this volume*). The principal objective of this portion of the study was to determine if the various zones of stratiform and discordant mineralization at the deposit and along strike from it are characterized by specific Pb isotopic signatures (Figs. 2.2 and 2.4).

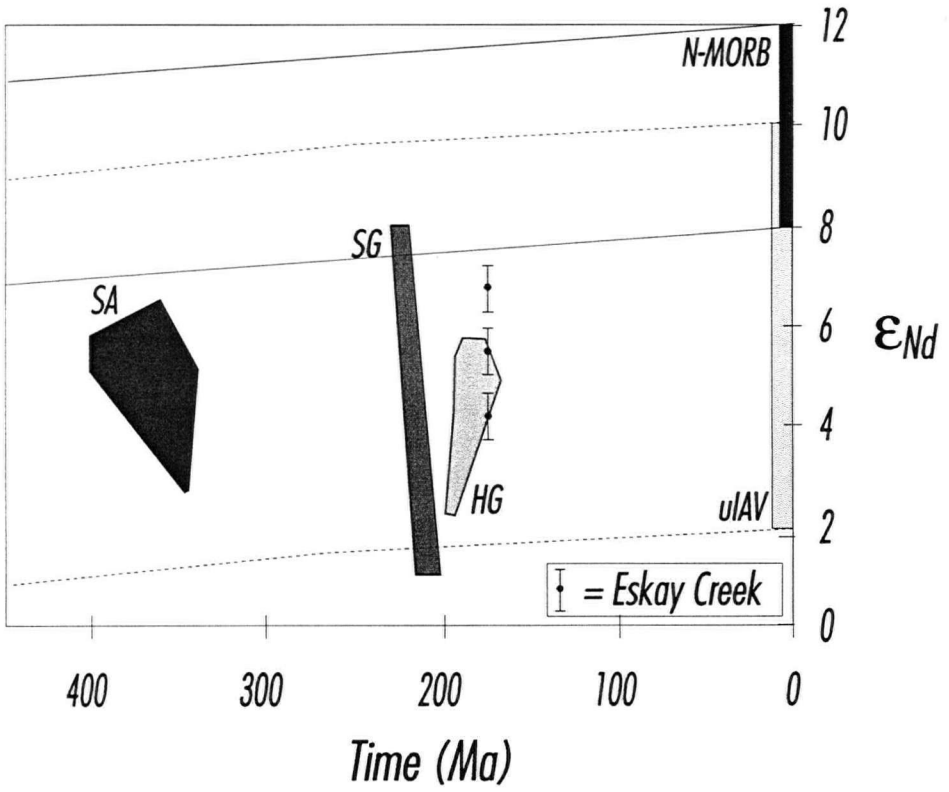

Figure 2. 8 Initial ε_{Nd} values and associated errors for volcanic rocks from the Eskay anticline. Shown for reference are fields for Paleozoic to Mesozoic arc assemblages of the Stikine terrane, uncontaminated island arc volcanic rocks (uIAV) [5,6,7], and mid-ocean ridge basalts (N-MORB) [8], evolution curves for uIAV and N-MORB are shown in dashed and solid lines, respectively. HG = felsic volcanic, and mafic to felsic intrusive rocks of the Hazelton Group [1,2,3], SG = mafic volcanic and intrusive rocks of the Stuhini Group [1,2,4], SA = mafic to felsic volcanic rocks of the Stikine Assemblage [1,4] ([1] Samson et al. (1989), [2] Jackson (1990), [3] Bevier and Anderson, (pers. comms., 1994), [4] Childe (*this volume*), [5] Nodah and Wasserburg (1981), [6] DePaolo and Wasserburg (1977), [7] Hawkesworth et al., (1993), [8] Jahn et al. (1980)).

In Figure 2.9 the lead isotopic signature of Eskay Creek mineralization is plotted relative to fields defined by Alldrick et al. (1987) for Lower Jurassic and Tertiary mineralization in the Stewart area. These fields represent data for sulfides (mainly galena) associated with a variety of

Table 2. 3 Common lead data for sulfides and sulfosalts from the Eskay anticline.

Sample[1] Number	Drill Hole Location	Zone	Mineral[2]	$^{206}Pb/^{204}Pb$ (error)[3,4]	$^{207}Pb/^{204}Pb$ (error)[3,4]	$^{208}Pb/^{204}Pb$ (error)[3,4]	$^{207}Pb/^{206}Pb$ (error)[3,4]	$^{208}Pb/^{206}Pb$ (error)[3,4]
E1a	surface	Emma Adit	gl	18.818 (0.003)	15.601 (0.003)	38.380 (0.008)	0.82905 (0.004)	2.0396 (0.009)
E2a	surface	Emma Adit	gl	18.824 (0.002)	15.611 (0.002)	38.396 (0.006)	0.82934 (0.004)	2.0398 (0.008)
E2b	surface	Emma Adit	py	18.834 (0.012)	15.618 (0.009)	38.409 (0.024)	0.82923 (0.009)	2.0394 (0.011)
E3a	surface	Mackay Adit	gl	18.840 (0.011)	15.629 (0.009)	38.436 (0.024)	0.82958 (0.012)	2.0402 (.0.019)
E4a	CA-215, 160.2m	Pathfinder	gl	18.876 (0.015)	15.651 (0.012)	38.495 (0.032)	0.82919 (0.010)	2.0394 (0.013)
E4b	CA-215, 160.2m	Pathfinder	cp	18.819 (0.003)	15.606 (0.003)	38.383 (0.008)	0.82927 (0.005)	2.0396 (0.008)
E5a	CA-215, 156.6m	Pathfinder	gl	18.823 (0.002)	15.606 (0.002)	38.366 (0.007)	0.82911 (0.004)	2.0383 (0.008)
E6a	U-04, 45.8m	109	gl	18.779 (0.009)	15.565 (0.008)	38.264 (0.020)	0.82884 (0.012)	2.0376 (0.014)
E6b	U-04, 45.8m	109	gl	18.799 (0.030)	15.588 (0.025)	38.319 (0.061)	0.82920 (0.008)	2.0383 (0.014)
E6c	U-04, 45.8m	109	sph	18.790 (0.009)	15.575 (0.008)	38.298 (0.020)	0.82891 (0.006)	2.0382 (0.011)
E7a	U-06, 7.5m	109	gl	18.811 (0.005)	15.596 (0.004)	38.354 (0.011)	0.82911 (0.005)	2.0390 (0.008)
E7b	U-06, 7.5m	109	gl	18.809 (0.041)	15.597 (0.034)	38.345 (0.084)	0.82923 (0.014)	2.0387 (0.018)
E8a	CA90-422, 52.1m	HW	gl	18.831 (0.012)	15.614 (0.010)	38.381 (0.024)	0.82919 (0.007)	2.0381 (0.011)
E8b	CA90-422, 52.1m	HW	py	18.821 (0.008)	15.602 (0.006)	38.346 (0.020)	0.82895 (0.022)	2.0374 (0.021)
E9b	U-56, 32.0m	21B	sph	18.816 (0.026)	15.601 (0.022)	38.356 (0.055)	0.82913 (0.017)	2.0385 (0.012)
E9c	U-56, 32.0m	21B	py	18.817 (0.005)	15.598 (0.004)	38.351 (0.013)	0.82895 (0.010)	2.0381 (0.014)
E9d	U-56, 32.0m	21B	boul	18.816 (0.003)	15.606 (0.002)	38.368 (0.008)	0.82939 (0.009)	2.0391 (0.012)
E11a	surface	FW Volcanic	gl	18.833 (0.004)	15.623 (0.003)	38.430 (0.009)	0.82952 (0.004)	2.0405 (0.009)
E11b	surface	FW Volcanic	gl	18.822 (0.004)	15.608 (0.003)	38.381 (0.010)	0.82922 (0.005)	2.0391 (0.009)
E12a	surface	Mackay Adit	gl	18.826 (0.003)	15.608 (0.003)	38.382 (0.009)	0.82908 (0.005)	2.0388 (0.009)
E13a	NEX 95-5, 71m	NEX	gl	18.833 (0.018)	15.621 (0.016)	38.424 (0.018)	0.82943 (0.009)	2.0402 (0.005)

[1] upper case letter and number refers to sample number, lower case letter refers to fraction number.
[2] mineral abreviations: gl=galena, py=pyrite, cp=chalcopyrite, sph=sphalerite, boul=boulangerite.
[3] errors are quoted at the 2ş (95% confidence) level.
[4] values are corrected for instrument fractionation by normalization based on replicate analyses of the NBS-981 standard.

styles of mineralization from more than 50 locations within the Iskut River and Stewart areas; also included within these fields are lead isotopic analyses of potassium feldspar from dated intrusive rocks (Alldrick et al., 1987; Godwin et al., 1988; J.K. Mortensen, unpublished data). These data show an evolution of lead to more radiogenic values from the Lower Jurassic to the Tertiary in this portion of the Stikine terrane. Eskay Creek lead analyzed in this study has a restricted range of values and partially overlaps the most radiogenic portion of the Lower Jurassic field. Sulfides and sulfosalts from the different zones and styles of mineralization in and along strike from the Eskay Creek deposit exhibit a remarkably homogeneous lead isotopic signature (Fig. 2.9, insert). This signature is found over a broad area extending from the Eskay Creek deposit, 4.5 km south to the Mackay adit.

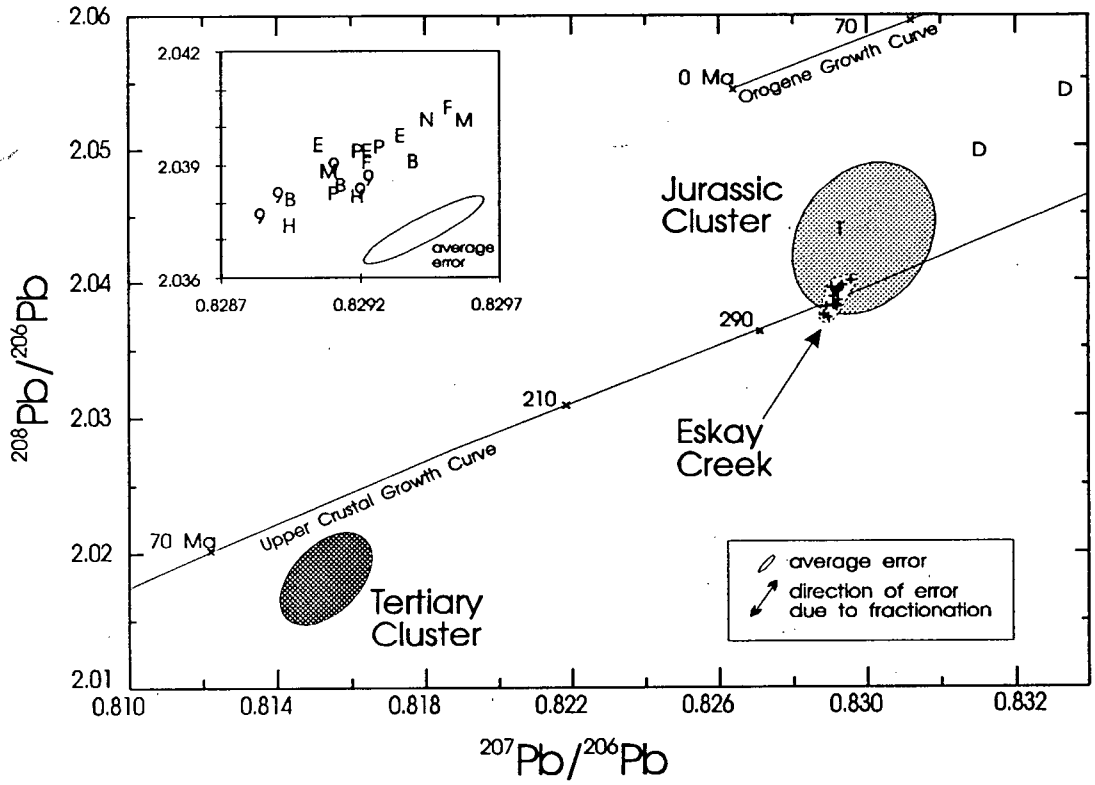

Figure 2. 9 $^{207}Pb/^{206}Pb$ vs. $^{208}Pb/^{206}Pb$ diagram for sulfide and sulfosalt samples from the Eskay anticline. Shown for reference are Lower Jurassic and Tertiary fields for the Iskut River and Stewart areas of the Stikine terrane (Alldrick et al., 1987; Godwin et al., 1988; J.K. Mortensen, unpublished data), Upper Crustal and Orogene Growth Curves (Zartman and Haines, 1988), and feldspar from Upper Triassic (T) and Devonian (D) intrusive rocks in the Stikine terrane, calculated to 175 Ma, assuming μ=9.74 and κ=3.78 (M.L. Bevier and R.G. Anderson, pers. comms., 1994; Childe, *this volume*). (B = 21 B zone, E = Emma Adit, F = footwall volcanic unit, H = hangingwall zone, M = Mackay Adit, N = northeast extension zone, P = pathfinder zone, 9 = 109 zone). Note that more radiogenic samples plot closer to the origin on this diagram.

Discussion

Regional Implications

The Stikine terrane is a complex volcanic arc characterized by a wide range of styles and ages of mineralization. Within the Iskut River area, mineralization related to the Hazelton Group consists primarily of Lower Jurassic epithermal and mesothermal gold±silver deposits and porphyry copper-gold deposits. The Middle Jurassic Eskay Creek deposit formed from a sea floor exhalative system which produced well-bedded clastic gold- and silver-rich sulfides and sulfosalts within argillite and in proximity to rhyolite-hosted stockwork zones. This degree of precious metal enrichment within a volcanogenic massive sulfide system is not only unique within the Stikine terrane, but also within the known ancient geologic record.

Prior to this study, the isotopic and biochronological age constraints on rocks within the Eskay anticline consisted of a U-Pb zircon age of 184 +5/-1 Ma for the Eskay porphyry (recalculated from Macdonald et al., 1992), Upper Pliensbachian ammonites, bivalves and corals from sedimentary rocks in the Betty Creek Formation, and Aalenian to possibly Early Bajocian radiolaria from the contact argillite in the immediate vicinity of the 21B zone (Nadaraju, 1993). The currently accepted lower stage boundary for the Aalenian (Harland et al., 1990) overlaps the isotopic age of the Eskay porphyry. Based on these data mineralization at Eskay Creek could be related to the Eskay porphyry, a felsic intrusive body coeval with the Texas Creek Plutonic and Premier Porphyry Suites, known mineralizing intrusive suites in the Iskut River and Stewart areas (Alldrick et al., 1986; Macdonald et al., 1996). However, the age of 175 +/-2 Ma determined for the Eskay rhyolite in this study demonstrates that mineralization at Eskay Creek formed in the Middle Jurassic, and is 7-16 Ma younger than the Eskay porphyry. Based on the ages of known mineral deposits in the Iskut River area, the period of time near the Lower Jurassic - Middle Jurassic boundary appears to mark a change in the metallogenic style of the Hazelton Group, from deeper, intrusion-related mineralization (approximately 197 to 184 Ma) to sea floor volcanogenic mineralization (approximately 177 to 173 Ma).

Chemical and isotopic characteristics of host rocks

On the basis of neodymium isotopic studies of intrusive and volcanic rocks, Samson et al. (1989) suggested that rocks of the Hazelton Group are the products of juvenile, mantle-derived material which formed in a volcanic arc setting, probably in an intra-oceanic environment. Recent studies of modern arc environments suggest that extension, rather than compression may be the dominant tectonic regime at consuming plate margins (Smellie, 1995). Within the immediate Eskay Creek area, the interpretation of rhyolitic magmas erupting along linear fissure vent zones, control on the facies distribution of volcanic and sedimentary rocks by regional and local fault blocks, and the transition to deep marine sedimentary sequences following the cessation of volcanism have been suggested to indicate formation in either a back arc or intra-arc basin environment (Bartsch, 1993). The trace and REE chemistry, and Nd signature of the Eskay rhyolite and hangingwall basalt are consistent with formation in an island arc environment.

The hangingwall basalt is characterized by a tholeiitic magmatic affinity. Both REE and Nd isotopic data indicate enrichment of the basalt relative to N-MORB, consistent with minor contamination from an E-MORB-type source. REE patterns and Zr/Y ratios indicate a tholeiitic magmatic affinity for the Eskay rhyolite, whereas coeval rhyolites on the east limb have transitional to calc-alkaline affinities. Regionally other rhyolites of the Salmon River Formation have more calc-alkaline affinities (A. Kaip, pers. comm., 1995). Rhyolites at Eskay Creek may be the products of fractional crystallization of mafic magma, partial melting of sialic crust, or some combination of these two sources. Barrett and Sherlock (1996) have noted that Nb/Zr ratios are inconsistent with derivation of the Eskay rhyolite entirely as a product of fractional crystallization of the hangingwall basalt, indicating that this unit may have some component of partial melt. Zircon inheritance in rhyolite from the east limb implies some component of crustal contamination within this unit. A more evolved magmatic affinity and Nd isotopic signature for the east limb rhyolite would suggest that this rhyolite either assimilated a greater component of partial melt, or slightly less juvenile sialic crust, than the Eskay rhyolite.

Metal source

Presently there is no clear consensus on the principal source of metals within ancient and modern submarine VMS deposits. The metals within these deposits may be leached from underlying volcanic and sedimentary strata, derived from magmatic sources, or some combination of these two processes (for example Doe and Zartman, 1979; Lydon, 1988; Stanton, 1990; Large, 1992, de Ronde, 1995; Huston et al., 1995). A review by Lydon (1988) concludes that a leaching model for the derivation of metals in VMS deposits is supported by experimental and computer-based studies, observation of sea floor basalts, and similarities of base metal ratios of mineralization with those of the dominant host lithologies. Stable and radiogenic isotopic studies have been cited as evidence for derivation of metals from both the leaching of strata below the ore deposit (for example Thorpe, et al., 1981; Fehn et al., 1983; Lydon, 1988) and , to a lesser extent, magmatic fluids (de Ronde, 1995 and references therein). Stanton (1990) argued for significant magmatic input for metals and fluids to VMS deposits, citing as evidence: (1) the concentration of mineralized zones at specific horizons, as opposed to throughout a volcanic cycle; (2) the apparent discrepancy between the generally smaller size of basalt-hosted VMS deposits relative to larger andesite- to rhyolite-hosted VMS deposits (given the abundance of sea floor basalts); and (3) variations in metal ratios in VMS orebodies relative to potential source rocks. Differences in the Se/S ratios of pyrite in Cu-rich and Cu-poor mineralization are consistent with a component of the sulfur in VMS deposits being derived from a magmatic hydrothermal sources (Huston et al., 1995).

Lead isotopic data, in combination with other information, may be used to constrain the source of lead, and by analogy other metals in VMS deposits (Gulson, 1986). In describing a model for the generation of ore fluids by leaching of metals from oceanic crust, Lydon (1988) suggested that the ore components to the fluids are not derived from the immediate footwall to mineralization, but rather from depths of 0.5 to 3 km below the paleo-sea floor, well below the present level of exposure in the Eskay anticline. Based on known stratigraphy in the Iskut River area, the basement to the Eskay Creek deposit at these depths may be composed of volcanic and sedimentary rocks of the Upper Triassic Stuhini Group and Paleozoic Stikine Assemblage, and their intrusive equivalents. Lead isotopic analysis of potassium feldspar from Devono-Mississippian and Upper Triassic intrusive rocks from the Iskut River area, when calculated

forward to the Middle Jurassic, show systematically less radiogenic lead isotopic compositions than Eskay Creek sulfides (M. L. Bevier and R. G. Anderson, pers. comms., 1994; Childe, *this volume*) (Fig. 2.9). These data indicate that leaching of lead from such sources would not result in the isotopic signature documented for Eskay Creek sulfides. Eskay Creek sulfides partially overlap the cluster for Lower Jurassic intrusions and mineralization in the Iskut River area and partially lie in a region that is more primitive, indicating derivation from either a Lower or Middle Jurassic source. Lead leached from Lower Jurassic intrusions of the Texas Creek Plutonic and Premier Porphyry Suites, such as the Eskay porphyry could contribute lead consistent with the observed isotopic signature of Eskay Creek sulfides. However, for intrusions of this age to be a principal source of metals within the deposit they would need to have been significantly more extensive at depth than their exposure in the Eskay anticline may suggest. Alternatively, lead derived from a Middle Jurassic magmatic source could also produce the lead isotopic signature of Eskay Creek sulfides. A potential source of Middle Jurassic magmatic fluids is the Eskay rhyolite. Without a better knowledge of the basement to the Eskay Creek deposit at the depths at which leaching is believed to take place, and a clearer understanding of the sources of metals to VMS deposits, it is not possible to determine which of these latter two potential reservoirs is the principal source of lead and other metals in the Eskay Creek deposit.

Modern Analogues

Studies of modern sea floor hydrothermal vent fields document the development of sulfide mounds and chimneys overlying stockwork zones hosted within altered volcanic rocks (for example Hannington et al., 1986; Herzig et al., 1993; and Gemmell, 1995). Mineralization at Eskay Creek may have formed in a similar manner, with degradation of accumulations of seafloor sulfides producing the graded sulfide and sulfosalt beds preserved within the deposit. Recently discovered exhalative, gold-rich polymetallic sulfide mineralization within back-arc basins of the western Pacific, such as the Okinawa and Mariana Troughs, and the Lau, Manus, and North Fiji Basins, may be representative of the tectonic settings in which some ancient VMS deposits formed (Herzig et al., 1993; Gemmell, 1995).

Herzig et al. (1993) have documented the presence of gold-rich (up to 29 ppm) sulfide chimneys, at water depths of 1600 to 2000 meters, hosted within a sequence of basalt to

rhyodacite on the Valu Fa Ridge in the southern Lau Basin. This region represents an active back arc spreading center built on remnant arc crust behind the Tonga-Kermadec subduction zone. The gross sulfide mineralogy, presence of iron-poor sphalerite and native gold in chimney samples, and a tholeiitic magmatic affinity of basalt and dacite from the Valu Fa Ridge have striking similarities to the Eskay Creek deposit (Sunkel, 1990; Herzig et al., 1993). Basalt and basaltic andesite from the Lau Basin show a wide range of ε_{Nd} values (+2.6 to +9.2), which have been interpreted to reflect multiple subduction components within a complex tectonic setting; ε_{Nd} values for basalts from the Valu Fa Ridge (+7.7 to +8.1) are some of the most primitive within the basin and are comparable to the hangingwall basalt at Eskay Creek (Volpe et al., 1988; Looke et al., 1990).

The PACMANUS deposit, located in the eastern Manus Basin, lies within a back arc basin built on remnant arc crust behind the New Britain arc (Gemmell, 1995). Within this deposit sulfides rich in gold and silver (averaging 15 and 230 ppm, respectively) are hosted by a volcanic sequence composed of andesite, dacite and rhyodacite between 1650 and 1680 meters water depth on the flanks of a dacite dome (Binns and Scott, 1993; Binns et al., 1995). Two samples of dacite (fresh and altered) dredged from the dacite dome exhibit a tholeiitic to transitional magmatic affinity based on Zr/Y ratios, and tholeiitic REE patterns intermediate in slope between those of the Eskay rhyolite and hangingwall basalt (Binns and Scott, 1993).

The mineralogy, gold concentrations, and spatial association with primitive felsic volcanic rocks of the PACMANUS and Valu Fa Ridge deposits, which are floored by older back-arc crust with no component of continental basement, have similarities to the Eskay Creek deposit and may represent modern equivalents.

Conclusions

Rhyolite which hosts stockwork mineralization and underlies clastic sulfide-sulfosalt mineralization at the Eskay Creek Au-Ag-rich VMS deposit erupted at 175 +/-2 Ma. This age is 7-16 Ma younger than mineralization associated with the Lower Jurassic Texas Creek Plutonic and Premier Porphyry Suites. A tholeiitic magmatic affinity and relatively primitive Nd signature for volcanic rocks within the footwall and hangingwall to mineralization at Eskay Creek suggest

that the deposit formed in an island-arc setting. The Eskay rhyolite, which hosts stockwork mineralization and underlies stratiform mineralization, is characterized by a more primitive magmatic affinity than contemporaneous rhyolites within the Iskut River area. Sulfides and sulfosalts from argillite-hosted stratiform mineralization and rhyolite-hosted discordant mineralization in and along strike from the Eskay Creek deposit are characterized by a homogeneous lead isotopic signature. This signature is consistent with derivation of lead, and presumably other metals, from either a Lower or Middle Jurassic source.

Plate 2. 2 Black matrix breccia, showing a brecciated, flow-banded rhyolite fragment in a black silicified matrix.

Plate 2. 3 Pillow basalts in the hangingwall to mineralization at Eskay Creek (hammer for scale).

Plate 2. 4 Flow-banded east limb rhyolite with aphanitic matrix and quartz and feldspar phenocrysts.

Plate 2. 5 21B zone argillite-hosted clastic sulfide and sulfosalt mineralization (hammer for scale).

Plate 2. 6 SEM backscatter image of feldspar inclusions in zircon, Eskay rhyolite (EC-GC-11) (scale bar 10 microns).

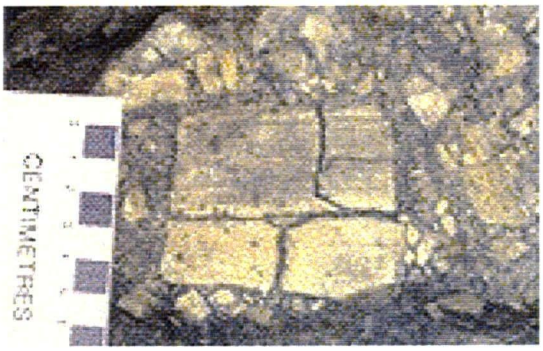

Plate 2.2

Plate 2.3

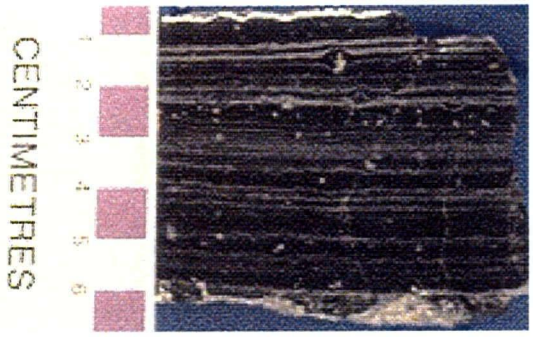

Plate 2.4

Plate 2.5

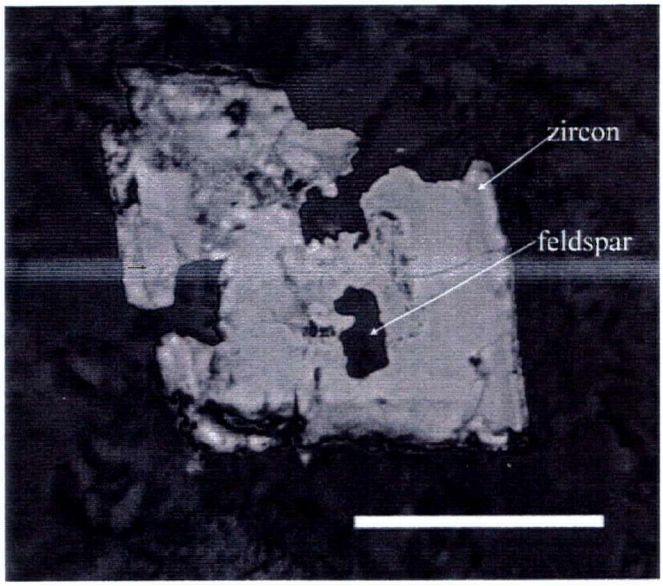

Plate 2.6

References

Alldrick, D.J., 1991, Geology and ore deposits of the Stewart Mining Camp, British Columbia: Unpublished Ph.D. thesis, Vancouver, Canada, The University of British Columbia, 347 p.

Alldrick, D.J., Mortensen, J.K., and Armstrong, R.L., 1986, Uranium-Lead age determinations in the Stewart area (104B/1), *in* Grant, B., and Newell, J.M., eds., Geological Fieldwork 1985, British Columbia Ministry of Energy, Mines and Petroleum Resources Paper 1986-1, p. 217-218.

Alldrick, D.J., Gabites, J.E., and Godwin, C.I., 1987 , Lead isotope data from the Stewart mining camp (104B/1), *in* Grant, B., and Newell, J.M., ed., Geological Fieldwork 1986, British Columbia Ministry of Energy, Mines and Petroleum Resources Paper 1987-1, p. 93-102.

Anderson, R.G., 1989, A Stratigraphic, Plutonic and Structural Framework for the Iskut River Map Area (NTS 104B), Northwestern British Columbia; Current Research, Part E, Geological Survey of Canada, Paper 89-1E, p. 145-154.

Anderson, R.G., and Thorkelson, D.J., 1990, Mesozoic stratigraphy and setting for some mineral deposits in Iskut River map area, northwestern British Columbia; Current Research, Part F, Geological Survey of Canada, Paper 90-1F, p. 131-139.

Barrett, T. J, and MacLean, W., 1994, Chemostratigraphy and hydrothermal alteration in exploration for VHMS deposits in greenstones and younger volcanic rocks: *in* Lentz, D.R., ed., Alteration and Alteration Processes Associated with Ore-forming Systems, Geological Association of Canada Short Course Notes, v. 11, p. 433-467.

Barrett, T. J, and Sherlock, R.L., 1996, Geology and Geochemistry of the Eskay Creek Deposit, Northwestern British Columbia, (submitted to Exploration and Mining Geology).

Bartsch, R.D., 1993, Volcanic stratigraphy and lithogeochemistry of the Lower Jurassic Hazelton Group, host to the Eskay Creek precious and base metal volcanogenic deposit: Unpublished M.Sc. thesis, Vancouver, Canada, The University of British Columbia, 178 p.

Binns, R.A., and Scott, S.D., 1993, Actively forming polymetallic sulfide deposits associated with felsic volcanic rocks in the eastern Manus back-arc Basin, Papua New Guinea: ECON. GEOL., v. 88, p. 2226-2236.

Binns, R.A., Parr, J.M., Scott, S.D., Gemmell, J.B., and Herzig, P.M, 1995, PACMANUS: an active, siliceous volcanic-hosted hydrothermal field in the eastern Manus Basin, Papua New Guinea: *in* Mauk, J.L., and St. George, J.D., eds., Proceedings of the 1995 PACRIM Congress, p. 49-54.

Blackwell, J.D., 1989, Eskay Creek Project: Exploration Review, 1932 to 1989, Report to Calpine Resources and Consolidated Stikine Silver Ltd. by Blackwell Mineral Exploration Consultants Ltd., 5 p.

Britton, J.M., Blackwell, J.D., and Schroter, T.G., 1989, #21 Zone Deposits, Eskay Creek, Northwestern British Columbia: Exploration in British Columbia, 1989, B.C. Ministry of Energy, Mines and Petroleum Resources, p. 197-223.

Childe, F., Barrett, T.J., and McGuigan, P.J., 1994, The Granduc VMS deposit, northwestern British Columbia: U-Pb ages and Pb isotope relations [abs.]: The Geological Society of America Program with Abstracts, p. A-381.

Davies. A.G.S., Lewis, P.D., and Macdonald, A.J., 1994, Stratigraphic and structural setting of mineral deposits in the Brucejack Lake area, northwestern British Columbia, Current Research, Part A, Geological Survey of Canada, Paper 94-A, p. 37-43.

DePaolo, D. J., 1988, Neodymium Isotope Geochemistry, An Introduction: Berlin, Springer-Verlag, 187 p.

DePaolo, D. J., and Wasserburg, G. J., 1977, The sources of island arcs as indicated by Nd and Sr studies: Geophysical Research Letters, v. 4, p. 465-468.

de Ronde, C.E.J., 1995, Fluid chemistry and isotopic characteristics of sea floor hydrothermal systems and associated VMS deposits: potential for magmatic contributions: *in* Thompson, J.F.H., ed., Magmas, Fluids and Ore Deposits, Mineralogical Association of Canada Short Course Notes, v. 23, p. 479-509.

Doe, B.R., and Zartman, R.E., 1979, Plumbotectonics: the Phanerozoic, *in* Barnes, H.L., ed., Geochemistry of hydrothermal ore deposits, Second Edition, Wiley, New York, p. 22-70.

Edmunds, F.C., and Kuran, D.L., 1991, TOK-KAY and GNC 1991 exploration program, geological and diamond drilling program, Prime Resources Group internal report.

Edmunds, F.C., Kuran, D.L., and Rye, K.A., 1994, The geology of the 21 Zone deposits at Eskay Creek northwestern British Columbia, Canada: Black Hills Fifth Western Regional Conference on Precious Metals, Coal and the Environment, p.154-175.

Faure, G., 1986, Principles of isotope geology: New York, John Wiley and Sons, Inc., 589p.

Fehn, U., Doe, B.R., and Delevaux, M.H., 1983, The Distribution of lead isotopes and the origin of Kuroko ore deposits in the Hokuroko District, Japan: ECON. GEOL. Monograph 5, p. 488-506.

Gemmell, J.B., 1995, Comparison of volcanic-hosted massive sulfide deposits in modern and ancient back-arc basins: examples from southwest Pacific and Australia: *in* Mauk, J.L., and St. George, J.D., eds., Proceedings of the 1995 PACRIM Congress, p. 227-232.

Godwin, C.I., Gabites, J.E., and Andrews, A., 1988, Leadtable: A galena lead isotope data base for the Canadian Cordillera, with a guide to its use by explorationists: British Columbia Ministry of Energy, Mines and Petroleum Resources Paper 1988-4, 188 p.

Grove, E.W., 1986, Geology and mineral deposits of the Unuk River-Salmon River-Anyox area: British Columbia Ministry of Energy, Mines and Petroleum Resources, Bulletin 63, 434 p.

Gulson, B. L., 1986, Lead isotopes in mineral exploration: Amsterdam, Elsevier, 244p.

Hannington, M.D., Peter, J.M., and Scott, S.D., 1986, Gold in sea-floor polymetallic sulfide deposits: ECON. GEOL., v. 81, p.1867-1883.

Harland, W.B., Armstrong, R.L., Cox, A.V., Craig, L.E., Smith, A., G., 1990, A Geologic Time Scale, 1989: Great Britain, Cambridge University Press, 263 p.

Hawkesworth, C.J., Gallagher, K., Hergi, J.M., and McDermott, F., 1993, Mantle and slab contributions in arc magmas: Annual Review of Earth and Planetary Science Letters, v. 21, p. 115-120.

Henderson, J.R., Kirkham, R.V., Henderson, M.N., Payne, J.G., Wright, T.O., and Wright, R.L., 1992, Stratigraphy and structure of the Sulphurets area, British Columbia: Current Research, Part A, Geological Survey of Canada, Paper 92-1A, p. 323-332.

Herzig, P.M., Hannington, M.D., Fouquet, Y., von Stackelberg, U., and Petersen, S., 1993, Gold-rich polymetallic sulfides from the Lau back arc and implications for the geochemistry of gold in sea-floor hydrothermal systems of the southwest Pacific: ECON. GEOL., v. 88, p. 2182-2209.

Huston, D.L., Sie, S.H., Suter, G.F., Cooke, D.R., and Both, R.A., 1995, Trace elements in sulfide minerals from eastern Australian volcanic-hosted massive sulfide deposits: Part I. Proton microprobe analyses of pyrite, chalcopyrite, and sphalerite, and Part II. Selenium levels

in pyrite: Comparison with $\delta^{34}S$ values and implications for the source of sulfur in volcanogenic hydrothermal systems: ECON. GEOL., v. 90, p.1167-1196.

Hutchison, C. S., 1974, Laboratory Handbook of Petrographic Techniques: New York, John Wiley and Sons, Inc., 527 p.

Jackson, J.L., 1990, Tectonic analysis of the Nisling, Northern Stikine and Northern Cache Creek terranes, Yukon and British Columbia: Unpublished Ph.D. thesis, Phoenix, United States of America, The University of Arizona, 200 p.

Jahn, B.-M., Griffiths, B., Charlot, R., Cornichet, J., and Vidal, F., 1980, Nd and Sr isotopic compositions and REE abundances of Cretaceous MORB (Holes 417D and 418A, Legs 51, 52 and 53): Earth and Planetary Science Letters, v. 48, p. 171-184.

Kirkham, R.V., and Margolis, J., 1995, Overview of the Sulphurets area, northwestern British Columbia, *in* Porphyry Deposits of the northwestern Cordillera of North America, T.G. Schroeter, ed., The Geological Society of the CIM, Special Volume 46, p. 473-498.

Large, R.R., 1992, Australian volcanic-hosted massive sulfide deposits: features, styles and genetic models, v. 87, p. 471-510.

Looke, G., McDonough, W.F., Goldstein, S.L., and Hoffman, A.W., 1990, Isotopic compositions of volcanic glasses from the Lau Basin: Marine Mining, v.9, p.235-245.

Lydon, J.W., 1988, Volcanogenic massive sulfide deposits Part 2: Genetic Models: *in* Roberts, R.G., and Sheahan, P.A., ed., Ore Deposit Models, Geoscience Canada Reprint Series 3, p. 155-181.

Macdonald, A.J., Lewis, P.D., Thompson, J.F.H., Nadaraju, G., Bartsch, R.D., Bridge, D.J., Rhys, D.A., Roth, T., Kaip, A., Godwin, C.I., and Sinclair, A.J., 1996, Metallogeny of an

Early to Middle Jurassic arc, Iskut River area, northwestern British Columbia: ECON. GEOL..

Macdonald, A.J., van der Heyden, P., Lefebure, D.V., and Alldrick, D.J., 1992, Geochronometry of the Iskut River Area - An update: *in* Grant, B., and Newell, J.M., eds., Geological Fieldwork 1991, British Columbia Ministry of Energy, Mines and Petroleum Resources Paper 1992-1, pp. 495-501.

MacLean, W.H., and Kranidiotis, P., 1987, Immobile element as monitors of mass transfer in hydrothermal alteration: Phelps Dodge massive sulfide deposits, Matagami, Quebec: ECON. GEOL., v. 82, p. 951-962.

Mortensen, J.K., Ghosh, D.K., and Ferri, F., 1995, U-Pb geochronology of intrusive rocks associated with copper-gold porphyry deposits in the Canadian Cordillera, *in* Porphyry Deposits of the northwestern Cordillera of North America, T.G. Schroeter, ed., The Geological Society of the CIM, Special Volume 46, p. 142-158.

Nadaraju, G.T., 1993, Triassic-Jurassic Biochronology of the Eastern Iskut River Map Area, Northwestern British Columbia: Unpublished M.Sc. thesis, Vancouver, Canada, The University of British Columbia, , 223 p.

Nodah, S. and Wasserburg, G. J., 1981, Nd and Sr isotopic study of volcanic rocks from Japan: Earth and Planetary Science Letters, v. 52, p. 264-276.

Roth, T., 1993, Geology, Alteration and Mineralization in the 21A Zone, Eskay Creek, northwestern British Columbia: Unpublished M.Sc. thesis, Vancouver, Canada, The University of British Columbia, 229 p.

Roth, T., 1995, Mineralization and facies variation in the Eskay Creek 21 Zone polymetallic sulfide-sulfosalt deposit, northwestern British Columbia [abs.]: Geological Association, Mineralogical Association of Canada Program with Abstracts, Victoria, p. A-91.

Rye, K., 1992, Geological and Geochemical Report on the 1991 Eskay Creek Diamond Drill Relog Program: Internal Report for International Corona Corporation.

Samson, S.D., McClelland, W.C., Patchett, P.J., Gehrels, G.E., and Anderson, R.G., 1989, Evidence from neodymium isotopes for mantle contributions to Phanerozoic crustal genesis in the Canadian Cordillera: Nature, v.337, p. 705-709.

Smellie, J.L., 1995, Volcanism associated with extension at consuming plate margins: Smellie, J.L, ed., London, The Geological Society, 293 p.

Stanton, R.L., 1990, Magmatic evolution and the ore type-lava type affiliations of volcanic exhalative ores: Geology of the mineral deposits of Australia and Papua New Guinea, Monograph Series of the Australasian Institute of Mining and Metallurgy, v.14, pp. 101-107.

Steiger, R.H., and Jäger, E., 1977, Subcommission on geochronology: Convention on the use of decay constants in geo- and cosmochronology: Earth and Planetary Science Letters, v. 14, p. 359-362.

Sun, S.S., and McDonough, W.F., 1989, Chemical and isotopic systematics of oceanic basalts: implications for mantle composition and process. , *in* Magmatism in the ocean basins, A.D. Saunders and M.J. Norry, ed., Geological Society Special Publication No. 42, p. 313-345.

Sunkel, G., 1990, Origin of petrological and geochemical variations of Lau Basin lavas (SW Pacific): Marine Mining, v.9, p. 205-234.

Thériault, R., J., 1990, Methods for Rb-Sr and Sm-Nd isotopic analyses at the geochronology laboratory, Geological Survey of Canada, *in* Radiogenic Age and Isotopic Studies: Report 2, Geological Survey of Canada, Paper 89-2, p. 3-6.

Thorpe, R. I., Franklin, J. M., and Sangster, D. F., 1981, Evolution of lead in massive sulfide ores of Bathurst District, New Brunswick, Canada: Institute of Mining and Metallurgy Transactions, Section B, p. B55-B56.

Volpe, A.M., Macdougall, J.D., and Hawkins, J.W., 1988, Lau Basin basalts (lbb): trace element and Sr-Nd isotopic evidence for heterogeneity in backarc basin mantle: Earth and Planetary Science Letters, v.90, p. 174-186.

York, D. 1969, Least-squares fit of a straight line with correlated errors: Earth and Planetary Science Letters, v. 5, p. 320-324.

Zartman, R.E., and Haines, S.M., 1988, The plumbotectonic model for Pb isotopic systematics among major terrestrial reservoirs - a case for bi-directional transport: Geochemica and Cosmochemica Acta, v.52, p. 1327-1339.

CHAPTER 3:

U-PB GEOCHRONOLOGY, ND AND PB ISOTOPIC SYSTEMATICS, AND GEOCHEMISTRY OF THE UPPER TRIASSIC GRANDUC VMS DEPOSIT, NORTHWESTERN BRITISH COLUMBIA

Plate 3.1. Granduc Mountain fly camp, looking north across North Leduc Glacier.

Introduction

The Granduc deposit is located 40 km northwest of Stewart, British Columbia, within the rugged Boundary Ranges of the Coast Mountains (Fig. 3.1 and Plate 3.2). Copper mineralization was first discovered and staked in the Granduc area in 1931. These claims lapsed and it was not until 1951, when the area was re-examined, that the level of the glaciers flanking Granduc Mountain had dropped sufficiently for the Granduc main ore zone to become exposed on surface (Dudas and Grove 1970). An underground mine was in production at Granduc from 1971 until 1978, and again from 1980 until 1984, when low metal prices forced final closure of the mine. Total production was 15.2 million tonnes grading 1.3% Cu, with a total of 124,000 kg Ag and 2,000 kg Au recovered (B.C. MINFILE 104B-021). Current published reserves indicate 9.9 million tonnes grading 1.79% copper, with minor gold and silver (Melville et al. 1992).

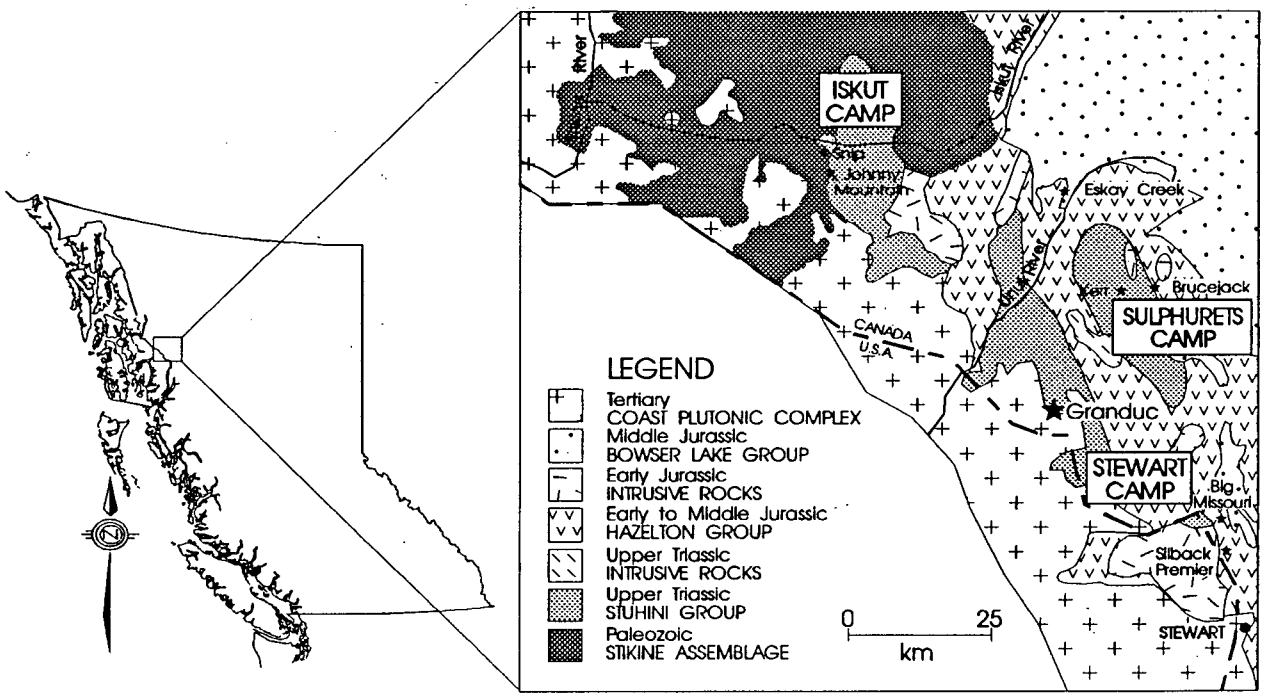

Figure 3. 1 Location map of the Granduc deposit, Stewart Mining Camp, northwestern British Columbia.

The Granduc deposit was initially classified as a mesothermal replacement type deposit (Davidson 1960). However, more recently Granduc has been interpreted to have a syngenetic,

volcanic-associated origin. The deposit has been classified as a cupriferous iron formation (Kirkham 1979), a concordant massive sulphide deposit (Grove 1986) and most recently a Besshi-type volcanogenic massive sulphide (VMS) deposit (Höy 1991). Re-classification was based on the recognition that copper-rich massive sulphide-oxide mineralization occurred within a deformed, but broadly conformable zone of sedimentary and volcanic rocks structurally overlying a thick sequence of mafic volcanic flow rocks and associated pyroclastic rocks (Grove 1986).

Prior to this study, the age of mineralization at Granduc was poorly constrained. It was not possible to correlate rocks which host the deposit with rocks off of Granduc Mountain, and sedimentary rocks in the area of mineralization lack preserved fossils. Previously the deposit has been assigned alternatively to the Upper Triassic Stuhini Group (Norman and McCue 1966; Höy 1991), and to the Lower to Middle Jurassic Hazelton Group (Dudas 1973; Grove 1986; Anderson and Thorkelson 1990; Lewis 1992) on the basis of regional correlations and lithological similarities. Grove (1986) assigned a Lower Jurassic age to the Granduc stratigraphy based in part on the presence of Pliensbachian fossils contained within a volcanic-sedimentary sequence from an unspecified locality near Granduc Mountain.

In this study, volcanic and intrusive rocks from Granduc Mountain were dated by U-Pb methods, and analyzed for their Nd isotopic signatures and major, trace and rare earth element compositions. The Pb isotopic compositions of mineralization from the Granduc deposit were also determined. New U-Pb age determinations on volcanic and intrusive rocks in the ore zone and footwall of the deposit, and the Pb isotopic composition of stratabound mineralization provide constraints on the age of VMS mineralization at the Granduc deposit, whereas the Nd isotopic signatures and lithogeochemical analyses constrain the tectonic environment in which the deposit formed.

Regional Geology

The Granduc Deposit occurs within the Stikine island arc terrane (hereafter referred to as Stikinia) along the western margin of the Intermontane Belt and is included within the Stewart Mining Camp in the southeast corner of the Iskut River map area (NTS 104 B) (Fig. 3.1). Regional mapping within the Iskut River map area has identified three Paleozoic to Mesozoic

volcanic-plutonic-sedimentary island arc assemblages. From oldest to youngest these are the Paleozoic Stikine Assemblage (Monger 1977), the Upper Triassic Stuhini Group (Souther 1971; Monger 1980) and the Lower to Middle Jurassic Hazelton Group (Leach 1909; Marsden and Thorkelson 1992). The Stikine Terrane is unconformably overlain by the Middle to Upper Jurassic Bowser Lake Group, an assemblage which overlaps the adjacent Cache Creek terrane (Monger and Berg 1984), and is intruded along its western margin by rocks of the Cretaceous to Tertiary Coast Plutonic Complex. The distribution of these units within the Iskut River map area is outlined by Anderson (1989).

The Paleozoic Stikine Assemblage is the oldest succession of rocks exposed within Stikinia, and consists of Devonian to Permian volcanic and sedimentary island arc successions (Monger 1977). Stikine Assemblage rocks have not been identified as far south as Granduc Mountain in the Iskut River map area.

Rocks of the Stikine Assemblage are unconformably overlain by the Upper Triassic Stuhini Group (Kerr 1948). The Stuhini Group is characterized by thick sequences of Carnian to Norian augite-phyric mafic volcanic pillow lavas, flows and volcaniclastic rocks intercalated with sedimentary sequences that include limestone reef sequences, greywacke, shale, chert and volcanic-derived sedimentary rocks. Local occurrences of bimodal volcanic rocks correlated with the Stuhini Group have been mapped in the northwest portion of the Iskut River map area (Anderson, 1989). Stuhini Group volcanism is contemporaneous with emplacement of the Stikine Plutonic Suite which has a compositional range of gabbro to diorite to monzonite (Woodsworth et al. 1992) . The volumetrically most significant member of the Stikine Plutonic Suite is the Hotailuh Batholith, a 1100 km^2 composite intrusion located on the eastern margin of the Stikine Terrane, 200 km northeast of the Granduc deposit (Anderson and Bevier 1992).

Mafic volcanic and sedimentary sequences of the Stuhini Group are unconformably overlain by mafic to felsic volcanic and related sedimentary rocks of the Lower to Middle Jurassic Hazelton Group, and cotemporal granodioritic to monzodioritic composition intrusions (Marsden and Thorkelson 1992; Macdonald et al 1996). The Hazelton Group is overlain by marine sedimentary rocks of the Bowser Lake Group. The onset of Bowser sedimentation marks a

change in the tectonic regime from an island arc setting producing rhyolitic to basaltic composition volcanic rocks, to the development of a passive basinal sequence characterized by deposition of shale, siltstone and conglomerate.

Prospecting in the Stewart Mining Camp has been active since the early 1900s and has led to the discovery of a large number of mineral deposits, including gold-silver-copper-zinc-lead Lower Jurassic mineralization at the Scottie Gold, Big Missouri and Premier-Silbak deposits (Alldrick 1991; Brown 1987); as well as Eocene silver-zinc-lead±molybdenum mineralization in the Prosperity/Porter Idaho camp (Alldrick 1991). Directly to the north of the Stewart Mining Camp is the Iskut River area, which contains a mesothermal gold deposit at Snip (Rhys 1993), complex intrusion-related epithermal gold-silver±base mineralization at Sulphurets (Margolis 1993), and a Au-Ag-rich VMS deposit at Eskay Creek, all of which formed in the Early to Middle Jurassic (Margolis 1993; Macdonald et al. 1996; Childe *this volume*) (Fig. 3.1). The presence of numerous deposits of widely varying genesis related to Jurassic magmatism has made Hazelton Group stratigraphy and cotemporal plutons a prime focus for mineral exploration. The present study investigates the possibility that economic mineral occurrences also formed in this region in Late Triassic time.

Geology of Granduc Mountain

Rocks on Granduc Mountain have been mapped by Davidson (1960), Klepacki and Read (1981), and McGuigan et al. (1992). These rocks can be divided into four main units; from east to west these are the Footwall, Mine, Lower Hangingwall and Upper Hangingwall Series (Fig. 3.2). The Mine Series and Lower Hangingwall Series are separated by the Granduc Fault; the Lower and Upper Hangingwall Series are separated by the Western Fault (Fig. 3.2 and Plate 3.3). The majority of the mined ore at Granduc came from the Main Zone of the deposit, with minor amounts from the North Zone (Grove 1986) (Fig. 3.2). Mineralization within the Main Zone of the Mine Series occurred within six zones, termed the A to F orebodies (Grove 1986) (Fig. 3.3).

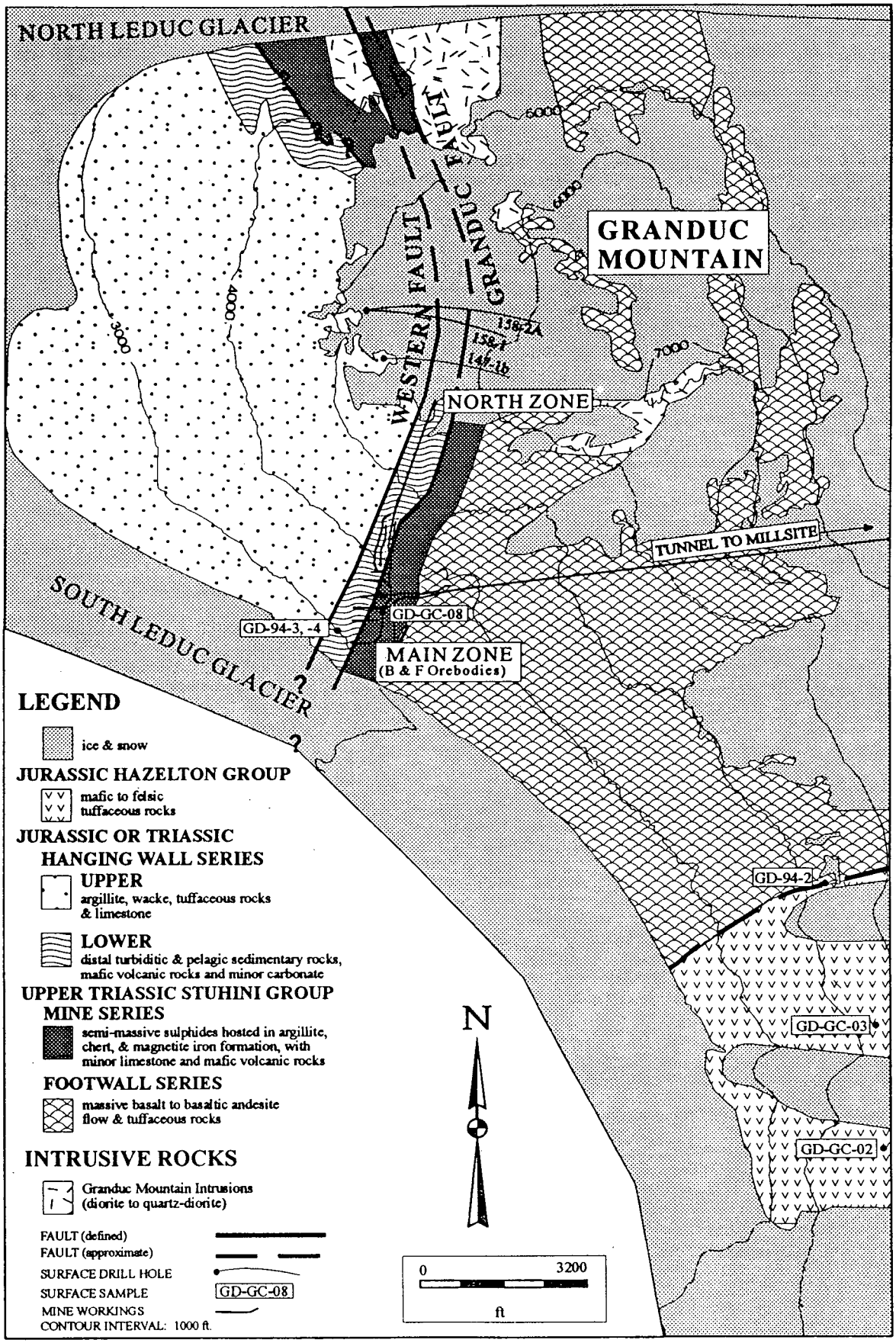

Figure 3. 2 Generalized geology of Granduc Mountain (after Davidson 1960; Klepacki and Read 1981; McGuigan et al. 1992).

Footwall Series

The Footwall Series consists of mafic volcanic flow rocks of basaltic to andesitic composition with sparse quartz + epidote amygdules and associated pyroclastic deposits. These rocks are intruded by coarse-grained, variably deformed sills of dioritic to quartz dioritic composition. Regional metamorphism reaches greenschist facies, with the development of metamorphic biotite and hornblende (Grove 1986). The Footwall Series are well exposed on the steep northern face of Granduc Mountain where they have been mapped by Davidson (1960); exposure across the top and the more gently sloping south face of the mountain is poor. However, a number of stratigraphic drill holes collared in the Hangingwall Series and drilled through the North Zone into the Footwall Series were archived and available for examination as part of this study. Rocks from the Footwall Series examined in this study do not show evidence of strong hydrothermal alteration and contain only minor pyrite+/-pyrrhotite+/-chalcopyrite veinlets, which are interpreted here to represent stockwork mineralization (Plate 3.4). Deformation through the Footwall Series varies from strong to weak. Localized zones of brecciation within thick sequences of massive fine-grained basaltic composition rock are interpreted to represent primary flow-tops. The variability of strain is particularly evident within thick intersections (up to 110 m apparent thickness) of the diorite sill, which shows textural variations ranging from undeformed equigranular zones to moderately sheared fabrics to sharply defined 0.5 to 2 cm thick mylonitic zones (Plate 3.5). In general, the degree of deformation increases uphole, towards the Mine Series and the Granduc and Western Faults. Intrusive contacts between the sills and volcanic rocks are typically sheared, diffuse, and chloritic over several 10s of centimeters. These contact zones also contain minor magnetite and up to a few percent disseminated sulphide, primarily pyrite. Mafic volcanic rocks of the Footwall Series are faulted along their southeastern margin against mafic to felsic tuffaceous and fragmental rocks (Fig. 3.2).

Mine Series

The Granduc Mine Series consists of semi-massive cupriferous iron sulphide lenses interbedded with argillite, chert, magnetite iron formation, limestone, tuffaceous rocks, and mafic

flows or sills within a cataclasite zone (Plate 3.6). The orebodies, with a maximum width of 60 m, strike approximately north-south and dip 60° to the west (Figs. 3.2 and 3.3) (Norman and McCue 1966). Sulphide mineralization consists of pyrite, pyrrhotite, chalcopyrite, sphalerite and galena, in order of decreasing abundance. Trace arsenopyrite, bornite and cobalite have also been reported from within the ore zones (Dudas and Grove 1970; Grove 1986). Primary sulphide-argillite bedding, indicative of subaqueous deposition, has been locally preserved despite large-scale folding and attenuation of the ore lenses (Kirkham 1979). However, the majority of the massive sulphide within the Granduc deposit has been remobilized and recrystallized (Kirkham 1979; Grove 1986). The presence of mafic rocks within the Mine Series suggests that mafic magmatism was occurring during sulphide accumulation.

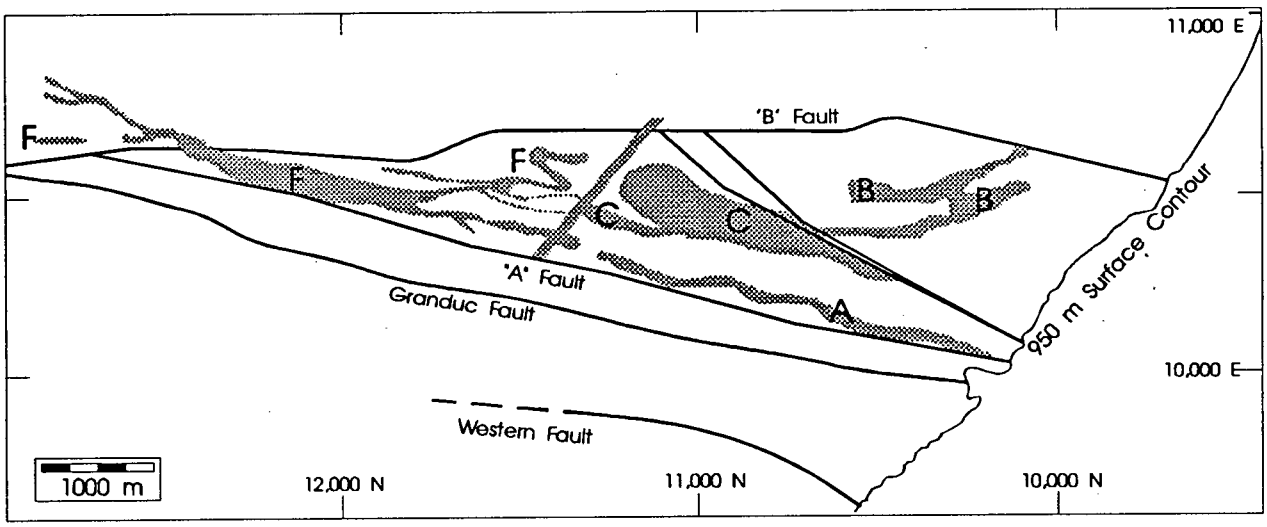

Figure 3. 3 Plan view of the 3100 (950 m) level of the Main Zone of the Granduc mine, showing relative positions of the A, B, C, and F orebodies (after Grove, 1986).

Hangingwall Series

The Lower Hangingwall Series, separated from the Mine Series by the Granduc Fault, has been coined the 'gash-banded tuff' sequence (McGuigan et al. 1992). It is composed primarily of distal turbiditic rocks, pelagic sedimentary rocks and possible fine-grained tuffaceous rocks, together with minor carbonate which often infills brittle fractures in these rocks. Fieldwork conducted as part of this study revealed the presence of local augite-phyric and plagioclase-

augite-phyric mafic volcanic flows or sills within this package (Fig. 3.2; samples GD-94-03, -04). The Upper Hangingwall Series, to the west of the Western Fault, is composed of thinly bedded brown to green siltstone and argillite, tuffaceous rocks of andesite composition and minor chert and limestone. The Hangingwall Series does not appear to be related to the Mine and Footwall Series.

Deformation

Two phases of regional deformation have been recorded in the Stewart area, the first occurring in the mid-Cretaceous (thermal peak = 110 +/-5 Ma) and the second in the Eocene (thermal peak = 54.8-44.8 Ma) (Alldrick 1991). Complex multi-stage deformation within the Iskut River map area has tectonically juxtaposed lithologically similar volcano-sedimentary sequences of the Triassic Stuhini Group and the Jurassic Hazelton Group, making the stratigraphic relations difficult to determine through field relationships alone.

Deformation on Granduc Mountain has been interpreted by Klepacki and Read (1981) to be the result of up to four phases of folding. However, a more recent interpretation by Lewis (1994) attributes deformation to a single event which is correlated with deformation along the Unuk River/Harrymel fault zone (South Unuk cataclasite zone in the terminology of Grove 1986). This fault zone is a north-south trending subvertical shear zone with sinistral displacement, characterized by variable strain gradients over a 60 km mappable extent, from the Iskut River in the north to the Granduc and Western Faults on Granduc Mountain in the south (Lewis 1994). South of Granduc Mountain the fault zone is abruptly truncated by intrusion of granodioritic composition rocks of the Coast Plutonic Complex.

U-Pb Geochronology

The U-Pb results reported in this paper are based on analysis of zircons recovered from 20-30 kilogram samples collected from drill core or outcrop; sample descriptions are given below. Heavy mineral extraction procedures and U-Pb analytical procedures follow those of Mortensen et al. (1995). All zircon fractions were abraded prior to analysis (Krogh 1982). Isotopic ratios were measured using a modified single collector VG-54R thermal ionization mass spectrometer

equipped with a Daly photomultiplier. Procedural blanks were 9-20 picograms for Pb and 1-2 picograms for U. Concordia intercept ages and associated errors were calculated using a modified York-II regression model (York 1969), and the algorithm of Ludwig (1980); ages were calculated using the decay constants recommended by Steiger and Jäger (1977). Age assignments follow the time scale of Harland et al. (1990). Analytical results are given in Table 3.1 and shown graphically in Figure 3.4.

Footwall Series quartz diorite sill

Sample GD-GC-01 was collected near the base of a 110 meter (drilling thickness) intersection of medium- to coarse-grained quartz dioritic composition sill which intrudes the Footwall Series in the North Zone of the Granduc deposit (158-2a, 630.9-641.0 m). Abundant prismatic to equant (l:w = 3:1 to 1:1) zircon with excellent clarity and minor bubble- and rod-shaped colourless inclusions were recovered (Plate 3.7) . Six fractions were analyzed; fraction E was concordant at 222.2 Ma, whereas all other fractions were slightly discordant, probably as a result of post-crystallization lead-loss (Fig. 3.4a). The $^{207}Pb/^{206}Pb$ ages of the discordant fractions ranged from 221.1 to 227.5 Ma. Because of the restricted range of $^{207}Pb/^{206}Pb$ ages and the lack of visible cores within zircon from this rock, the weighted mean $^{207}Pb/^{206}Pb$ age of 223 +/-3 Ma is considered to be the best estimate of the age of crystallization of this unit.

Footwall Series basalt flow

Sample GD-GC-04 was collected from the Footwall Series within the North Zone of the deposit (Hole 158-2a, 695.8-709.6 m). The sample consisted of a single dark green chlorite-altered basaltic composition flow, with poorly preserved metamorphic hornblende porphyroblasts, sparse quartz + epidote-filled vesicles and 2-3 % disseminated pyrite. Heavy mineral separates yielded a small quantity of equant multi-faceted zircon with few inclusions and high clarity (Plate 3.8). All zircons recovered from the rock were analyzed, and fractions were slightly discordant, probably as a result of post-crystallization lead-loss; the $^{207}Pb/^{206}Pb$ ages ranged from 221.4 to 224.3 Ma (Fig. 3.4b). Because of the restricted range of $^{207}Pb/^{206}Pb$ ages and the lack of visible cores within zircon from this rock, the weighted mean $^{207}Pb/^{206}Pb$ age of 223 +/-5 Ma is considered to be the best estimate of the age of this unit.

Table 3. 1 U-Pb analytical data for samples from Granduc Mountain.

Fraction[1]	Wt.	U	Pb[2]	^{206}Pb[3]	Pb[4]	^{208}Pb[5]	Isotopic ratios(±1σ,%)[6]			Isotopic dates(Ma,±2σ)[6]		
	mg	ppm	ppm	^{204}Pb	pg	%	$^{206}Pb/^{238}U$	$^{207}Pb/^{235}U$	$^{207}Pb/^{206}Pb$	$^{206}Pb/^{238}U$	$^{207}Pb/^{235}U$	$^{207}Pb/^{206}Pb$
Footwall Series quartz diorite sill (GD-GC-01: DDH 158-2a, 630.9-641.0 m)												
A,m,N1,p	0.030	888	30.0	1618	24	7.0	0.03475±0.14	0.24231±0.30	0.05057±0.22	220.2±0.6	220.3±1.2	221.3±9.9
B,mN1,p	0.083	1798	60.9	20460	15	8.2	0.03434±0.09	0.2396±0.10	0.05061±0.03	217.7±0.4	218.1±0.4	222.9.±1.4
C,m,N1,p	0.350	852	28.8	11660	54	9.0	0.03403±0.11	0.2379±0.19	0.05071±0.10	215.7±0.5	216.7±0.8	227.5±4.6
D,c,N1,p	0.155	422	14.2	2201	64	8.2	0.03413±0.12	0.2384±0.25	0.05066±0.17	216.3±0.5	217.1±1.0	225.3±7.7
E,m,N1,p	0.077	367	12.7	3989	14	9.3	0.03488±0.11	0.2433±0.22	0.05059±0.13	221.0±0.5	221.1±0.9	222.2±6.2
F,m,M1,p	0.170	652	22.3	7208	32	9.5	0.03434±0.16	0.2394±0.23	0.05057±0.12	217.7±0.7	218.0±0.9	221.1±5.3
Footwall Series basalt flow (GD-GC-04: DDH 158-2a, 695.8-709.6 m)												
A,f,N1,eq	0.015	322	10.6	293	34	5.5	0.03460±0.19	0.2414±0.84	0.05061±0.72	219.3±0.8	219.6±3.3	223.0±33.1
B,f,N1,eq	0.032	485	16.8	564	55	10.6	0.03419±0.14	0.2387±0.44	0.05064±0.34	216.7±0.6	217.4±1.7	224.3±15.7
D,f,N1,eq	0.014	1036	36.5	2230	16	11.4	0.03450±0.12	0.2409±0.29	0.05057±0.22	218.9±0.5	219.1±1.1	221.4±10.2
E,f,N1,eq	0.020	1583	55.6	2144	32	11.7	0.03432±0.10	0.2395±0.24	0.05061±0.15	217.5±0.4	218.0±0.9	223.0±7.1
Mine Series basaltic andesite (GD-GC-08: surface)												
A,m,N1,s	0.128	127	4.3	1763	20	6.6	0.03515±0.11	0.2452±0.29	0.05059±0.22	222.7±0.5	222.7±1.2	222.4±10.1
B,m,N1,s	0.077	139	4.7	1245	19	6.8	0.03503±0.13	0.2444±0.34	0.05061±0.28	221.9±0.6	222.0±1.4	223.1±12.9
C,f,N1,s	0.031	131	4.5	561	16	7.7	0.03506±0.13	0.2446±0.57	0.05059±0.50	222.2±0.6	222.2±2.3	222.3±23.1
Felsic lapilli tuff (GD-GC-02: surface)												
A,c,N1,mf	0.127	163	4.6	1828	19	7.2	0.02921±0.11	0.2005±0.27	0.04980±0.20	185.6±0.4	185.6±0.9	185.4±9.1
B,m,N1,mf	0.143	483	13.7	6863	18	8.6	0.02864±0.11	0.1974±0.13	0.05001±0.06	182.0±0.4	183.0±0.4	195.3±2.7
C,f,N1,p	0.081	193	5.4	2629	10	9.4	0.02828±0.10	0.1942±0.24	0.04981±0.16	179.8±0.3	180.2±0.8	186.3±7.5

[1]All fractions are air abraded; Grain size, smallest dimension: c= +134μm, m=-134μm+74μm, f=-74μm; Magnetic codes
Franz magnetic separator sideslope at which grains are nonmagnetic; e.g., N1=nonmagnetic at 1°; Field strength for all fractions =1.8A; Front slope for all fractions=20°; Grain character codes: eq=equant, p=prismatic, mf=multi-faceted, s=subhedral
[2]Radiogenic Pb
[3]Measured ratio corrected for spike and Pb fractionation of 0.0043/amu ±20% (Daly collector)
[4]Total common Pb in analysis based on blank isotopic composition
[5]Radiogenic Pb
[6]Corrected for blank Pb, U and common Pb (Stacey-Kramers model Pb composition at the $^{207}Pb/^{206}Pb$ date of fraction, or age of sample)

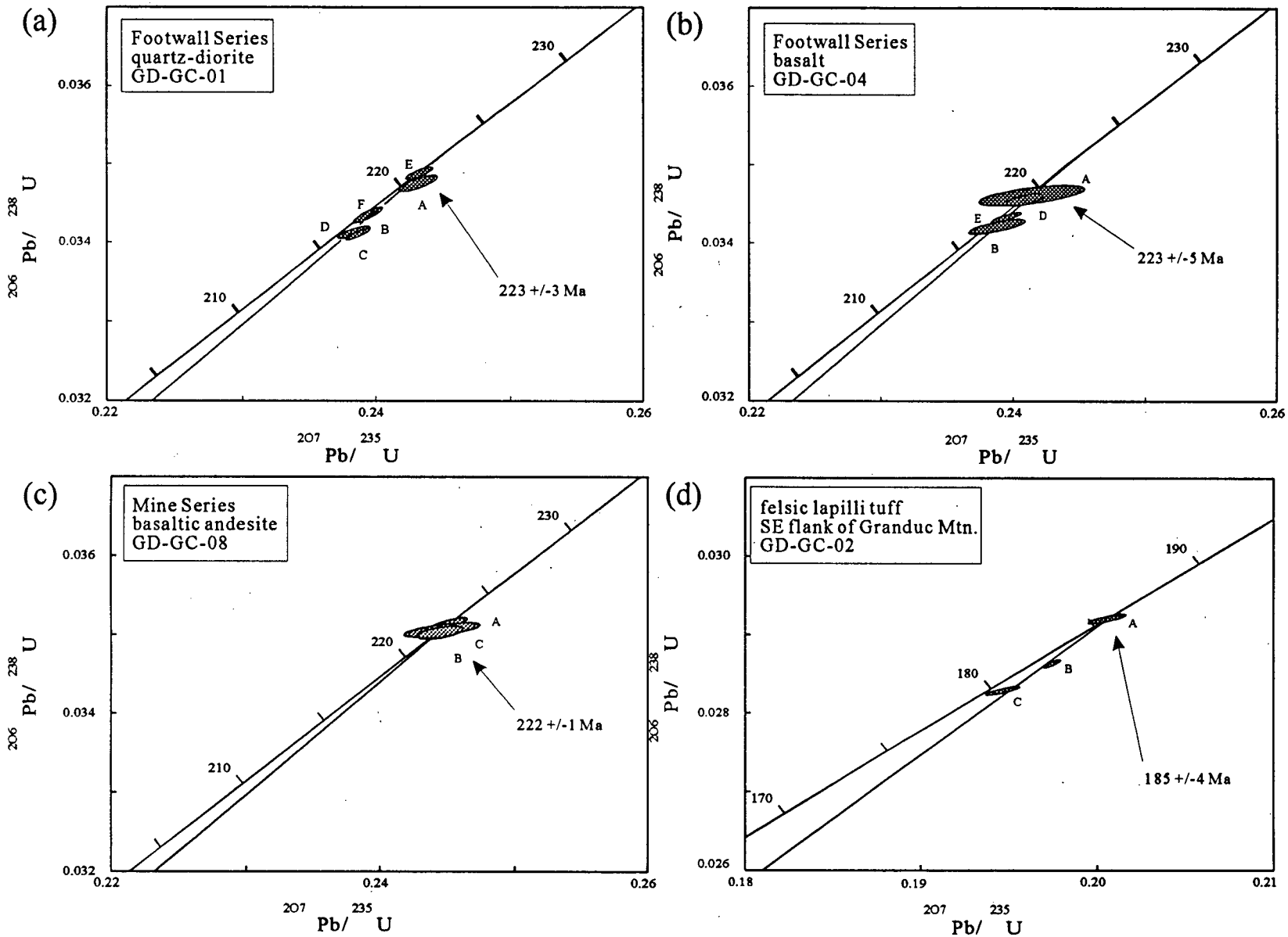

Figure 3.4 U-Pb concordia diagrams for a) Granduc Footwall Series quartz diorite; b) Granduc Footwall Series basalt; c) Granduc Mine Series basaltic andesite; and d) felsic lapilli tuff on the southeast flank of Granduc Mountain.

Mine Series basaltic andesite

An intensely sheared rock of basaltic andesitic composition from the Granduc Mine Series was collected on surface (sample GD-GC-08) from within the Glory Hole area (Fig. 3.2). Primary textures were not sufficiently preserved to determine if this unit represents a flow, tuff or sill. A small quantity of ovoid zircons (l:w = 3:1 to 2:1) with resorption pits and no remnant crystal faces were recovered (Plate 3.9). All the zircon from this rock were analyzed in three fractions, all three fractions were concordant, with $^{207}Pb/^{206}Pb$ ages of 222.3 to 223.1 Ma (Fig. 3.4c). An age of 222 +/-1 Ma, encompassing the $^{206}Pb/^{238}U$ ages and associated errors of the three concordant fractions is considered the best estimate of the age of this unit.

Dacite fragmental, southeast of Granduc Mountain

Felsic tuffaceous and fragmental rocks occur on the southeast flank of Granduc Mountain, as well as north and south of the Leduc Glaciers (Fig. 3.2 and Plate 3.10). On the southeast flank of Granduc Mountain these rocks, which are in fault contact with mafic volcanic rocks of the Footwall Series, consist of mafic to felsic debris flows and felsic lapilli to ash tuffs. Two samples of dacitic composition volcaniclastic rocks were collected as part of this study (GD-GC-02 and -03); sample GD-GC-02, from a zone of deformed, variably altered felsic lapilli tuff was dated by U-Pb methods. Three fractions were analyzed, one fraction was concordant at 185.4 Ma, whereas the other two were slightly discordant, with $^{207}Pb/^{206}Pb$ ages of 186.3 and 195.3 Ma (Fig. 3.4d). An age of 185 +/-4 Ma, based on the weighted mean $^{207}Pb/^{206}Pb$ age and error of all fractions is considered the best estimate of the age of this unit.

Lithogeochemistry

A suite of samples from drill core and surface were analyzed by X-ray fluorescence at McGill University using glass beads for major elements and pressed pellets for trace elements (Table 3.2). A subset of these samples were analyzed for rare earth element (REE) concentrations by instrumental neutron activation at Actlabs (Table 3.3). The purpose of this portion of the study was to determine the compositional range and tectonic affinity of volcanic and intrusive rocks on Granduc Mountain.

Table 3.2 Major and trace element chemistry for the Granduc deposit.

Sample	LITHOLOGY	SiO2 %	TiO2 %	Al2O3 %	Fe2O3 %	MnO %	MgO %	CaO %	Na2O %	K2O %	P2O5 %	LOI	Total
GD-GC-01	quartz-diorite sill/dyke	57.78	0.76	16.69	5.03	0.20	1.98	4.14	5.88	2.88	0.34	4.13	99.92
GD-GC-02	dacitic tuff	63.81	0.41	13.91	4.31	0.12	1.45	4.24	4.25	2.29	0.17	4.80	99.87
GD-GC-03	dacitic tuff	64.80	0.38	16.68	3.26	0.09	0.37	5.16	3.95	1.48	0.13	3.34	99.74
GD-GC-04	basalt	48.82	0.64	11.32	10.75	0.19	13.06	10.43	1.38	1.37	0.33	2.15	100.63
GD-GC-05	feldspar porphyry	72.14	0.45	8.06	4.84	0.08	1.87	4.46	1.21	1.90	0.20	4.17	99.73
GD-GC-06	basalt	45.50	0.59	10.94	11.53	0.24	15.81	11.21	1.04	1.86	0.16	2.16	101.27
GD-GC-07	tuffaceous chert	89.55	0.19	3.54	2.86	0.00	0.28	0.00	0.08	1.68	0.03	1.50	99.71
GD-GC-08	basaltic-andesite	52.40	0.84	17.55	7.70	0.15	3.00	7.05	3.36	1.97	0.38	6.17	100.57
GD-94-2	basalt	47.66	0.59	12.56	14.78	0.17	9.31	7.65	1.97	3.30	0.20	1.87	100.06
GD-94-3	plag. porphyritic basalt	49.43	1.15	17.36	10.34	0.17	3.26	8.89	4.10	0.69	0.23	4.83	100.45
GD-94-4	plag+aug-porphyritic basalt	47.69	1.03	17.28	9.77	0.17	6.49	9.66	3.50	0.78	0.26	3.65	100.28
146-3, 5.5 m	basalt	47.02	0.86	14.30	12.30	0.18	9.58	8.62	1.85	1.97	0.29	3.35	100.47
146-3, 56.7 m	basalt	44.20	0.62	11.22	9.99	0.19	9.67	9.68	0.27	4.97	0.20	8.56	99.77
146-3, 102.4 m	basalt	47.49	0.83	14.09	12.66	0.16	6.22	6.07	1.28	5.92	0.23	4.89	100.08
146-3, 145.1 m	altered zone	54.67	1.52	21.92	3.35	0.17	0.41	5.47	2.85	6.56	0.03	2.38	99.67
146-3, 203.3 m	quartz-diorite sill/dyke	58.99	0.70	18.04	2.93	0.12	1.62	4.86	6.51	2.19	0.41	3.08	99.51
146-3, 275.2 m	basalt	47.00	0.71	13.13	9.43	0.29	9.44	9.01	2.53	2.83	0.28	4.90	99.75
146-3, 303.3 m	cherty tuff	50.62	0.91	15.38	10.95	0.15	7.07	8.15	3.43	2.06	0.27	1.22	100.34
158-1, 587.1 m	feldspathic tuff	48.14	0.92	17.66	8.60	0.16	4.17	7.42	3.58	1.69	0.25	7.87	100.54
158-1, 634.0 m	cherty tuff	88.00	0.24	4.40	1.61	0.02	1.50	1.21	0.89	0.96	0.09	1.29	100.27
158-1, 654.4 m	basalt	48.50	0.74	11.66	11.54	0.21	11.65	11.74	1.67	0.85	0.27	2.13	101.16
158-1, 665.4 m	basalt	43.08	0.71	13.40	11.73	0.22	7.70	9.47	2.19	3.30	0.23	6.90	99.32
158-1, 670.3 m	diorite sill/dyke	50.99	0.68	14.86	3.05	0.20	2.71	11.65	4.37	2.30	0.27	8.54	99.73
158-1, 816.9 m	basalt	47.66	0.71	12.77	11.10	0.22	13.06	7.88	1.87	3.34	0.23	1.63	100.67
158-1, 846.1 m	basaltic andesite	52.45	0.98	16.28	11.60	0.10	4.03	6.95	5.21	0.84	0.30	1.38	100.25
158-1, 686.1 m	basalt	50.48	0.77	14.05	9.77	0.16	9.60	8.68	3.27	1.20	0.23	2.00	100.40
158-1, 907.7 m	basaltic andesite	52.73	0.71	13.44	8.60	0.20	9.96	8.02	3.22	1.85	0.29	1.04	100.23
147-1b, 252.7 m	basalt	48.54	2.78	13.44	15.52	0.28	5.70	7.66	3.32	1.58	0.42	1.38	100.77
147-1b, 259.7 m	feldspathic tuff?	50.03	0.88	19.59	9.06	0.14	3.28	8.49	4.23	1.42	0.49	2.40	100.13
147-1b, 272.8 m	cherty tuff	82.31	0.32	6.35	4.00	0.03	1.37	0.85	0.55	3.21	0.11	0.90	100.63
147-1b, 304.8 m	basalt	47.00	0.75	12.63	12.86	0.15	11.26	8.11	1.50	3.67	0.27	2.28	100.73
147-1b, 351.1 m	diorite sill/dyke	50.15	0.85	15.97	6.33	0.14	6.36	11.39	3.54	1.14	0.32	3.74	100.02
147-1b, 373.4 m	quartz-diorite sill/dyke	58.46	0.83	18.89	3.64	0.07	1.74	4.95	7.34	1.36	0.08	2.33	99.74

Sample	LITHOLOGY	SiO2 %	TiO2 %	Al2O3 %	Fe2O3 %	MnO %	MgO %	CaO %	Na2O %	K2O %	P2O5 %	LOI	Total
147-1b, 415.1 m	black mudstone	47.13	0.84	13.59	14.41	0.16	7.74	3.97	0.20	6.68	0.30	4.34	99.59
147-1b, 473.1 m	diorite sill/dyke	50.38	1.02	16.77	2.90	0.19	2.82	9.37	5.76	2.51	0.21	7.33	99.34
147-1b, 485.9 m	sheared sill/dyke margin?	37.80	0.59	11.63	29.89	0.10	4.65	4.87	1.64	3.96	0.27	3.45	99.91
147-1b, 517.3 m	basalt	46.14	0.79	15.27	9.46	0.14	6.89	8.71	2.64	2.73	0.24	7.41	100.54
102-77, 42.7 m	basalt	44.22	2.03	9.41	23.39	0.38	5.45	10.33	1.50	1.17	0.49	0.81	99.51
102-77, 58.2 m	feldspathic tuff?	46.90	0.81	18.02	10.67	0.19	3.23	11.12	1.92	2.48	0.35	4.20	100.06
147-1b, 332.2 m	gash-banded andesite?	43.01	0.62	10.70	12.75	0.34	10.11	9.16	0.00	3.1	0.23	9.4	99.42
102-77, 127.7 m	gash-banded andesite?	50.38	0.92	19.00	10.58	0.17	2.95	7.67	2.31	3.36	0.41	1.49	99.24
119-66, 4.0 m	andesite	56.09	0.71	17.87	6.48	0.13	2.02	3.25	4.38	4.75	0.27	2.42	98.37
119-66, 23.6	diorite sill/dyke ?	50.52	0.76	17.74	5.00	0.14	3.35	6.97	5.20	2.4	0.31	5.29	97.68
119-66, 34.7 m	basalt	47.82	0.60	10.52	9.79	0.23	12.33	10.32	1.14	2.96	0.19	4.11	100.01
119-66, 54.9 m	cherty tuff?	80.57	0.43	7.65	1.61	0.06	0.98	1.53	1.33	2.12	0.1	2.09	98.47
102-79, 2.4 m	basalt?	48.20	0.81	15.87	14.61	0.21	5.69	3.03	2.72	4.32	0.3	3.66	99.42
102-79, 12.2 m	argillaceous chert	90.51	0.08	1.73	2.85	0.04	0.88	2.00	0.00	0.25	0.31	1.22	99.87
102-79, 87.8 m	basaltic andesite	53.79	0.76	14.46	12.58	0.22	5.44	6.72	2.77	2.67	0.35	0.92	100.68
102-79, 111.9 m	andesite	63.25	0.61	13.22	9.12	0.09	0.39	2.34	4.20	4.18	0.03	1.7	99.13
158-2a, 422.7 m	lapilli tuff	50.15	1.25	17.26	12.77	0.19	3.75	7.47	4.04	0.74	0.26	2.34	100.22
158-2a, 512.1 m	banded chert w/ sulphides	83.99	0.28	4.83	4.72	0.06	1.21	1.55	1.01	1.3	0.06	2.09	101.1
158-2a, 523.0 m	basalt	50.85	1.06	17.41	11.14	0.16	5.14	7.07	4.24	1.97	0.34	1.13	100.51
158-2a, 586.7 m	quartz diorite sill/dyke	57.74	0.66	17.27	5.01	0.15	1.60	3.39	5.35	4.74	0.36	2.64	98.91
158-2a, 737.0 m	basalt	47.63	0.63	10.54	12.02	0.18	14.09	8.80	1.61	1.17	0.15	3.29	100.11
158-2a, 784.8 m	basalt	46.21	0.63	11.63	10.70	0.24	9.89	16.35	0.45	1.08	0.26	2.56	100
158-2a, 816.5 m	basalt	48.27	0.68	12.17	10.12	0.21	13.22	10.26	1.25	2.19	0.2	1.52	100.09
153-1, 250.2 m	basalt	50.44	0.93	17.98	11.15	0.18	3.54	9.08	3.70	0.62	0.17	1.94	99.73
153-1, 420.0 m	chlorite schist	57.74	0.95	21.62	1.57	0.08	0.27	3.75	6.61	3.37	0.02	3.12	99.1
153-1, 444.4 m	quartz diorite sill/dyke	57.94	0.63	17.46	4.86	0.11	1.38	3.94	6.07	4.04	0.35	3.02	99.8
153-1, 521.8 m	basalt	47.50	0.83	14.30	12.80	0.18	9.66	7.50	1.85	3.25	0.27	1.76	99.9
153-1, 478.2 m	diorite sill/dyke	51.81	0.90	16.90	4.40	0.07	6.63	8.72	4.34	2.13	0.74	3.97	100.61
153-1, 588.6 m	basalt	49.68	0.68	12.05	8.61	0.16	11.70	9.80	2.66	1.06	0.17	3.18	99.75
153-1, 64.9 m	basalt	48.77	0.72	12.73	10.88	0.18	11.67	10.01	1.37	1.68	0.21	2.34	100.56

Sample	BaO	Co	Cr2O3	V	Cu	Ni	Zn	Ga	Nb	Rb	Sr	Pb	Zr	Y	Zr/Y
	ppm	ppm	ppm	ppm	ppm	ppm	ppm	ppm	ppm	ppm	ppm	ppm	ppm	ppm	
GD-GC-01	344	28	int	106	261	10	211	16	10	135	159	9	146	25	5.8
GD-GC-02	829	18	50	71	76	14	45	10	7	54	210	5	99	15	6.6
GD-GC-03	654	19	47	45	96	20	44	16	7	35	395	4	98	10	9.8
GD-GC-04	279	71	814	213	115	226	57	11	2	51	174	10	50	14	3.6
GD-GC-05	2817	66	268	133	88	50	52	8	5	57	176	8	78	19	4.1
GD-GC-06	198	65	1176	204	108	414	169	10	2	87	128	11	48	11	4.4
GD-GC-07	4618	44	58	60	85	0	188	8	8	18	39	1102	46	36	1.3
GD-GC-08	711	20	0	197	140	4	106	18	3	63	284	3	65	18	3.6
GD-94-2	675	39	961	269	92	199	129	13	1	126	149	6	33	17	2.0
GD-94-3	386	25	33	312	53	11	101	19	2	11	432	2	100	24	4.3
GD-94-4	395	26	207	269	37	88	92	17	1	13	489	2	64	16	4.0
146-3, 5.5 m	0.03	35	561	305	34	129	87	14	4	73	268	8	61	16	3.8
146-3, 56.7 m	0.02	18	694	249	460	112	181	10	3	326	90	10	44	10	4.4
146-3, 102.4 m	0.03	60	369	314	1013	130	120	15	4	403	102	9	59	12	4.9
146-3, 145.1 m	0.23	8	381	42	480	11	92	11	10	236	304	22	69	7	9.9
146-3, 203.3 m	0.04	16	2	90	27	6	71	19	11	87	416	7	73	29	2.5
146-3, 275.2 m	0.03	62	572	266	413	181	168	13	4	178	233	10	51	13	3.9
146-3, 303.3 m	0.03	30	348	271	147	98	86	16	5	103	198	9	70	18	3.9
158-1, 587.1 m	0.03	26	21	231	93	25	89	17	5	68	262	6	60	15	4.0
158-1, 634.0 m	0.03	38	67	33	71	20	53	4	6	32	49	0	89	14	6.4
158-1, 654.4 m	0.02	50	847	261	290	175	90	12	4	23	189	7	51	14	3.6
158-1, 665.4 m	0.07	45	559	275	1886	182	175	14	5	137	182	18	54	15	3.6
158-1, 670.3 m	0.06	8	97	145	68	22	69	13	6	78	264	7	66	19	3.5
158-1, 816.9 m	0.03	42	740	259	144	230	183	12	4	163	168	7	50	14	3.6
158-1, 846.1 m	0.02	54	87	330	499	30	41	16	5	27	275	9	71	20	3.6
158-1, 686.1 m	0.02	38	740	294	342	116	42	14	4	40	176	9	57	17	3.4
158-1, 907.7 m	0.04	20	616	232	95	139	97	12	5	64	415	8	65	17	3.8
147-1b, 252.7	0.06	36	91	400	182	74	58	21	14	49	240	9	514	41	12.5
147-1b, 259.7	0.06	16	48	251	192	20	31	17	4	32	565	10	66	17	3.9
147-1b, 272.8	0.52	37	78	76	774	42	17	5	6	53	84	1	71	12	5.9
147-1b, 304.8	0.05	17	902	249	353	184	265	15	5	131	99	17	60	11	5.5
147-1b, 351.1	0.02	10	149	235	46	40	70	15	4	35	371	9	60	17	3.5
147-1b, 373.4	0.02	5	87	132	64	9	31	12	10	50	308	3	77	30	2.6

Sample	BaO	Co	Cr2O3	V	Cu	Ni	Zn	Ga	Nb	Rb	Sr	Pb	Zr	Y	Zr/Y
	ppm	ppm	ppm	ppm	ppm	ppm	ppm	ppm	ppm	ppm	ppm	ppm	ppm	ppm	
147-1b, 415.1	0.12	80	340	293	113	76	104	14	5	250	59	10	59	13	4.5
147-1b, 473.1	0.03	16	70	122	106	53	95	12	6	129	227	5	73	11	6.6
147-1b, 485.9	0.02	54	278	481	9284	120	102	21	5	277	144	15	54	7	7.7
147-1b, 517.3	0.02	14	327	269	117	87	81	15	3	150	228	69	54	14	3.9
102-77, 42.7 m	0.04	20	41	375	1889	48	404	25	15	31	105	38	158	49	3.2
102-77, 58.2 m	0.1	20	85	282	211	37	85	19	4	68	541	21	58	15	3.9
147-1b, 332.2	361	23	1023	293	388	157	222	14	7	133	49	2	34	16	2.1
102-77, 127.7	1509	13	20	295	81	18	57	19	4	87	400	17	58	22	2.6
119-66, 4.0 m	1548	17	4	143	65	14	44	18	7	126	261	11	93	16	5.8
119-66, 23.6	614	31	7	174	557	52	86	17	4	99	308	15	64	19	3.4
119-66, 34.7 m	205	24	880	250	105	168	168	14	5	188	108	4	36	17	2.1
119-66, 54.9 m	2383	136	29	143	20	14	24	8	9	39	96	7	103	28	3.7
102-79, 2.4 m	1483	120	182	264	248	47	186	16	6	146	171	10	61	23	2.7
102-79, 12.2 m	206	57	22	190	157	73	33	7	8	2	40	13	31	16	2.0
102-79, 87.8 m	911	34	111	244	322	25	199	17	6	85	228	15	66	22	3.1
102-79, 111.9	437	14	3	22	43	8	63	33	53	59	84	19	859	79	10.8
158-2a, 422.7	361	26	48	328	121	23	102	20	5	20	287	9	100	29	3.4
158-2a, 512.1	871	98	19	156	452	70	32	9	9	22	50	14	62	19	3.4
158-2a, 523.0	1143	26	124	324	141	35	46	17	6	63	240	8	73	25	2.9
158-2a, 586.7	1048	16	14	102	183	8	138	18	10	133	355	22	215	28	7.7
158-2a, 737.0	251	46	941	261	101	223	56	12	6	38	139	3	33	20	1.7
158-2a, 784.8	368	46	728	260	34	162	106	12	6	22	223	15	40	21	1.9
158-2a, 816.5	311	57	878	259	79	290	120	13	6	73	204	7	41	22	1.9
153-1, 250.2 m	350	37	24	295	124	9	67	18	4	10	364	7	71	25	2.9
153-1, 420.0 m	529	12	132	60	30	5	25	15	10	90	394	15	69	11	6.2
153-1, 444.4 m	817	10	13	113	83	11	170	20	12	114	290	10	176	31	5.6
153-1, 521.8 m	693	5	487	308	46	80	121	16	5	131	256	9	48	20	2.4
153-1, 478.2 m	213	19	272	182	31	139	27	16	5	109	365	4	57	15	3.9
153-1, 588.6 m	147	26	851	240	137	139	58	11	6	38	219	3	35	21	1.7
153-1, 64.9 m	394	33	649	273	57	177	171	13	5	57	263	12	40	21	1.9

Table 3.3 Rare earth element chemistry for the Granduc deposit.

Sample	Hf ppm	Sc ppm	Ta ppm	Th ppm	U ppm	W ppm	La ppm	Ce ppm	Nd ppm	Sm ppm	Eu ppm	Tb ppm	Yb ppm	Lu ppm
GD-GC-01	4.4	9.2	1.2	3.0	2.3	54	13.9	33	17	4.04	0.89	0.7	2.78	0.36
GD-GC-04	0.9	41.5	<d/l	1.1	1.0	33	8.7	18	10	2.56	0.86	0.4	1.44	0.20

Major and Trace Elements

Igneous rocks sampled for geochemical analysis from the Granduc Mine and Footwall Series can be divided into two main groups on the basis of lithology: mafic volcanic and volcaniclastic rocks, and mafic to intermediate sills and dykes. Mafic volcanic and volcaniclastic rocks range in composition from Mg-rich basalt to basalt and basaltic andesite, with SiO_2=43-53 %, TiO_2=0.6-2.8 %, Al_2O_3=9.4-19.6 %, MgO=3.0-15.8 %, and Cr_2O_3=33-1176 ppm. These rocks have Zr/Y ratios of 1.7 to 5.5, which are consistent with tholeiitic to transitional magmatic affinities, with the exception of two samples with extremely high concentrations of Zr (514 and 859 ppm), and correspondingly high Zr/Y ratios (12.5 and 10.8, respectively) (Table 3.2 and Fig. 3.5a). The Zr/Y ratios determined for these rocks in part overlap the more primitive end of the data cluster determined for mafic rocks the Stuhini Group in the Telegraph Creek map area, north of Granduc (Fig. 3.5b). A trend from low to high Zr, TiO_2, and Al_2O_3, and high to low Cr_2O_3, can be established for mafic volcanic and volcaniclastic rocks from Granduc Mountain (Figs. 3.6a, b, and c). This variation in composition corresponds to the geographic location of samples, with the most primitive compositions (lowest Zr, TiO_2, and Al_2O_3, highest Cr_2O_3) occurring at the greatest depths in drill core (all drill holes sampled were drilled from west to east) and at the easternmost surface exposures of the Footwall Series, a few meters west of the shear zone that separates Footwall Series rocks from volcaniclastic rocks of Jurassic age discussed above (Fig. 3.2). This variation in the chemical composition of the mafic volcanic rocks may represent the fractionation of a mafic magma from more primitive to more evolved compositions, and if so would suggest the VMS mineralization within the Mine Series may be overlying a chemically evolving volcanic pile.

Variably deformed sills and dykes which intrude mafic volcanic and volcaniclastic rocks of the Footwall Series range in composition from diorite to quartz diorite, and are compositionally similar to the basalt to basaltic andesite composition flows and tuffaceous rocks they intrude (SiO_2=50-59 %, TiO_2=0.6-1.0 %, Al_2O_3=14.9-18.9 %, MgO=1.4-6.6 %, and Cr_2O_3=7-278 ppm). Intrusive equivalents of the most primitive Mg-rich basaltic rocks were not represented in the drill core sampled in this study. Ratios of Zr/Y of 2.5 to 7.7 for the sills and dykes are consistent with predominantly tholeiitic to transitional magmatic affinities (Fig. 3.5a). Diorite to quartz diorite

sills and dykes lie along the trends established for the mafic volcanic rocks, with the exception of three rocks, which have markedly higher Zr concentrations (146-215 ppm), and slightly elevated Y concentrations and Zr/Y ratios relative to other samples of the sills analyzed in this study (Fig. 3.6a, b, and c). These high Zr concentrations may represent a high Zr mineral, such as zircon, becoming concentrated by chemical or physical mechanisms within some parts of these sills.

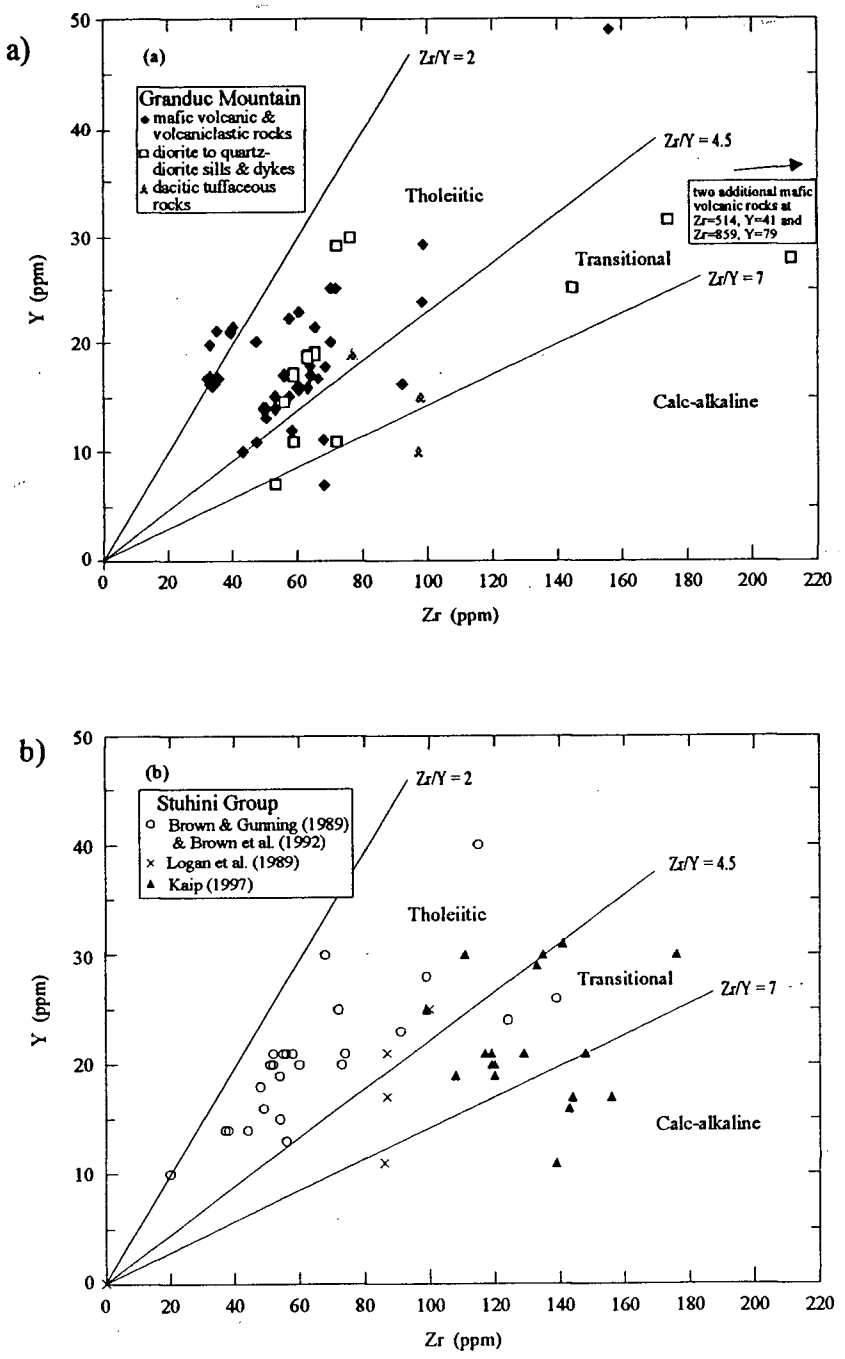

Figure 3. 5 Plot of Y *versus* Zr for a) rocks from Granduc Mountain; and b) regional samples from the Stuhini Group (data from Logan et al., 1989; Brown and Gunning 1989; Brown et al. 1992; Kaip, 1997) (limits after Barrett and MacLean 1994).

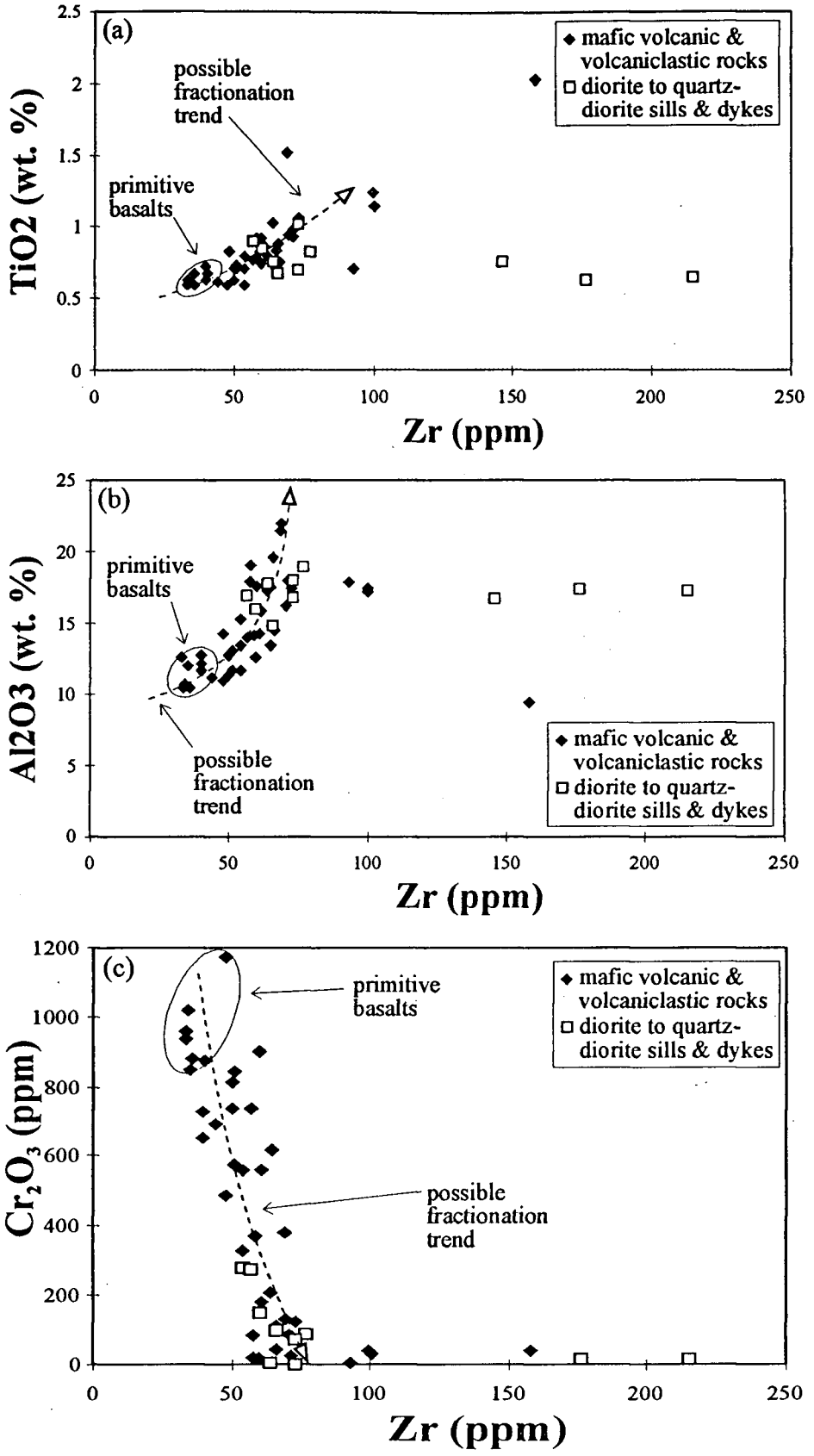

Figure 3. 6 Plots of a) TiO_2 *versus* Zr; b) Al_2O_3 *versus* Zr; and c) Cr_2O_3 *versus* Zr for mafic volcanic and volcaniclastic rocks and diorite to quartz diorite sills and dykes from Granduc Mountain.

Rare Earth Elements

Basalt and quartz diorite from the Footwall Series of the Granduc deposit have similar REE patterns, characterized by depletion in heavy-REE relative to light-REE, and Ce_n/Yb_n ratios of 3.2 and 3.8, respectively (Fig. 3.7). The sample of quartz diorite has a minor negative Eu anomaly, which is consistent with plagioclase fractionation. This sample also corresponds to one of the samples noted above to have an elevated Zr concentration. The similarity between the pattern for this rock and the basalt, combined with the higher overall REE concentrations of the sill sample is consistent with concentration of zircon or some other Zr- and REE-rich mineral within portions of the sill. The REE patterns of these rocks are slightly enriched relative to basalts of N- and E-MORB character, and indicate derivation from somewhat more evolved sources than N- and E-MORB lavas (Sun and McDonough 1989).

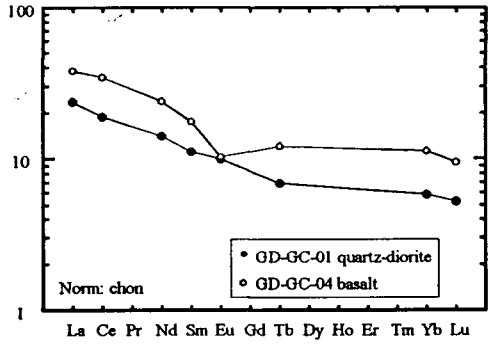

Figure 3. 7 REE plot for basalt and quartz diorite from the Granduc Footwall Series.

Nd Isotope Data

The samples of basaltic volcanic rock from the Footwall Series and quartz dioritic intrusion, both of which were dated in this study, were analyzed for their Nd isotopic compositions to further constrain potential magmatic source regions for these rocks. Neodymium isotopic analyses were conducted by R. Thériault at the Geochronology Laboratory of the Geological Survey of Canada; analytical procedures are described by Thériault (1990). Analytical uncertainty is ± 0.5 ε_{Nd} units; abundances of Sm and Nd were determined by isotope dilution and have an uncertainty of 1% or less. Analytical results are presented in Table 3.4 and are shown graphically in Figure 3.8.

Basalt from the Granduc Footwall Series and quartz diorite intrusive into it have initial ε_{Nd} values of +6.1 and +6.8, respectively. These values, which are within error of each other, indicate that these rocks were derived from primitive magmatic sources with no detectable component of old, evolved sialic basement. For comparison, initial ε_{Nd} values determined in this study are plotted with those of regional samples of mafic volcanic and volcaniclastic rocks of the Stuhini Group (n = 4, initial ε_{Nd} = +1.3 to +7.7) and mafic intrusions of the Stikine Plutonic Suite (n = 3, initial ε_{Nd} = +4.0 to +7.7) (Fig. 3.8) (Samson et al. 1989; Jackson 1990); values determined in this study overlap the most primitive end of the data array.

Table 3. 4 Neodymium isotopic data.

Sample	Sm (ppm)	Nd (ppm)	$^{147}Sm/^{144}Nd$	meas. $^{143}Nd/^{144}Nd$ (error x 10^{-6}, 2σ)	ε_{Nd}[2] (present day)	age[1] (Ma)	ε_{Nd}[2] (initial)
GRANDUC							
GD-GC-01 Footwall Series quartz diorite sill	4.43	18.48	0.1448	0.512908 (7)	+5.3	223	+6.8
GD-GC-04 Footwall Series basalt flow	3.36	13.46	0.1511	0.512884 (6)	+4.8	223	+6.1

[1]used for the calculation of ε_{Nd} (initial).
[2]error = ±0.5 ε_{Nd} units.

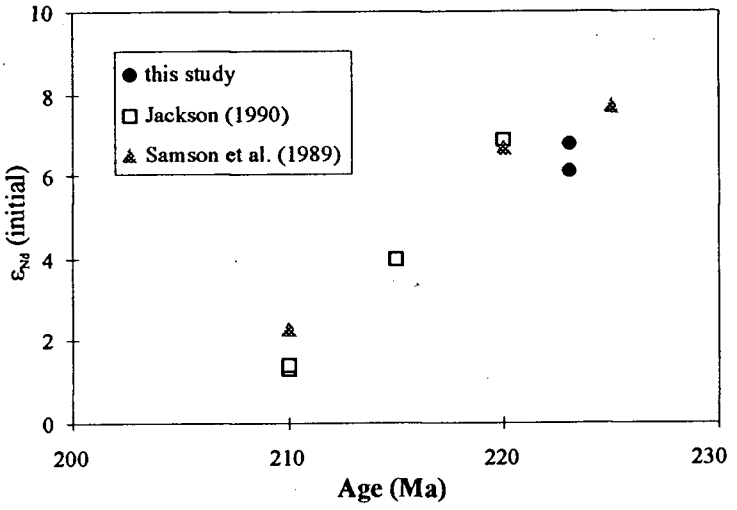

Figure 3. 8 Plot of ε_{Nd} (initial) *versus* age for basalt and quartz diorite from the Granduc Footwall Series, plotted with Late Triassic rocks of the Stuhini Group and Stikine Plutonic Suite (Samson et al. 1989; Jackson 1990).

Pb Isotope Data

Lead isotopic compositions were determined for sulphides from the B and F ore zones in the Granduc deposit, as well as for galena and potassium feldspar from Pb-Zn-Ag veins which cross cut the Footwall Series (Fig. 3.3). Sample preparation and Pb isotopic analyses were carried out at the Geochronology Laboratory at the University of British Columbia. Analytical procedures are outlined in Appendix 1; analytical results are given in Table 3.5 and shown graphically in Figure 3.9.

Table 3. 5 Lead isotopic data for samples from the Granduc deposit.

SAMPLE [1] NUMBER	DRILL HOLE LOCATION	SAMPLE DESCRIPTION	MIN [2]	$^{206}Pb/^{204}Pb$ (% error)[3,4]	$^{207}Pb/^{204}Pb$ (% error)[3,4]	$^{208}Pb/^{204}Pb$ (% error)[3,4]	$^{207}Pb/^{206}Pb$ (% error)[3,4]	$^{208}Pb/^{206}Pb$ (% error)[3,4]
G1a	102-77, 112ft.	B orebody	gl	18.62 (0.027)	15.56 (0.027)	38.19 (0.030)	0.8358 (0.008)	2.051 (0.009)
G1b	102-77, 112ft.	B orebody	gl	18.64 (0.022)	15.59 (0.023)	38.27 (0.026)	0.8362 (0.006)	2.053 (0.008)
G2a	102-77, 356ft.	B orebody	gl	18.65 (0.015)	15.59 (0.017)	38.27 (0.021)	0.8359 (0.006)	2.052 (0.009)
G2b	102-77, 356ft.	B orebody	gl	18.65 (0.019)	15.58 (0.021)	38.27 (0.024)	0.8355 (0.005)	2.052 (0.010)
G2c	102-77, 356ft.	B orebody	py	18.65 (0.044)	15.58 (0.038)	38.24 (0.056)	0.8355 (0.025)	2.051 (0.032)
G3a	158-1, 3135ft.	vein	gl	19.18 (0.019)	15.64 (0.021)	38.70 (0.024)	0.8151 (0.006)	2.018 (0.009)
G3b	158-1, 3135ft.	vein	gl	19.18 (0.012)	15.63 (0.014)	38.71 (0.019)	0.8151 (0.007)	2.018 (0.010)
G3c	158-1, 3135ft.	vein	kf	19.19 (0.011)	15.63 (0.013)	38.71 (0.018)	0.8146 (0.006)	2.017 (0.009)
G3d	158-1, 3135ft.	vein	kf	19.18 (0.026)	15.62 (0.027)	38.66 (0.030)	0.8144 (0.006)	2.015 (0.008)
G9a	119-57, 97ft.	F orebody	gl	18.64 (0.010)	15.58 (0.013)	38.25 (0.017)	0.8357 (0.005)	2.052 (0.008)
G9b	119-57, 97ft.	F orebody	gl	18.63 (0.014)	15.57 (0.016)	38.24 (0.019)	0.8359 (0.005)	2.052 (0.008)

[1] upper case letter and number refers to sample number, lower case letter refers to fraction number.
[2] mineral abreviations: gl=galena, py=pyrite, kf=potassium feldspar.
[3] errors are quoted at the 2σ (95% confidence) level.
[4] values are corrected for instrument fractionation by normalization based on replicate analyses of the NBS-981 standard.

Alldrick (1991) has characterized the Pb isotopic signature of Jurassic and Tertiary mineralization in the Stewart Mining Camp. Lead isotopic values group in two distinct clusters, the isotopically more primitive cluster correspond to Jurassic gold-silver-copper-zinc-lead mineralization, and the isotopically more evolved cluster to Tertiary silver-zinc-lead±molybdenum mineralization associated with Hyder Plutonism. Values determined in the present study are plotted relative to Alldrick's (1991) Jurassic and Tertiary clusters (Fig. 3.9).

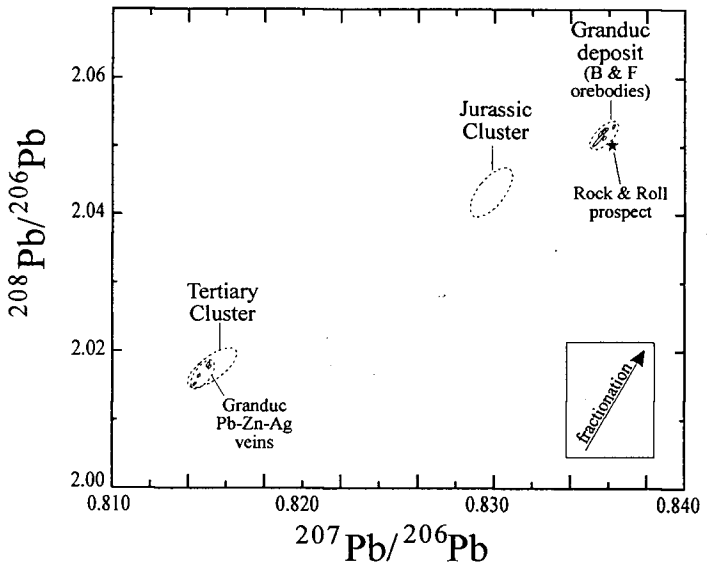

Figure 3. 9 Plot of $^{207}Pb/^{206}Pb$ *versus* $^{208}Pb/^{206}Pb$ for sulphides from B and F orebodies of the Granduc deposit, veins which cross cut the Footwall Series of the deposit, and the Rock and Roll prospect (Dean and Carr, 1991). Plotted for comparison are clusters defined for Jurassic and Tertiary mineralization in the Stewart Mining Camp (Alldrick, 1991).

Syngenetic Cu-rich VMS mineralization

Mineralization within the main orebodies at Granduc consists primarily of laminated and variably deformed massive to semi-massive pyrite-pyrrhotite-chalcopyrite in an argillaceous and variably magnetite-rich matrix (Plate 3.11). In the archived core examined, galena occurs as thin (1-3mm) quartz-calcite-galena±pyrite veinlets cross-cutting the banded copper-rich mineralization. On first inspection, the intimate relationship between the galena-rich veinlets and the banded mineralization within these highly deformed rocks appeared to reflect a remobilization of the galena. However, the possibility that the galena was part of a younger mineralizing event could not be dismissed. Therefore, laminated pyrite, as well as galena was analyzed for its Pb

isotopic composition. Analysis of six galena samples from the B and F orebodies in the Main Zone of the Granduc deposit yielded ratios of $^{207}Pb/^{206}Pb$ = 0.8355-0.8362 and $^{208}Pb/^{206}Pb$ = 2.051-2.052 (Fig. 3.9 and Table 3.5). Lead values determined for pyrite from the B orebody plots within the range of galena values ($^{207}Pb/^{206}Pb$ = 0.8355 and $^{208}Pb/^{206}Pb$ = 2.051), suggesting that Pb within the two minerals was derived from the same metallogenic source. Thus the galena analyzed in this study appears to represent a minor, yet primary component to Granduc mineralization which was preferentially remobilized during deformation. The values determined for galena and pyrite from the Granduc deposit are less radiogenic than Jurassic mineralization in the Stewart area, and therefore suggest a pre-Jurassic age for this style of mineralization, consistent with the age of the host rocks.

Pb-Zn-Ag Veins

A limited number of undeformed, coarse-grained microcline-calcite-sulphide veins (10-15 cm apparent thickness) cross cut Footwall Series in the North Zone of the Granduc deposit; insufficient core is preserved from the mined-out zones to determine if these veins cross cut the orebodies in significant quantities. Sulphides in these veins consist of pyrite, galena, and sphalerite; original assays of bulk rocks containing these veins show enrichments of lead, zinc and silver (Plate 3.12). Galena and microcline from one of these veins yielded Pb isotopic ratios of $^{207}Pb/^{206}Pb$ = 0.8144-0.8151 and $^{208}Pb/^{206}Pb$ = 2.015-2.018 (Fig. 3.9 and Table 3.5). These values are significantly more radiogenic than the Pb isotopic signature determined for syngenetic mineralization in the Granduc deposit and plot within the cluster defined by Alldrick (1991) for mineralization related to Tertiary intrusions in the Stewart Mining Camp.

Discussion

Ages of magmatic rocks on Granduc Mountain

In the current study mafic volcanic rocks from the Footwall and Mine Series of the Granduc deposit were dated by U-Pb methods at 223 +/-5 and 222 +/-1 Ma, respectively, and are therefore assigned to the Upper Triassic Stuhini Group. These results establish that magmatic

rocks in the Mine and Footwall Series are the same age, a association that could not be confirmed by field relationships alone, due to the high degree of deformation on Granduc Mountain.

A quartz diorite body which intrudes the Footwall Series was dated by U-Pb methods at 223 +/-3 Ma; this unit is therefore assigned to the Stikine Plutonic Suite. The age determined for this unit is within error of those determined for mafic volcanic rocks in this study and establishes that plutonism was contemporaneous with volcanism in the Footwall and Mine Series of the Granduc deposit. The age of this intrusion is also identical to an age of approximately 223 Ma determined for the Bucke Glacier Stock, 6 -8 km north of Granduc Mountain (Lewis 1994), and indicates that Late Triassic plutonism in the area was not restricted to Granduc Mountain.

On the southeast flank of Granduc Mountain mafic volcanic rocks of the Footwall Series are in fault contact with deformed mafic to felsic tuffaceous and fragmental rocks (Fig. 3.2). A tuffaceous rock of dacitic composition was dated by U-Pb methods at 185 +/-4 Ma, and these rocks are therefore assigned to the Lower Jurassic Hazelton Group. An Early Jurassic age for volcanic rocks in the southeast flank of Granduc Mountain implies that these rocks are unrelated to volcanic and intrusive rocks of the Granduc Mine and Footwall Series.

Age of Cu-rich VMS mineralization

As a result of the high degree of deformation, determining the age of the magmatic rocks is not sufficient to establish an age for VMS mineralization at Granduc. Therefore the Pb isotopic signature of mineralization at Granduc was determined as part of this study. The Pb isotopic signatures of Jurassic and Tertiary age mineralization in the Stewart Mining Camp has been documented by Alldrick (1991); the data clusters can be used in a comparative way to establish an age for other mineralization in the region. In this study, Cu-rich VMS mineralization at Granduc was determined to have a Pb isotopic signature that is distinctly more primitive than both Tertiary and Jurassic mineralization in the region; these data imply a pre-Jurassic age for VMS mineralization at Granduc (Fig. 3.9). Together, the Pb isotopic data and U-Pb age determinations for igneous rocks in the Mine and Footwall Series suggest a Late Triassic age for Cu-rich VMS mineralization at Granduc, consistent with a syngenetic interpretation of mineralization (Grove 1986; Höy 1991).

An interpreted Late Triassic age for Granduc VMS mineralization indicates that in addition to the Jurassic and Tertiary metallogenic epochs in the region, there was also a Late Triassic metallogenic event. The Pb isotopic signature of this mineralization is distinct, and more primitive than signatures of Jurassic and Tertiary mineralization in the region. It should therefore be possible to use sulphide Pb isotopic signatures from other syngenetic mineral occurrences to determine if they are related to this Late Triassic mineralizing event. The Rock and Roll prospect, located 7 km west of the Snip deposit, is interpreted to be a VMS occurrence of probable Late Triassic age (B.C. MINFILE # 104B 377). The prospect, with indicated reserves of 0.58 million tonnes grading 3.1 % Zn, 0.8 % Pb, 0.6 % Cu, 2.8 g/t Au and 336 g/t Ag, consists of sediment-hosted base metal sulphides which occur in proximity to mafic volcanic and volcaniclastic rocks, interpreted to be part of the Upper Triassic Stuhini Group (B.C. MINFILE). Galena from the Rock and Roll prospect has a Pb isotopic signature that is very close to that determined in this study for mineralization at Granduc ($^{207}Pb/^{206}Pb = 0.8363$ and $^{208}Pb/^{206}Pb = 2.050$) (Dean and Carr 1991) (Fig. 3.9). The similarity in the Pb isotopic signatures for mineralization from the two areas suggest that a Late Triassic age designation for mineralization at the Rock and Roll prospect is valid.

Age of Pb-Zn-Ag veins

Galena and microcline from undeformed, coarse-grained Pb-Zn-Ag veins which cross cut the Footwall Series have a Pb isotopic signature which is significantly more evolved than that of the Cu-rich VMS mineralization discussed above. These veins have a Pb isotopic composition which plots within the cluster defined for Tertiary mineralization in the region (Fig. 3.9) (Alldrick 1991). This Tertiary mineralization is characterized by Ag-rich galena-sphalerite veins and includes the Prosperity, Porter-Idaho and Indian deposits (Alldrick 1991). Based on the Pb isotopic signature of these veins and the similarity in the styles of mineralization, these veins are interpreted to be of Tertiary age. Although Pb and Zn were not present in recoverable amounts at the Granduc deposit, Ag was recovered. It is possible that Tertiary Pb-Zn-Ag veins may have locally contributed to the silver content of the deposit.

Lithogeochemistry and Nd isotopic signatures

The Granduc Footwall, Mine and locally Lower Hangingwall Series contain mafic volcanic and volcaniclastic rocks of high-Mg basaltic to basaltic andesitic composition. The most primitive compositions occur at the southeast extreme of the Footwall Series and at the greatest depths in drill core; the most evolved compositions occur in the Mine Series and near the top of the drill holes, if this trend in the geochemical data is reflecting a fraction trend from less to more evolved affinities, it would suggest that this sequence was younging from east to west, towards the Mine Series. The Footwall Series is intruded by dioritic to quartz dioritic composition sills and dykes of comparable age and chemical compositions similar to those of the basaltic to andesitic volcanic and volcaniclastic rocks which they intrude, and these rocks have tholeiitic to transitional magmatic affinities.

Two samples, consisting of basalt from the Footwall Series and quartz diorite which intrudes it have similar REE patterns and initial ε_{Nd} values which are identical within error (+6.1 and +6.8, respectively) (Figs. 3.7 and 3.8). The light-REE enriched and heavy-REE depleted REE patterns suggest derivation from magmatic sources which are slightly enriched relative to MORB, and are consistent with formation in an oceanic back arc basin or an early, tholeiitic stage of island arc formation, and inconsistent with formation in either a mid-ocean ridge or continental margin setting. The primitive Nd isotopic signatures indicate that these rocks are the products of juvenile magmatic sources and have not interacted with significant amounts of old, evolved sialic crust. The similarities in age, Nd isotopic signature, and major, trace and rare earth element chemistry indicate that mafic volcanic and volcaniclastic rocks of the Granduc Mine and Footwall Series are probably comagmatic with the diorite to quartz diorite sills and dykes which intrude the Footwall Series.

Regionally, volcanic rocks of the Upper Triassic Stuhini Group have tholeiitic to calc-alkaline magmatic affinities and initial ε_{Nd} values of +1.3 to +7.7 (Figs. 3.5b and 3.8). Upper Triassic volcanic and intrusive rocks from Granduc lie at the more primitive end of the regional data set, both in terms of Zr/Y ratios and Nd isotopic signatures. Based on the available Nd data and the ages assigned to the rocks analyzed, these data suggest that Late Triassic mafic rocks of the Stuhini Group and Stikine Plutonic Suite become more evolved (i.e., tend towards lower

initial ε_{Nd} values) with time, which is consistent with the broad-scale maturation of an island arc (c.f. Donnelley 1968; Baker 1968; Gill 1970). These data indicate that to this point, economic VMS mineralization has been found in the oldest, and most chemically and isotopically primitive part of the Stuhini Group.

Comparison with the Late Triassic Windy Craggy deposit

The Alexander terrane is host to the world class mafic volcanic and sediment-hosted Early Norian Windy Craggy deposit, with reserves of 300 Mt of 1.4 % copper (Orchard 1986; Höy 1991; B.C. MINFILE #114P-002). The Granduc and Windy Craggy deposits, which formed more or less contemporaneously in different island arc terranes, both comprise copper-rich mineralization hosted within variably calcareous and argillaceous sedimentary and mafic submarine volcanic rocks which are intruded by diorite sills. Both deposits have similar ore mineralogy, including locally high concentrations of magnetite within the ore zones. However, the Windy Craggy deposit is significantly larger than the Granduc deposit. The two deposits differ in other respects as well; lithogeochemical analyses of mafic rocks from Windy Craggy have been interpreted by MacIntyre (1986) to have a calc-alkaline to alkaline affinity, with Zr/Y ratios mainly of 6 to 18 and REE patterns which show a strong LREE-enrichment relative to MORB. The range of Pb isotopic compositions determined for Windy Craggy mineralization is $^{207}Pb/^{206}Pb$ = 0.8332-0.8341, and $^{208}Pb/^{206}Pb$ = 2.037-2.040 (Peter, 1992); these values are markedly more radiogenic than those of syngenetic mineralization from the Granduc deposit. Windy Craggy has been interpreted to have formed within subaqueous rift valleys associated with spreading centers as part of a transform fault system adjacent to a continental mass, analogous to the present day Guaymas Basin (MacIntyre 1986). In comparison, mafic rocks from Granduc are mainly tholeiitic, with a lesser degree of LREE-enrichment, and the associated mineralization has a less evolved Pb isotopic signature. These comparisons suggest that VMS mineralization in the Granduc deposit formed in a more oceanic, or primitive tectonic setting than contemporaneous mineralization at Windy Craggy.

A model for the formation of the Granduc deposit

VMS mineralization at Granduc is interpreted to have accumulated within a subaqueous sediment-dominated sequence overlying a mafic volcanic pile. Contemporaneous, and probably comagmatic mafic intrusive rocks within the Footwall Series may be related to more extensive intrusions at depth, such as are seen to the north at the Bucke Glacier Stock, and may have acted as a heat source to drive a hydrothermal system. Kirkham (1979) has suggested that the bedded oxide-sulphide metalliferous sediments produced in the Red Sea brine deeps might be a possible modern day analogue to the Granduc deposit, and adopted Sato's (1972) model invoking expulsion of high density Type I brines from source vents. If these vents were located in areas of high relief on the paleo-seafloor, brines could have flowed downslope and pooled within local depressions, to produce distal, layered sulphide-oxide-silicate accumulations. Accumulation of sulphides by this mechanism is consistent with the apparent lack of hydrothermal alteration, and paucity of stringer mineralization within the volcanic pile underlying the Granduc ore lenses. This allows for the preservation of multiple ore lenses, such as those seen at Granduc, either by multiple, probably linear vents or within multiple localized depressions in which sulphides accumulated. The high degree of deformation precludes determining unequivocally if VMS mineralization at Granduc formed by the mechanism described above. However, this model is consistent with the observations made and data presented in this study.

Conclusions

Mafic volcanic rocks of the Granduc Footwall and Mine Series, and similar composition sills and dykes which intrude the Footwall Series, are of Late Triassic age and therefore are assigned to the Stuhini Group and Stikine Plutonic Suite, respectively. These volcanic and intrusive rocks are characterized by predominantly tholeiitic to transitional magmatic affinities, primitive Nd isotopic signatures and REE patterns which are slightly enriched relative to N- and E-MORB; the chemical signatures of these rocks suggest formation within an oceanic back arc basin or early stages of island arc magmatism. The similarity in age and isotopic and chemical signatures of the volcanic and intrusive rocks suggest that they are comagmatic. The age of igneous host rocks, along with a Pb isotopic signature of syngenetic mineralization which is less radiogenic than Jurassic and Tertiary mineralization in the region, supports a Late Triassic age for VMS mineralization at Granduc.

Plate 3. 2 Snow capped north face of Granduc Mountain.

Plate 3. 3 Granduc Glory Hole photo showing surface traces of the Granduc and Western faults and sample locations, looking northeast.

Plate 3. 4 massive basalt from the Granduc Footwall Series with weak pyrite veining.

Plate 3. 5 Moderately to strongly sheared sill cross cutting the Granduc Footwall Series.

Plate 3. 6 Strongly deformed limestone, Granduc Mine Series (hammer for scale).

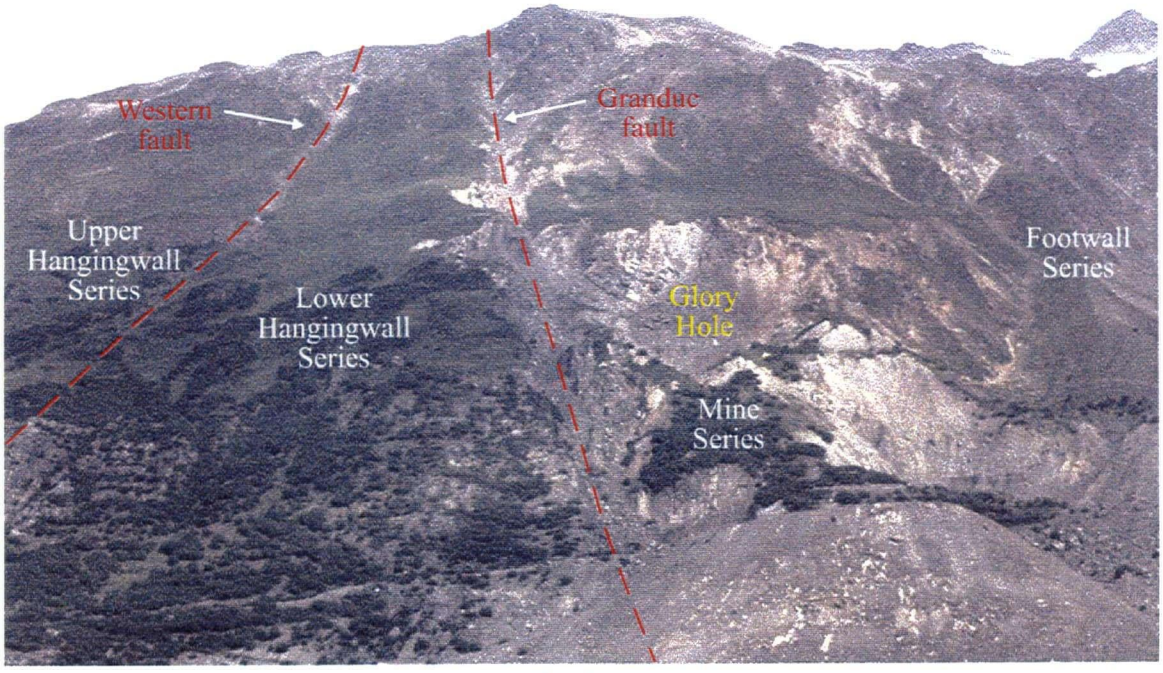

Plate 3.3

Plate 3.2

Plate 3.4

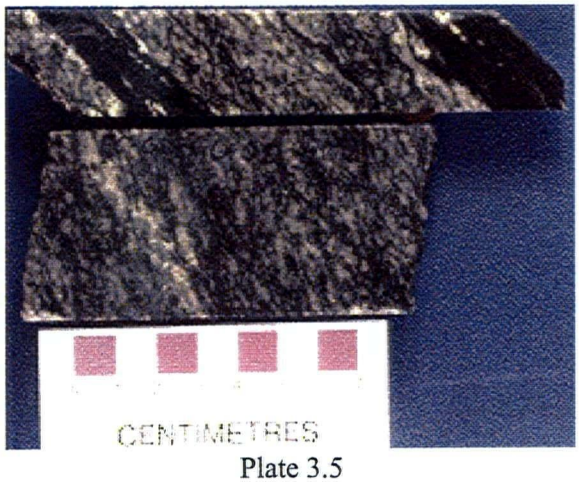

Plate 3.5

Plate 3.6

Plate 3. 7 Prismatic zircon, sample GD-GC-01, quartz diorite sill (grain length = 100μ)

Plate 3. 8 Equant zircon, sample GD-GC-04, Footwall Series basalt (grain length = 50μ)

Plate 3. 9 Ovoid zircon, sample GD-GC-08, Mine Series basaltic andesite (grain length = 100μ)

Plate 3. 10 Felsic volcanic fragmental rock, southeast flank of Granduc Mountain, close to locality of sample GD-GC-02 (hammer for scale).

Plate 3. 11 Semi-massive sulphides (pyrite, chalcopyrite, and pyrrhotite) within an argillaceous matrix, Granduc B orebody.

Plate 3. 12 Microcline-calcite-galena-sphalerite veins, which cross cut mafic volcanic rocks of the Granduc Footwall Series.

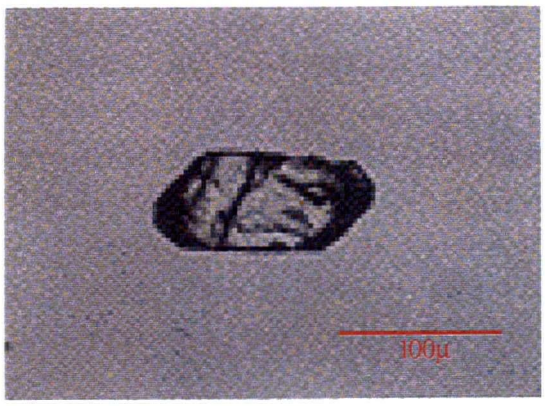

Plate 3.7

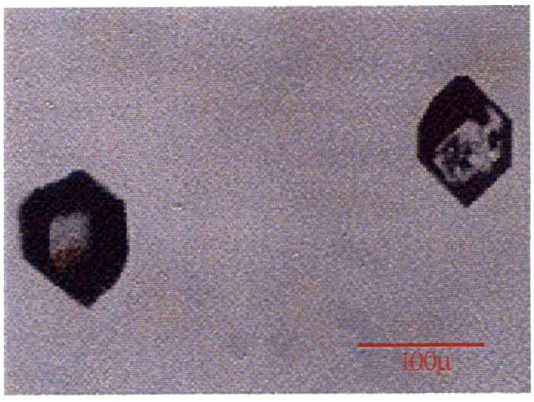

Plate 3.8

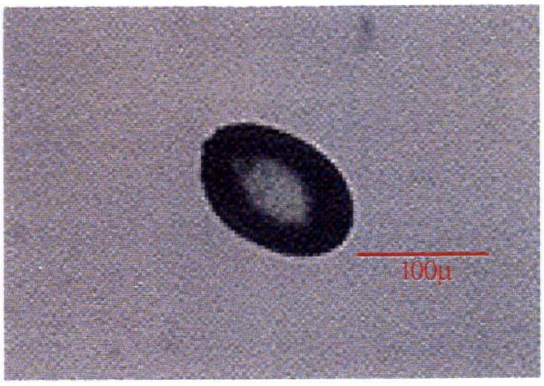

Plate 3.9

Plate 3.10

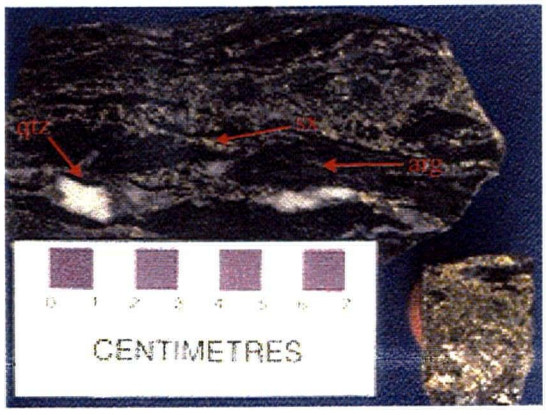

Plate 3.11

Plate 3.12

References

Anderson, R.G. 1989. A stratigraphic, plutonic and structural framework for the Iskut River map area, northwestern British Columbia. *In* Current Research, Part E, Geological Survey of Canada Paper 89-1E, pp. 145-154.

Anderson, R.G., and Bevier, M.L. 1992. New Late Triassic and Early Jurassic U-Pb zircon ages from the Hotailuh Batholith, cry Lake map area, north-central British Columbia. *In* Radiogenic Age and Isotopic Studies: Report 6; Geological Survey of Canada, Paper 92-2, pp. 145-152.

Anderson, R.G., and Thorkelson, D.J. 1990. Mesozoic stratigraphy and setting for some mineral deposits in Iskut River map area, northwestern British Columbia. *In* Current Research, Part E, Geological Survey of Canada, Paper 90-1F, pp. 131-139.

Alldrick, D.J. 1991. Geology and Ore Deposits of the Stewart Mining Camp. Ph.D. thesis, The University of British Columbia, Vancouver, 417p.

Baker, P.E. 1968. Comparative volcanology and petrology of the Atlantic island-arcs. Bulletin of Volcanology, **32**: 189-206.

Barrett, T.J., and MacLean, W.H. 1994. Chemostratigraphy and hydrothermal alteration in exploration for VHMS deposits in greenstones and younger volcanic rocks. *In* Alteration and Alteration Processes associated with Ore-forming Systems, Geological Association of Canada, Short Course Notes. *Edited by* D.R. Lentz, **11**: 433-467.

Brown, D.A. 1987. Geological setting of the Silbak Premier Mine, northwestern B.C. M.Sc. thesis, University of British Columbia, Vancouver, 216 p.

Brown, D.A., and Gunning, M.G. 1989. Geochemistry and mineral occurrences of the Scud River area, northwestern British Columbia (104G/5, 6). British Columbia Ministry of Energy, Mines and Petroleum Resources, Open File Map 1989-7.

Brown, D.A., Neill, I., Timmerman, J., Harvey-Kelly, F.E.L., Gunning, M.G., and Greig, C.J. 1992. Geology, mineral occurrences and geochemistry of the Tahltan Lake and Chutine River area (104G/12W, 13). British Columbia Ministry of Energy, Mines and Petroleum Resources, Open File Map 1992-2.

Childe, F.C. 1996. U-Pb geochronology and Nd and Pb isotopic characteristics of the Au-Ag-rich Eskay Creek VMS deposit, British Columbia. Economic Geology.

Davidson, D.A. 1960. Surface Geology at the Granduc Mine. M.A.Sc. thesis, The University of British Columbia, Vancouver, 106 p.

Dean, J.A., and Carr, G.R. 1991. Report to Prime Exploration on the lead isotopic compositions of samples from Galore Creek and Iskut River, British Columbia. *Unpublished Sirotope Report SR 154, CSIRO Australia*, 16 p.

Donnelley, T.W. 1968. Caribbean island arcs in light of the sea floor spreading hypothesis. Transactions of the New York Academy of Science, **30**: 745-750.

Dudas, M. 1973. Granduc Mine. *In* British Columbia Ministry of Energy, Mines and Petroleum Resources, Geology, Exploration and Mining in British Columbia, 1973, p. 497-499.

Dudas, M. and Grove, E.W. 1970. *In* British Columbia Ministry of Energy, Mines and Petroleum Resources, Geology, Exploration and Mining in British Columbia, 1970, p. 66-73.

Gill, J.B. 1970. Geochemistry of Viti Levu, Fiji, and its evolution as an island arc. Contributions to Mineralogy and Petrology, **44**: 179-203.

Grove, E.W. 1986. Geology and mineral deposits of the Unuk River-Salmon River-Anyox area; British Columbia Ministry of Energy, Mines and Petroleum Resources, Bulletin 63, 152 p.

Harland, W.B., Armstrong, R.L., Cox, A.V., Craig, L.E., Smith, A.G., and Smith, D.G. 1990. A Geological Time Scale, 1989, Cambridge University Press, Cambridge, 263 p.

Höy, T. 1991. Volcanogenic Massive Sulphide Deposits in British Columbia: in Ore Deposits, Tectonics and metallogeny in the Canadian Cordillera. British Columbia Ministry of Mines and Petroleum Resources, Paper 1991-4, pp. 89-123.

Jackson, J.L. 1990. Tectonic analysis of the Nisling, Northern Stikine and Northern Cache Creek terranes, Yukon and British Columbia. Ph.D. thesis, University of Arizona, Tucson, Arizona, 200 p.

Kaip, A.W. 1997. Geology, alteration, and mineralization on the Hank property, northwest British Columbia: A near-surface, low-sulphidation epithermal system, M.Sc. thesis, University of British Columbia, Vancouver, 198 p.

Kirkham, R.V. 1979. Copper in Iron Formation: *In* Current Research, Part B, Geological Survey of Canada, Paper 79-1B, p. 17-22.

Kerr, F.A. 1948. Lower Stikine and Iskut River Areas, British Columbia. Geological Survey of Canada, Memoir 246, 94 p.

Klepacki, D.W., and Read, P.B. 1981. Surface structural analysis, Granduc Mine area. Unpublished Report.

Krogh, T.E. 1982. Improved accuracy of U-Pb zircon ages by the creation of more concordant systems using an air abrasion technique. Geochemica and Cosmochemica Acta, **46**: 637-649.

Leach, W.W. 1909. The Bulkley Valley and vicinity, Geological Survey of Canada, Summary Report, 1908.

Lewis, P.D. 1992. Structural evolution of the Iskut River area: Preliminary Results. *In* Mineral Deposit Research Unit "Metallogeny of the Iskut River Area, British Columbia", Annual Technical Report Year 2, The University of British Columbia, Vancouver, British Columbia, 23p.

Lewis, P.D. 1994. Structural and Stratigraphic Setting of the South Unuk River / Granduc Mountain Area, Stewart Mining Camp, Northwestern British Columbia. *In* Mineral Deposit Research Unit "Volcanogenic Massive Sulphide Deposit Project", Annual Technical Report year 2, The University of British Columbia, Vancouver, British Columbia, 24p.

Logan, J. Koyanagi, V., and Rhys, D. 1989. Geology and mineral occurrences of the Galore Creek area (104G/3, 4). British Columbia Ministry of Energy, Mines and Petroleum Resources Open File Map 1989-8.

Ludwig, K.R. 1980. Calculation of uncertainties of U-Pb isotope data. Earth and Planetary Science Letters, **46**: 212-220.

Macdonald, A.J., Lewis, P.D., Thompson, J.F.H., Nadaraju, G., Bartsch, R.D., Bridge, D.J., Rhys, D.A., Kaip, A.W., Godwin, C.I., and Sinclair, A.J. 1996. Metallogeny of an Early to Middle Jurassic arc, Iskut River area, northwestern British Columbia. Economic Geology, **91**: 1098-1114.

MacIntyre, D.G. 1986. The geochemistry of basalts hosting massive sulphide deposits, Alexander terrane northwest British Columbia (114P). *In* British Columbia Ministry of Mines and Petroleum Resources, Paper 1996-1. *Edited by* W.J. McMillan, pp. 89-123.

Margolis, J., 1993. Geology and intrusion-related copper-gold mineralization, Sulphurets, British Columbia. Ph.D. thesis. University of Oregon, Eugene, 289 p.

Marsden, H., and Thorkelson, D.J. 1992. Geology of the Hazelton Volcanic Belt in British Columbia: Implications for the Early to Middle Jurassic Evolution of Stikinia. Tectonics, **11**: 1266-1287.

McGuigan, P.J., Melnyk, W., and Dawson, G.L. 1992. Compilation Report on the Granduc Property. Unpublished Report by Cambria Geological.

Melville, D.M., Faulkner, E.L., Meyers, R.E., Wilton, H.P., and Malot, M-L. 1992. 1991 Producers and Potential Producers, Mineral and Coal; British Columbia Ministry of Energy, Mines and Petroleum Resources, Open File 1992-1.

Monger, J.W.H. 1977. Upper Paleozoic Rocks of the Western Canadian Cordillera and their bearing on Cordilleran Evolution. Canadian Journal of Earth Sciences, **14**: 1832-1859.

Monger, J.W.H. 1980. Upper Triassic stratigraphy, Dease Lake and Tulsequah map areas, northwestern British Columbia. *In* Current Research, Part B, Geological Survey of Canada Paper 80-1b, p. 1-9.

Monger, J.W.H., and Berg, H.C. 1984. Part B--Lithotectonic terrane map of western Canada and southeastern Alaska; *In* Lithotectonic Terrane Maps of the North American Cordillera, *Edited by* N.J. Siberling and D.L. Jones, United States Geological Survey, Open-File Report 84-523.

Mortensen, J.K., Ghosh, D.K., and Ferri, P. 1995. U-Pb geochronology of intrusive rocks associated with Cu-Au deposits in the Canadian Cordillera. *In* Porphyry Deposits in the Northwestern Cordillera of North America. *Edited by* T.G. Schroter. **G-2**: 491-531.

Norman, G.W.H., and McCue, J., 1966. Relations of ore to fold patterns at Granduc, B.C., *In* Tectonic History and Mineral Deposits of the Western Cordillera; Canadian Institute of Mining and Metallurgy Special Volume 8, p. 305-314.

Orchard, M.J., 1986. Conodonts from western Canadian chert: Their nature, distribution and stratigraphic application, in Investigative Techniques and Applications. Ellis Horwood Ltd., Chichester, England, p. 94-119.

Peter, J.M. 1992. Comparative Geochemical Studies of the Upper Triassic Windy Craggy and Modern Guaymas Basin Deposits: A contribution to the understanding of massive sulphide formation in volcano-sedimentary environments. Ph.D. thesis, University of Toronto, Toronto, 235p.

Rhys, D.A. 1993. Geology of the Snip Mine, and its relationship to the magmatic and deformational history of the Johnny Mountain area, northwestern British Columbia. M.Sc. thesis, University of British Columbia, Vancouver, British Columbia, 278 p.

Samson, S.D., McClelland, W.C., Patchett, P.J., Gehrels, G.E., and Anderson, R.G. 1989. Evidence from neodymium isotopes for mantle contributions to Phanerozoic crustal genesis in the Canadian Cordillera. Nature, **337**: 705-709.

Sato, T. 1972. Behaviors of ore-forming solutions in seawater. Mining Geology, **22**, p. 31-42.

Souther, J.G. 1971. Telegraph Creek map-area. Geological Survey of Canada Paper 77-44, 34 p.

Steiger, R.H., and Jäger, E. 1977. Subcommission on geochronology: Convention on the use of decay constants in geo- and cosmochronology. Earth and Planetary Science Letters, **14**: 359-362.

Sun, S-S. and McDonough, W.F. 1989. Chemical and isotopic systematics of oceanic basalts; implications for mantle composition and processes. *In* Magmatism in the ocean basins, *Edited by* A.D. Saunders and M.J. Norry. Geological Society Special Publication **42**: 313-345.

Thériault, R., J. 1990. Methods for Rb-Sr and Sm-Nd isotopic analyses at the geochronology laboratory, Geological Survey of Canada. *In* Radiogenic Age and Isotopic Studies, Report 2, Geological Survey of Canada, Paper 89-2, pp. 3-6.

Woodsworth, G.J., Anderson, R.G., Armstrong, R.L., Struik, L.C., and van der Heyden, P. 1992. Plutonic Regimes. Chapter 15 *In* Geology of the Cordilleran Orogen in Canada, Geological Survey of Canada. *Edited by* H. Gabrielse and C.J. Yorath, p. 491-531.

York, D. 1969. Least-squares fit of a straight line with correlated errors. Earth and Planetary Science Letters, **5**: 320-324.

CHAPTER 4:

U-PB GEOCHRONOLOGY, GEOCHEMISTRY, AND RADIOGENIC ISOTOPIC CHARACTERISTICS OF THE KUTCHO ASSEMBLAGE, HOST TO THE KUTCHO CREEK DEPOSIT, AND RELATED TECTONIC SLIVERS WITHIN THE CANADIAN CORDILLERA

Plate 4.1. East face of Sumac Ridge, Kutcho Assemblage.

PART 1:

Geological Setting, U-Pb Geochronology, and Radiogenic Isotopic Characteristics of the Permo-Triassic Kutcho Assemblage, North-Central British Columbia

Abstract

The Kutcho Assemblage is a latest Permian to Early Triassic volcano-sedimentary sequence within the fault-bounded King Salmon Allochthon. Volcanic and volcaniclastic rocks consist of massive to pillowed flows and tuffs of basaltic to basaltic andesitic composition, as well as flows, mass flows, and pyroclastic flows of rhyodacitic to rhyolitic composition. The volcanic sequence is intruded by gabbro, diorite, trondhjemite and quartz-plagioclase porphyry. Volcanic and intrusive rocks have tholeiitic magmatic affinities, with the exception of the gabbro sills and dykes, which are chemically similar to alkaline arc magmas. Cu-Zn volcanogenic massive sulphide mineralization at the Kutcho Creek deposit is hosted by rhyolite mass flows near the top of the Kutcho Assemblage. Rhyolite mass flows from the hangingwall and footwall to mineralization have U-Pb ages of 242 +/-1 Ma and 246 +7/-5 Ma, respectively, whereas a quartz-plagioclase porphyritic intrusion to the south of the mineralization has a U-Pb age of 244 +/-6 Ma.

The age of the Kutcho Assemblage, and the primitive Pb isotopic signature of its contained massive sulphide mineralization ($^{207}Pb/^{206}Pb$ = 0.83988-0.84112 and $^{208}Pb/^{206}Pb$ = 2.0517-2.0556) are inconsistent with formation as part of the adjacent Stikine or Quesnel terranes. Primitive Nd isotopic signatures (initial ε_{Nd} = +7.5 to +7.8), and trace and rare earth element chemistry indicate that volcanic rocks of the Kutcho Assemblage, related intrusions and VMS mineralization formed in an intraoceanic island arc environment, probably directly on oceanic crustal basement. Gabbro sills and dykes, which are interpreted to be slightly younger than volcanic rocks of the Kutcho Assemblage, appear to have formed in response to a change in the tectonic regime, perhaps as a result of a collisional event.

Introduction

The Kutcho Assemblage, previously termed the Kutcho sequence and Kutcho Formation, occurs within the King Salmon Allochthon in north-central British Columbia. It is host to the Kutcho Creek Cu-Zn volcanogenic massive sulphide (VMS) deposit (Monger and Thorstad 1978; Bridge et al. 1986; Thorstad and Gabrielse 1986). The King Salmon Allochthon lies in thrust and fault contact with the island arc Stikine and Quesnel terranes, and the oceanic Cache Creek terrane (hereafter called Stikinia, Quesnellia and Cache Creek, respectively) (Fig. 4.1). The King Salmon Allochthon has been tectonically emplaced onto Cache Creek, which is a Mississippian to Jurassic oceanic melange composed of mafic to ultramafic volcanic and intrusive rocks, and thick sequences of shallow water carbonates, ribbon chert and argillaceous sediments (Monger et al. 1991). Stikinia and Quesnellia, which lie in fault contact with the King Salmon Allochthon, are Paleozoic and Mesozoic island-arc assemblages, consisting of mafic to felsic arc-related volcanic rocks and associated plutonic and sedimentary rocks (Monger et al. 1991). Stikinia is host to several significant VMS deposits, including the Tulsequah Chief, Granduc, and Eskay Creek deposits; VMS deposits of comparable size and grade are not known in Cache Creek or Quesnellia (Höy 1986).

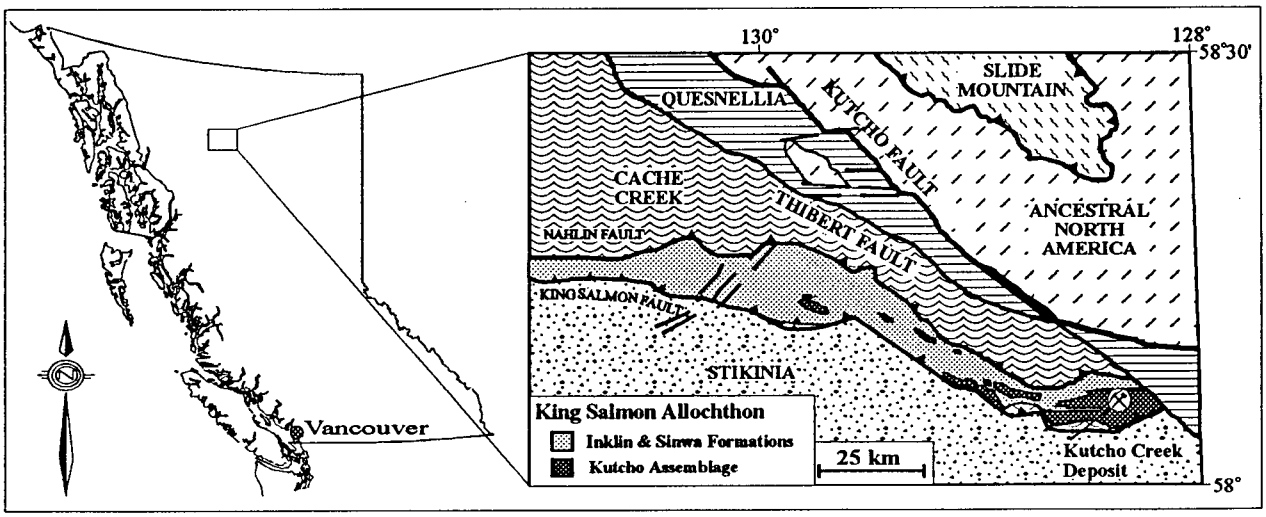

Figure 4. 1 Regional setting of the King Salmon Allochthon (modified from Thorstad and Gabrielse, 1986).

In this study, magmatic rocks of the Kutcho Assemblage were dated by U-Pb methods. Samples were also analyzed for their Nd isotopic signatures and major, trace and rare earth element compositions. Lead isotopic compositions were determined for their contained sulphides. The ages determined in this study are of regional significance, as they define the time period in which the Kutcho Assemblage formed, and they bracket the age of VMS mineralization at Kutcho Creek. Radiogenic isotopic compositions, and lithogeochemical and REE signatures determined in this study and parallel studies (Barrett et al. 1996) provide new information on the tectonic setting and terrane affiliation of the Kutcho Assemblage, and the environment of formation of the Kutcho Creek deposit. New constraints on the timing and setting of VMS mineralization at Kutcho Creek has implications for mineral exploration.

Geology of the King Salmon Allochthon

The King Salmon Allochthon is composed of three lithologically distinct packages of rocks. From oldest to youngest these are: 1) volcanic rocks of the Kutcho Assemblage; 2) limestone and marble which have been correlated with the Upper Triassic Sinwa Formation (Monger and Thorstad 1978); and 3) argillaceous sediments and siltstones which have been correlated with the Inklin Formation of the Lower Jurassic Laberge Group (Gabrielse 1962) (Fig. 4.1). The Kutcho Assemblage is intruded by gabbro, diorite, trondhjemite and quartz-plagioclase porphyry.

Previous studies on the Kutcho Assemblage include those by Gabrielse (1962) and (1978), Pearson and Panteleyev (1975), Panteleyev and Pearson (1976), Monger and Thorstad (1978), Thorstad (1983), and Thorstad and Gabrielse (1986). Extensive drilling, mapping and geophysical studies were conducted by Esso Minerals Canada and Sumitomo Metal Mining Co. Ltd. Results of this work are in part summarized by Bridge et al. (1986).

Kutcho Assemblage

Rocks of the Kutcho Assemblage can be broadly divided into southern and northern sequences (Fig. 4.2). The northern sequence, which hosts the Kutcho Creek deposit, consists of

northward younging rhyolitic mass flows and tuffs, overlain by fine-grained volcanic and sedimentary rocks, which are intruded by gabbro sills and dykes (Fig. 4.3). The southern sequence is compositionally bimodal and consists of basaltic and rhyolitic flows and tuffaceous sedimentary rocks, with minor argillite, cross-cut by mafic and felsic intrusive rocks. As a result of limited exposure and small scale folding and faulting within the central part of the Kutcho Assemblage, the relationship between the northern and southern sequences is unclear. The southern sequence may represent either a lower portion of the assemblage, or a fine-grained distal equivalent to the coarse, proximal mass flows of the northern sequence (P. Lewis, pers. comm. 1995).

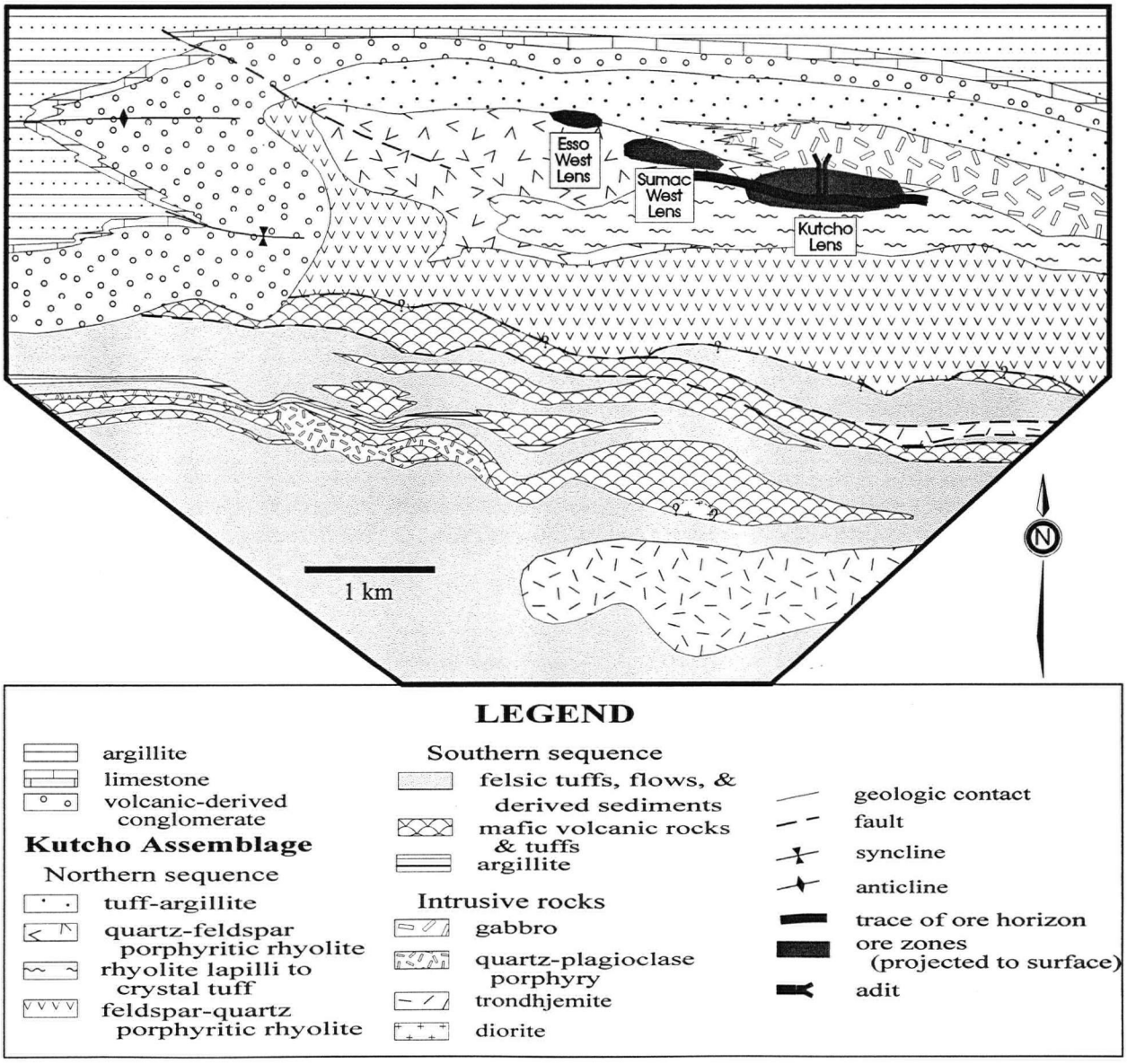

Figure 4. 2 Geology of the Kutcho Assemblage (modified from Holbek et al., 1991).

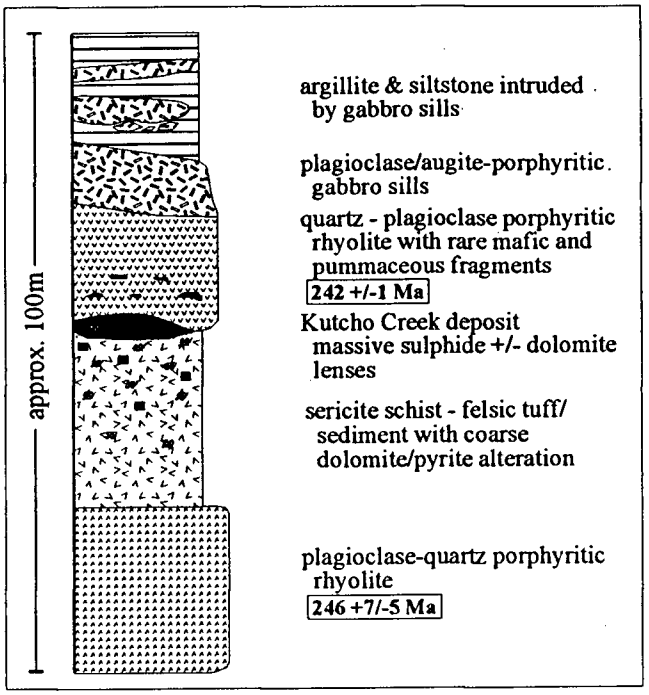

Figure 4. 3 Schematic stratigraphic section for the northern sequence of the Kutcho Assemblage.

Within the northern sequence, the oldest exposed unit consists of coarse-grained plagioclase-quartz porphyritic rhyolite fragmental rocks which are interpreted to have formed from mass flows and pyroclastic flows. Plagioclase is the dominant phenocryst, with lesser quartz and granophyric intergrowths of plagioclase and quartz (Plate 4.2). This unit is overlain by rhyolite lapilli and crystal tuffs, which form the immediate footwall to massive sulphide mineralization at Kutcho Creek. The hangingwall to mineralization consists of coarse-grained quartz-plagioclase porphyritic rhyolite fragmental rocks of probable mass flow origin; quartz phenocrysts are dominant and are characterized by numerous embayments and undulatory extinction (Plate 4.3). Rhyolite within the footwall and immediate hangingwall to mineralization has experienced intense sericite-pyrite-carbonate alteration which obscures primary textures (Plate 4.4). Where preserved, angular to rounded fragments up to 25 cm across occur in a crystal-rich matrix. Interbedded within the rhyolite mass flows in the hangingwall are rare mafic and pumiceous clasts (Plate 4.5). These clasts are flattened parallel to the regional east-west foliation which affects all rocks in the Kutcho Assemblage to varying degrees, and appear to occur along specific stratigraphic horizons.

The hangingwall rhyolite is overlain by bedded felsic tuffaceous rocks which grade upward into argillite. Coarse-grained plagioclase-augite porphyritic gabbro sills and dykes intrude the upper portion of the volcano-sedimentary sequence, at and above the rhyolite-sediment contact (Plate 4.6). Rare narrow porphyritic gabbroic dykes also occur lower in the sequence of rhyolite mass flows; these are interpreted to be feeders to the extensive sills emplaced higher in the stratigraphy. Interaction zones between the gabbro and rhyolite, and the local presence of peperitic textures at the contact between gabbro and argillite suggest that gabbro sills and dykes were emplaced prior to lithification of the upper tuffaceous rhyolitic units and the overlying argillite. Minor alteration of the lower portions of the gabbroic bodies suggest emplacement during the waning stages of hydrothermal activity.

Within the southern sequence, basalt occurs as massive to pillowed flows and tuffs, and rhyolite forms fine-grained quartz-plagioclase porphyritic flows, tuffs and coarse fragmental rocks. Thin beds of argillite occur as rare interbeds in the tuffaceous rocks; the presence of argillite and pillowed basalt indicate deposition of the Kutcho Assemblage in a subaqueous environment. Trondhjemite, quartz-plagioclase porphyry, and diorite intrude the southern sequence (Fig. 4.2).

The mineralogy and texture of felsic units which intrude the southern sequence are very similar to those of the rhyolite in the northern sequence. These units consist predominantly of quartz and plagioclase, with no potassium feldspar. In both the rhyolitic volcanic rocks and porphyry, quartz and plagioclase occur as individual phenocrysts or as glomerocrystic and granophyric intergrowths (Plates 4.2 and 4.8). Unlike the other felsic units, the trondhjemite intrusion has a medium-grained equigranular texture. However, quartz-plagioclase intergrowths similar to those observed in porphyritic units also occur in the trondhjemite.

Deformation in the Kutcho Assemblage is interpreted to have occurred in Jurassic time, contemporaneously with emplacement of the King Salmon Allochthon onto Cache Creek. Deformation resulted in a penetrative axial planar foliation and the formation of upright to overturned southwest vergent asymmetric to near isoclinal folds (Thorstad and Gabrielse 1986).

Sinwa and Inklin Formations

Tuff and argillite at the top of the northern sequence of the Kutcho Assemblage are capped by coarse conglomeratic sedimentary rocks, composed primarily of clasts of the underlying mafic and felsic volcanic rocks, as well as rare limestone clasts (Fig. 4.2). Conglomerate is interbedded with, and overlain by lenses of foliated limestone and finely crystalline marble. Limestone interbedded with the conglomerate was sampled for micropaleontological analysis in an attempt to constrain the age of sedimentation, but microfossils were not recovered.

Regionally, limestone which overlies the Kutcho Assemblage contains a sparse fauna of crinoids, corals, bryoza and pelecypods of probable Triassic age (Panteleyev 1977; Monger and Thorstad 1978). Upper Triassic index fossils reported by Panteleyev (1977) and Thorstad and Gabrielse (1986) from west of the Kutcho Assemblage include the bivalves *Lima* sp. (?), a probable *Palaeocardita*, (*Minetrigonia*, sp.) as well as a Mesozoic scleractinian coral; these rocks have been correlated with the Upper Triassic Sinwa Formation (Monger and Thorstad 1978) (Fig. 4.2).

Overlying the limestone, and locally directly overlying the Kutcho Assemblage, are thick sequences of argillite and siltstone (Monger and Thorstad 1978). These sedimentary rocks, which have not yielded fossils in the Cry Lake map area, have been correlated with the Inklin Formation of the Lower Jurassic Laberge Group, on the basis of lithology and regional relationships (Monger and Thorstad 1978; Gabrielse 1962) (Fig. 4.2).

Kutcho Creek deposit

Mineralization at the Kutcho Creek deposit consists of three massive sulphide lenses interpreted to lie at the same stratigraphic level; from east to west these are the Kutcho, Sumac West and Esso West zones (Bridge et al. 1986). The sulphide lenses are conformable to bedding, with a general strike of 280° and dips of 45° to 50° north (Bridge et al. 1986) (Fig. 4.2). The largest and closest to surface of the three is the Kutcho lens, with a length of 1400 meters and a maximum thickness of 27 meters, containing probable reserves of 14 Mt, grading 1.8% copper,

3.0% zinc, 28 g/t Ag and 0.34 g/t Au (Holbek et al. 1991). The smaller, and deeper Sumac West and Esso West lenses have reserves of 5.3 Mt of 1.1% copper, 1.6% zinc, 14 g/t Ag and 0.10 g/t Au, and 3.3 Mt of 3.4% copper, 5.6% zinc, 63 g/t Ag and 0.56 g/t Au, respectively (Holbek et al. 1991).

The lower margins of the sulphide lenses are gradational into pyrite-sericite-carbonate-altered lapilli to crystal tuffs (Bridge et al. 1986). Within the altered footwall, pyrite occurs as fine- to coarse-grained (1 mm to 1.5 cm) cubes; sericite is typically wispy and outlines the foliation in the rocks. Carbonate alteration consists of coarse-grained (0.5 to 1.5 cm) dolomite rhombs and fine-grained ankerite. The upper contacts of the lenses are typically sharp, and the immediate hangingwall to mineralization consists of coarse-grained quartz-plagioclase porphyritic rhyolite mass flows; localized alteration extends a short distance upwards into the hangingwall (Plate 4.4). The main sulphide minerals within the deposit are pyrite, sphalerite, chalcopyrite, and bornite, with minor chalcocite (Plate 4.9). Galena has been reported from within the sulphide lenses (Bridge et al. 1986), but we observed it only within cross cutting fractures during this study. Within the exploration adit a laminated dolomitic rock occurs as a discrete zone within massive sulphide of the Kutcho lens. This unit contains fine-grained disseminated sulphides, which in part define the laminations, and is brecciated and infilled with an assemblage of quartz-calcite-pyrite-bornite-covellite. The laminated dolomite facies is interpreted to be exhalitive in origin.

The Kutcho Creek deposit is jointly owned by Homestake Canada Ltd. and Sumac Mines Ltd. (controlled by Sumitomo Metal Mining Co. Ltd.). The Kutcho lens has been considered for open pit mining due to its proximity to surface, the general topography of the area and continuity of the orebody (Bridge et al 1986). However, location and lack of road access has made development of the Kutcho Creek deposit non-economic to this time.

Previous Correlations and Rb-Sr Geochronology

The Kutcho Assemblage was originally correlated with the Lower Permian Asitka Group of the Stikine terrane on the basis of lithological similarities and a Lower Permian Rb-Sr whole rock age of 275 $\pm$25 Ma (Panteleyev and Pearson 1976; Monger 1977). However, the presence

of gradational contacts with overlying limestones and a second Rb-Sr whole rock age of 210 ±10 Ma led Monger and Thorstad (1978) and Thorstad and Gabrielse (1986) to suggest that the Kutcho Assemblage was Upper Triassic in age. Thorstad and Gabrielse (1986) correlated the Kutcho Assemblage with Upper Triassic arc sequences, most notably the Takla Group, and concluded that the Kutcho Assemblage could have formed as an island arc built directly on Cache Creek. An Upper Triassic age designation for the Kutcho Assemblage implied that mineralization at Kutcho Creek formed in the same time interval as several other significant VMS deposits in the North American Cordillera, including the Windy Craggy (Orchard 1986), Greens Creek (Newberry et al. 1990) and Granduc (Childe et al. 1994) deposits. The Upper Triassic age assignment and correlations with VMS deposits elsewhere in the Cordillera is inconsistent with U-Pb zircon geochronology presented in this paper.

U-Pb Geochronology of the Kutcho Assemblage

Three units were dated using U-Pb zircon methods in the Geochronology Laboratory at the University of British Columbia. Samples included quartz-plagioclase porphyritic rhyolite from the immediate hangingwall to the Kutcho Creek deposit (KC-GC-01) and plagioclase-quartz porphyritic rhyolite from the footwall of the deposit (KC-GC-04), both from within the northern sequence, and quartz-plagioclase porphyry which intrudes the southern sequence (KC-GC-03) (Figs. 4.2 and 4.3). Multiple samples of the trondhjemite and hangingwall gabbro were also collected for U-Pb dating, but failed to yield zircon or other dateable minerals.

Heavy mineral extraction procedures and U-Pb zircon analytical procedures follow those of Mortensen et al. (1995). Isotopic ratios were measured using a modified single collector VG-54R thermal ionization mass spectrometer equipped with a Daly photomultiplier. Uranium and Pb analytical blanks were in the range of 1-2 and 6-15 picograms, respectively. Concordia intercept ages and associated errors were calculated using a modified York-II regression model (York 1969), and the algorithm of Ludwig (1980); ages were calculated using the decay constants recommended by Steiger and Jäger (1977). Age assignments follow the time scale of Harland et al. (1990), except for the age of the Permo-Triassic boundary, which follows the designation of Renne et al. (1995). Analytical results are given in Table 4.1 and shown graphically in Figure 4.4.

Fraction[1]	Wt.	U	Pb[2]	^{206}Pb[3]	Pb[4]	^{208}Pb[5]	Isotopic ratios(±1σ,%)[6]			Isotopic dates(Ma,±2σ)[6]		
	mg	ppm	ppm	^{204}Pb	pg	(%)	$^{206}Pb/^{238}U$	$^{207}Pb/^{235}U$	$^{207}Pb/^{206}Pb$	$^{206}Pb/^{238}U$	$^{207}Pb/^{235}U$	$^{207}Pb/^{206}Pb$
hangingwall quartz-plagioclase porphyritic rhyolite (KC-GC-01)												
C,m,N1,p,t	0.096	137	5	2242	14	6.2	0.03791±0.10	0.2668±0.26	0.05104±0.18	239.9±0.5	240.1±1.1	242.8±8.5
K,f,M1,p	0.096	157	6	1656	21	7.0	00.03738±0.15	0.2627±0.28	0.05097±0.18	236.6±0.7	236.8±1.2	239.6±8.4
M,m,N1,p	0.717	138	5	3290	72	6.6	0.03755±0.45	0.2648±0.48	0.05114±0.13	237.7±2.1	238.5±2.1	247.0±6.0
N,m,N1,p	0.280	140	5	3611	27	6.7	0.03822±0.15	0.2689±0.24	0.05102±0.13	241.8±0.7	241.8±1.0	241.8±6.0
O,m,N1,p	0.101	145	5	2916	12	6.8	0.03818±0.31	0.2686±0.39	0.05102±0.20	241.5±1.5	241.5±1.7	241.8±9.2
P,f,N1,p	0.072	151	5	1774	15	6.5	0.03737±0.45	0.2633±0.52	0.05111±0.21	236.5±2.1	237.3±2.2	245.7±9.8
footwall plagioclase-quartz porphyritic rhyolite (KC-GC-04)												
A,m,N2,p	0.165	80	3	651	46	6.4	0.03690±0.16	0.2595±0.55	0.05101±0.47	233.6±0.7	234.3±2.3	241.1±21.7
D,m,N2,p	0.598	79	3	718	155	6.5	0.03704±0.12	0.2611±0.40	0.05112±0.32	234.5±0.5	235.6±1.7	246.3±14.7
E,m,M2,p	0.424	74	3	656	111	8.7	0.03722±0.12	0.2624±0.566	0.05113±0.49	235.6±0.5	236.6±2.3	246.8±22.6
F,m,N2,p	0.630	78	3	989	123	6.8	0.03842±0.35	0.2704±0.54	0.05116±0.33	243.0±1.7	243.0±2.3	242.7±16.8
G,m,N2,p	0.170	73	3	691	43	6.7	0.03747±0.13	0.2646±0.38	0.05122±0.33	237.2±0.6	238.4±1.6	250.6±13.0
H,f,N2,p	0.036	90	3	731	10	6.8	0.03624±0.17	0.2552±0.56	0.05108±0.48	229.5±0.7	230.8±2.3	244.6±21.9
plagioclase-quartz porphyry (KC-GC-03)												
D,m,M1,p	0.192	103	4	649	71	8.2	0.03687±0.18	0.2601±0.44	0.05116±0.33	233.4±0.8	234.7±1.8	247.9±15.2
E,f,N1,p	0.368	101	4	1164	74	7.8	0.03641±0.10	0.2562±0.27	0.05102±0.19	230.6±0.5	231.6±1.1	241.6±8.6
F,m,N1,p	0.303	76	3	1080	51	7.4	0.03728±0.11	0.2626±0.29	0.05110±0.21	235.9±0.5	236.8±1.2	245.2±9.5

[1]All fractions are air abraded; Grain size, smallest dimension: m=-134μm+74μm, f=-74μm;
Magnetic codes: Franz magnetic separator sideslope at which grains are nonmagnetic; e.g., N1=nonmagnetic at 1°; Field strength for all fractions =1.8A; Front slope for all fractions=20°; Grain character codes: p=prismatic, t=tips
[2]Radiogenic Pb
[3]Measured ratio corrected for spike and Pb fractionation of 0.0043/amu ±20% (Daly collector)
[4]Total common Pb in analysis based on blank isotopic composition
[5]Radiogenic Pb
[6]Corrected for blank Pb, U and common Pb (Stacey-Kramers model Pb composition at the $^{207}Pb/^{206}Pb$ date of fraction, or age of sample)

Table 4 1 U-Pb zircon analytical data for samples from the Kutcho Assemblage.

Zircons from the three units were visually and chemically similar. Zircons were small and prismatic (length:width = 2:1 to 3:1), with few inclusions, good clarity, and no visible cores, but numerous fractures and generally rough surfaces. Only the best quality grains, free of opaque inclusions were selected, and all zircon fractions were abraded prior to analysis (Krogh 1982).

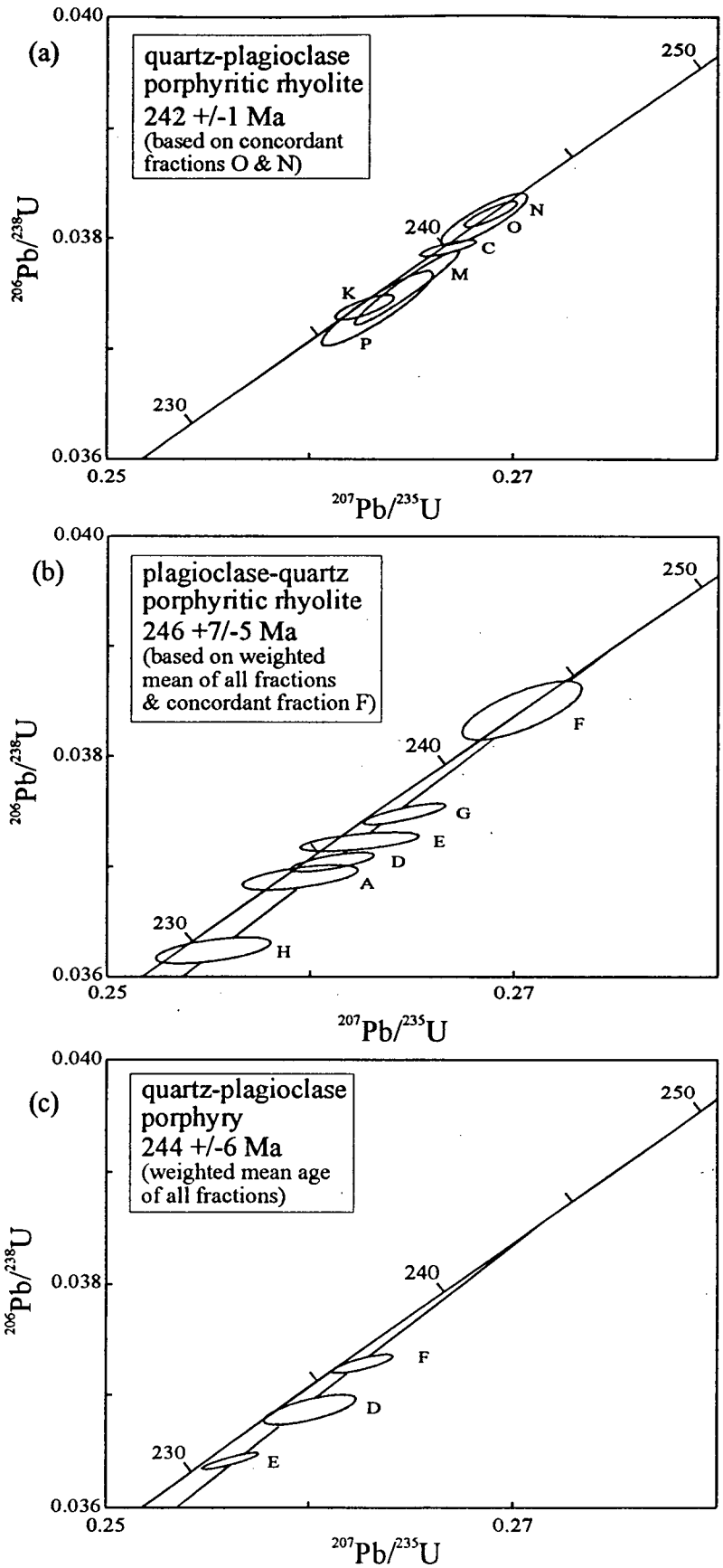

Figure 4. 4 U-Pb concordia plots of a) hangingwall quartz-plagioclase porphyritic rhyolite (KC-GC-01); b) footwall plagioclase-quartz porphyritic rhyolite (KC-GC-04); and c) quartz - plagioclase porphyry (KC-GC-03).

Hangingwall quartz-plagioclase porphyritic rhyolite (KC-GC-01)

Analysis of six fractions of zircon from this rock yielded $^{207}Pb/^{206}Pb$ ages of 240 to 247 Ma (Table 4.1, Fig. 4.4a). Fractions O and N were overlapping and concordant; all other fractions were slightly discordant, probably as a result of post-crystallization Pb-loss. An Earliest Triassic age of 242 +/-1 Ma was calculated for this unit based on the $^{206}Pb/^{238}U$ ages and errors of the two concordant fractions.

Footwall plagioclase-quartz porphyritic rhyolite (KC-GC-04)

Analysis of six fractions of zircon from this rock yielded $^{207}Pb/^{206}Pb$ ages of 241 to 251 Ma (Table 4.1, Fig. 4.4b). Fraction F was concordant, whereas all other fractions were slightly discordant, probably as a result of post-crystallization Pb-loss. The weighted mean of the $^{207}Pb/^{206}Pb$ ages of all six fractions from this unit is 246 +/-7 Ma. A weighted mean age is considered valid for this rock due to the restricted range of $^{207}Pb/^{206}Pb$ ages and the lack of visible cores within the zircon. An Earliest Triassic age of 246 +7/-5 Ma, based on the $^{207}Pb/^{206}Pb$ weighted mean age and upper intercept error of all fractions and the upper error limit for the $^{206}Pb/^{238}U$ age of concordant fraction F, is considered to be the best estimate of the age of this unit.

Quartz-plagioclase porphyry (KC-GC-03)

Analysis of three fractions of zircon from this rock yielded $^{207}Pb/^{206}Pb$ ages of 242 to 248 Ma (Table 4.1, Fig. 4.4c). All fractions were slightly discordant, probably as a result of post-crystallization Pb-loss. Because of the restricted range of $^{207}Pb/^{206}Pb$ ages and the lack of visible cores within zircon from this rock, the weighted mean $^{207}Pb/^{206}Pb$ age of all fractions (244 +/-6 Ma) is considered to be the best estimate of the age of this unit.

Zircon geochemistry

Zircon from all three units are characterized by low U concentrations; this feature is consistent with the low concentrations of high field strength and rare earth elements in rocks of

the Kutcho Assemblage (Tables 4.1 and 4.2). In addition, there is a strong positive correlation between the weight of individual zircon fractions and the total common Pb in each analysis (Table 4.1), indicating that the source of the common Pb may have been in the zircon crystals themselves, perhaps as microinclusions of colourless minerals with high common Pb concentrations, such as feldspar or apatite. The combination of low U concentrations and increasing common Pb with sample size contributed to relatively low ratios of radiogenic to common Pb ($^{206}Pb/^{204}Pb$) in zircon from the Kutcho Assemblage.

Lithogeochemistry

Major, trace, and rare earth (REE) element concentrations were determined for volcanic rocks of the Kutcho Assemblage and intrusions that cross cut it (Table 4.2). The chondorite-normalized Ce/Yb ratio (Ce_n/Yb_n) is used to describe the slope of the REE patterns, and therefore the degree of evolution of the rocks.

Rocks of the Kutcho Assemblage are compositionally bimodal, comprising basalt to basaltic andesite and their intrusive equivalents (SiO_2 = 45 to 55%), and rhyodacite to rhyolite and their intrusive equivalents (SiO_2 = 65 to 80%) (Table 4.2). On the basis of chemical composition these rocks can be divided into four main groups: 1) felsic volcanic and intrusive rocks; 2) mafic volcanic rocks and related intrusions; 3) gabbro sills and dykes; and 4) compositionally distinctive mafic, pumiceous, and dacitic fragments and basalt.

Felsic volcanic and intrusive rocks

Rhyodacite and rhyolite are compositionally indistinguishable from trondjhemite and quartz-plagioclase porphyry (Table 4.2). These rocks are characterized by low concentrations of K and high field strength elements (HFSE) (i.e. Th, U, Zr, Hf), high concentrations of Na, and Zr/Y ratios of 2.2-4.0. (Table 4.2 and Fig. 4.5). Rhyolite, trondhjemite, and quartz-plagioclase porphyry have near-flat REE patterns (Ce_n/Yb_n = 0.7-1.0), low overall REE concentrations, and negative Eu anomalies, the latter being consistent with plagioclase fractionation (Fig. 4.6a). Both the REE signatures and Zr/Y ratios of these rocks indicate a tholeiitic magmatic affinity.

Table 4.2 Major, trace, and rare earth element data for samples from the Kutcho Assemblage.

Sample Number	Lithology	SiO2 %	TiO2 %	Al2O3 %	Fe2O3 %	MnO %	MgO %	CaO %	Na2O %	K2O %	P2O5 %	LOI	Total
KC-GC-01	HW qtz + plag porph. rhyolite	77.40	0.27	12.11	2.16	0.02	0.42	1.88	4.45	0.89	0.05	0.88	100.60
KC-GC-02	quartz + plag porphyry	71.25	0.51	13.51	4.46	0.08	1.20	2.34	4.80	0.25	0.09	1.89	100.40
KC-GC-03	trondhjemite	77.22	0.25	12.54	2.48	0.08	0.16	0.06	5.54	0.95	0.04	1.34	100.70
KC-GC-04	FW plag + qtz. porph. rhyolite	80.22	0.13	11.73	1.06	0.04	0.57	0.04	5.95	0.06	0.02	0.79	100.60
KC-GC-05	gabbro sill	47.57	0.80	11.76	12.79	0.22	8.02	11.55	2.76	2.59	0.77	1.94	100.90
KC-GC-06	gabbro sill	53.36	0.61	18.37	8.09	0.17	2.88	5.62	3.77	4.15	0.60	2.47	100.28
KC-GC-07	trondhjemite	74.16	0.50	13.55	3.37	0.05	0.98	0.26	6.05	0.14	0.09	1.22	100.39
KC-GC-08	gabbro sill	51.68	0.61	18.19	8.27	0.20	3.17	6.80	3.31	3.58	0.60	3.62	100.13
JTK-1	felsic fragment	77.67	0.21	10.17	3.26	0.06	0.41	3.70	3.00	0.66	0.04	1.44	100.66
JTK-2	mafic fragment	62.13	0.55	15.50	4.35	0.10	2.36	3.84	3.92	2.53	0.07	4.96	100.38
JTK-4	quartz + plag porphyry	72.86	0.54	13.43	3.68	<dl	0.81	1.73	5.67	0.29	0.12	1.27	100.47
JTK-6	chlorite schist	48.00	0.59	16.70	9.28	0.16	8.24	9.25	3.89	0.10	0.05	4.22	100.55
JTK-8	biotite - chlorite schist	63.78	0.63	15.62	6.66	0.14	2.89	1.22	5.56	1.38	0.08	2.54	100.54
JTK-11	rhyolite	76.47	0.40	12.51	2.62	0.13	0.19	0.16	5.78	0.08	0.07	1.41	99.83
JTK-13	basalt	47.90	1.11	16.40	11.05	0.21	7.92	9.58	2.88	0.03	0.12	3.51	100.79
JTK-18	basalt	50.28	0.81	16.59	9.77	0.14	8.79	7.24	3.40	0.12	0.09	3.40	100.72
JTK-19	quartz + plag porphyry	76.91	0.25	12.43	2.30	0.03	0.33	0.12	6.12	0.92	0.04	0.78	100.26
JTK-20	rhyolite	76.28	0.38	12.21	3.15	0.19	1.03	0.12	5.73	0.10	0.07	1.16	100.50
JTK-22	quartz + plag porphyry	66.08	0.57	14.64	6.39	0.16	3.01	1.79	5.50	0.16	0.08	2.62	101.03
JTK-27	plag. porphyritic fragment	64.77	0.44	14.62	6.48	0.09	3.62	4.45	2.53	0.93	0.10	2.61	100.70
JTK-28	pumiceous fragment	48.88	0.58	17.36	8.63	0.31	2.91	8.29	1.18	4.18	0.08	7.67	100.18
JTK-29	mafic fragment	44.36	0.51	15.96	6.48	0.28	1.95	13.25	2.47	3.36	0.07	11.05	99.84
JTK-30	gabbro dyke/sill	51.48	0.71	16.47	9.15	0.26	6.25	5.70	3.00	1.19	0.89	5.61	100.82
JTK-31	mafic fragment	41.20	0.94	14.34	7.41	0.32	8.62	8.46	3.69	0.10	0.06	14.19	99.49
JTK-34	vesicular basaltic flow	46.76	0.64	16.49	9.73	0.15	7.57	9.17	2.77	0.02	0.05	7.11	100.54
JTK-39	diorite	48.52	1.31	15.52	11.90	0.18	7.49	9.00	3.47	0.12	0.13	2.92	100.67
JTK-45	tuffaceous sediment	49.06	1.87	15.07	12.78	0.19	5.93	9.36	3.08	0.07	0.16	2.99	100.64
JTK-48	tuffaceous sediment ?	49.11	0.67	14.33	8.63	0.19	6.80	13.82	2.04	0.05	0.07	5.06	100.88
90-K11-44.2m	rhyolite	78.13	0.12	10.60	2.78	0.03	0.18	0.63	5.97	0.07	0.02	1.46	100.04
90-K11-46.6m	vesicular basaltic flow	55.23	2.01	14.28	11.36	0.18	5.02	3.69	6.13	0.04	0.28	2.19	100.48
90-K11-132.6m	fine tuffaceous sediment ?	45.59	1.31	15.91	9.51	0.12	6.63	11.56	3.76	0.03	0.11	5.00	99.64
90-K11-214.9m	fine tuffaceous sediment	61.46	0.46	17.67	4.87	0.08	2.16	3.21	7.17	0.31	0.11	1.91	99.44
90-K11-443.2m	basalt	47.44	1.13	16.20	10.04	0.16	7.92	11.25	2.86	0.05	0.10	3.01	100.28
detection limit		60 ppm	35 ppm	120 ppm	30 ppm	30 ppm	95 ppm	15 ppm	75 ppm	25 ppm	35 ppm		

Table 4.2 (con't).

Sample Number	BaO ppm	Co ppm	Cr2O3 ppm	V ppm	Cu ppm	Ni ppm	Zn ppm	Ga ppm	Nb ppm	Rb ppm	Sr ppm	Pb ppm	Th ppm	U ppm	Y ppm	Zr ppm
KC-GC-01	126	37	<dl	37	45	<dl	63	12.0	4.0	12.0	71.0	<dl	<dl	2.0	39.0	125.0
KC-GC-02	57	25	16	58	166	16	50	15.0	4.0	2.0	102.0	<dl	<dl	2.0	43.0	110.0
KC-GC-03	276	45	2	21	14	<dl	90	15.0	5.0	9.0	39.0	<dl	<dl	3.0	55.0	175.0
KC-GC-04	13	42	<dl	10	24	<dl	55	12.0	5.0	1.0	21.0	<dl	<dl	2.0	52.0	138.0
KC-GC-05	532	39	249	350	153	40	114	16.0	1.0	61.0	441.0	4.0	1.0	2.0	17.0	55.0
KC-GC-06	1125	27	15	162	292	5	168	18.9	3.0	73.8	708.5	4.7	2.2	<dl	22.3	87.9
KC-GC-07	60	34	<dl	37	13	<dl	66	13.5	5.0	<dl	37.3	<dl	<dl	<dl	36.5	132.4
KC-GC-08	495	27	22	170	238	5	161	17.6	4.4	63.9	267.6	8.2	1.3	<dl	22.6	86.7
JTK-1	322	36	11	36	9	3	43	12.0	4.0	8.0	73.0	<dl	<dl	2.0	47.0	103.0
JTK-2	290	6	22	61	9	8	110	15.0	2.0	32.0	50.0	<dl	<dl	6.0	73.0	44.0
JTK-4	34	17	<dl	44	12	<dl	98	13.0	4.0	4.0	104.0	<dl	<dl	1.0	46.0	100.0
JTK-6	39	36	232	272	73	52	83	15.0	1.0	1.0	226.0	<dl	<dl	4.0	14.0	24.0
JTK-8	234	10	<dl	155	28	<dl	110	17.0	3.0	11.0	39.0	<dl	<dl	6.0	25.0	78.0
JTK-11	<dl	25	<dl	14	23	<dl	89	14.0	5.0	1.0	49.0	<dl	<dl	2.0	42.0	121.0
JTK-13	24	34	254	331	5	43	100	16.0	2.0	2.0	156.0	3.0	<dl	9.0	21.0	45.0
JTK-18	23	31	407	274	43	80	109	15.0	2.0	2.0	106.0	<dl	<dl	8.0	18.0	39.0
JTK-19	300	25	<dl	19	2	<dl	61	14.0	6.0	9.0	36.0	<dl	<dl	3.0	44.0	175.0
JTK-20	3	18	13	22	85	1	669	14.0	5.0	2.0	34.0	<dl	<dl	3.0	32.0	119.0
JTK-22	7	25	<dl	104	10	<dl	94	15.0	4.0	2.0	67.0	<dl	<dl	5.0	23.0	79.0
JTK-27	183	38	74	154	58	8	91	12.1	3.6	13.9	121.3	<dl	<dl	<dl	29.1	80.8
JTK-28	553	36	27	272	85	14	165	23.2	3.0	60.0	102.5	7.2	<dl	<dl	25.9	15.7
JTK-29	571	23	43	264	103	7	125	19.4	2.6	55.8	122.7	<dl	<dl	<dl	28.6	16.9
JTK-30	129	21	178	199	336	34	278	16.3	5.1	11.9	239.6	12.7	<dl	<dl	18.2	63.6
JTK-31	88	39	351	172	519	69	358	15.3	3.6	<dl	51.5	1.8	<dl	<dl	31.6	49.3
JTK-34	70	31	288	244	58	49	91	13.2	2.8	<dl	260.2	<dl	<dl	<dl	10.6	16.9
JTK-39	148	43	244	384	78	33	104	16.5	3.1	<dl	225.8	<dl	<dl	<dl	21.3	49.1
JTK-45	148	33	148	359	37	21	112	17.9	3.3	<dl	103.2	<dl	<dl	<dl	27.1	72.1
JTK-48	69	32	552	249	51	83	90	14.5	2.9	<dl	222.8	1.0	<dl	<dl	12.8	28.0
90-K11-44.2m	<dl	31	39	0.0	441	<dl	123	14.7	5.0	<dl	27.5	<dl	<dl	<dl	96.4	224.8
90-K11-46.6m	139	34	60	263	64	16	134	18.0	3.2	<dl	59.4	<dl	<dl	<dl	54.4	185.1
90-K11-132.6m	95	47	376	281	108	92	115	16.3	3.4	<dl	116.4	<dl	<dl	<dl	28.7	76.1
90-K11-214.9m	67	18	19	68	68	6	79	16.3	5.1	1.8	116.9	<dl	<dl	<dl	8.0	50.8
90-K11-443.2m	108	34	522	285	49	93	97	14.8	3.5	<dl	98.4	<dl	<dl	<dl	20.2	52.2
detection limit	17 ppm	10 ppm	15 ppm	10 ppm	2 ppm	3 ppm	2 ppm	1 ppm	1 ppm	1 ppm	1 ppm	1 ppm	1 ppm	1 ppm	1 ppm	1 ppm

Table 4.2 (con't).

Sample Number	Hf ppm	Sc ppm	Ta ppm	Th ppm	U ppm	W ppm	La ppm	Ce ppm	Nd ppm	Sm ppm	Eu ppm	Tb ppm	Yb ppm	Lu ppm
KC-GC-01	3.8	8.9	1.1	0.9	0.5	262	5.1	17	12	3.15	0.56	0.8	4.28	0.62
KC-GC-02	2.9	14.0	0.8	0.8	0.6	181	5.3	15	12	3.71	1.03	1.0	5.18	0.73
KC-GC-03	4.6	6.8	0.6	1.0	0.7	168	9.5	29	19	4.33	0.73	1.0	5.83	0.84
KC-GC-04	2.9	10.8	1.1	0.4	0.5	260	3.6	13	10	3.50	0.67	1.2	6.49	0.93
KC-GC-05	1.0	37.9	0.3	1.5	0.8	73	8.2	20	12	2.85	0.92	0.5	1.39	0.20
JTK-18	0.8	36.9	<dl	0.2	0.3	14	1.8	5	4	1.44	0.53	0.5	1.68	0.25
JTK-34	1.5	27.1	<dl	<dl	<dl	32	4.5	13	10	3.36	1.19	0.9	3.12	0.43
detection limit	0.2 ppm	0.1 ppm	0.3 ppm	0.1 ppm	0.1 ppm	1 ppm	0.1 ppm	1 ppm	1 ppm	0.01 ppm	0.05 ppm	0.1 ppm	0.05 ppm	0.01 ppm

Mafic volcanic rocks and related intrusions

Basalt to basaltic andesite and diorite have low concentrations of both HFSE and large ion lithofile elements (LILE) (i.e. K, Ba, Rb, Sr, Pb) and Zr/Y ratios of 2.1-3.4 (Table 4.2 and Fig. 4.5). A sample of basalt (JTK-18) has low overall concentrations of REE and a slightly light REE depleted pattern ($Ce_n/Yb_n = 0.8$) (Fig. 4.6b). Similar to felsic rocks of the Kutcho Assemblage, mafic volcanic and related intrusive rocks have Zr/Y ratios and a REE pattern indicative of a tholeiitic magmatic affinity.

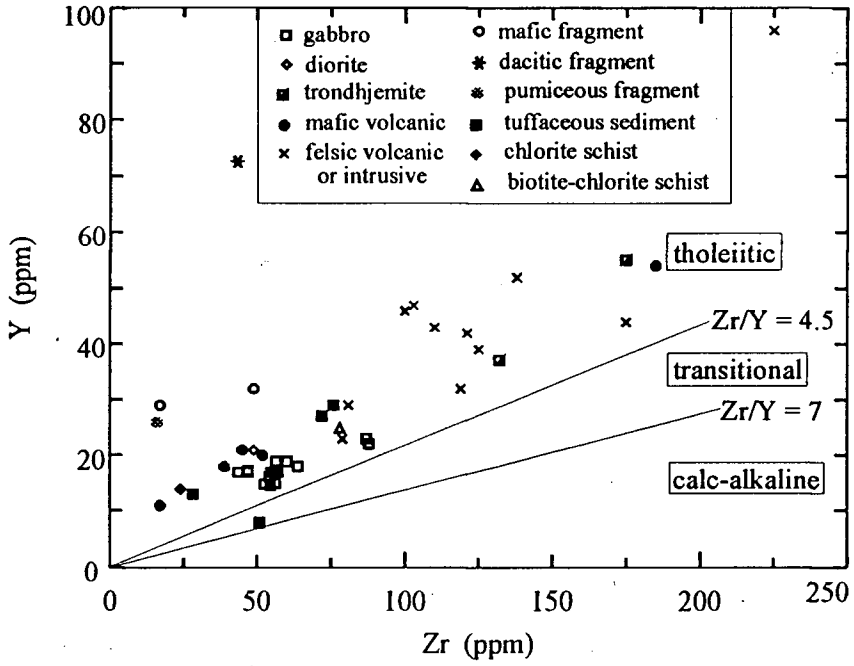

Figure 4. 5 Plot of Y *versus* Zr (fields from Barrett and MacLean, 1994).

Gabbro sills and dykes

The chemical signature of the gabbro is distinct from that of mafic volcanic rocks of the Kutcho Assemblage. Gabbro has low concentrations of HFSE and Zr/Y ratios of 2.6-3.9, but high concentrations of P, Cu and LILE (Table 4.2 and Fig. 4.5). On a plot of P_2O_5 vs. K_2O the fields for gabbro and basalt are distinct from each other, with gabbro having high P_2O_5 and variable K_2O, whereas basalt has both low P_2O_5 and K_2O (Fig. 4.7).

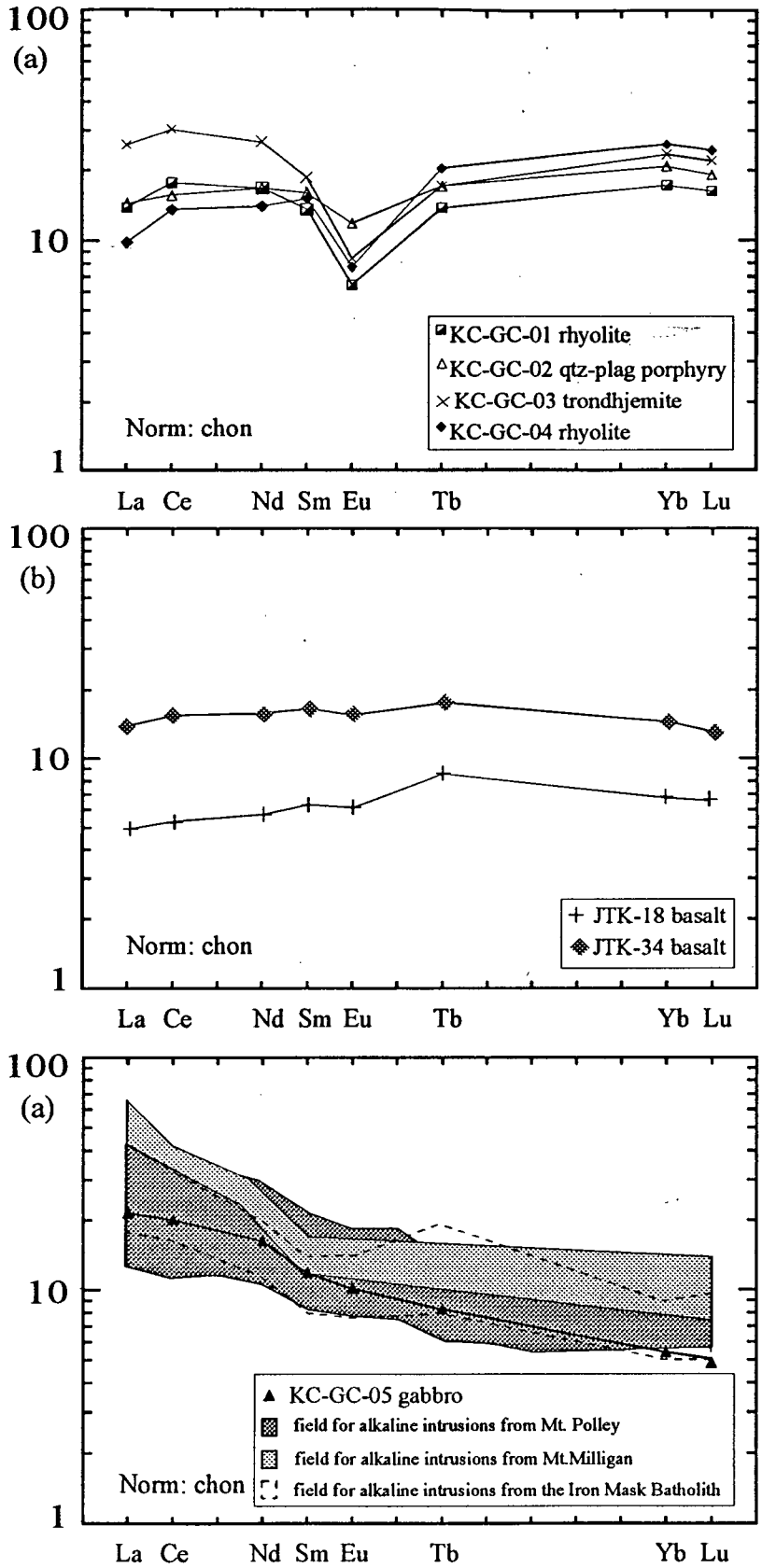

Figure 4. 6 REE plots of a) felsic volcanic and intrusive rocks; b) mafic volcanic rocks; and c) gabbro, fields of data from alkaline mafic rocks in Quesnellia at Mt. Polley (Fraser et al. 1995), Mt. Milligan (Barrie 1993), and the Iron Mask Batholith (Snyder and Russell 1995) are shown for comparison.

Gabbro is depleted in heavy-REE relative to light-REE, with a near-constant slope that decreases from La to Lu ($Ce_n/Yb_n = 3.6$) (Fig. 4.6c). This pattern is significantly more evolved than those of volcanic rocks of the Kutcho Assemblage and is comparable to patterns determined for alkaline arc magmas which intrude the northern Cordillera (Fig. 4.6c). On a plot of alkali vs. silica the gabbroic sills and dykes have an alkaline affinity; in comparison, volcanic rocks of the Kutcho Assemblage and related felsic intrusions have a predominantly subalkaline affinity (Fig. 4.8).

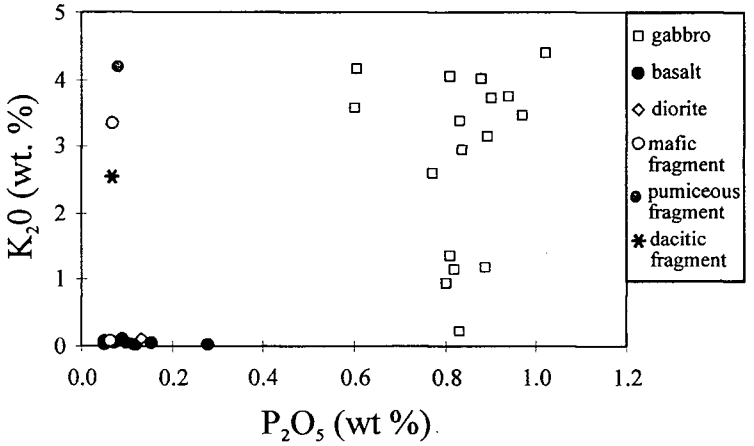

Figure 4. 7 Plot of K_2O *versus* P_2O_5 which differentiates tholeiitic basalt in the Kutcho Assemblage from gabbroic rocks which intrude the upper part of the assemblage and clasts in felsic fragmental units.

Compositionally distinctive mafic, dacitic, and pumiceous fragments and basalt

A distinct group of mafic to intermediate composition volcanic rocks is recognized on the basis of extremely low Zr/Y ratios (0.6-1.6) (Table 4.2 and Fig. 4.5). This group consist of dacitic (JTK-2), mafic (JTK-29, -31) and pumiceous (JTK-28) fragments interbedded with rhyolite mass flows of the northern sequence, and a vesicular basaltic flow (JTK-34) (Plate 4.5). The basalt from this group has a near-flat REE pattern ($Ce_n/Yb_n = 1.1$), with slightly higher light REE concentrations than the other sample of basalt analyzed in this study (Fig. 4.6b). Sample JTK-28, -29, and -31 have high concentrations of alkali earths, whereas the other two have low concentrations (Fig. 4.9). The rocks from this group with the lowest Zr/Y ratios (0.6; JTK-2, -28, -29) have high concentrations of K and other LILE, the range of which overlap those of the gabbro, but low P concentrations, comparable to those of the basalts (Table 4.2 and Fig. 4.7); the rocks with slightly higher Zr/Y (1.6; JTK-31, -34) are more similar to basalt of the Kutcho Assemblage.

It is unclear from these data whether these mafic, dacitic, and pumiceous fragments and basalt represent the most primitive end member of mafic volcanic rocks in the Kutcho Assemblage, or if they are a second, extremely primitive alkaline to subalkaline basalt type characterized by low Zr/Y ratios but variable major element chemistry.

Nd isotope data

The Nd isotopic signatures of hangingwall rhyolite and gabbro from the northern sequence, and trondhjemite and quartz-plagioclase porphyry from the southern sequence were determined to further constrain potential magmatic source regions. Neodymium isotopic analyses were conducted by R. Thériault at the Geochronology Laboratory of the Geological Survey of Canada. Analytical procedures are described by Thériault (1990). Analytical uncertainty is ± 0.5 ε_{Nd} unit; abundances of Sm and Nd were determined by isotope dilution and have an uncertainty of 1% or less.

High positive initial ε_{Nd} values of +7.5 to +9.1 for the five units analyzed attest to the primitive nature of volcanic and related intrusive rocks in the Kutcho Assemblage (Table 4.3). In Figure 4.8 these values are compared with those of island arc and oceanic terranes which now lie in proximity to the Kutcho Assemblage. The Nd isotopic signature of felsic rocks of the Kutcho Assemblage are comparable to those of mafic rocks of the Nicola Group (+6.8 to +7.8) and Fennel Formation (+7.7 to +10.2), the most primitive mafic rocks of the Stuhini Group (+1.3 to +7.7), and mafic to intermediate composition alkaline arc magmas which intrude Quesnellia and northern Stikinia (+2.7 to +7.9) (Samson et al. 1989; Jackson 1990; Smith and Lambert 1995; Cassidy et al. 1996; Childe *this volume*) (Fig. 4.9). Rhyolite from the Sitlika Assemblage, in central British Columbia has a comparable Nd signature to those determined in this study, whereas Paleozoic and Jurassic rocks from Stikinia have more evolved signatures (Samson et al. 1989; Childe 1997; Childe and Schiarizza 1997; Childe *this volume*) (Fig. 4.8).

Table 4 3 Neodymium isotopic data for samples from the Kutcho Assemblage.

Sample	Sm (ppm)	Nd (ppm)	$^{147}Sm/^{144}Nd$	meas. $^{143}Nd/^{144}Nd$ (error x 10^{-6}, 2σ)	ε_{Nd}[2] (present day)	age[1] (Ma)	ε_{Nd}[2] (initial)
KC-GC-01 HW quartz porphyritic mass flow	3.69	11.84	0.1884	0.513024 (5)	+7.5	245	+7.8
KC-GC-02 trondhjemite	3.88	11.93	0.1966	0.513029 (5)	+7.6	245	+7.6
KC-GC-03 quartz + plagioclase porphyritic felsic intrusive	5.22	19.88	0.1586	0.512969 (5)	+6.6	245	+7.8
KC-GC-05 HW gabbro	3.77	14.97	0.1521	0.512942 (9)	+6.1	245	+7.5
JTK-34 basaltic flow	3.58	10.51	0.2058	0.513117 (12)	+9.4	245	+9.1

[1]used for the calculation of ε_{Nd} (initial).
[2]error = $\pm$0.5 ε_{Nd} units.

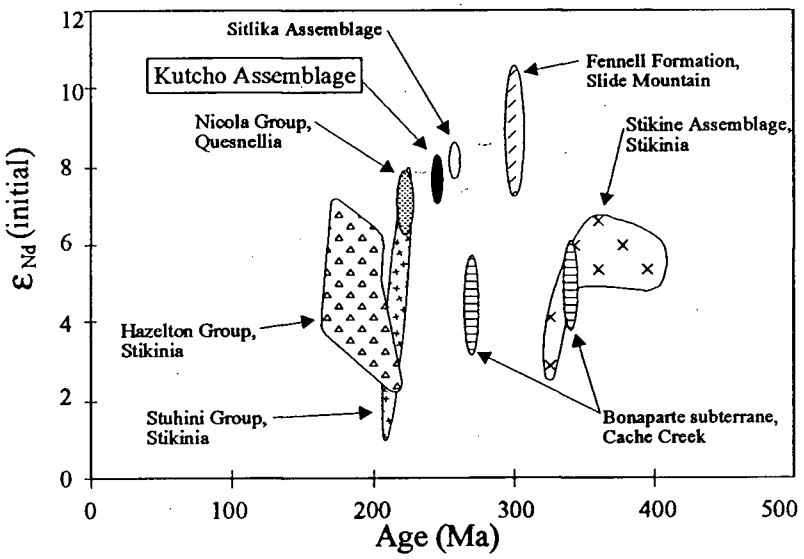

Figure 4. 8 ε_{Nd}(initial) *versus* age plot of rhyolite from the Kutcho Assemblage, and trondhjemite, quartz-plagioclase porphyry, and gabbro intrusions. Shown for comparison are fields for various volcanic assemblages in the Canadian Cordillera (Stikine Assemblage and Stuhini Groups: Samson et al., 1989; Jackson, 1990; Childe, this volume; Hazelton Group: Samson et al., 1989, Bevier and Anderson, pers. comm., 1995; Childe, 1997; Sitlika Assemblage, Childe and Schiarizza, 1997; Bonaparte subterrane: Jackson, 1990; Smith and Lambert, 1995; Fennell Formation: Smith and Lambert, 1995).

Pb isotope data

Lead isotopic compositions were determined for copper- and iron-rich sulphides from the Kutcho, Esso West and Sumac West lenses. Analytical procedures are outlined in Childe (*this volume*), and analytical results are given in Table 4.4 and Figure 4.9.

Table 4 4 Lead isotopic data for samples from the Kutcho Assemblage.

SAMPLE NUMBER	SAMPLE LOCATION	MIN. [1]	$^{206}Pb/^{204}Pb$ (% error) [2,3]	$^{207}Pb/^{204}Pb$ (% error) [2,3]	$^{208}Pb/^{204}Pb$ (% error) [2,3]	$^{207}Pb/^{206}Pb$ (% error) [2,3]	$^{208}Pb/^{206}Pb$ (% error) [2,3]
K1a	Kutcho lens	bn	18.514 (0.037)	15.568 (0.037)	38.039 (0.038)	0.84089 (0.004)	2.0546 (0.005)
K1c	Kutcho lens	bn	18.508 (0.037)	15.561 (0.031)	38.044 (0.041)	0.84080 (0.020)	2.0556 (0.019)
K1d	Kutcho lens	cp	18.471 (0.018)	15.520 (0.017)	37.895 (0.020)	0.84022 (0.007)	2.0517 (0.007)
K2a	Sumac West lens	py	18.584 (0.086)	15.614 (0.079)	38.128 (0.089)	0.84000 (0.034)	2.0520 (0.024)
K3a	Esso West lens	py+cp	18.434 (0.107)	15.507 (0.107)	37.872 (0.108)	0.84123 (0.014)	2.0545 (0.012)
K3b	Esso West lens	py	18.494 (0.324)	15.555 (0.324)	37.986 (0.325)	0.84112 (0.020)	2.0540 (0.019)
K4b	Esso West lens	py	18.377 (0.345)	15.451 (0.344)	37.774 (0.346)	0.84075 (0.025)	2.0538 (0.023)
K6b	Sumac West lens	bn	18.510 (0.032)	15.546 (0.029)	37.990 (0.033)	0.83988 (0.012)	2.0524 (0.010)

[1] mineral abbreviations: py=pyrite, bn=bornite, cp=chalcopyrite.
[2] errors are quoted at the 2σ (95% confidence) level.
[3] values are corrected for instrument fractionation by normalization based on replicate analyses of the NBS-981 standard

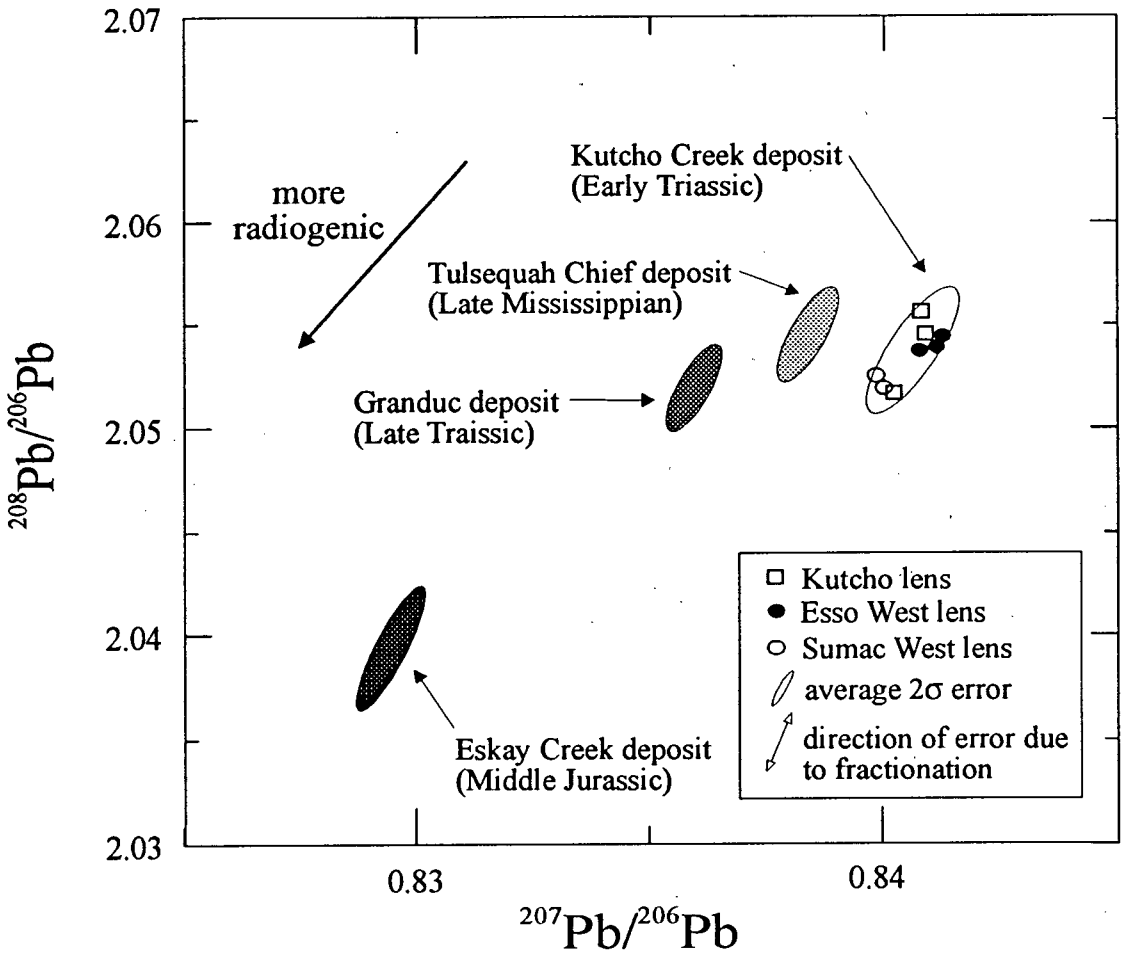

Figure 4. 9 $^{207}Pb/^{206}Pb$ *versus* $^{208}Pb/^{206}Pb$ plot of sulphides from the Kutcho Creek deposit. Shown for comparison are fields for the Tulsequah Chief, Granduc and Eskay Creek deposits (Childe, 1997; Childe et al., 1994; Childe, 1994).

Sulphides from the Kutcho Creek deposit have a restricted range of Pb isotopic compositions, with no distinction between values for the three sulphide lenses. For comparison, the Pb isotopic signature of Kutcho Creek mineralization is plotted relative to Early Mississippian to Middle Jurassic VMS deposits in Stikinia (Fig. 4.9) (Childe 1997; Childe *this volume*). The Pb isotopic signature of Permo-Triassic Kutcho Creek mineralization is distinctly more primitive than Mississippian to Jurassic VMS mineralization in Stikinia.

Discussion

Age of volcanic and intrusive rocks

U-Pb dating indicates that rhyolite from the top of the northern sequence has an Early Triassic age of 242 +/-1 Ma, whereas rhyolite from the base of the northern sequence and porphyry which intrudes the southern sequence have ages of 246+7/-5 and 244 +/-6 Ma, respectively, which overlap the Permo-Triassic boundary. The Early Triassic age of 242 +/-1 Ma from the northern sequence constrains the minimum age of volcanism in the Kutcho Assemblage (Fig. 4.3). Within terranes of island arc affinity in the Cordillera, such as Stikinia and Quesnellia, the Late Permian to Early Triassic typically corresponds to a hiatus in volcanism, marked by regional unconformities (Gabrielse and Yorath 1991). The discrepancy between the age of the Kutcho Assemblage and island arc assemblages of Stikinia and Quesnellia suggests that the Kutcho Assemblage did not form as part of one of these terranes (Childe et al. submitted).

The absolute age of the gabbro, which is chemically distinct from rocks of the majority of the Kutcho Assemblage remains unconstrained. However, rhyolite which is cross cut by the gabbro is dated at 242 +/-1 Ma and therefore provides a maximum age for the gabbro. In addition, field observations indicate that the gabbro was emplaced prior to both lithification of the stratified rocks that overlie the Kutcho Assemblage and cessation of the hydrothermal system associated with VMS mineralization. Consequently, the gabbro sills and dykes are interpreted to be only slightly younger than the felsic volcanic rocks which they intrude.

Lithogeochemistry and Nd isotopic signatures

Basalt of the Kutcho Assemblage, and diorite which intrudes it have low-K tholeiitic compositions; a sub-group of basaltic to dacitic fragments and basalt is characterized by lower Zr/Y ratios and variable K concentrations. Rhyodacite and rhyolite of the Kutcho Assemblage, and trondhjemite and quartz-plagioclase porphyry which intrude it are low-K, high-Na tholeiites. The Zr/Y ratios and REE patterns of the felsic volcanic rocks are indistinguishable from those of the felsic intrusive rocks, and indicate derivation from tholeiitic magmatic sources. The Nd isotopic signatures of rhyolite, trondhjemite and quartz-plagioclase porphyry indicate derivation from primitive sources, with little or no interaction with old, evolved sialic crustal components. The similarity in age, mineralogy, Nd isotopic signature, and trace, major and rare earth element chemistry suggests that volcanic rocks of the Kutcho Assemblage and felsic intrusions which cross cut it are cogenetic.

Gabbro has a high initial ε_{Nd}, comparable to values determined for felsic volcanic rocks of the Kutcho Assemblage. However, the major and REE chemistry of these high-K alkaline gabbros is more evolved than that of mafic volcanic and related intrusions of the Kutcho Assemblage, and are chemically and isotopically similar to Triassic to Jurassic alkaline (shoshonitic) arc magmas which intrude Quesnellia and northern Stikinia (Barrie 1993; Mortimer 1987; Lang et al. 1995; Mortensen et al. 1995).

Kutcho Creek deposit

The Kutcho Creek VMS deposit is hosted by rhyolite mass flows in the northern sequence of the Kutcho Assemblage. The coarse, angular nature of rhyolite clasts, the lack of sorting and the presence of pumiceous fragments within the northern sequence indicates that VMS mineralization formed proximal to a felsic volcanic source. The Kutcho Creek deposit has previously been described as having aspects of both a Besshi-type deposit (Pearson and Panteleyev 1975), based primarily on the recognition of concordant, bedded cupriferous iron sulphide lenses, and a Kuroko-type deposit (Thorstad and Gabrielse 1986), based on the association of massive sulphide mineralization with thick sequences of what were interpreted to be predominantly calc-alkaline felsic volcaniclastic rocks, in a bimodal volcanic sequence. However,

the Cu-Zn-rich and Pb-poor metal suite, the lack of sulphate facies, and host rocks consisting of low-K tholeiitic rhyolite are fundamentally different from either Besshi- or Kuroko-type deposits.

The U-Pb zircon ages of 242 +/-1 Ma and 246+7/-5 Ma determined for rhyolites from the northern sequence bracket the age of VMS mineralization at Kutcho Creek (Fig. 4.3). The Pb isotopic signature of Kutcho Creek mineralization is more primitive than signatures of Paleozoic to Jurassic VMS deposits in Stikinia, implying that Pb, and by implication other metals in the Kutcho Creek deposit were derived from more primitive sources than metals in VMS deposits in Stikinia. A latest Permian to Early Triassic age implies that the Kutcho Creek deposit did not form contemporaneously with Upper Triassic VMS deposits elsewhere in the Cordillera, and the isotopic data indicates that the Kutcho Assemblage and its contained mineralization is unlikely to have formed as part of Stikinia.

Tectonic setting

The primitive trace and rare earth element chemistry, and Nd isotopic signature of volcanic rocks from the Kutcho Assemblage suggests formation in an intraoceanic island arc built directly on oceanic crustal basement (Childe et al. submitted). Compositionally bimodal volcanic rocks, which are chemically and mineralogically similar to the Kutcho Assemblage have been documented by Vallier (1995) in the Blue Mountains Region of the northwestern United States. Vallier (1995) suggests that these rocks may have formed in the fore-arc portion of an intraoceanic island arc; Barrett et al. (1996) and Childe et al. (submitted) suggest that the Kutcho Assemblage may have formed in a similar tectonic environment. Cu-Zn VMS mineralization formed proximal to a felsic volcanic center near the end of this volcanic episode.

Following rhyolitic volcanism, and during the waning stages of hydrothermal activity, gabbro dykes and sills intruded the upper part of the volcanic sequence and overlying volcano-sedimentary rocks. The gabbroic rocks have the chemical signature of alkaline arc magmas, in contrast with the low-K tholeiitic signature of the underlying felsic and mafic rocks. Alkaline arc magmas commonly form in complex tectonic settings related to subduction or post-subduction processes such as collision (e.g. Box and Flowers 1989; Barrie 1993; Lang et al. 1995; Cassidy et al. 1996). The Tabar-Feni chain of volcanic islands consists of alkaline arc magmas

compositionally similar to those which intrude the Kutcho Assemblage (Wallace et al. 1983; Kennedy et al. 1990; McInnes and Cameron 1994). The Tabar-Feni chain occurs in a fore-arc position and is interpreted to have formed following collision of the Ontong-Java oceanic plateau with the subduction zone and consequent cessation of subduction (McInnes and Cameron 1994). Although a collisional origin for the gabbroic rocks which intrude the Kutcho Assemblage cannot be demonstrated, a fore-arc setting similar to Tabar-Feni appears likely. Regardless, the chemistry of the gabbroic rocks which intrude the upper part of the Kutcho Assemblage strongly suggests that a tectonic change occurred immediately after formation of massive sulphide mineralization and the deposition of extensive rhyolitic mass flow deposits.

Conclusions

The Kutcho Assemblage consists of compositionally bimodal tholeiitic volcanic rocks of latest Permian to Early Triassic age. The volcanic sequence is intruded by compositionally similar diorite, trondhjemite and quartz-plagioclase porphyry, as well as alkaline gabbro. The age and Nd isotopic signature of volcanism, and the Pb isotopic signature of VMS mineralization indicate that the Kutcho Assemblage did not form as part of Stikinia or Quesnellia. The Kutcho Assemblage and contained mineralization is interpreted to have formed as part of an intraoceanic island arc. Gabbro which intrudes it may have formed in response to a change in the tectonic environment.

Table 4.5 Major and trace element data for 14 additonal samples of gabbro which intrude the Kutcho Assemblage.

Sample Number	Lithology	SiO2 %	TiO2 %	Al2O3 %	Fe2O3 %	MnO %	MgO %	CaO %	Na2O %	K2O %	P2O5 %	LOI	Total
90-K27-116m	gabbro	49.06	0.71	13.27	11.48	0.20	7.25	10.25	2.70	2.96	0.84	1.62	100.50
E-53, 58.5m	gabbro	47.12	0.71	13.47	9.86	0.19	6.39	7.53	3.26	4.01	0.88	6.12	99.72
E-53, 100m	gabbro	48.38	0.62	16.17	8.72	0.15	4.92	7.34	3.86	1.35	0.81	8.26	100.72
E-53, 118m	gabbro	44.26	0.66	14.18	9.82	0.18	6.5	9.63	2.69	0.24	0.83	11.48	100.62
KT50, 60m	gabbro	47.99	0.83	12.68	12.94	0.21	8.14	10.82	0.79	3.39	0.83	1.78	100.63
86, 5.3m	gabbro	51.53	0.60	17.49	8.53	0.15	3.15	7.16	3.06	4.05	0.81	3.29	100.04
KT30, 44.5m	gabbro	50.59	0.76	14.62	11.19	0.19	6.22	7.88	3.10	3.46	0.97	1.37	100.56
KT30,64m	gabbro	47.23	0.81	15.51	12.20	0.19	6.79	6.87	2.71	4.38	1.02	2.57	100.50
KT30,101.5m	gabbro	50.03	0.71	14.45	10.30	0.19	5.68	8.45	2.63	3.74	0.90	3.06	100.33
KT30,150m	gabbro	50.50	0.73	14.09	11.01	0.19	6.26	7.95	3.18	3.14	0.89	1.95	100.10
KT30,180m	gabbro	49.50	0.75	13.80	11.57	0.20	7.02	8.17	2.53	3.75	0.94	2.07	100.51
KT30,201.5m	gabbro	45.97	0.68	12.01	10.70	0.21	6.57	10.02	1.90	1.15	0.82	10.17	100.40
KT30,224m	gabbro	46.02	0.63	15.08	9.36	0.16	5.81	6.35	4.54	0.95	0.80	10.61	100.45
detection limit		60 ppm	35 ppm	120 ppm	30 ppm	30 ppm	95 ppm	15 ppm	75 ppm	25 ppm	35 ppm		

Sample Number	BaO ppm	Co ppm	Cr2O3 ppm	V ppm	Cu ppm	Ni ppm	Zn ppm	Ga ppm	Nb ppm	Rb ppm	Sr ppm	Pb ppm	Th ppm	U ppm	Y ppm	Zr ppm
90-K27-116m	459	37	364	280	247	62	151	15.2	3.4	64.8	274.4	5.3	2.9	1.1	17.3	47.0
E-53, 58.5m	258	36	281	267	646	51	215	15.3	3.1	102.8	279.2	6.2	<dl	<dl	17.0	54.7
E-53, 100m	126	33	163	195	606	35	211	16.2	3.8	21.5	258.5	7.8	<dl	<dl	16.9	55.8
E-53, 118m	33	34	253	241	663	56	219	15.1	3.3	4.2	335.7	15.2	<dl	<dl	14.8	52.7
KT50, 60m	893	33	298	360	434	48	181	15.5	1.7	71.4	667.9	6.9	0.9	1.1	17.0	43.7
86, 5.3m	1010	23	57	181	654	12	216	16.1	2.3	75.8	986.3	7.9	<dl	<dl	14.6	54.5
KT30, 44.5m	575	38	258	275	637	46	219	15.3	1.8	71.2	714.2	9.6	<dl	1.1	17.5	56.7
KT30,64m	636	36	258	292	648	51	237	16.9	2.1	92.3	756.7	9.7	1.1	1.0	18.9	60.3
KT30,101.5m	624	32	240	254	489	44	185	14.9	2.8	78.2	342.9	8.5	<dl	1.5	17.4	56.4
KT30,150m	616	41	258	262	656	51	218	14.9	2.6	65.5	499.0	7.5	<dl	0.5	17.0	57.3
KT30,180m	658	36	297	274	542	54	209	15.4	3.0	76.1	339.5	8.5	<dl	2.3	18.9	56.6
KT30,201.5m	397	29	347	231	591	181	212	13.6	3.2	16.0	164.1	4.3	<dl	0.2	16.2	54.2
KT30,224m	269	30	165	199	452	32	191	15.4	4.3	13.2	124.7	2.3	<dl	<dl	15.0	56.4
detection limit	17 ppm	10 ppm	15 ppm	10 ppm	2 ppm	3 ppm	2 ppm	1 ppm	1 ppm	1 ppm	1 ppm	1 ppm	1 ppm	1 ppm	1 ppm	1 ppm

References

Barrett, T.J., and MacLean, W.H. 1994. Chemostratigraphy and hydrothermal alteration in exploration for VHMS deposits in greenstones and younger volcanic rocks. *In* Alteration and Alteration Processes associated with Ore-forming Systems: Geological Association of Canada, Short Course Notes. *Edited by* D.R. Lentz, **11**: 433-467.

Barrett, T.J., Thompson, J.F.H., and Sherlock, R.L. 1996. Geology and Geochemistry of the Kutcho Creek VMS deposit, Northern British Columbia. Exploration and Mining Journal.

Barrie, C.T. 1993. Petrochemistry of shoshonitic rocks associated with porphyry copper-gold deposits of central Quesnellia, British Columbia, Canada. Journal of Geochemical Exploration, **48**, 225-258.

Box, S.E., and Flower, M.F.J. 1989. Introduction to special section on alkaline arc magmas. Journal of Geophysical Research, **94**: 4467-4468.

Bridge, D.A., Marr, J.M., Hashimoto, K., Obara, M., and Suzuki., R. 1986. Geology of the Kutcho Creek volcanogenic massive sulphide deposits, northern British Columbia. *In* Mineral Deposits of Northern Cordillera, CIM Special Volume 37. *Edited by* J.A. Morin, pp. 115-128.

Cassidy, K.F., Lang, J.R., Lueck, B.A., Mortensen, J.K., Russell, J.K., and Thompson, J.F.H. 1996. Geochemical and isotopic characteristics of Mesozoic alkalic intrusions in the Cordillera of British Columbia: Tectonic significance and implications for Cu-Au metallogeny. Geological Society of Australia, Abstracts number 41, Canberra, p. 81.

Childe. F.C. 1994. Chronology and Radiogenic Isotopic Studies of the Kutcho, Granduc, Anyox and Tulsequah Chief Volcanogenic Massive Sulphide Deposits; *in* Mineral Deposit Research Unit, Volcanogenic Massive Sulphide Deposit Project Annual Report, Year 2, pp. 1-37.

Childe, F.C. 1997. U-Pb geochronology and Nd and Pb isotopic characteristics of the Au-Ag-rich Eskay Creek VMS deposit, British Columbia. Economic Geology.

Childe, F.C., and Schiarizza, P. 1997. U-Pb geochronology, geochemistry and Nd isotopic systematics of the Sitlika Assemblage, northcentral British Columbia. *In* Geological Fieldwork 1996. *Edited by* B. Grant. B.C. Ministry of Employment and Investment, Paper 1997-1, p.69-78.

Childe. F., Barrett. T.J., and McGuigan. P.J. 1994. The Granduc VMS deposit northwest British Columbia: U-Pb ages and Pb isotopic relations. Geological Society of America Annual Meeting Program with Abstracts, Seattle, p. A-381.

Childe, F.C., Thompson, J.F.H., Mortensen, J.K., Friedman, R.M., Schiarizza, P., Bellefontaine, K., and Marr, J. submitted. Primitive Permo-Triassic volcanism in the Canadian Cordillera: Tectonic and metallogenic implications. Geology.

Fraser, T.M., Stanley, C.R., Nikic, Z.T., Pesalj, R., and Gorc, D. 1995. The Mount Polley alkalic porphyry copper-gold deposit, south-central British Columbia. *In* Porphyry Deposits in the Northwestern Cordillera of North America. *Edited by* T. Schroter. **G-2**: 609-622.

Gabrielse, H. 1962. Cry Lake, British Columbia: Geological Survey of Canada, Map 29-1962.

Gabrielse, H. 1978. Operation Dease, *In* Report of Activities, Part A, Geological Survey of Canada, Paper 78-1A, p.1-4.

Gabrielse, H., and Yorath, C.J. 1991. Tectonic Synthesis, Chapter 18. *In* Geology of the Canadian Orogen in Canada. *Edited by* H. Gabrielse and C.J. Yorath. Geological Survey of Canada, Geology of Canada, **4**: 677-705.

Harland, W.B., Armstrong, R.L., Cox, A.V., Craig, L.E., Smith, A., G. 1990. A Geologic Time Scale, 1989. 263 pages.

Holbek, P., McPherson, M., and Oiye, P. 1991. 1990 exploration report on the Kutcho Creek property. Internal Report for Homestake Canada Ltd., 210 pages.

Höy, T. 1991. Volcanogenic Massive Sulphide Deposits in British Columbia: in Ore Deposits, Tectonics and metallogeny in the Canadian Cordillera. B.C. Ministry of Mines and Petroleum Resources, Paper 1991-4, pp. 89-123.

Irvine, T.N., and Baragar, W.R.A. 1971. A guide to the chemical classification of the common volcanic rocks. Canadian Journal of Earth Sciences, **8**: 523-548.

Jackson, J.L. 1990. Tectonic analysis of the Nisling, Northern Stikine and Northern Cache Creek terranes, Yukon and British Columbia. Ph.D. thesis, The University of Arizona, Tucson, Arizona, 200 pages.

Kennedy, A.K., Hart, S.R., and Frey, F.A. 1990. Composition and isotopic constraints on the petrogenesis of alkaline arc lavas: Lihir Island, Papua New Guinea. Journal of Geophysical Research, **95**: 6929-6942.

Krogh, T.E. 1982. Improved accuracy of U-Pb zircon ages by the creation of more concordant systems using an air abrasion technique. Geochemica and Cosmochemica Acta, **46**: 637-649.

Lang, J.R., Lueck, B.A., Mortensen, J.K., Russell, J.K., Stanley, C.R., and Thompson, J.F.H. 1995. Triassic-Jurassic silica-undersaturated and silica-saturated alkalic intrusions in the Cordillera of British Columbia: Implications for arc magmatism. Geology, **23**: 451-454.

Ludwig, K.R. 1980. Calculation of uncertainties of U-Pb isotope data. Earth and Planetary Science Letters, **46**: 212-220.

McInnes, B.I.A., and Cameron, E.M. 1994. Carbonated, alkaline hybridizing melts from a sub-arc environment: Mantle wedge samples from the Tabar-Lihir-Tanga-Feni arc, Papua New Guinea. Earth and Planetary Sciences, **122**, 125-141.

Monger, J.W.H. 1977. Upper Paleozoic Rocks of the Western Canadian Cordillera and their bearing on Cordilleran Evolution. Canadian Journal of Earth Sciences, **14**: 1832-1859.

Monger, J.W.H., and Thorstad, L. 1978. Lower Mesozoic stratigraphy, Cry Lake (104I) and Spatsizi (104H) map areas, British Columbia. *In* Current Research, Part A, Geological Survey of Canada, Paper 78-1A, pp. 21-24.

Monger, J.W.H, Wheeler, J.O., Tipper, H.W., Gabrielse, H., Harms, T., Struik, L.C., Campbell, R.B., Dodds, C.J., Gehrels, G.E., and O'Brien, J. 1991. Part B. Cordilleran terranes. *In* Upper Devonian to Middle Jurassic assemblages, Chapter 8 of Geology of the Cordilleran Orogen in Canada. *Edited by* H. Gabrielse and C.J. Yorath. Geological Survey of Canada, **4**: 281-327.

Mortensen, J.K., Ghosh, D.K., and Ferri, P. 1995. U-Pb geochronology of intrusive rocks associated with Cu-Au deposits in the Canadian Cordillera. *In* Porphyry Deposits in the Northwestern Cordillera of North America. *Edited by* T.G. Schroter. **G-2**: 491-531.

Mortimer, N. 1987. Late Triassic, arc-related, potassic igneous rocks in the North American Cordillera. Geology, **14**: 1035-1038.

Newberry, R.J., Brew, D.A., and Crafford, T.C. 1990. Genesis of the Greens Creek (GC) volcanogenic massive sulphide (VMS) deposit, S.E. Alaska: A geochemical study. Geological Association of Canada Annual Meeting Program with Abstracts, pp. A-96.

Orchard, M.J. 1986. Conodonts from western Canadian chert: Their nature, distribution and stratigraphic application. *In* Investigative Techniques and Applications, Ellis Horwood Ltd., Chichester, pp. 94-119.

Panteleyev, A. 1977. Kutcho Creek Map-Area (104I/1W). *In* Geological Fieldwork. *Edited by* N.C. Carter and R.J, Moir. B.C. Ministry of Mines and Petroleum Resources, p. 43.

Panteleyev, A., and Pearson., D.E. 1976. Kutcho Creek Map-Area (104I/1W). *In* Geological Fieldwork, B.C. Ministry of Mines and Petroleum Resources, pp. 74-76.

Pearson., D.E., and Panteleyev, A. 1975. Cupiferous Iron Sulphide Deposits, Kutcho Creek Map-Area (104I/1W); *in* Geological Fieldwork, B.C. Ministry of Mines and Petroleum Resources, pp. 86-92.

Renne, P.R. 1995. Synchrony and Causal Relations Between Permian-Triassic Boundary Crises and Siberian Flood Volcanism. Science, **269**: 1413-1416.

Samson, S.D., McClelland, W.C., Patchett, P.J., Gehrels, G.E., and Anderson, R.G. 1989. Evidence from neodymium isotopes for mantle contributions to Phanerozoic crustal genesis in the Canadian Cordillera: Nature, **337**: 705-709.

Smith, A.D., and Lambert, R.S. 1995. Nd, Sr, and Pb isotopic evidence for contrasting origins of ;ate Paleozoic volcanic rocks from the Slide Mountain and Cache Creek terranes, south-central British Columbia. Canadian Journal of Earth Sciences, **32**: 447-459.

Snyder, L. and Russell, J.K. 1995. Petrogenetic relationships and assimilation processes in the alkalic Iron Mask batholith, south-central British Columbia. *In* Porphyry Deposits in the Northwestern Cordillera of North America. *Edited by* T.G. Schroter, **G-2**: 593-608.

Steiger, R.H., and Jäger, E. 1977. Subcommission on geochronology: Convention on the use of decay constants in geo- and cosmochronology. Earth and Planetary Science Letters, **14**: 359-362.

Thompson, J.F.H., Mortensen, J.K., and Lang, J.R. 1995. Magma suites and metallogeny - examples from the Canadian Cordillera. PACRIM '95 Abstracts, pp. 569-574.

Thériault, R., J. 1990. Methods for Rb-Sr and Sm-Nd isotopic analyses at the geochronology laboratory, Geological Survey of Canada. *In* Radiogenic Age and Isotopic Studies, Report 2, Geological Survey of Canada, Paper 89-2, pp. 3-6.

Thorstad, L.E. 1983. The Upper Triassic "Kutcho Formation" Cassiar Mountains, North-Central British Columbia. M.Sc. thesis, University of British Columbia, Vancouver, British Columbia, 271 pages.

Thorstad, L., and Gabrielse, H. 1986. The Upper Triassic Kutcho Formation Cassiar Mountains, North-Central British Columbia. Geological Survey of Canada Paper 86-16, 53 pages.

Vallier, T.L. 1995. Petrology of pre-Tertiary igneous rocks in the Blue Mountains region of Oregon, Idaho, and Washington: Implications for the geologic evolution of a complex island arc. *In* Geology of the Blue Mountains region of Oregon, Idaho, and Washington: Petrology and tectonic evolution of pre-Tertiary rocks of the Blue Mountains Region. *Edited by* T.L. Vallier, and H.C. Brooks. U.S. Geological Survey Professional Paper 1438, pp. 125-209.

Wallace, D.A., Johnson, R.W., Chappell, B.W., Arculus, R.J., Perfit, M.R., and Crick, I.H. 1983. Cainozoic volcanism of the Tabar, Lihir, Tanga, and Feni Islands, Papua New Guinea: Geology, whole-rock analyses, and rock-forming mineral compositions. Bureau of Mineral Resources, Geology, and Geophysics, Australian Department of Resources and Energy, Report 243, 62 pages.

York, D. 1969. Least-squares fit of a straight line with correlated errors. Earth and Planetary Science Letters, **5**: 320-324.

PART 2:

U-Pb Geochronology, Geochemistry and Nd Isotopic Systematics
of the Sitlika Assemblage, Central British Columbia

Introduction

Rocks of the Sitlika assemblage occur within the eastern Sitlika Range and adjacent parts of the Hogem Batholith, east of Takla Lake in central British Columbia (Figs. 4.10 and 4.11). The Sitlika assemblage is currently the focus of a two year 1:50,000 scale mapping project headed by one of the authors of this report (Schiarizza and Payie, 1997; Schiarizza *et al.*, 1997). This report presents U-Pb zircon geochronology for felsic volcanic and intrusive rocks, major and trace element analyses for the principal igneous lithologies of the Sitlika assemblage and Nd isotopic and rare earth analyses for rocks dated in this study.

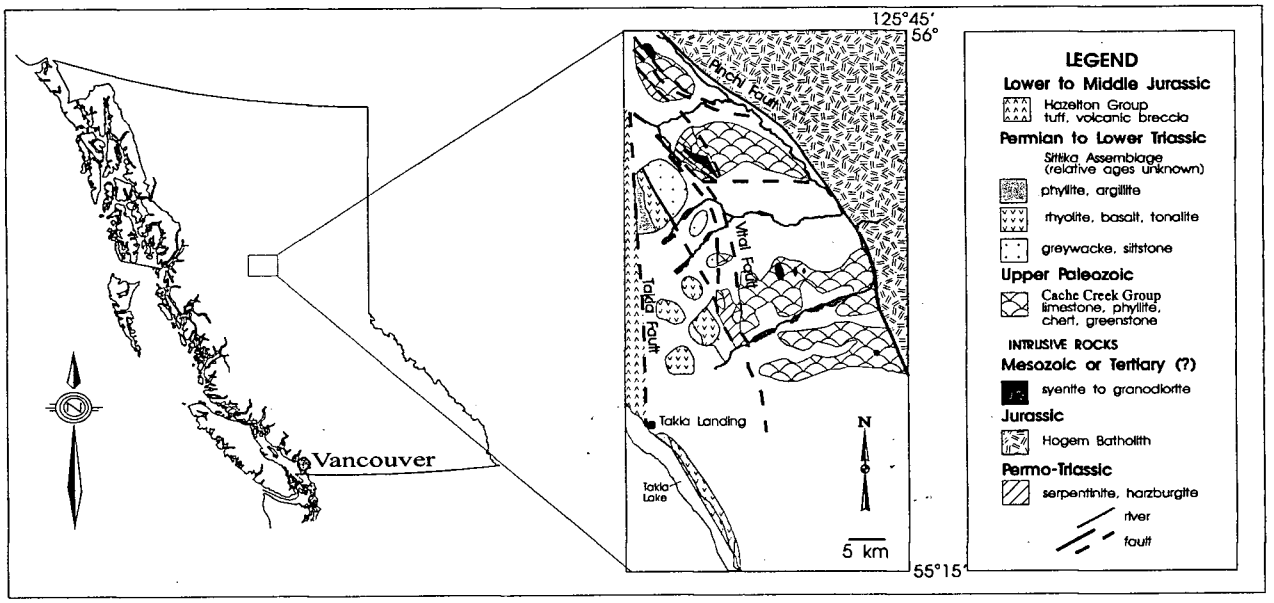

Figure 4. 10 Location and Generalized geology of the Sitlika Assemblage, northcentral British Columbia (after Paterson 1974).

Previous work

Volcanic and sedimentary rocks, directly east of the Takla Fault, were originally correlated with the Cache Creek Group (Armstrong, 1949). Further mapping by Paterson (1974) identified the presence of three principal lithologies within and south of the Sitlika Range: argillite, volcanic

rock and greywacke. Based on the occurrence of felsic volcanic and volcaniclastic rocks within this sequence, Paterson (1974) concluded that these rocks were not part of the Cache Creek Group, and hence informally named them the Sitlika assemblage.

On the basis of similarities in lithologies and structural style Monger *et al.* (1978) suggested that the Sitlika assemblage may represent an offset portion of the Kutcho Assemblage, a fault-bounded volcano-sedimentary sequence which lies some 300 km north of the Sitlika assemblage. The Kutcho Assemblage is host to the Kutcho Creek volcanogenic massive sulphide deposit, with reserves of 17 Mt, grading 1.6% Cu and 2.3% Zn, 29 g/t Ag and 0.3 g/t Au (Bridge *et al.*, 1986); the identification of displaced slivers of the Kutcho Assemblage in the Cordillera has implications for base metal exploration. Recent studies have documented the precise age and geochemical characteristics of the Kutcho Assemblage and provide a basis for comparison between the Kutcho and Sitlika Assemblages (Childe and Thompson, 1995; Thompson *et al.*, 1995; Childe and Thompson, submitted). One of the most distinctive characteristic of the Kutcho Assemblage is the Permo-Triassic to earliest Triassic age of magmatism (Childe and Thompson, submitted). This time period is typically characterized by a regional unconformity in terranes of island-arc affinity in the Cordillera (Gabrielse and Yorath, 1991).

Geology

The Sitlika assemblage comprises greenschist facies metavolcanic and metasedimentary rocks in the central part of the Intermontane Belt. They are in fault contact with the Stuart Lake Belt of the Cache Creek terrane to the east, and juxtaposed against unmetamorphosed volcanic and sedimentary rocks of the Stikine terrane to the west, across the Late Cretaceous or Early Tertiary Takla fault. In the Kenny Creek - Mount Olson area, the Sitlika Assemblage is subdivided into three units, corresponding to the divisions originally defined by Paterson (1974) (Fig. 4.11). The volcanic unit comprises mafic to felsic flow and fragmental rocks, along with comagmatic intrusions. Mafic rocks are dominant, and include thoroughly reconstituted actinolite-epidote-chlorite schists, as well as more massive greenstone with variable preservation of vesicles, plagioclase phenocrysts and pillow structures. The subordinate felsic volcanic rocks include quartz-sericite schists, with or without relict quartz and feldspar phenocrysts, as well as massive feldspar porphyry and quartz-feldspar porphyry. Light grey felsic volcanic rocks also

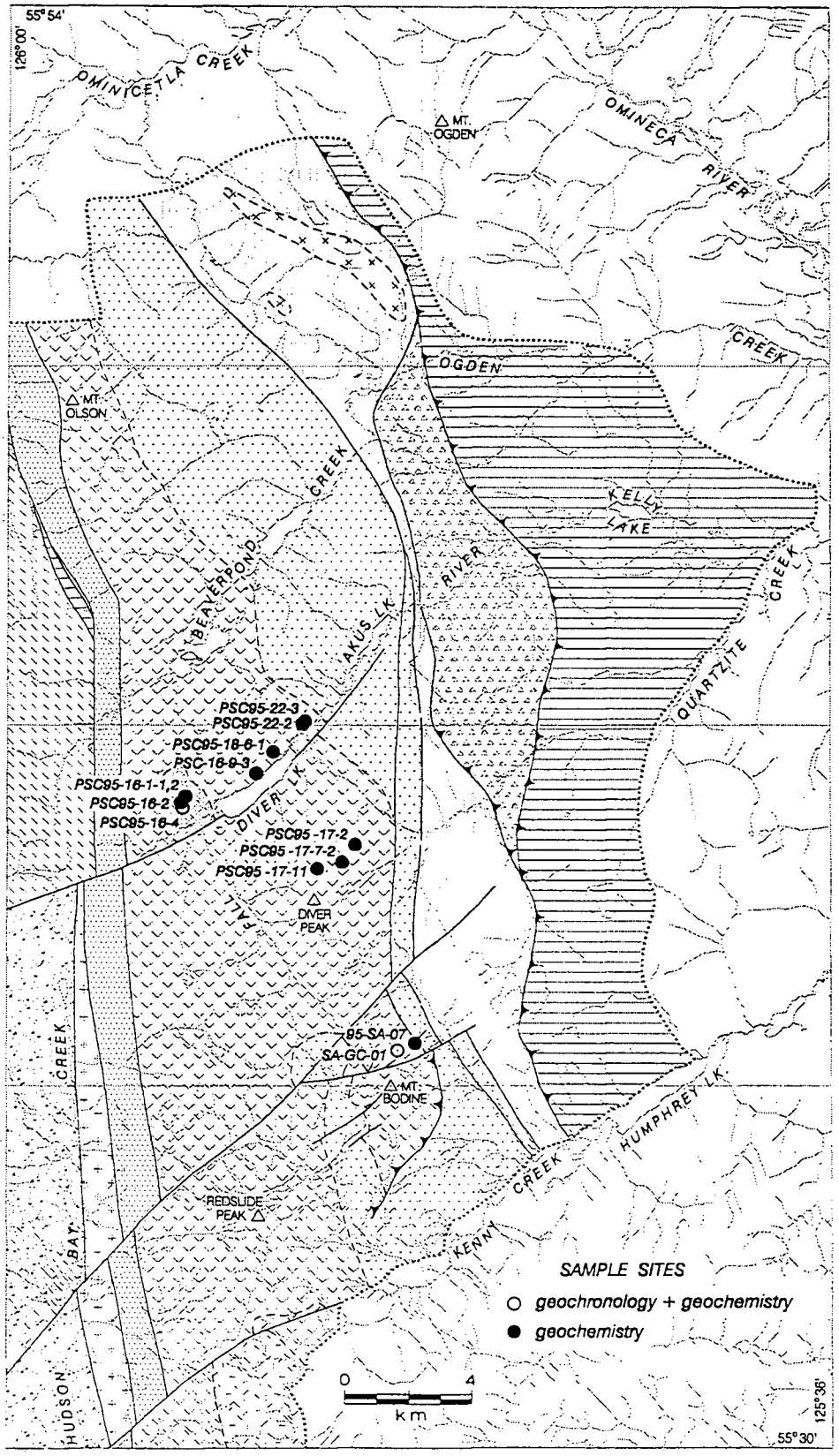

Figure 4. 11 Generalized geology of the Kenny Creek - Mount Olsen area (after Schiarizza and Payie 1997), showing geochemistry and geochronology sample locations.

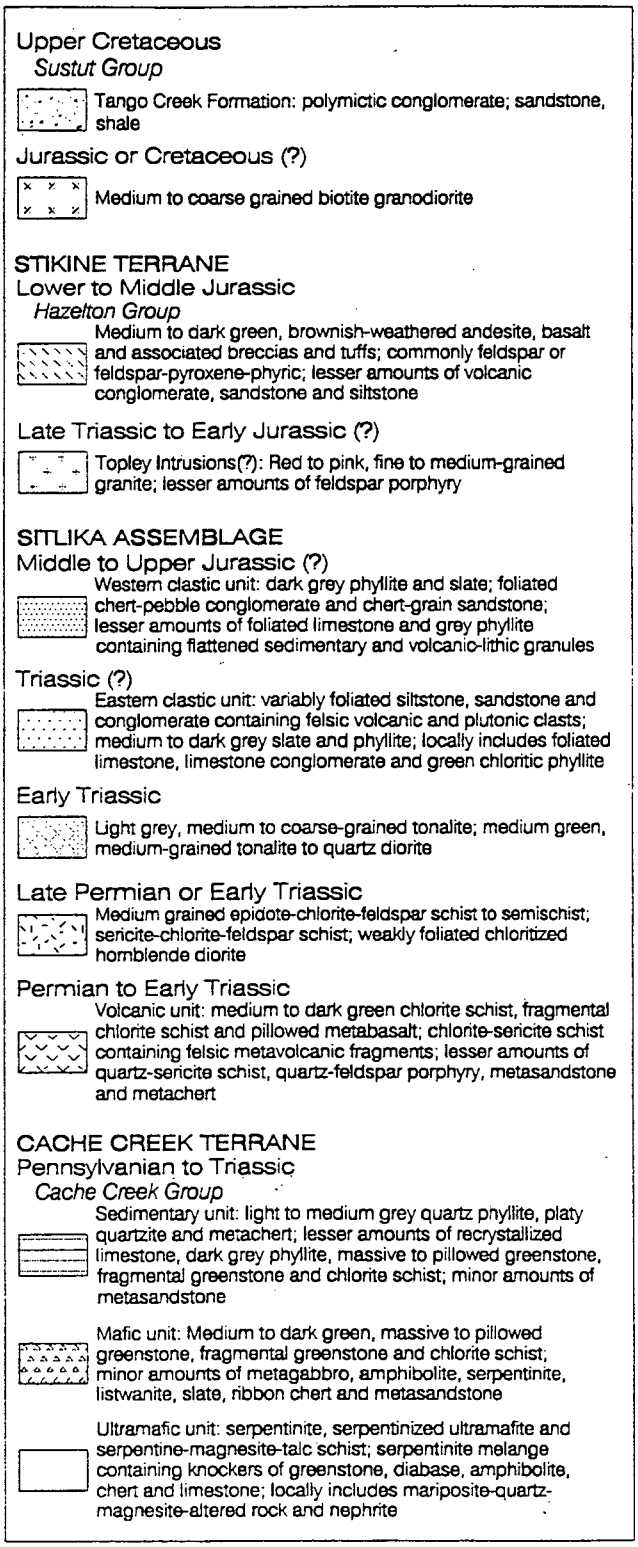

Legend to accompany Figure 4.11.

constitute the dominant clast type in fragmental sericite-chlorite schists that are common within the unit. These fragmental rocks generally interfinger with pillowed mafic volcanic rocks, and may represent mass flow deposits derived from adjacent felsic volcanic buildups. Mafic to intermediate composition intrusive rocks within the volcanic unit include fine- to medium-grained feldspar-chlorite schist and semischist, derived from sills, dykes and small plugs of diabase, gabbro, and diorite. Felsic intrusive rocks include widespread dykes and sills of variably foliated quartz-feldspar porphyry, as well as a small multiphase tonalite stock that intrudes pillowed volcanic rocks and fragmental schist west of Diver Lake (Fig. 4.11).

Clastic sedimentary rocks that crop out mainly east of the volcanic unit correspond to Paterson's (1974) greywacke division. These rocks rest stratigraphically above the volcanic unit in sections exposed north of Beaverpond Creek and west of Mount Bodine; the contact is abrupt but apparently conformable. The basal part of the eastern clastic unit comprises green chloritic phyllite containing lenses of recrystallized limestone and dolostone, as well as conglomerate and coarse sandstone. The conglomerates contain mainly felsic volcanic clasts, with some felsic plutonic clasts, limestone clasts and mafic volcanic clasts. The volcanic and plutonic clasts are lithologically similar to rocks found within the Sitlika volcanic unit. Higher stratigraphic levels consist mainly of dark green slate intercalated with thin to thick, massive to graded beds of volcanic-lithic sandstone and siltstone. The eastern clastic unit is not dated, but is presumed to be Early Triassic and/or younger as it conformably overlies the volcanic unit.

Clastic metasedimentary rocks that crop out west of the Sitlika volcanic unit are equivalent to Paterson's (1974) argillite division, and consist of dark grey phyllite, chert-pebble conglomerate, chert-quartz sandstone, and limestone. These rocks are not well exposed, but apparently form a narrow continuous belt that occurs east of the Takla fault over the full length of the map area (Fig. 4.11). The contact with the adjacent Sitlika volcanic unit is not well exposed, but is inferred to be a fault. The western clastic unit is not dated, but is tentatively correlated with the Middle to Upper Jurassic Ashman Formation at the base of the Bowser Lake Group (Tipper and Richards, 1976). This correlation is based on their general lithologic similarity, and in particular on the predominance of chert clasts in the coarser clastic intervals, which apparently does not occur in older rocks found in this part of the central Intermontane Belt.

All three units of the Sitlika assemblage are characterized by a single penetrative cleavage or schistosity defined by the preferred orientation of metamorphic minerals and variably flattened clastic grains or volcanic fragments. This metamorphic foliation is axial planar to folds that are most commonly observed in the eastern clastic unit. The folds are upright, with axes that plunge north to northwest or south to southeast. North of Beaverpond Creek, the volcanic unit and lower portion of the overlying eastern clastic unit comprise a moderately east-dipping homocline cut by a steep, east-dipping cleavage. Farther east, the eastern clastic unit is repeated across several upright folds. The wide outcrop expanse of the eastern clastic unit thins dramatically to the south, apparently due to truncation along the fault system that marks the Sitlika - Cache Creek contact. The volcanic belt is correspondingly wider in the south, in part due to internal folding, as indicated by a faulted anticline and adjacent syncline that repeat the volcanic unit and overlying eastern clastic unit south and west of Mount Bodine.

The Sitlika assemblage is bounded to the east by a unit of serpentinite melange that is included in the Cache Creek Group. Metasedimentary and metavolcanic rocks comprising the bulk of the Cache Creek Group farther east rest structurally above the serpentinite melange unit across an east-dipping thrust fault (Paterson, 1974). Limited structural data suggests that the Sitlika - Cache Creek contact (specifically, the contact between the Sitlika assemblage eastern clastic unit and the serpentinite melange) is a steeply dipping dextral strike-slip fault that postdates the contractional deformation within the Cache Creek Group (Schiarizza and Payie, 1997).

U-Pb geochronology

Two samples were collected for U-Pb zircon geochronology. These consisted of a tonalite from the Diver Lake area, with abundant 3-6 mm glassy quartz phenocrysts set in a fine-grained crystalline groundmass (PSC95-16-4), and a rhyolite from the Mount Bodine area, with 1-2 mm quartz and plagioclase phenocrysts (SA-GC-01) (Plates 4.10 and 4.11).

Sample preparation and U-Pb analyses were carried out at the Geochronology Laboratory of the University of British Columbia. The samples were processed and zircon was separated using conventional crushing, grinding, Wilfley table and heavy liquid techniques. All fractions

Fraction[1]	Wt.	U	Pb[2]	^{206}Pb[3]	Pb[4]	^{208}Pb[5]	Isotopic ratios(±1σ,%)[6]			Isotopic dates(Ma,±2σ)[6]		
	mg	ppm	ppm	^{204}Pb	pg	%	$^{206}Pb/^{238}U$	$^{207}Pb/^{235}U$	$^{207}Pb/^{206}Pb$	$^{206}Pb/^{238}U$	$^{207}Pb/^{235}U$	$^{207}Pb/^{206}Pb$
Mount Bodine rhyolite SA-GC-01												
A,m,M1,p	0.120	77	3	1730	14	9.7	0.04082±0.13	0.2892±0.29	0.05138±0.23	257.9±0.7	257.9±1.3	257.8±10.5
B,f,M1,p	0.122	60	2	604	29	8.9	0.03680±0.13	0.2603±0.43	0.05129±0.34	233.0±0.6	234.9±1.8	253.9±15.7
C,f,M1,p	0.102	53	2	917	14	8.1	0.03782±0.12	0.2671±0.35	0.05123±0.28	239.3±0.6	240.4±1.5	251.0±12.7
J,f,M2,p	0.052	67	2	579	15	8.5	0.03714±0.14	0.2632±0.48	0.05140±0.40	235.1±0.7	237.2±2.0	258.7±18.2
Diver Lake tonalite PSC95-16-4												
A,c,N1,p	0.099	194	7	2469	19	7.8	0.03801±0.22	0.2682±0.31	0.05112±0.19	240.5±1.0	241.2±1.3	248.8±8.3
B,c,N2Ip	0.035	174	7	1254	12	8.6	0.03807±0.18	0.2689±0.40	0.05122±0.32	240.9±0.8	241.8±1.7	250.9±14.6
C,m,N1,p	0.140	244	9	4202	19	7.7	0.03771±0.11	0.2652±0.21	0.05100±0.13	238.6±0.8	238.8±0.9	240.7±5.9
D,c,M1,p	0.285	230	37	6801	23	8.1	0.03816±0.12	0.2689±0.21	0.05111±0.11	241.4±0.6	241.8±0.9	245.7±5.0
E,c,N1,p	0.196	199	32	3925	24	7.5	0.03816±0.10	0.2686±0.21	0.05105±0.13	241.4±0.5	241.6±0.9	243.0±6.2

[1]All fractions are air abraded; Grain size, smallest dimension: c= +134μm, m=-134μm+74μm, f=-74μm; Magnetic codes: Franz magnetic separator sideslope at which grains are nonmagnetic; e.g., N1=nonmagnetic at 1°; Field strength for all fractions =1.8A; Front slope for all fractions=20°; Grain character codes: p=prismatic.
[2]Radiogenic Pb
[3]Measured ratio corrected for spike and Pb fractionation of 0.0043/amu ±20% (Daly collector)
[4]Total common Pb in analysis based on blank isotopic composition
[5]Radiogenic Pb
[6]Corrected for blank Pb, U and common Pb (Stacey-Kramers model Pb composition at the $^{207}Pb/^{206}Pb$ date of fraction, or age of sample).

Table 4 6 U-Pb zircon analytical data for samples from the Sitlika assemblage.

were air abraded prior to analysis, to reduce the effects of surface-correlated lead loss (Krogh, 1982). Zircon grains were selected based on criteria such as magnetic susceptibility, clarity, morphology and size. Procedures for dissolution of zircon and extraction and purification of uranium and lead follow those of Parrish et al. (1987). Uranium and lead were loaded onto single, degassed refined rhenium filaments using the silica gel and phosphoric acid emitter technique. Procedural blanks were 9 and 6 picograms for lead and uranium, respectively. Errors assigned to individual analyses were calculated using the numerical error propagation method of Roddick (1987) and all errors are quoted at the 2σ level. Ages were calculated using the decay constants recommended by Steiger and Jäger (1977). Common lead corrections were made using the two-stage growth model of Stacey and Kramers (1975). Discordia lines were regressed using a modified York-II model (York, 1969; Parrish et al., 1987). Uranium-lead analytical results are presented in Table 4.6.

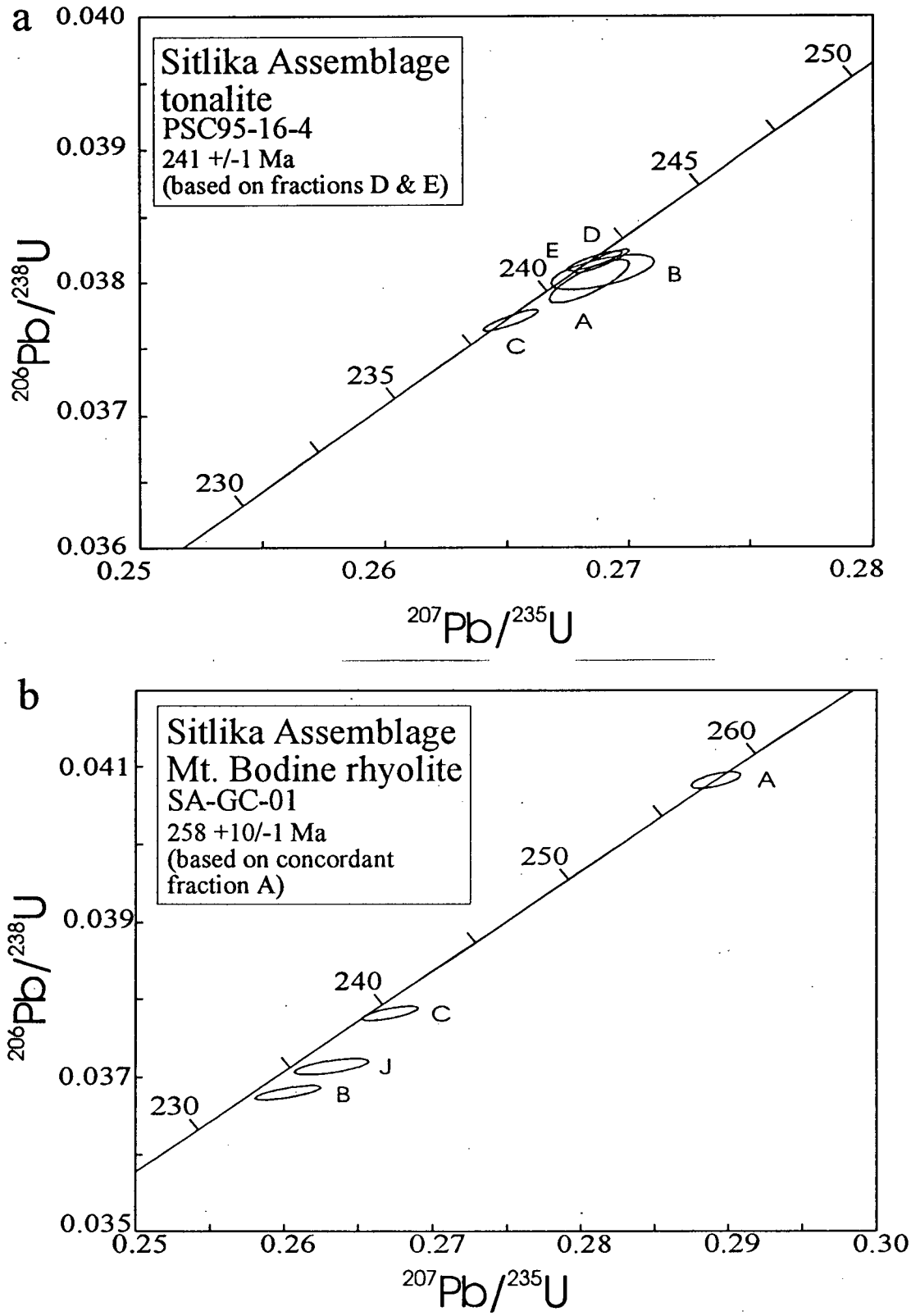

Figure 4. 12 U-Pb concordia diagrams for a) Diver Lake tonalite (PSC95-16-4); and b) Mount Bodine rhyolite (SA-GC-01).

Diver Lake tonalite

The Diver Lake tonalite (PSC95-16-4) contained abundant coarse-grained, prismatic zircon with few inclusions and good clarity. Analysis of five fractions yielded $^{207}Pb/^{206}Pb$ ages of 241 to 251 Ma. Fraction E was concordant, with a $^{206}Pb/^{238}U$ age of 241.4 Ma, while fraction D slightly overlapped concordia, with a $^{206}Pb/^{238}U$ age of 241.4 Ma (Fig. 4.12a). An Early Triassic age of 241 +/-1 Ma, which is based on the $^{206}Pb/^{238}U$ age and associated errors of fractions E and D, is considered to be the best estimate for the age of this rock.

Mount Bodine rhyolite

The Mount Bodine rhyolite (SA-GC-01) contained a small quantity of fine-grained prismatic zircon with few inclusions and good clarity. Zircon from this rock was characterized by extremely low U concentrations (53 to 77 ppm), which is in part reflected in low $^{206}Pb/^{204}Pb$ ratios (Table 4.6). All of the zircon recovered from this rock was divided into four fractions, analyses yielded $^{207}Pb/^{206}Pb$ ages of 251 to 259 Ma. Fraction A was concordant, with a $^{206}Pb/^{238}U$ age of 257.9 Ma (Fig. 4.12b). A Permian age of 258 +10/-1 Ma, based on the $^{206}Pb/^{238}U$ age and $^{206}Pb/^{238}U$ and $^{207}Pb/^{206}Pb$ errors of fraction A, is considered to be the best estimate of the age of this rock.

Geochemistry

Major and Trace Elements

A suite of thirteen igneous rock samples from the Sitlika assemblage were analyzed for major and trace element abundances. Based on these analyses, the Sitlika assemblage has a roughly bimodal distribution of compositions, containing basalt (47-50% SiO_2) and dacite to rhyolite, and their intrusive equivalents (62-85% SiO_2) (Table 4.7). The Mount Bodine rhyolite (SA-GC-01) has a high SiO_2 concentration (85%), combined with relatively low concentrations of other major elements (Al_2O_3, Fe_2O_3, CaO, Na_2O) which indicates silicification of this rock, and is

Table 4.7 Major and trace element data for rocks from the Sitlika assemblage.

sample number	lithology	SiO2 %	TiO2 %	Al2O3 %	Fe2O3 %	MnO %	MgO %	CaO %	Na2O %	K2O %	P2O5 %	LOI	Total	BaO ppm
SA-GC-01	rhyolite	85.25	0.16	8.40	1.58	0.02	0.00	0.15	4.53	0.23	0.02	0.25	100.59	<d/l
95-SA-07	dacite	67.86	0.70	11.37	5.93	0.26	2.46	0.44	3.04	0.55	0.19	4.35	100.31	103
PSC95-16-1-1	tonalite	74.47	0.30	13.45	2.55	0.05	0.65	1.95	5.09	0.69	0.06	0.99	100.28	181
PSC95-16-1-2	QFP	66.42	0.65	16.01	4.72	0.11	1.35	3.66	5.56	0.30	0.18	1.34	100.33	170
PSC95-16-2	QFP to tonalite	65.18	0.74	16.12	5.17	0.10	1.56	3.72	5.34	0.34	0.18	1.82	100.30	116
PSC95-16-4	tonalite	74.43	0.31	13.92	2.09	0.03	0.71	2.45	5.16	0.62	0.06	0.87	100.69	258
PSC95-16-9-3	pillowed metabasalt	49.00	2.17	16.40	12.62	0.19	4.79	5.08	5.38	0.04	0.24	3.85	99.85	191
PSC95-17-2	biot-chl. schist	48.53	1.81	14.64	15.65	0.24	5.56	6.37	3.79	0.45	0.11	3.42	100.67	257
PSC95-17-7-2	chlorite schist	62.09	1.38	15.02	8.18	0.17	2.53	2.68	7.23	0.18	0.20	0.98	100.68	132
PSC95-17-11	chlorite schist	46.98	1.53	16.15	12.36	0.19	5.04	9.05	4.24	0.07	0.28	4.70	100.67	135
PSC95-18-6-1	pillowed metabasalt	49.89	1.42	15.64	13.91	0.22	4.92	7.70	4.38	0.12	0.14	2.56	100.98	138
PSC95-22-2	chl-ser-qtz schist	74.14	0.12	14.68	1.29	0.04	0.35	0.31	7.05	1.28	0.02	0.82	100.13	125
PSC95-22-3	chlorite schist	43.91	1.35	17.13	11.78	0.18	6.84	7.89	4.20	0.22	0.18	6.68	100.46	119
Detection Limits (ppm):		60	35	120	30	30	95	15	75	25	35			17

sample number	Co ppm	Cr2O3 ppm	Cu ppm	Ni ppm	V ppm	Zn ppm	Ga ppm	Nb ppm	Pb ppm	Rb ppm	Sr ppm	Th ppm	U ppm	Y ppm	Zr ppm
SA-GC-01	47	<d/l	7	<d/l	<d/l	68	9.8	5.3	<d/l	<d/l	23.1	<d/l	<d/l	40.0	180.3
95-SA-07	18	<d/l	83	<d/l	83	1219	19.0	3.3	160.9	4.6	35.6	<d/l	<d/l	50.2	166.0
PSC95-16-1-1	54	<d/l	5	<d/l	25	57	13.9	4.1	<d/l	8.8	132.5	<d/l	4.3	27.4	139.3
PSC95-16-1-2	36	<d/l	4	<d/l	56	60	16.6	3.9	<d/l	2.7	200.2	<d/l	4.5	40.4	131.0
PSC95-16-2	14	<d/l	3	<d/l	68	59	15.0	4.1	<d/l	3.9	217.0	<d/l	4.4	42.7	117.8
PSC95-16-4	60	<d/l	4	<d/l	27	43	13.7	3.9	<d/l	5.4	110.9	<d/l	4.2	29.4	127.3
PSC95-16-9-3	44	66	46	11	402	136	20.1	3.6	2.3	<d/l	106.4	4.2	6.7	43.6	121.1
PSC95-17-2	45	35	32	<d/l	490	117	18.1	3.4	2.1	5.7	118.9	5.1	7.1	30.6	46.5
PSC95-17-7-2	19	<d/l	12	<d/l	164	111	19.5	4.0	1.0	1.0	73.9	1.3	5.8	53.2	268.1
PSC95-17-11	37	217	27	45	253	118	18.0	2.8	1.8	<d/l	133.2	4.0	6.6	37.6	109.9
PSC95-18-6-1	37	<d/l	53	3	391	126	19.2	3.0	1.6	<d/l	125.0	4.7	7.0	37.4	106.6
PSC95-22-2	30	<d/l	23	9	<d/l	60	17.2	8.2	<d/l	8.5	25.6	<d/l	4.0	85.5	233.7
PSC95-22-3	47	271	89	62	288	124	14.9	3.8	1.9	2.6	73.5	3.0	6.6	28.0	74.6
Detection Limits (ppm):	10	15	2	3	10	2	1	1	1	1	1	1	1	1	1

Table 4.7 Major and trace element data for samples from the Sitlika assemblage.

consistent with field observations. In a plot of SiO_2 vs. K_2O (Pecerrillo and Taylor, 1976), unaltered rocks from the Sitlika assemblage lie within the field for low-K magmas (Fig. 4.13a). A plot of Zr vs. Y indicates that intrusive and volcanic rocks of the Sitlika assemblage have a predominantly tholeiitic magmatic affinity, with Zr/Y ratios of 1.5 to 5.0 (Fig. 4.13b and Table 4.7).

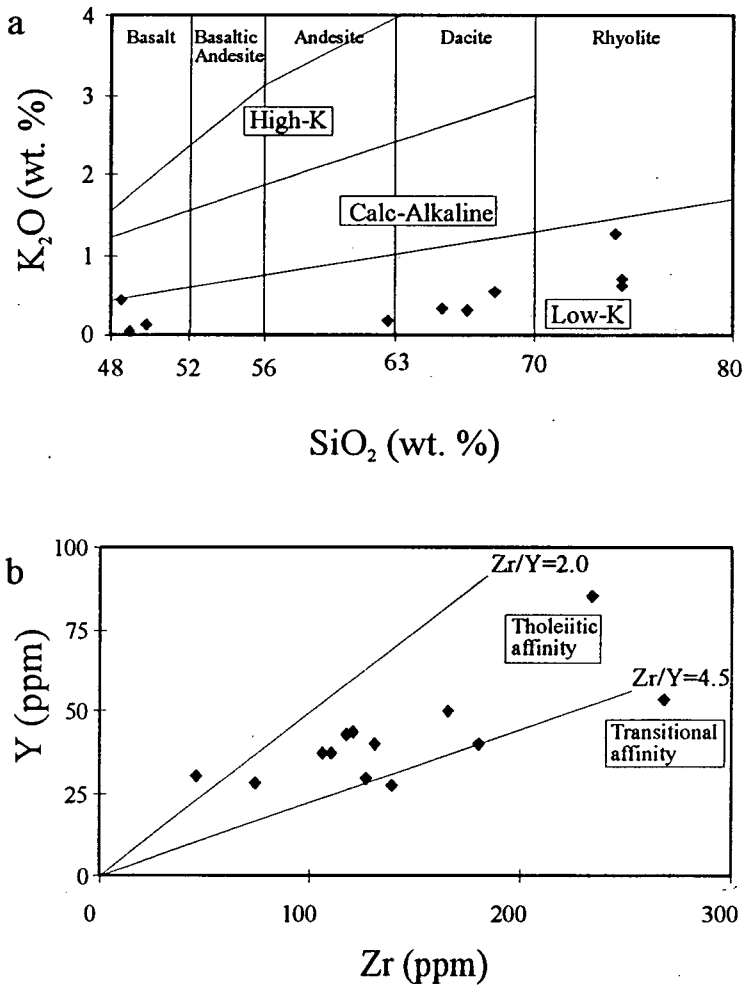

Figure 4. 13 a) SiO_2 vs. K_2O diagram for unaltered rocks of the Sitlika Assemblage (fields from Peccerillo and Taylor, 1976); b) Zr vs. Y diagram for all samples from the Sitlika Assemblage (fields from Barrett and MacLean, 1994).

Rare Earth Elements

Rare earth element (REE) concentrations were determined for samples of rhyolite, tonalite, and basalt from the Sitlika Assemblage (Table 4.9 and Figs. 4.14a and b). All three rocks are characterized by low REE abundances and near-flat REE patterns. A small negative europium

Table 4.8 Rare earth element data for samples from the Sitlika assemblage.

sample number	Au ppb	Ag ppm	As ppm	Br ppm	Cs ppm	Hf ppm	Hg ppm	Ir ppb	Sb ppm	Sc ppm	Se ppm	Ta ppm	W ppm	La ppm	Ce ppm	Nd ppm	Sm ppm	Eu ppm	Tb ppm	Yb ppm	Lu ppm
SA-GC-01	<d/l	<d/l	<d/l	<d/l	<d/l	<d/l	<d/l	<d/l	0.1	6.4	<d/l	1.4	251	6.6	23	16	4.4	0.8	1.0	4.4	0.6
PSC95-16-4	<d/l	<d/l	<d/l	<d/l	<d/l	4.5	<d/l	<d/l	0.6	6.1	0.8	1.6	302	5.8	<d/l	16	2.3	0.9	0.6	3.1	0.5
PSC95-18-6-1	<d/l	<d/l	2.0	<d/l	<d/l	2.9	<d/l	<d/l	0.6	39.1	<d/l	<d/l	15	4.3	<d/l	16	3.6	1.4	0.9	3.6	0.5
Detection Limits:	2 ppb	2 ppm	1 ppm	0.5 ppm	0.2 ppm	0.2 ppm	1 ppm	1 ppm	0.1 ppm	0.1 ppm	0.5 ppm	0.3 ppm	1 ppm	0.1 ppm	1 ppm	1 ppm	0.01 ppm	0.05 ppm	0.1 ppm	0.05 ppm	0.01 ppm

anomaly for the rhyolite is consistent with fractionation of plagioclase in this unit. With the exception of the europium anomaly, the patterns for the rhyolite and tonalite are extremely similar (Fig. 4.14a). The low overall REE concentrations and near-flat REE patterns for rocks of the Sitlika Assemblage suggest derivation from primitive magmatic sources.

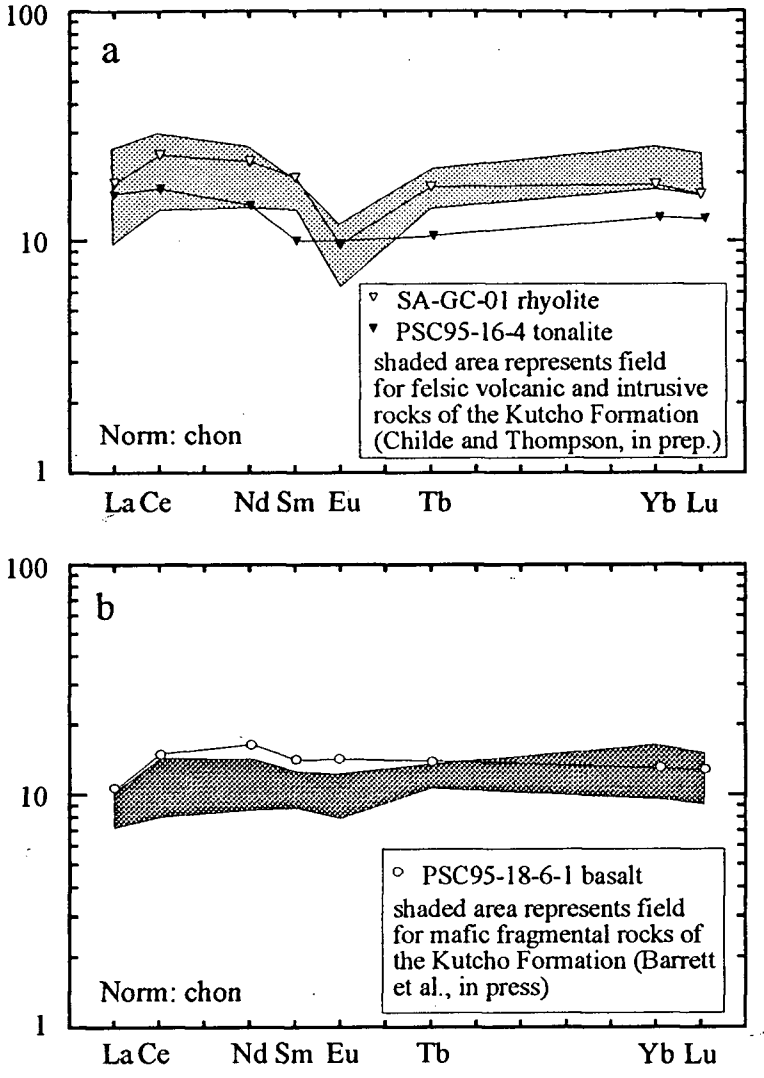

Figure 4. 14 Chondorite-normalized rare earth element diagram for a) rhyolite (SA-GC-01) and tonalite (PSC95-16-4), showing the field for felsic volcanic and intrusive rocks of the Kutcho Assemblage (Childe and Thompson, submitted), and b) basalt (PSC95-18-6-1) from the Sitlika Assemblage, showing the field for mafic volcanic rocks of the Kutcho Assemblage (Childe and Thompson, submitted).

Nd Isotopic Systematics

The Nd isotopic ratio of rhyolite and tonalite dated in this study were determined to further constrain the degree of evolution of this magma. Isotopic analysis of the rhyolite was conducted by R. Thériault at the Geochronology Laboratory of the Geological Survey of Canada;

analysis of the tonalite was conducted at Memorial University. Analytical procedures are described by Thériault (1990). Abundances of Sm and Nd determined by isotope dilution have an uncertainty of 1% or less. Uncertainty for calculated ε_{Nd} values is ± 0.5 ε_{Nd} units. Neodymium analytical results are presented in Table 4.9.

An initial ε_{Nd} value of +8.2 for the Mount Bodine rhyolite is one of the highest values reported for a felsic rock within the Cordillera and indicates derivation of this magma from primitive, unenriched magmatic sources, with no evidence for contamination by old, isotopically evolved sialic crust. An initial ε_{Nd} value of +2.7 for tonalite that intrudes the Sitlika assemblage indicates that this unit is also derived from primitive magmatic sources.

Table 4 9 Nd isotopic data for samples from the Sitlika assemblage.

Sample	Sm (ppm)	Nd (ppm)	$^{147}Sm/^{144}Nd$	meas. $^{143}Nd/^{144}Nd$ (error x 10^{-6}, 2σ)	ε_{Nd}[2] (present day)	age[1] (Ma)	ε_{Nd}[2] (initial)
Mount Bodine rhyolite SA-GC-01	**4.77**	**16.12**	**0.1789**	**0.513029 (6)**	**+7.6**	**258**	**+8.2**
Diver Lake tonalite PSC95-16-4	**2.61**	**9.99**	**0.16158**	**0.512723 (19)**	**+1.7**	**241**	**+2.7**

[1]used for the calculation of ε_{Nd} (initial).
[2]error = ± 0.5 ε_{Nd} units.

Discussion

Ages of 258 +10/-1 Ma and 241 +/-1 Ma, determined for rhyolite and tonalite, respectively, indicate that magmatic activity in the Sitlika assemblage was occurring in the Permo-Triassic, and in part overlapped in time with magmatism in the Kutcho Assemblage. Major and trace element chemistry shows that the Sitlika assemblage is composed of low-K intrusive and bimodal volcanic rocks with a tholeiitic magmatic affinity. Rare earth element chemistry and Nd isotopic systematics indicate derivation from primitive magmas, uncontaminated by old, evolved crust.

Rocks of the Sitlika assemblage formed in the same time period as the Kutcho Assemblage, and the principal lithologies are indistinguishable from those of the Kutcho Assemblage. As such, this region represents a viable exploration target for Kutcho Creek-equivalent VMS mineralization in the Cordillera.

References

Armstrong, J.E. (1949): Fort St. James Map Area, Cassiar and Coast Districts, British Columbia; *Geological Survey of Canada,* Memoir 252.

Barrett, T.J., and MacLean, W.H. (1994): Chemostratigraphy and Hydrothermal Alteration in Exploration for VHMS Deposits in Greenstones and Younger Volcanic Rocks, *in* Alteration and Alteration Processes Associated with Ore-forming Systems, Lentz, D.R., Editor, *Mineral Deposits Division, Geological Association of* Canada, Short Course Notes Volume 11, pages 433-467.

Bridge, D.A., Marr, J.M., Hasimoto, K., Obara, M., and Suzuki, R. (1986): Geology of the Kutcho Creek Volcanogenic Massive Sulphide Deposit, Northern British Columbia; *in* Mineral Deposits of the Northern Cordillera, *Canadian Institute of Mining and Metallurgy Special Volume 37*, Morin, J.A., Editor, pages 115-128.

Childe, F.C., and Thompson, J.F.H. (submitted): Geological Setting, U-Pb Geochronology and Radiogenic Isotopic Characteristics of the Permo-Triassic Kutcho Assemblage, Northcentral British Columbia.

Childe, F.C., and Thompson, J.F.H. (1995): U-Pb Age Constraints and Pb Isotopic Signature of the Kutcho VMS Deposit: Implications for the Terrane Affiliation of the Kutcho Formation, North Central British Columbia; *Geological Association of Canada - Mineralogical Association of Canada Program with Abstracts*, page A 16.

Gabrielse, H., and Yorath, C.J. (1991): Tectonic synthesis, Chapter 18, *in* Geology of the Canadian Orogen in Canada, Gabrielse, H., and Yorath, C., Editors, *Geological Survey of Canada,* Geology of Canada, Number 4, pages 677-705.

Krogh, T. (1982): Improved Accuracy of U-Pb Zircon Ages by the Creation of More Concordant Systems Using Air Abrasion Technique; *Geochemica et Cosmochemica Acta*, Volume 46, pages 637-649.

Monger, J.W.H., Richards, T.A., and Paterson, I.A. (1978): The Hinterland Belt of the Canadian Cordillera: New Data from Northern and Central British Columbia; *Canadian Journal of Earth Sciences*, Volume 15, pages 823-830.

Paterson, I.A. (1974): Geology of the Cache Creek Group and Mesozoic Rocks at the Northern End of the Stuart Lake Belt, Central British Columbia; *Geological Survey of Canada Special Paper 74-1*, Part B, pages 31-41.

Parrish, R.R., Roddick, J. C., Loveridge, W. D. and Sullivan, R. W. (1987): Uranium-Lead Analytical Techniques at the Geochronological Laboratory, Geological Survey of Canada; *in* Radiogenic Age and Isotopic Studies, Report 1, *Geological Survey of Canada*, Paper 87-2, pages 3-7.

Peccerillo, A., and Taylor, S.R. (1976): Geochemistry of Eocene Calc-alkaline Volcanic Rocks from the Kastamonu Area, Northern Turkey; *Contributions to Mineralogy and Petrology*, Volume 68, pages 61-81.

Roddick, J.C. (1987): Generalized Numerical Error Analysis with Applications to Geochronology and Thermodynamics; *Geochimica et Cosmochimica Acta*, Volume 51, pages 2129-2135.

Schiarizza, P., and Payie, G. (1997): Geology of the Sitlika Assemblage in the Kenny Creek - Mount Olson Area (93n/12, 13), Central British Columbia; *In* Geological Fieldwork 1996, Grant, B., Editor, *British Columbia Ministry Of Employment And Investment*, Paper 1997-1, 79-100.

Schiarizza, P., Payie, G., Holunga, S., and Wright, D. (1997): Geology, Mineral Occurrences and Geochemistry of the Kenny Creek - Mount Olson Area (93n/12, 13), British

Columbia; *In* Geological Fieldwork 1996, Grant, B., Editor, *British Columbia Ministry of Employment and Investment*, Open File 1997-2.

Stacey, S.J. and Kramers, J.D. (1975): Approximation of Terrestrial Lead Isotope Evolution by a Two-stage Model; *Earth and Planetary Science Letters*, Volume 26, pages 207-221.

Steiger, R. H. and Jäger, E. (1977): Subcommission on Geochronology: Convention on the Use of Decay Constants in Geo- and Cosmochronology; *Earth and Planetary Science Letters*, Volume 36, pages 359-362.

Thompson, J.F.H., Barrett, T.J., Sherlock, R.L., and Holbec, P. (1995): The Kutcho VMS deposit, British Columbia: A Felsic Volcanic-hosted Deposit in a Tholeiitic Bimodal Sequence, *Geological Association of Canada - Mineralogical Association of Canada Program with Abstracts*, page A 104.

Tipper, H.W., and Richards, T.A. (1976): Jurassic Stratigraphy and History of North-Central British Columbia; *Geological Survey of Canada*, Bulletin 270, 73 pages.

Thériault, R.J. (1990): Methods for Rb-Sr and Sm-Nd Isotopic Analyses at the Geochronology Laboratory, Geological Survey of Canada, *in* Radiogenic Age and Isotopic Studies: Report 2, *Geological Survey of Canada*, Paper 89-2, pages 3-6.

York, D. (1969): Least-squares Fitting of a Straight Line with Correlated Errors; *Earth and Planetary Science Letters*, Volume 5, pages 320-324.

PART 3:

Evidence for Early Triassic Felsic Magmatism in the Ashcroft (92I) Map Area, British Columbia

Introduction

This report presents U-Pb geochronology, and major, trace and rare earth element data for a package of felsic to intermediate composition volcanic and intrusive rocks. These rocks, previously correlated with the Nicola Group, occur within the western portion of the Ashcroft (92I) map area in southwestern British Columbia (Fig. 4.15).

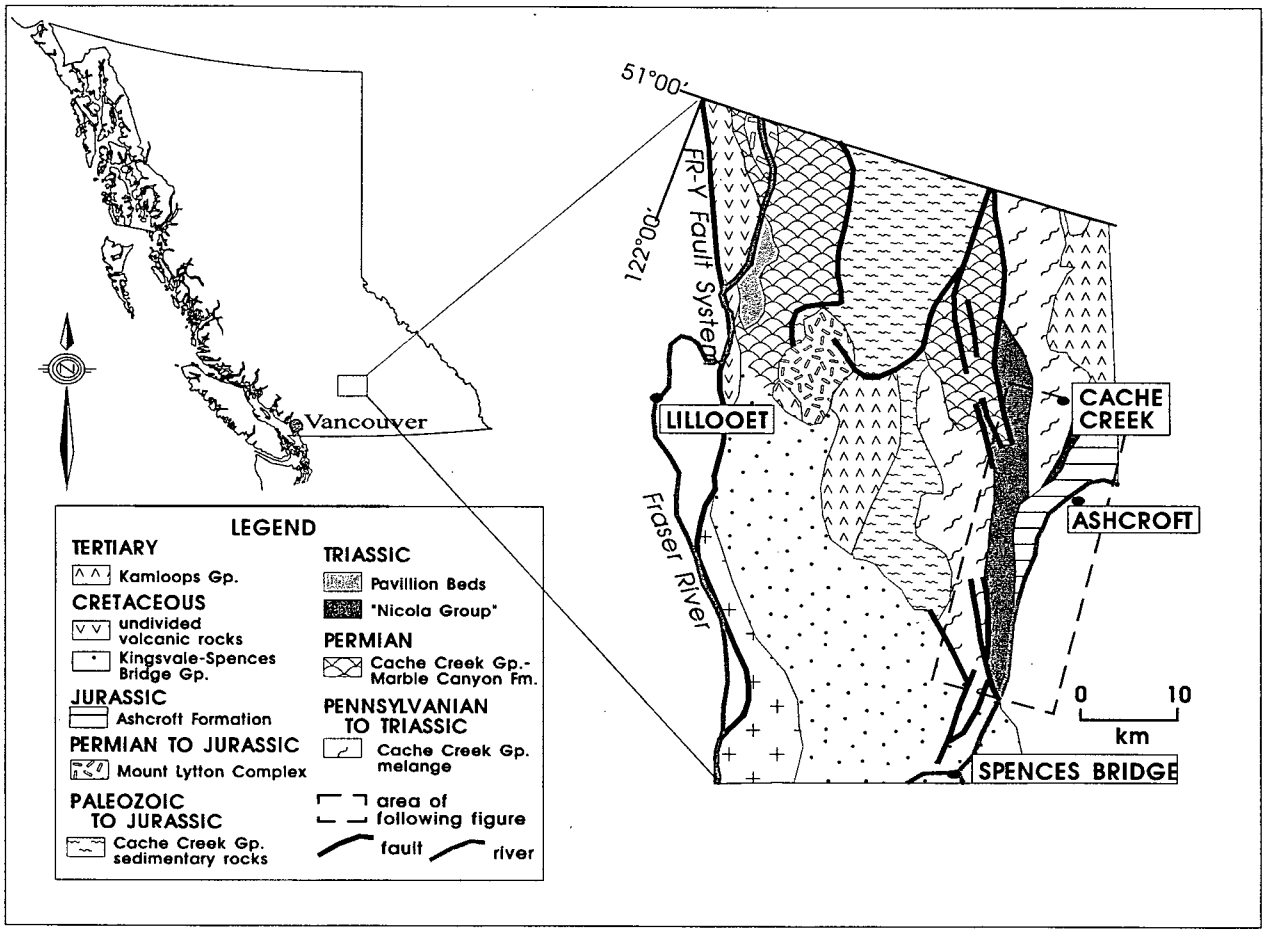

Figure 4. 15 Generalized geology between Lillooet and Ashcroft, the outlined area is detailed in Figure 2 (FR-Y = Fraser River - Yalakom); (modified from Monger et al., 1991).

Rocks examined in the current study include silicic ash and crystal tuffs, and an intrusion of dioritic to tonalitic composition. These units are lithologically similar to volcanic rocks of the Kutcho Assemblage and contemporaneous plutonic bodies which intrude the Kutcho Assemblage, 950 km to the north (Marr, pers. comm., 1995; Childe and Thompson, 1995b). The objectives of this study were to obtain precise age and geochemical data for these rocks, to determine if they could represent an offset portion of the Kutcho Assemblage.

Nicola Group

The Nicola Group is a Late Triassic to Early Jurassic island arc assemblage within the Quesnel terrane. It is comprised of submarine to subaerial, predominantly mafic volcanic and volcaniclastic rocks, their intrusive equivalents and associated clastic and chemical sedimentary rocks (Preto, 1977; Monger *et al.*, 1991). The Nicola Group has been broadly divided into western, central and eastern belts on the basis of lithology and lithogeochemistry (Mortimer, 1986; Monger *et al.*, 1991). Variation from calc-alkaline to shoshinitic compositions from west to east has been interpreted to reflect eastward dipping subduction in the Nicola arc (Mortimer, 1986).

Mafic and lesser felsic volcanic and intrusive rocks previously assigned to the western belt of the Nicola Group have been mapped in the Ashcroft (92I) and Hope (92H) map areas by Preto (1977), Grette (1978), Travers (1978), Shannon (1982), and Monger and McMillan (1984).

Kutcho Assemblage

The Kutcho Assemblage, in north-central British Columbia, forms the lowermost unit in the fault-bounded King Salmon Allochthon. It is composed of tholeiitic bimodal volcanic rocks and sedimentary rocks and is intruded by contemporaneous, probably comagmatic plutonic rocks (Gabrielse, 1979; Thorstad and Gabrielse, 1986; Childe and Thompson, 1995a and b, submitted). Magmatism occurred in the Latest Permian to Early Triassic (Childe and Thompson, 1995a and b). The Kutcho Assemblage is host to the Kutcho Creek volcanogenic massive sulphide deposit, with reserves of 17 Mt, grading 1.6% Cu, 2.3% Zn, 29 g/t Ag and 0.3 g/t Au (Bridge *et al.*, 1986).

Geology

The current study examines felsic volcanic and intrusive rocks formerly assigned to the Nicola Group between the Martell and Bonaparte Faults, in the Venables Valley and Red Hill areas (Fig. 4.16). Within the Venables Valley area, Grette (1978) divided rocks into three main units. From inferred oldest to youngest these units are: (1) mafic to felsic volcanic rocks, related intrusive rocks, and volcanic derived sedimentary rocks; (2) thick, massive to bedded limestone; and (3) argillite and thin bedded limestone, with minor volcanic rocks.

To the north, in the Red Hill area, Ladd (1981) proposed four subdivisions for volcanic rocks, thought to be interbedded, and hence of contemporaneous age, which were assigned to the Nicola Group. These are (1) felsic crystal tuffs characterized by large quartz grains; (2) chlorite-rich mafic schist, with relict phenocrysts; (3) silicified greenstone; and (4) altered massive chloritic basalt. On Red Hill, Ladd (1981) mapped felsic tuffs cross cut by a series of fine- to coarse-grained granodioritic to tonalitic plutons. Three kilometers southwest of Red Hill, Ladd (1981) observed trondhjemite grading into rhyolite tuffs, and suggested that the intrusion was hypabyssal, with the volcanic and intrusive units being emplaced in the same magmatic event.

Felsic volcanic rocks from the Venables Valley and Red Hill consist of massive to bedded crystal to ash tuffs. Crystal tuffs are characterized by 2 to 5 mm diameter glassy quartz and/or plagioclase phenocrysts within a fine-grained quartzo-feldspathic matrix. Quartz and plagioclase commonly occur as broken grains, reflecting the pyroclastic nature of these rocks (Plate 4.12). The crystal tuffs contain scattered flow-banded, aphanitic clasts and sporadic layers of wispy chlorite, which may be remnants of flattened pumice fragments. Ash tuffs are characterized by a fine-grained quartzo-feldspathic matrix with rare 1 to 2 mm diameter quartz and plagioclase crystals.

The diorite to tonalite body that intrudes the volcanic rocks on Red Hill has a medium-grained granitic texture, and contains varying proportions of plagioclase, hornblende and quartz, with minor secondary calcite and epidote (Plate 4.13).

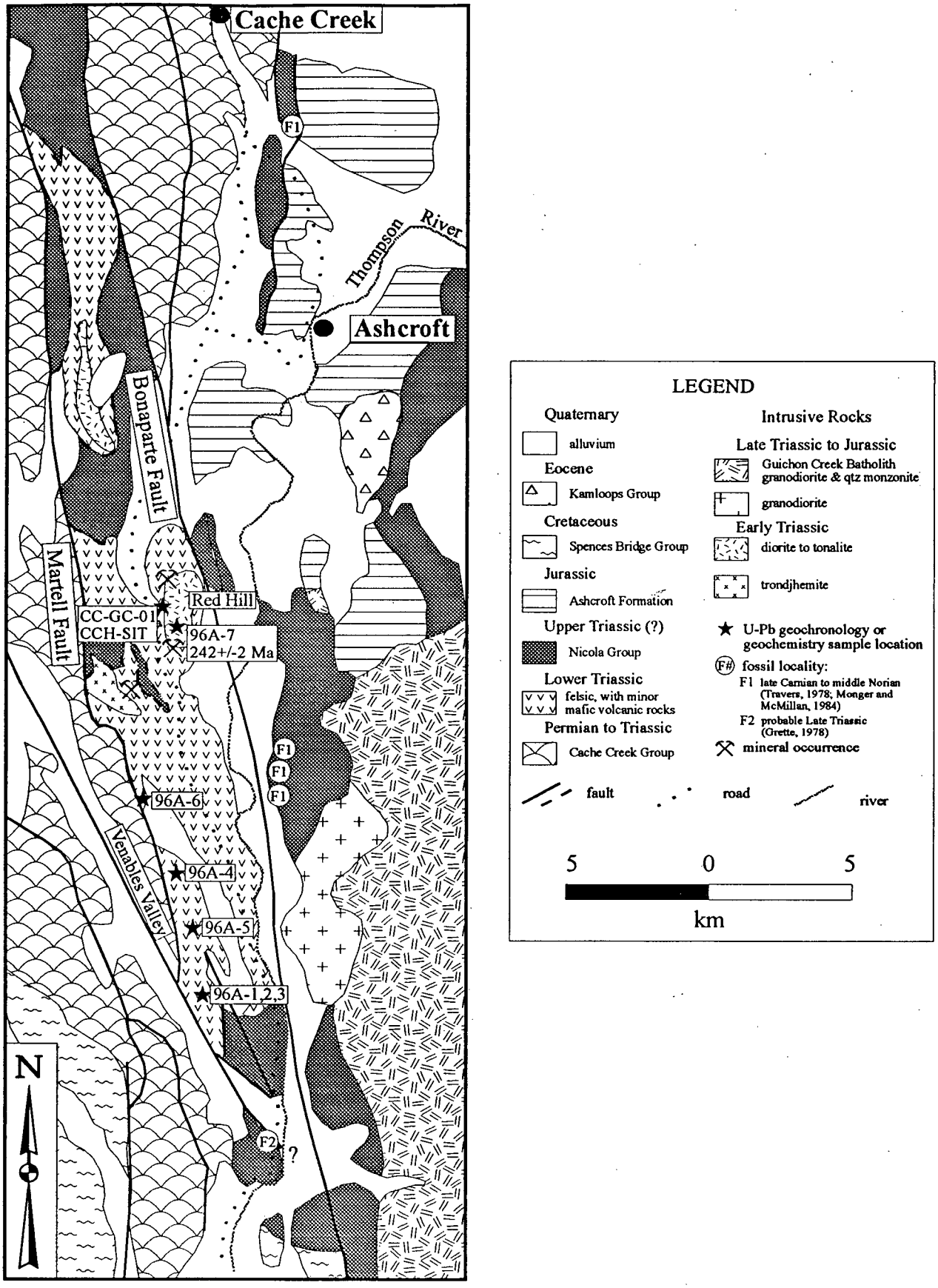

Figure 4. 16 Geology of the Spences Bridge - Cache Creek area (modified from Ladd, 1981; Monger and McMillan, 1984).

Biochronological constraints from south, east and north of the study area consist of probable Late Triassic conodonts from limestone (Grette, 1978), Late Triassic ammonites and pelecypods from argillite (Monger and McMillan, 1984), and middle Norian ammonites from sediments overlain by mafic volcanic rocks of the Nicola Group (Travers, 1978) (Fig. 4.16). However, these age determinations do not assist in constraining the age of felsic magmatism, as the dated sedimentary rocks are not found in conformable contact with the felsic rocks.

Grette (1978) obtained an Early Jurassic Rb-Sr whole rock isochron age of 196 +/-15 Ma, with a Sr_i of 0.7043 ($\pm$0.0002) from felsic volcanic and intrusive rocks within the study area; Grette attributed the elevated Sr_i to contamination by seawater Sr. The isochron is highly dependent on a sample of altered dacite. Hydrothermal alteration has the potential to perturb Rb-Sr systematics (Shirey, 1991). Regardless of the mechanism of isotopic disturbance, the validity of this age determination is suspect.

U-Pb geochronology

One sample of tonalite (96A-7) and three samples of crystal tuff (96A-1, 96-A3, and CC-GC-01) were collected and processed for U-Pb zircon analysis, as described below. Of the four samples, only the tonalite contained sufficient zircon for U-Pb analysis. The low Zr concentrations in the crystal tuffs (65-91 ppm), along with the relatively fine grain size may be responsible for the scarcity of recoverable zircon in the tuffs.

Sample preparation and U-Pb analyses were carried out at the Geochronology Laboratory of the University of British Columbia. The samples were processed and zircon was separated using conventional crushing, grinding, Wilfley table and heavy liquid techniques. All fractions were air abraded prior to analysis, to reduce the effects of surface-correlated lead loss (Krogh, 1982). Zircon grains were selected based on criteria such as magnetic susceptibility, clarity, morphology and size. Procedures for dissolution of zircon and extraction and purification of uranium and lead follow those of Parrish *et al.* (1987). Uranium and lead were loaded onto single, degassed refined rhenium filaments using the silica gel and phosphoric acid emitter technique. Procedural blanks were 9 and 6 picograms for lead and uranium, respectively. Errors assigned to individual analyses were calculated using the numerical error propagation method of Roddick

(1987) and all errors are quoted at the 2σ level. Ages were calculated using the decay constants recommended by Steiger and Jäger (1977). Age designations were based on the time scale of Harland *et al.* (1990) and the revised age of the Permo-Triassic boundary by Renne *et al.* (1995). Common lead corrections were made using the two-stage growth model of Stacey and Kramers (1975). Discordia lines were regressed using a modified York-II model (York, 1969; Parrish *et al.*, 1987). Uranium-lead analytical results are presented in Table 4.10.

Table 4 10 U-Pb zircon analytical data for a sample from the Ashcroft map area.

Fraction[1]	Wt.	U	Pb[2]	^{206}Pb	Pb^{4}	^{208}Pb[5]	Isotopic ratios(±1σ,%)[6]			Isotopic dates(Ma,±2σ)[6]		
	mg	ppm	ppm	^{204}Pb	pg	%	$^{206}Pb/^{238}U$	$^{207}Pb/^{235}U$	$^{207}Pb/^{206}Pb$	$^{206}Pb/^{238}U$	$^{207}Pb/^{235}U$	$^{207}Pb/^{206}Pb$
tonalite 96A-7												
A,c,N1,t	0.455	183	7	7528	26	8.3	0.03694±0.09	0.2601±0.09	0.05107±0.06	233.8±0.4	234.8±0.4	244.0±2.7
B,c,N1,t	0.204	139	5	8223	8	7.3	0.03712±0.13	0.2610±0.20	0.05100±0.11	235.0±0.6	235.5±0.8	240.9±5.2
C,c,N1,t	0.226	135	5	7877	9	7.6	0.03723±0.10	0.2615±0.19	0.05095±0.10	235.7±0.5	235.9±0.8	238.4±4.8
D,m,N1,t	0.265	169	6	8496	12	7.8	0.03666±0.14	0.2578±0.15	0.05101±0.05	232.1±0.7	232.9±0.6	241.2±2.5

[1]All fractions are air abraded; Grain size, smallest dimension: c= +134μm, m=-134μm+74μm
Magnetic codes: Franz magnetic separator sideslope at which grains are nonmagnetic; e.g., N1=nonmagnetic at 1°; Field strength for all fractions =1.8A; Front slope for all fractions=20°
Grain character codes: t=tabular
[2]Radiogenic Pb
[3]Measured ratio corrected for spike and Pb fractionation of 0.0043/amu ±20% (Daly collector)
[4]Total common Pb in analysis based on blank isotopic composition
[5]Radiogenic Pb
[6]Corrected for blank Pb, U and common Pb (Stacey-Kramers (1975) model Pb composition at the $^{207}Pb/^{206}Pb$ age of fraction, or age of sample)

Red Hill tonalite

The tonalite (96A-7) contained abundant coarse-grained tabular to prismatic zircon with few colourless baguette-shaped inclusions and good clarity. Analysis of four fractions of zircon yielded $^{207}Pb/^{206}Pb$ ages of 238 to 244 Ma (Fig. 4.17 and Table 4.10). The error ellipse of fraction C slightly overlaps the concordia curve, with a $^{206}Pb/^{238}U$ age of 236 Ma, which provides a minimum age for this rock. However, an Early Triassic age of 242 +/-2 Ma, based on the weighted mean $^{207}Pb/^{206}Pb$ age of all four fractions, is considered the best estimate of the age of this rock.

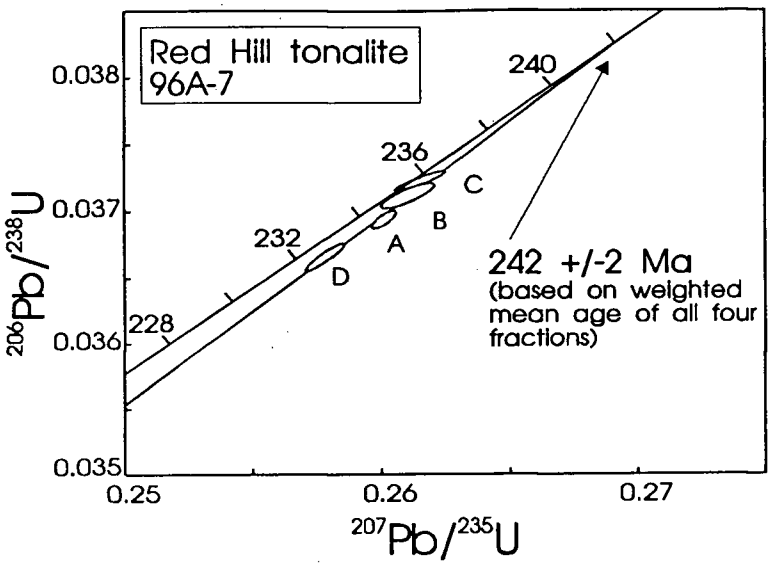

Figure 4. 17 U-Pb concordia diagram for tonalite sample 96A-7.

Geochemistry

major and trace elements

A suite of one intrusive and eight volcanic rock samples were analyzed for major and trace element abundances, using x-ray fluorescence at McGill University in Montreal, Quebec. Volcanic rocks range in composition from dacite to rhyolite (61-80% SiO_2, 0.19-0.30% TiO_2), whereas the intrusive rock has a tonalitic composition (63% SiO_2, 0.62% TiO_2) (Fig. 4.18a and Table 4.11). All samples have relatively low K_2O (0.05-1.70%) and high Na_2O (3.18-6.26%) concentrations.

Volcanic and intrusive rocks analyzed in this study have Zr/Y ratios of 1.1 to 5.5 (Table 4.11). Using the limits defined by Barrett and MacLean (1994), these rocks have a predominantly tholeiitic magmatic affinity (Fig. 4.18b).

rare earth elements

Rare earth element (REE) concentrations were determined for samples of two rhyolite crystal tuffs and the tonalite by neutron activation analysis at Actlabs in Ancaster, Ontario. All samples are characterized by near-flat patterns (Fig. 4.19 and Table 4.12). These patterns,

Table 4.11. Major and trace element data for samples from the Ashcroft map area.

sample number	lithology	SiO2 %	TiO2 %	Al2O3 %	Fe2O3 %	MnO %	MgO %	CaO %	Na2O %	K2O %	P2O5 %	LOI	Total	BaO ppm
96A-1	qtz+plag crystal tuff	69.76	0.30	12.12	2.77	0.15	1.54	3.79	3.18	1.70	0.06	4.21	99.63	309
96A-2	qtz+plag crystal tuff	79.63	0.22	11.88	0.78	0.02	0.41	0.27	6.26	0.07	0.05	0.53	100.13	28
96A-3	qtz+plag crystal tuff	77.90	0.19	10.00	1.72	0.10	0.70	2.40	4.45	0.22	0.04	2.45	100.19	95
96A-4	plag crystal tuff	60.80	0.60	15.24	8.61	0.16	3.64	1.53	6.00	0.05	0.11	3.43	100.21	64
96A-5	siliceous ash tuff	76.77	0.26	9.78	2.79	0.10	1.22	2.00	4.95	0.20	0.07	2.36	100.52	37
96A-6	qtz+plag crystal tuff	75.58	0.26	12.18	1.96	0.08	0.63	1.27	6.15	0.20	0.06	1.66	100.04	46
96A-7	tonalite	62.54	0.62	15.59	7.11	0.13	2.78	4.83	3.27	1.61	0.09	1.97	100.61	433
CC-GC-01	qtz crystal tuff	76.79	0.24	13.70	0.57	0.01	1.12	0.23	4.46	1.45	0.04	1.30	99.95	251
CCH-SIT	qtz+plag crystal tuff	76.51	0.27	13.65	1.23	0.00	0.20	0.27	5.90	0.92	0.03	1.03	100.03	137
Detection Limits (ppm):		60	35	120	30	30	95	15	75	25	35			17

sample number	Co ppm	Cr2O3 ppm	Cu ppm	Ni ppm	V ppm	Zn ppm	Ga ppm	Nb ppm	Pb ppm	Rb ppm	Sr ppm	Th ppm	U ppm	Y ppm	Zr ppm
96A-1	23	17	11	7	26	103	13	3.4	1.1	20.7	170.1	<d/l	4.5	35.6	84.0
96A-2	44	<d/l	<d/l	<d/l	<d/l	51	10	3.7	<d/l	<d/l	111.1	<d/l	3.6	34.2	108.1
96A-3	44	27	6	11	<d/l	72	10	3.0	<d/l	2.8	163.5	<d/l	3.8	33.7	91.4
96A-4	36	<d/l	6	4	197	104	16	4.3	2.7	<d/l	91.9	<d/l	5.2	25.6	27.8
96A-5	28	16	7	<d/l	49	67	8	3.8	<d/l	<d/l	82.8	<d/l	4.1	27.4	60.7
96A-6	36	20	<d/l	7	23	61	10	4.7	<d/l	1.6	69.2	<d/l	3.9	21.5	79.1
96A-7	31	47	68	9	150	97	14	3.1	2.5	36.4	155.6	3.3	5.5	36.8	112.2
CC-GC-01	30	<d/l	4	<d/l	23	45	15	7.6	<d/l	14.5	61.6	<d/l	<d/l	11.9	65.0
CCH-SIT	44	<d/l	12	<d/l	17	40	13	5.5	<d/l	7.9	75.4	<d/l	<d/l	32.2	88.8
Detection Limits (ppm)	10	15	2	3	10	2	1	1	1	1	1	1	1	1	1

Table 4.12. Rare earth element data for samples from the Ashcroft map area.

sample number	Au ppb	Ag ppm	As ppm	Br ppm	Cs ppm	Hf ppm	Hg ppm	Ir ppb	Sb ppm	Sc ppm	Se ppm	Ta ppm	W ppm	La ppm	Ce ppm	Nd ppm	Sm ppm	Eu ppm	Tb ppm	Yb ppm	Lu ppm
96A-3	<d/l	<d/l	<d/l	<d/l	<d/l	3.3	<d/l	<d/l	0.4	10.8	<d/l	0.9	212	5.5	14	9	2.64	0.80	0.7	3.17	0.44
96A-6	<d/l	<d/l	1	<d/l	<d/l	2.3	<d/l	<d/l	0.5	7.9	<d/l	1.0	150	4.4	11	7	1.66	0.51	0.4	1.79	0.25
96A-7	<d/l	<d/l	2	<d/l	1.1	4.5	<d/l	<d/l	0.6	23.1	<d/l	<d/l	108	6.5	19	11	3.18	0.86	0.8	3.48	0.48
Detection Limits	2 ppb	2 ppm	1 ppm	0.5 ppm	0.2 ppm	0.2 ppm	1 ppm	1 ppm	0.1 ppm	0.1 ppm	0.5 ppm	0.3 ppm	1 ppm	0.1 ppm	1 ppm	1 ppm	0.01 ppm	0.05 ppm	0.1 ppm	0.05 ppm	0.01 ppm

combined with low REE concentrations indicate derivation of the rhyolite tuffs and tonalite from primitive magmatic sources.

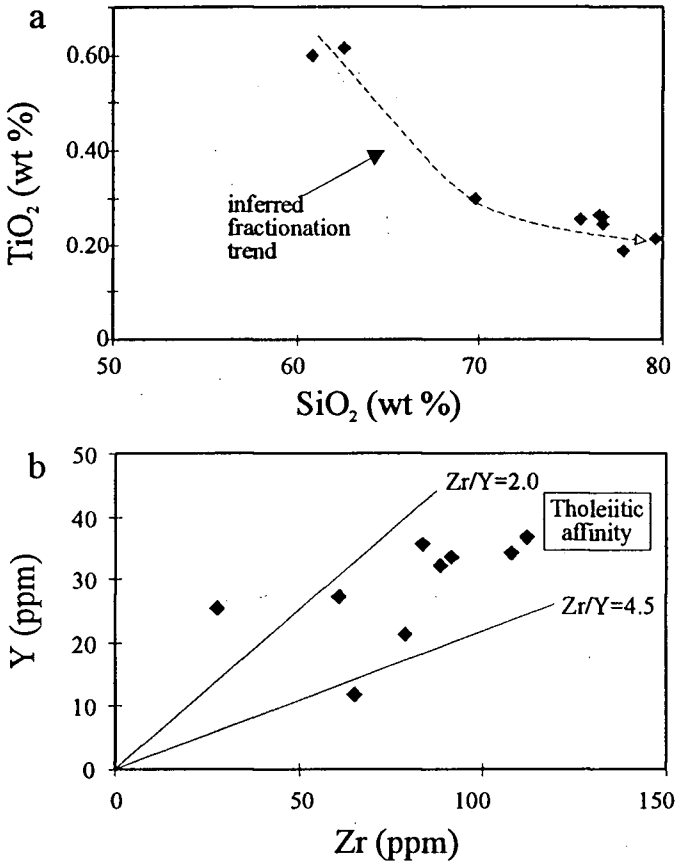

Figure 4. 18 a) TiO_2 versus SiO_2 diagram b) Zr versus Y diagram (Barrett and MacLean, 1994) for samples of volcanic and intrusive rocks from the Ashcroft area.

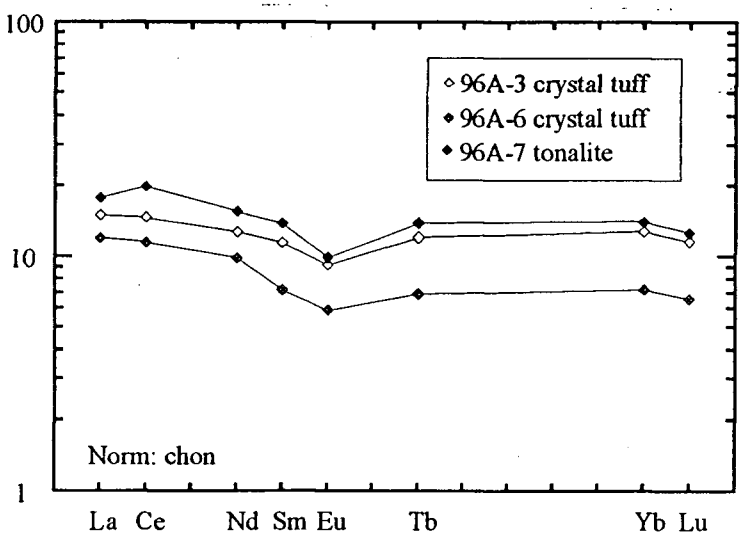

Figure 4. 19 Rare earth element diagram for one tonalite and two rhyolite crystal tuffs.

Discussion and Tectonic Implications

An Early Triassic age of 242 +/-2 Ma for the tonalite dated in this study is older than rocks of the Nicola Group and contemporaneous plutonism, but is indistinguishable from rocks of the Kutcho Assemblage (McMillan et al., 1982; Monger and McMillan, 1984; Childe and Thompson, 1995a and b).

The strong similarity between the REE patterns of the rhyolites and tonalite suggests that the volcanic and intrusive rocks were derived from the same magmatic source, and are probably of similar age. The low-K tholeiitic chemistry of these rocks is comparable to those of the Kutcho Assemblage, and dissimilar from the calc-alkaline to shoshinitic chemistry characteristic of the Nicola Group (Mortimer, 1986; Thompson *et al.*, 1995; Childe and Thompson, submitted). Based on the data presented in this paper, felsic volcanic and intrusive rocks which occur between the Martell and Bonaparte Faults, near Ashcroft, are tentatively correlated with the Permo-Triassic Kutcho Assemblage, rather than the Late Triassic to Early Jurassic Nicola Group. Mafic volcanic rocks assigned to the Nicola Group occur both to the east and west of the Bonaparte Fault (Fig. 4.16). The presence of Late Triassic fossils imply that this correlation is valid for basaltic rocks which occur east of the Bonaparte Fault. However, the age of basaltic rocks that occur west of the Bonaparte Fault, in proximity to, and possibly interbedded with rhyolite tuffs, is not constrained. These basaltic rocks may be contemporaneous with the Early Triassic felsic rocks, rather than the younger Nicola Group lavas. Detailed mapping and geochemistry, accompanied by additional U-Pb geochronology are necessary in order to determine the extent of Early Triassic age rocks with primitive arc affinity in this region.

VMS Potential

The presence of rocks of Kutcho Assemblage age and affinity within the Ashcroft map area raises the potential for Kutcho Creek-equivalent Cu-Zn volcanogenic massive sulphide mineralization.

A number of copper occurrences are known within the Venables Valley - Red Hill area. The Red Hill showing (B.C. MINFILE 092INW042) contains chalcopyrite, chalcocite, and secondary Cu minerals that occur within chlorite and sericite altered pyritic greenstone, in proximity to Early Triassic rhyolite tuffs and tonalite. Also on Red Hill are unnamed gossans containing malachite and azurite (Ladd, 1981). Rhyolite tuff-hosted mineralization includes two unnamed copper occurrences, which occur approximately 1 km east of the trondhjemite body, southwest of Red Hill (Ladd, 1981). Based on the correlation of these rocks with the Kutcho Assemblage proposed in this paper, mineralized occurrences within this area should be explored for Cu-Zn VMS potential.

References

Barrett, T.J., Sherlock, R.L. and Thompson, J.F.H. (1996): Geology and Geochemistry of the Kutcho Creek VMS deposit, northern British Columbia; *Exploration and Mining Journal.*

Barrett, T.J. and MacLean, W.H. (1994): Chemostratigraphy and Hydrothermal Alteration in Exploration for VHMS Deposits in Greenstones and Younger Volcanic Rocks, *in* Alteration and Alteration Processes associated with Ore-forming Systems, Lentz, D.R., Editor, *Geological Association of Canada*, Short Course Notes volume 11, pages 433-467.

Bridge, D.A., Marr, J.M., Hashimoto, K., Obara, M. and Suzuki., R. (1986): Geology of the Kutcho Creek Volcanogenic Massive Sulphide deposits, Northern British Columbia; *in* Mineral Deposits of Northern Cordillera, *Canadian Institute of Mining Special Volume 37*, Morin, J.A. Editor, pages 115-128.

Childe, F.C. and Thompson, J.F.H. (1995a): U-Pb Age Constraints and Pb Isotopic Signature of the Kutcho VMS Deposit: Implications for the Terrane Affiliation of the Kutcho Formation, North Central British Columbia; *Geological Association of Canada Mineralogical Association of Canada Program with Abstracts*, page A 16.

Childe, F.C. and Thompson, J.F.H. (1995b): U-Pb Age Constraints and Pb Isotopic Signature of the Kutcho VMS Deposit: Implications for the Terrane Affiliation of the Kutcho Formation, North Central British Columbia; *The Gangue*, Grant, B. Editor, Issue 49, pages 6-8.

Childe, F.C. and Thompson, J.F.H. (submitted): Geological Setting, U-Pb geochronology, and Radiogenic Isotopic Characteristics of the Permo-Triassic Kutcho Assemblage, Northcentral British Columbia.

Gabrielse, H. (1979): Geology of the Cry Lake Map Area; *Geological Survey of Canada*, Open File Report 610.

Grette, J. (1978): Cache Creek and Nicola Groups near Ashcroft, B.C.; unpublished M.Sc. thesis, *University of British Columbia*, 88 pages.

Harland, W.B., Armstrong, R.L., Cox, A.V., Craig, L.E., Smith, A., G. (1990): A Geologic Time Scale, 1989: 263 pages.

Krogh, T. (1982): Improved Accuracy of U-Pb Zircon Ages by the Creation of More Concordant Systems Using Air Abrasion Technique; *Geochemica et Cosmochemica Acta*, Volume 46, pages 637-649.

Ladd, J.H. (1981): A Report on the Geology of the Cache Creek - Nicola Contact Southwest of Ashcroft (92I/11); *in* Geology in British Columbia, *B.C. Ministry of Energy, Mines and Petroleum Resources*, pages 91-97.

McMillan, W.J., Armstrong, R.L. and Harakal, J. (1982): Age of the Coldwater Stock and Nicola Batholith, Near Merritt; *in* Geological Fieldwork 1981, *B.C. Ministry of Energy, Mines and Petroleum Resources*, Paper 1982-1, pages 102-105.

Monger, J.W.H. and McMillan, W.J. (1984): Bedrock geology of the Ashcroft (92I) Map Area; *Geological Survey of Canada,* Open File 980.

Monger, J.W.H, Wheeler, J.O., Tipper, H.W., Gabrielse, H., Harms, T., Struik, L.C., Campbell, R.B., Dodds, C.J., Gehrels, G.E. and O'Brien, J. (1991): Part B, Cordilleran terranes; Upper Devonian to Middle Jurassic assemblages, *in* Geology of the Cordilleran Orogen in Canada, Gabrielse, H. and Yorath, C.J. Editors; *Geological Survey of Canada*, pages 281-327.

Mortimer, N. (1986): The Nicola Group: Late Triassic and Early Jurassic Subduction-Related Volcanism in British Columbia; *Canadian Journal of Earth Sciences,* Volume 24, pages 2521-2536.

Parrish, R.R., Roddick, J. C., Loveridge, W. D. and Sullivan, R. W. (1987): Uranium-Lead Analytical Techniques at the Geochronological Laboratory, Geological Survey of Canada; *in* Radiogenic Age and Isotopic Studies, Report 1, *Geological Survey of Canada*, Paper 87-2, pages 3-7.

Preto, V.A. (1977): The Nicola Group: Mesozoic Volcanism Related to Rifting in Southern British Columbia; *Geological Association of Canada,* Special Paper Number 16, pages 39-57.

Renne, P.R. (1995): Synchrony and Causal Relations Between Permian-Triassic Boundary Crises and Siberian Flood Volcanism; *Science*, Volume 269, pages 1413-1416.

Roddick, J, C. (1987): Generalized Numerical Error Analysis with Applications to Geochronology and Thermodynamics; *Geochimica et Cosmochimica Acta*, Volume 51, pages 2129-2135.

Shannon, K. (1982): Cache Creek Group and Contiguous Rocks Near Cache Creek, B.C.; unpublished M.Sc. thesis, *University of British Columbia*, 72 pages.

Shirey, S.B. (1991): The Rb-Sr, Sm-Nd and Re-Os Isotopic Systematics: A Summary and Comparison of Their Applications to the Cosmochronology and Geochronology of Igneous Rocks; *Mineralogical Association of Canada* Short Course Handbook on Applications of Radiogenic Isotope Systems to Problems in Geology, Heaman, L. and Ludden, J.N. Editors, pages 103-166.

Stacey, S. J. and Kramers, J. D. (1975): Approximation of Terrestrial Lead Isotope Evolution by a Two-stage Model; *Earth and Planetary Science Letters*, Volume 26, pages 207-221.

Steiger, R. H. and Jäger, E. (1977): Subcommission on Geochronology: Convention on the Use of Decay Constants in Geo- and Cosmochronology; *Earth and Planetary Science Letters*, Volume 36, pages 359-362.

Thompson, J.F.H., Barrett, T.J., Sherlock, R.L. and Holbec, P. (1995): The Kutcho VMS Deposit, British Columbia: A Felsic Volcanic-hosted Deposit in a Tholeiitic Bimodal Sequence, *Geological Association of Canada - Mineralogical Association of Canada Program with Abstracts*, page A 104.

Thorstad, L. and Gabrielse, H. (1986): The Upper Triassic Kutcho Formation, Cassiar Mountains, North-Central British Columbia; *Geological Survey of Canada*, Paper 86-16, 53 pages.

Travers, W.B. (1978): Overturned Nicola and Ashcroft strata and their relation to the Cache Creek Group, Southwestern Intermontane Belt, British Columbia; *Canadian Journal of Earth Sciences*, Volume 15, pages 99-116.

York, D. (1969): Least-squares Fitting of a Straight Line with Correlated Errors; *Earth and Planetary Science Letters*, Volume 5, pages 320-324.

PART 4:

Primitive Permo-Triassic volcanism in the Canadian Cordillera:
Tectonic and metallogenic implications

Abstract

Permo-Triassic volcanic rocks of the Kutcho and Sitlika Assemblages, and the Venables Valley - Red Hill area occur as fault-bounded slivers adjacent to the Cache Creek terrane in the Canadian Cordillera. Rocks from the three areas consist of isotopically primitive (initial ε_{Nd} = +7.6 to +8.2), compositionally bimodal low-K tholeiitic basalt and rhyolite, with associated intrusions. These arc sequences are distinct in age, chemistry and radiogenic isotopic signature from other allochthonous arc sequences in the Cordillera. Data presented in this paper suggest that these primitive arc assemblages were built directly on oceanic crustal basement, and as such may represent a previously unrecognized intraoceanic arc terrane.

Introduction

The Kutcho Assemblage (KA), and overlying marine sediments comprise the King Salmon Allochthon, a tectonic wedge which lies in thrust and fault contact with the oceanic Cache Creek terrane and the island-arc Stikine and Quesnel terranes (Fig. 4.20a). The age, terrane affiliation, and tectonic setting of the KA have been the subject of considerable debate (e.g., Monger, 1977; Panteleyev and Pearson, 1976; Thorstad and Gabrielse, 1986). Recent U-Pb zircon geochronology has yielded Latest Permian to Early Triassic ages for volcanic rocks of the KA and plutons which intrude it (Childe and Thompson, 1995; Childe and Thompson, submitted), whereas geochemical (Barrett et al., 1996; Childe and Thompson, submitted) and radiogenic isotope (Childe and Thompson, submitted) data define a distinctive primitive arc chemistry for the KA. These characteristics are inconsistent with formation of the KA within the recognized elements of the adjacent Quesnel or Stikine island arc terranes, as defined by Souther (1991). In this paper the age, geochemistry and Nd isotopic signature of magmatic rocks of the KA are

compared with two lithologically similar, fault-bounded sequences which occur in similar tectonic positions within the Canadian Cordillera; these are the Sitlika Assemblage (SA) in the Manson River (NTS 93N) map area, and a sequence of felsic volcanic and intrusive rocks of the Venables Valley - Red Hill area (VV-RH) in the Ashcroft (NTS 92I) map area (Figs. 4.20b and c).

Geology of the Kutcho Assemblage (KA)

Childe and Thompson (submitted) divide rocks of the KA into northern and southern sequences; the stratigraphic relationship between the two sequences is unclear. The Kutcho Creek volcanogenic massive sulfide (VMS) deposit, with reserves of 14 Mt grading 1.8% Cu, 3% Zn, 29 g/t Ag and 0.3 g/t Au is hosted within rhyolite near the top of the northern sequence (Fig. 4.20a) (Bridge et al., 1986).

The southern sequence contains compositionally bimodal volcanic rocks, consisting of interbedded basalt and rhyodacite to rhyolite, with minor sedimentary intervals. Mafic volcanic rock types consist of pillowed to massive basalt flows and possible basaltic tuffs. Felsic volcanic components consist of aphanitic to fine-grained plagioclase±quartz porphyritic flow and fragmental rocks, mass flows, and crystal to ash tuffs. Sedimentary rocks consist of thin (<0.5 m) beds of argillite. The presence of pillowed lavas and argillite attest to deposition in a subaqueous environment. Facing directions in the southern sequence are rare, but where present indicate younging to the south. The southern sequence is intruded by trondhjemite and quartz-plagioclase porphyry, as well as minor diorite (Fig. 4.20a). Quartz-plagioclase porphyry from the southern sequence has been dated at 244±6 Ma (Table 4.13) (Childe and Thompson, submitted).

The northern sequence, which youngs consistently to the north, consists of fragmental coarse-grained plagioclase±quartz porphyritic rhyodacite, overlain by lapilli to crystal tuffs, which in turn are overlain by coarse-grained quartz±plagioclase porphyritic fragmental rocks. Massive sulphide mineralization occurs at the base of the upper unit (Fig. 4.20a). The coarse fragmental rocks, of probable mass flow and pyroclastic origin, are overlain by fine-grained rhyolite tuffs which grade upward into argillite. Plagioclase-augite porphyritic gabbros intrude the upper part of the volcanic section and overlying argillite. Tuff and argillite are overlain by conglomeratic sediments, derived at least in part from the underlying volcanic rocks, and lenses of unfossiliferous

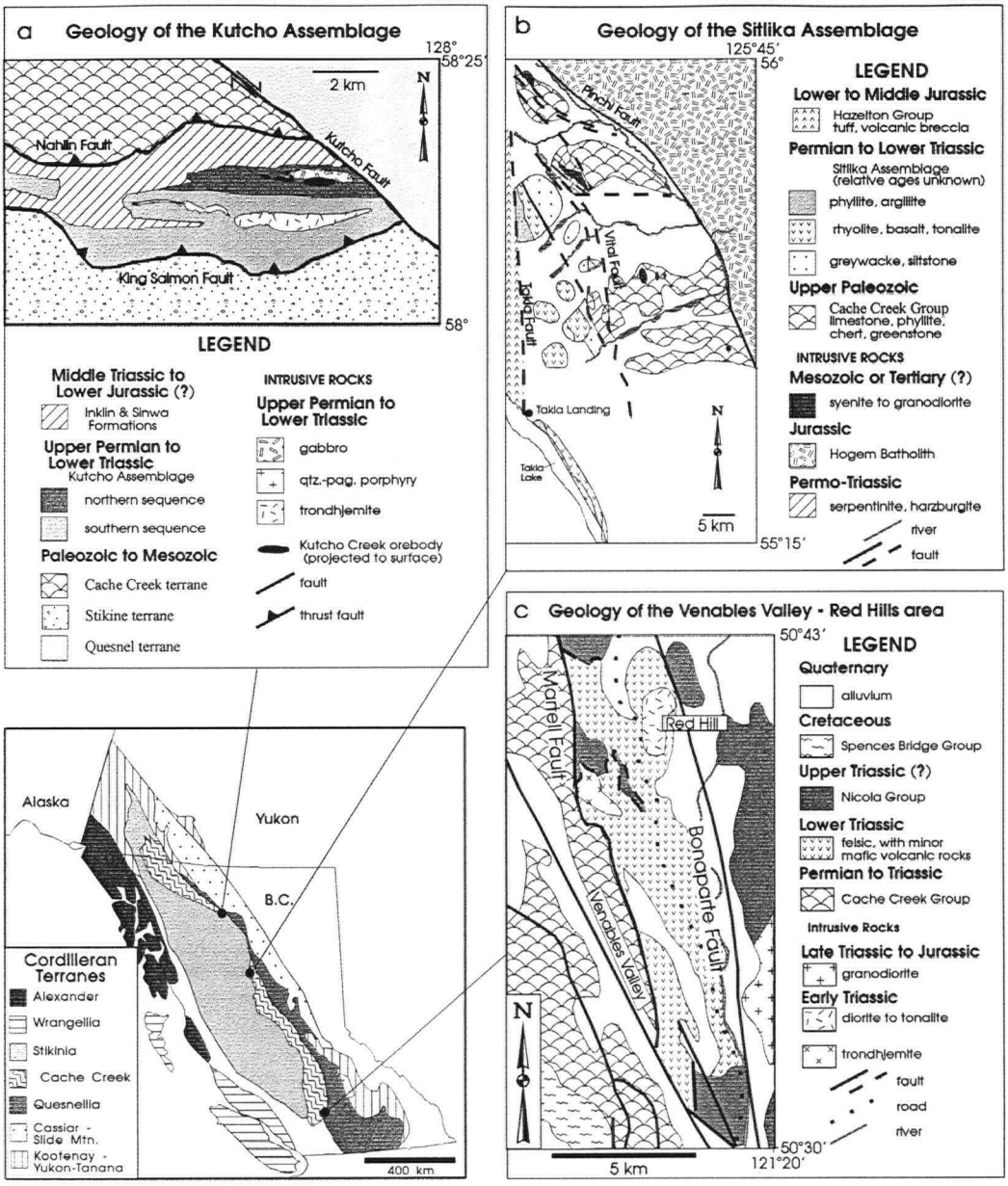

Figure 4. 20 Terrane map of the Canadian Cordillera, a) geology of the Kutcho Assemblage and adjacent rocks; b) geology of the Sitlika Assemblage and adjacent rocks; and c) geology of the Venables Valley - Red Hills area (modified from Thorstad and Gabrielse, 1986; Paterson, 1974; Monger and McMillan, 1984).

limestone, which is correlated on the basis of lithology, with the Upper Triassic Sinwa Formation (Thorstad and Gabrielse, 1986). Plagioclase±quartz porphyritic rhyodacite in the lower part of the northern sequence has been dated at 246 +7/-5 Ma, and quartz±plagioclase porphyritic rhyolite has been dated at 242 ±1 Ma (Table 4.13, Childe and Thompson, submitted). The later

date constrains the upper age limit for volcanism in the KA, but the base of the KA is not exposed, and therefore the maximum age of volcanism in the KA remains unconstrained.

Geology of the Sitlika Assemblage (SA)

The SA, which lies between the Takla and Vital faults in central British Columbia, consists of sedimentary and compositionally bimodal volcanic rocks (Paterson, 1974; Schiarizza and Payie, 1997; Childe and Schiarizza, 1997) (Fig.4.20b). Volcanic rocks of the SA consist of quartz and/or plagioclase porphyritic rhyodacite to rhyolite flows and tuffs, and pillowed to massive basalt flows, and are intruded by gabbro, diorite, and tonalite (Schiarizza and Payie, 1997); several volcanic-hosted base metal showings occur within the SA. Quartz porphyritic rhyolite from the SA, and equigranular to quartz+plagioclase porphyritic tonalite which intrudes it have been dated at 258 +10/-1 Ma and 241 +/-1 Ma, respectively (Table 4.13) (Childe and Schiarizza, 1997). Volcanic rocks of the SA are conformably overlain by marine sedimentary rocks, which include siltstone, sandstone, conglomerate, and limestone; this sequence is similar to sedimentary rocks which overlie the KA.

Previous workers (Monger et al., 1978; Thorstad and Gabrielse, 1986) have observed that the SA resembles the KA in terms of general composition and structural style; these observations are now reflected in the tectonic assemblage map of the Canadian Cordillera (Wheeler and McFeely, 1991). The present study provides the first geochronological and geochemical data which verifies a correlation between the SA and KA.

Geology of Volcanic and Plutonic Rocks in the Venables Valley - Red Hill Area (VV-RH)

Fault-bounded volcanic and plutonic rocks correlated by Grette (1978) and Ladd (1981) with the western belt of the Upper Triassic Nicola Group occur between the Martell and Bonaparte faults in the VV-RH of southern British Columbia (Fig. 4.20c). Felsic volcanic rocks in the VV-RH consist of massive to bedded rhyolite ash tuff and quartz and/or plagioclase crystal tuffs; mafic volcanic rocks consist of schistose and altered basalt, which may either be interbedded and coeval with the rhyolite tuffs, or fault-bounded slivers of the Nicola Group or Cache Creek terrane; volcanic-hosted Cu showings occur on Red Hill (Ladd, 1981). Trondhjemite intrusions

cross cut and grade into the rhyolite tuffs (Ladd, 1981). A diorite to tonalite body which intrudes the rhyolite tuffs was dated at 242 ±2 Ma, precluding correlation of the rhyolite tuffs with Late Triassic rocks (Childe et al., 1997).

Geochemistry

Major and Trace Elements

The ranges of selected major and trace element concentrations, and Zr/Y ratios for rocks of the KA, SA and VV-RH are summarized in Table 2. Volcanic rocks of the KA and SA are compositionally bimodal, with basalt and dacite to rhyolite, whereas those from the VV-RH are dacite to rhyolite, but as discussed above may include interbedded basalt. Volcanic rocks from the three areas are geochemically similar and characterized by low K and Zr and high Na contents (Table 4.14). Zircon in the felsic volcanic and intrusive rocks in all areas have distinctly low U contents (Table 4.13). Based on the limits defined by Barrett and MacLean (1994), Zr/Y ratios from the three areas indicate tholeiitic magmatic affinities (Fig. 4.21). Felsic plutonic rocks from each of the three regions are comparable in composition to the felsic volcanic rocks which they intrude.

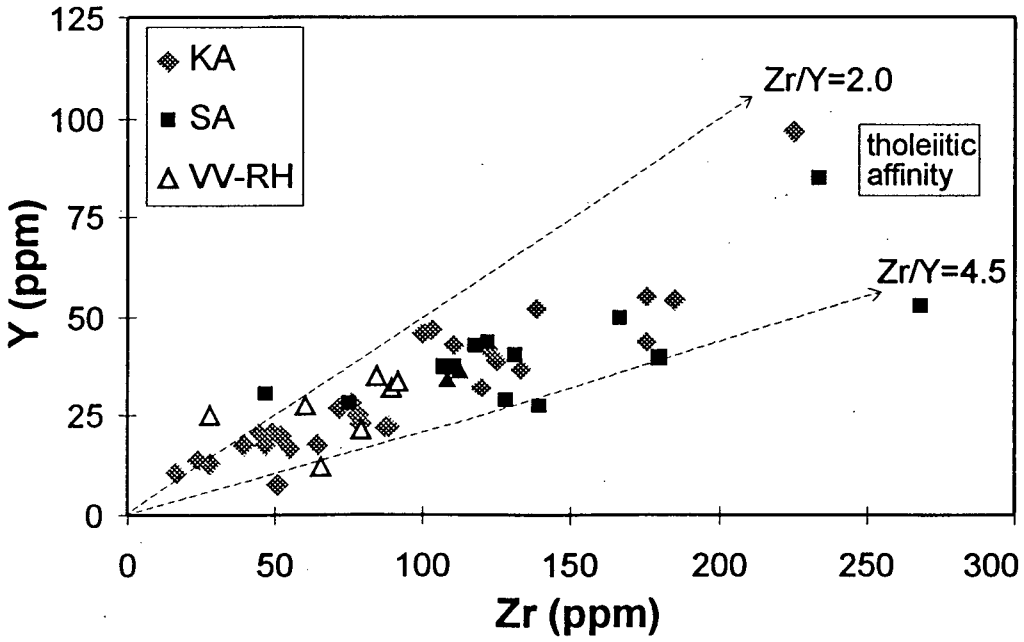

Figure 4. 21 Plot of Zr *versus* Y for volcanic rocks of the KA, SA, and VV-RH, and associated felsic plutonic rocks (data from Childe and Thompson, submitted; Childe and Schiarizza, 1997; Childe et al., 1997).

Table 4 13 U-Pb zircon ages and initial ε_{Nd} for the Kutcho Assemblage (KA), Sitlika Assemblage (SA), and felsic volcanic and intrusive rocks from the Venables Valley - Red Hill area (VV-RH); abbreviations: eP = Early Permian lP = Late Permian, eTr = Early Triassic, *age designations are based on the time scale of Harland et al. (1991) and the age of the Permian-Triassic boundary determined by Renne et al., (1995); data sources: KA = Childe and Thompson, (submitted), SA = Childe and Schiarizza, (1997), VV-RH = Childe et al., (1997), **error = $\pm$0.5 ε_{Nd} units.

Region	Lithology	U-Pb age	Period*	U in zircon (ppm)	ε_{Nd} (initial)**
KA	qtz.-plag. porphyritic rhyolite	242 +/-1 Ma	eTr	137-157	+7.8
KA	plag.-qtz. porphyritic rhyolite	246 +7/-5 Ma	lP-eTr	73-90	-
KA	qtz.-plag. porphyry	244 +/-6 Ma	lP-eTr	76-103	+7.8
KA	trondhjemite	-	-	-	+7.6
SA	tonalite	241 +/-1 Ma	eTr	174-244	-
SA	qtz. porphyritic rhyolite	258 +10/-1 Ma	eP-lP	53-77	+8.2
VV-RH	tonalite	242 +/-2 Ma	eTr	135-183	-

Table 4 14 Ranges of selected major and trace element concentrations for rocks of the KA, SA and VV-RH; data sources KA = Childe and Thompson, (submitted); SA = Childe and Schiarizza, (1997); VV-RH = Childe et al., (1997).

Region	Lithology	SiO_2 (%)	K_2O (%)	Na_2O (%)	Zr (ppm)	Zr/Y	Ce_n/Yb_n
KA	basalt	41-52	0.02-0.12	2.86-3.69	17-45	1.6-2.6	0.8-1.1
KA	rhyodacite to rhyolite	76-80	0.06-0.89	3.00-5.95	103-225	2.2-3.7	0.7-1.0
KA	qtz.-plag. porphyry & trondhjemite	66-77	0.14-0.95	4.80-6.12	79-175	2.2-4.0	0.9-1.4
SA	basalt	47-50	0.04-0.45	3.79-5.38	47-121	1.5-2.9	-
SA	dacite to rhyolite	62-85	0.18-1.28	3.04-7.23	166-268	2.7-5.0	1.3
SA	tonalite	65-74	0.30-0.69	5.09-5.56	118-139	2.8-5.1	1.4
VV-RH	dacite to rhyolite	61-80	0.07-1.70	3.18-6.26	28-108	1.1-3.7	1.4-1.5
VV-RH	tonalite	63	1.61	3.27	112	3.0	1.1

Rare Earth Elements

Rare Earth Element (REE) plots of felsic volcanic rocks of the KA, SA, and VV-RH, and felsic plutonic rocks are presented in Figure 4.22. The slope, and therefore degree of evolution, of REE patterns is described using the chondorite-normalized Ce/Yb ratio (Ce_n/Yb_n), thereby removing the potential problem of La mobility due to alteration or metamorphism, and utilizing the better precision of Yb measurements. REE signatures from felsic rocks in all three areas are similar and are characterized by near-flat REE patterns (Ce_n/Yb_n = 0.9-1.5) and low overall REE concentrations. All rocks, with the exception of tonalite from the SA, have negative europium anomalies, consistent with plagioclase fractionation. Within each area, volcanic and plutonic rocks have comparable REE signatures. Basalt from the KA reported by Childe and Thompson (submitted) have near-flat to slightly LREE depleted (Ce_n/Yb_n = 0.8-1.1) REE patterns, consistent with derivation from an N-MORB-type source (Sun and McDonough, 1989).

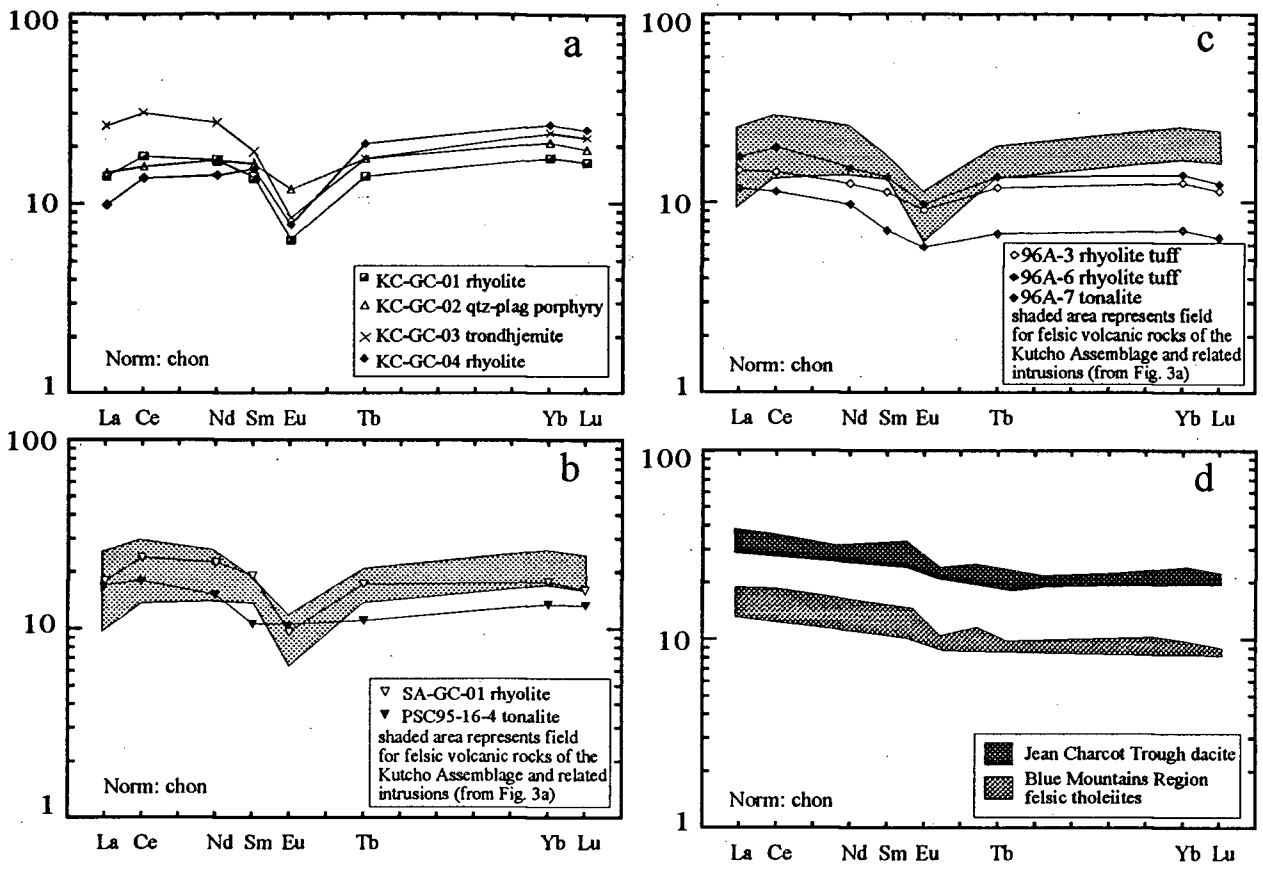

Figure 4. 22 Chondorite-normalized REE diagrams for a) rhyolite of the KA, and quartz-plagioclase porphyry and trondhjemite which intrude the KA (Childe and Thompson, submitted); b) rhyolite of the SA, and tonalite which intrudes the SA (Childe and Schiarizza, 1997); c) rhyolite tuffs of the VV-RH, and tonalite which intrudes the rhyolite tuffs (Childe et al., 1997); and d) Permian to Triassic felsic volcanic and plutonic rocks of the Blue Mountains terrane, northwest United States (Vallier, 1995), and felsic volcanic rocks of the Jean Charcot Trough, Vanuatu arc, Southwest Pacific (Nakada et al., 1994).

Nd Isotope Data

Rhyolite mass flows of the KA, and trondhjemite which intrudes it, have initial ε_{Nd} values of +7.6 to 7.8, while rhyolite from the SA has an initial ε_{Nd} value of +8.2 (Childe and Thompson, submitted; Childe and Schairizza, 1997). These high positive values suggest derivation from primitive magmatic sources, with no incorporation of old, evolved sialic components. In comparison, felsic rocks of the Stikine island arc terrane have reported values of +2.7 to 5.8, which, while still primitive, are more evolved than those from the KA and SA (Samson et al., 1989; Bevier and Anderson, pers. comms., 1995; Childe, unpublished data). No comparable database exists for felsic rocks in Quesnellia.

Discussion

Comparison of the KA, SA and VV-RH

Rocks of the KA, SA, and VV-RH are comprised of Permo-Triassic quartz- and plagioclase-porphyritic felsic volcanic rocks, with related intrusions. Contemporaneous basaltic flow rocks exist in the KA and SA, and may also be present in the VV-RH. Silicic rocks from the three areas include low-K, high-Na tholeiitic volcanic rocks and related plutons, with near-flat REE patterns; Nd isotopic signatures of these rocks in the KA and SA are extremely primitive. Basaltic volcanic rocks of the KA and SA are low-K, with a N-MORB REE signature. The similarities in mineralogy, chemistry, radiogenic isotopic signature and age indicate that rocks of the KA, SA, and VV-RH could have formed either as a single assemblage, which was subsequently dispersed by faulting, or as separate arc assemblages which formed within the same environment in the same time period. It is not possible to distinguish between these two alternatives on the basis of field and laboratory data, and therefore we favor the second, more conservative interpretation.

Tectonic Environment

The chemical and isotopic characteristics of the KA, SA and VV-RH summarized above are consistent with formation within an intraoceanic island arc environment. Barrett et al. (1996) have suggested that rocks of the KA probably formed within a fore-arc setting above a subduction zone, an interpretation which is consistent with the data presented in this paper.

Permo-Triassic rocks with similar chemistry and mineralogy to those of the KA, SA and VV-RH occur within the Wallowa and Baker terranes of the Blue Mountains Region (BMR) of Oregon, Idaho, and Washington (Vallier, 1995). These felsic volcanic-dominated sequences are characterized by low-K, high-Na tholeiitic quartz and/or plagioclase porphyritic dacite to rhyolite and trondhjemite, and low-K tholeiitic basalt, with near-flat REE patterns that remain almost constant with increasing SiO_2 (Ce_n/Yb_n = 1.0-1.9, Fig. 4.22d) (Vallier, 1995). These rocks are interpreted by Vallier (1995) to have formed as early, probably fore-arc sequences, within a Permo-Triassic intraoceanic island arc. The recognition of several sequences of Permo-Triassic tholeiitic volcanic rocks throughout the Cordillera, usually occurring as tectonic slivers, suggests

that this magmatic event may have been widespread. The Kutcho Creek Cu-Zn and Iron Dyke Cu-Au VMS deposits are hosted within tholeiitic rhyolites of the KA and the Wallowa terrane of the BMR, respectively (Bridge et al., 1986; Bussey and LeAnderson, 1994). The presence of significant VMS mineralization in the KA and BMR indicates a potential for comparable deposits within rocks of this age and chemical affinity, such as the SA and VV-RH, which are already know to host showings of possible volcanogenic origin, and other not yet recognized correlative tectonic slices.

Magmatic Source

Chemically similar rocks to the KA, SA and VV-RH are found in the northern Jean Charcot back-arc Trough (NJC) of the Vanuatu arc, in the southwest Pacific. Igneous rocks from the NJC include a compositionally bimodal volcanic assemblage, with low-K (<1%) N-MORB-type basalt, and low-K (<1%), high-Na (>6%) dacite that compositionally resembles trondhjemite; basalt has a tholeiitic affinity, and dacite has a tholeiitic to transitional affinity (Nakada et al., 1994). The two rock types have comparable, near-flat REE patterns (basalt: Ce_n/Yb_n= 0.9-1.6; dacite: Ce_n/Yb_n= 1.6-1.7) and almost identical ratios of incompatible elements (Fig. 4.22d) (Nakada et al., 1994). Nakada et al. (1994) concluded that production of the dacite by partial melting of crustal material would not produce the geochemical coherence observed between the basalt and dacite; rather the high-Na dacite evolved from a mantle-derived basaltic magma as a product of fractional crystallization. Permian to Early Triassic tholeiitic compositionally bimodal rocks of the BMR, which are discussed above, are interpreted to have formed by the same process, but within a fore-arc setting (Vallier, 1995). Low-K, high-Na felsic lavas of the KA, SA and VV-RH, and low-K basalt of the KA and SA exhibit nearly identical geochemical relations as bimodal rocks of the NJC and BMR. We suggest, that similar to the NJC and BMR, felsic rocks of the KA, SA and VV-RH formed as the products of fractional crystallization of a mantle derived, low-K tholeiitic basalt. The chemical similarities between bimodal volcanic rocks of the NJC, a young back-arc trough, and the BHR, KA, SA and VV-RH, which are interpreted to represent ancient fore-arc assemblages, suggest felsic magmas produced through the fractional crystallization of mafic melts can form in different tectonic settings within the arc environment.

Terrane Affiliation of the KA, SA and VV-RH

The present tectonic position of the KA, SA, and VV-RH suggests that these rocks may have formed either as part of Stikinia or Quesnellia, directly on the Cache Creek terrane, or as a discrete, previously unrecognized intraoceanic arc terrane. Rocks of the KA, SA and VV-RH formed in the Permian to Early Triassic. Within Stikinia and Quesnellia this period corresponds to a hiatus in volcanism, marked by regional unconformities; therefore correlation of the volcanic sequences from the KA, SA and VV-RH with these terranes is unlikely.

The primitive arc chemistry and Nd signatures of rocks of the KA, SA and VV-RH indicate formation in an intracoeanic island arc, probably built directly on oceanic crustal basement. Thorstad and Gabrielse (1986) suggest that the KA formed on the Cache Creek terrane. However, where visible, the contact between the Cache Creek and KA, SA and VV-RH is tectonic. Furthermore, the distinctive Tethyan faunal assemblages that characterize Cache Creek (Gabrielse and Yorath, 1991) have not been identified in the KA. In the French Range (FR), 150 km north of the KA, undated mafic to felsic volcanic rocks and Permian sedimentary rocks, which may be correlative with the KA, directly overlie Cache Creek rocks (Monger, 1975); further work in this area is required to document a potential relationship among the FR, KA, and Cache Creek terrane.

Conclusions

Low-K tholeiitic felsic $\pm$ mafic lavas and associated plutons of the KA, SA and VV-RH are primitive arc magmas which have experienced no significant contamination by sialic crust, and probably formed in an intraoceanic island arc setting. These magmatic rocks are distinct in age, chemistry and radiogenic isotopic signature from the Stikine and Quesnel island arc terranes and may have formed on a substrate of oceanic affinity, such as the Cache Creek terrane.

Plate 4. 2 Quartz-plagioclase granophyric intergrowth in rhyolite, northern sequence (field of view = 8 mm).

Plate 4. 3 Quartz grain with undulatory extinction, northern sequence (field of view = 8 mm).

Plate 4. 4 Sericite-pyrite alteration in quartz-plagioclase porphyritic rhyolite in the immediate hangingwall of the Kutcho Creek deposit (hammer for scale).

Plate 4. 5 Basaltic (dark) and rhyolitic (light) fragments in rhyolite mass flow from the northern sequence (ruler for scale).

Plate 4. 6 Plagioclase-augite porphyritic gabbro (ruler for scale).

Plate 4. 7 Rhyolite mass flow from the Kutcho Assemblage.

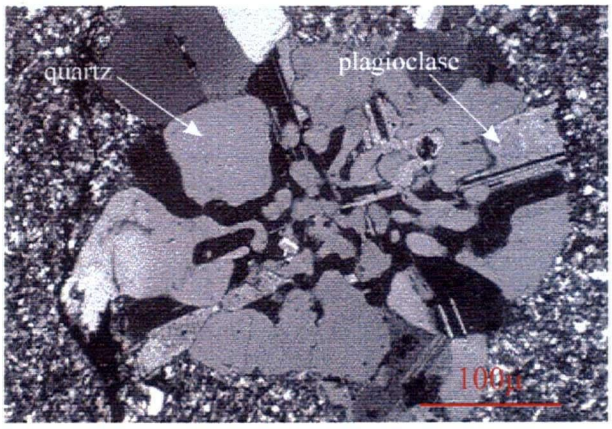

Plate 4.2

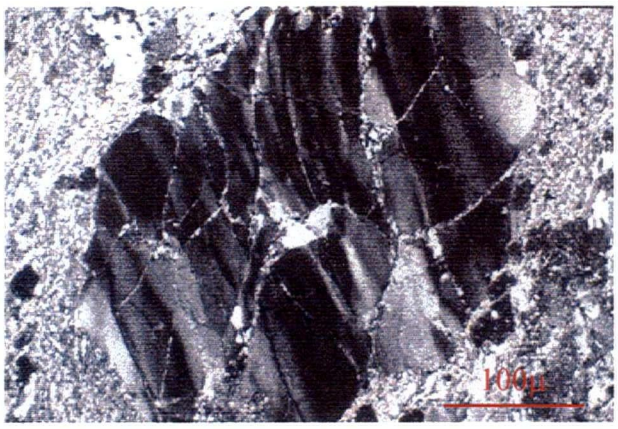

Plate 4.3

Plate 4.4

Plate 4.5

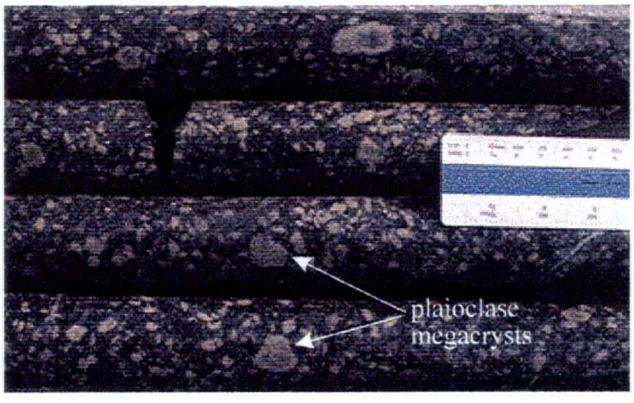

Plate 4.6

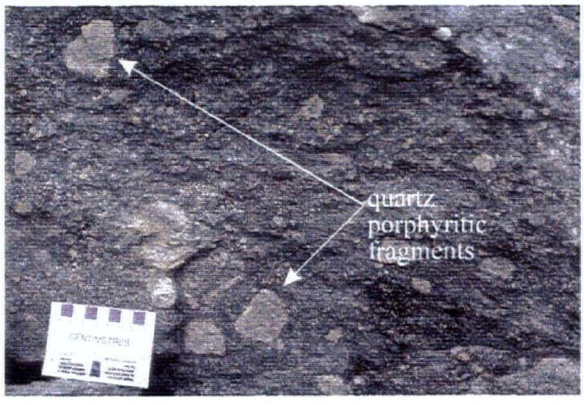

Plate 4.7

Plate 4. 8 Quartz-plagioclase glomerocryst.

Plate 4. 9 Massive sulphide from the Kutcho lens, Kutcho Adit (mainly pyrite and chalcopyrite), small scale faults outlined by white chalk).

Plate 4. 10 Photomicrograph of quartz-plagioclase glomerocryst in a quartzo-feldspathic groundmass, Mount Bodine rhyolite, sample SA-GC-01 (field of view = 5 mm).

Plate 4. 11 Photomicrograph of intergrown quartz and plagioclase grains, tonalite, sample PSC95-16-4 (field of view = 5 mm).

Plate 4. 12 Photomicrograph of rhyolite crystal tuff (96A-2) showing a broken quartz grain (photograph width 5 mm).

Plate 4. 13 Photomicrograph of tonalite (96A-7) showing equigranular texture (photograph width 5 mm), p = plagioclase, q = quartz.

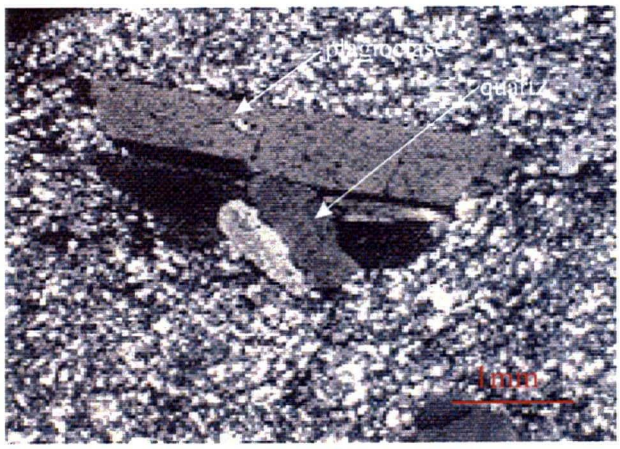

Plate 4.8

Plate 4.9

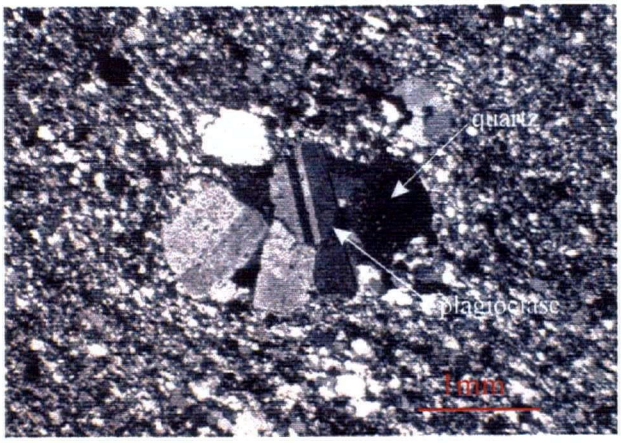

Plate 4.10

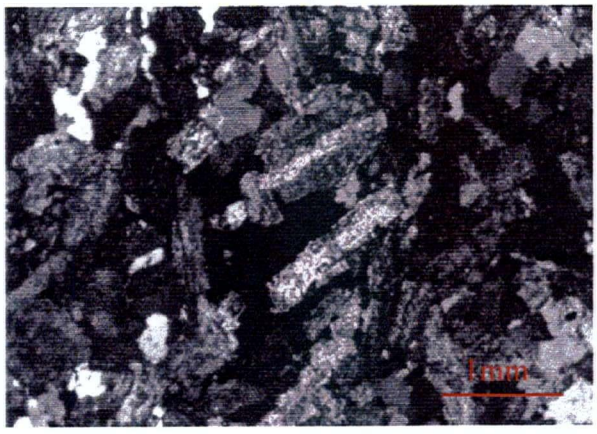

Plate 4.11

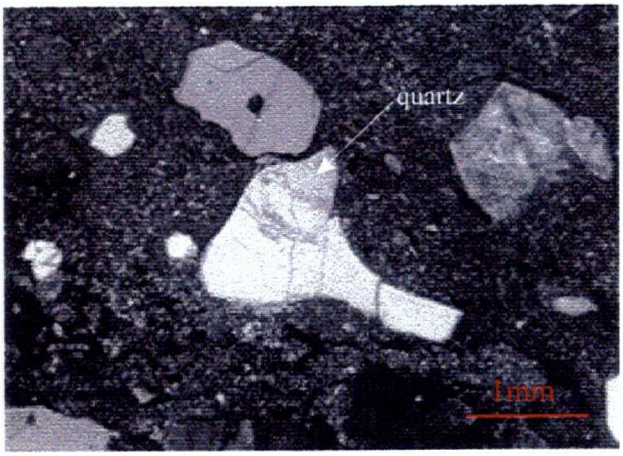

Plate 4.12

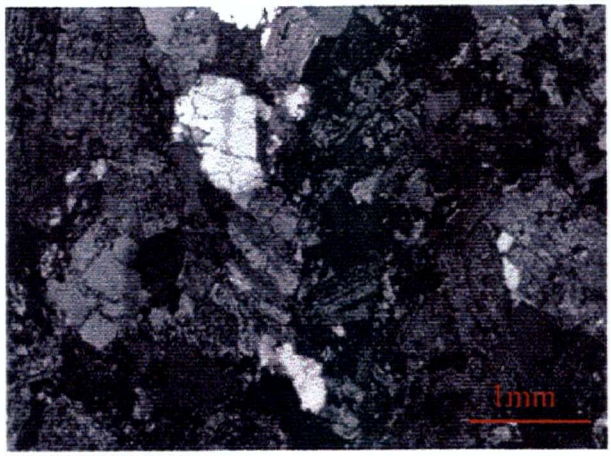

Plate 4.13

References

Barrett, T.J., and MacLean, W.H., 1994, Chemostratigraphy and hydrothermal alteration in exploration for VHMS deposits in greenstones and younger volcanic rocks, *in* Lentz, D.R., ed., Alteration and Alteration Processes associated with Ore-forming Systems: Geological Association of Canada, Short Course Notes, v.11, p. 433-467.

Barrett, T.J., Sherlock, R.L., and Thompson, J.F.H., 1996, Geology and geochemistry of the Kutcho Creek VMS deposit, northern British Columbia: Exploration and Mining Journal.

Bridge, D.A., Marr, J.M., Hashimoto, K., Obara, M., and Suzuki., R., 1986, Geology of the Kutcho Creek volcanogenic massive sulphide deposits, northern British Columbia: *in* Mineral Deposits of Northern Cordillera, Canadian Institute of Mining Special Volume 37, Morin, J.A., ed., p. 115-128.

Bussey, S.D., and LeAnderson, P.J., 1994, Geology of the Iron Dyke Mine and surrounding Permian Hunsaker Creek Formation: *in* Geology of the Blue Mountains region of Oregon, Idaho, and Washington: Stratigraphy, Physiography, and Mineral Resources of the Blue Mountains Region, Vallier, T.L., and Brooks, H.C., eds., U.S. Geological Survey Professional Paper 1439, p.151-181

Childe, F.C., and Thompson, J.F.H., 1995, U-Pb age constraints and Pb isotopic signature of the Kutcho Deposit: Implications for the terrane affiliation of the Kutcho Assemblage, north central British Columbia: Geological Association of Canada - Mineralogical Association of Canada Annual Meeting, Program with Abstracts, p. a 17.

Childe, F.C., and Thompson, J.F.H., submitted, Geological setting, age, and radiogenic isotopic characteristics of the Permo-Triassic Kutcho Creek Cu-Zn VMS deposit, northcentral British Columbia: Canadian Journal of Earth Sciences.

Childe, F.C., and Schiarizza, P., 1997, U-Pb geochronology, geochemistry and Nd isotopic systematics of the Sitlika Assemblage, northcentral British Columbia: *in* Geological

Fieldwork 1996, Grant, B., ed., B.C. Ministry of Employment and Investment, Paper 1997-1, p. 69-78.

Childe, F.C., Friedman, R.M., Mortensen, J.K., and Thompson, J.F.H., 1997, Evidence for Early Triassic felsic magmatism in the Ashcroft (92I) map area, British Columbia: *in* Geological Fieldwork 1996, Grant, B., ed., B.C. Ministry of Employment and Investment, Paper 1997-1, p. 117-124.

Gabrielse, H., and Yorath. C.J., 1991, Tectonic synthesis; *in* Geology of the Cordilleran Orogen in Canada, H. Gabrielse and C.J. Yorath (ed.); Geological Survey of Canada, no. 4, p. 677-705.

Grette, J., 1978, Cache Creek and Nicola Groups near Ashcroft, British Columbia: unpublished M.Sc. thesis, University of British Columbia, 88p.

Harland, W.B., Armstrong, R.L., Cox, A.V., Craig, L.E., Smith, A., G., 1990, A Geologic Time Scale, 1989: 263 pages.

Ladd, J.H., 1981, A report on the geology of the Cache Creek - Nicola contact southwest of Ashcroft (92I/11): *in* Geology in British Columbia, B.C. Ministry of Energy, Mines and Petroleum Resources, pages 91-97.

Monger, J.W.H., 1975, Upper Paleozoic rocks of the Atlin terrane, northwestern British Columbia and south-central Yukon: Geological Survey of Canada Paper 74-47, 63p.

Monger, J.W.H., 1977, Upper Paleozoic rocks of northwestern British Columbia: Report of Activities, Part A, Geological Survey of Canada Paper 77-1A, p. 255-262.

Monger, J.W.H., and McMillan, W.J., 1984, Bedrock geology of Ashcroft (92I) map area: Geological Survey of Canada, Open File Map 980.

Monger, J.W.H., Richards, T.A., and Paterson, I.A., 1978, The Hinterland Belt of the Canadian Cordillera: new data from northern and central British Columbia, Canadian Journal of Earth Sciences, v. 15, p. 823-830.

Nakada, S., Maillet, P., Monjaret, M-C., Funjinawa, A., and Urabe, T., 1994, High-Na dacite from the Jean Charcot Trough (Vanuatu), southwest Pacific: Marine Geology, v. 116, p. 197-213.

Panteleyev, A., and Pearson., D.E., 1976, Kutcho Creek Map-Area (104I/1W): *in* Geological Fieldwork, B.C. Ministry of Mines and Petroleum Resources, p.74-76.

Paterson, I.A., 1974, Geology of the Cache Creek Group and Mesozoic rocks at the northern end of the Stuart Lake Belt, central British Columbia; Geological Survey of Canada Special Paper 74-1, Part B, pages 31-41.

Renne, P.R., 1995, Synchrony and Causal Relations Between Permian-Triassic Boundary Crises and Siberian Flood Volcanism: Science, Volume 269, pages 1413-1416.

Samson, S.D., McClelland, W.C., Patchett, P.J., Gehrels, G.E., and Anderson, R.G., 1989, Evidence from neodymium isotopes for mantle contributions to Phanerozoic crustal genesis in the Canadian Cordillera: Nature, v.337, p. 705-709.

Schiarizza, P., and Payie, G., 1997, Geology of the Sitlika Assemblage in the Kenny Creek - Mount Olson area (93N/12, 13), central British Columbia: *in* Geological Fieldwork 1996, Grant, B., ed., B.C. Ministry of Employment and Investment, Paper 1997-1, p. 79-100.

Souther, J.O., 1991, Volcanic Regimes, *in* Geology of the Canadian Orogen in Canada, Gabrielse, H., and Yorath, C., eds.; Geological Survey of Canada, Geology of Canada, no. 4, p. 457-490.

Sun, S. -s., and McDonough, W.F., 1989, Chemical and Isotopic systematics of oceanic basalts: implications for mantle composition and processes: *in* Magmatism in the Ocean Basins, Saunders, A.D., and Norry, M.J., eds., Geological Society Special Publication Number 42, p. 313-345.

Thorstad, L., and Gabrielse, H., 1986, The Upper Triassic Kutcho Formation, Cassiar Mountains, North-Central British Columbia: Geological Survey of Canada Paper 86-16, 53 p.

Vallier, T.L., 1995, Petrology of pre-Tertiary igneous rocks in the Blue Mountains region of Oregon, Idaho, and Washington: Implications for the geologic evolution of a complex island arc: *in* Geology of the Blue Mountains region of Oregon, Idaho, and Washington: Petrology and tectonic evolution of pre-Tertiary rocks of the Blue Mountains Region, Vallier, T.L., and Brooks, H.C., eds., U.S. Geological Survey Professional Paper 1438, p. 125-209.

Wheeler, J.O., and McFeely, P., 1991, Tectonic Assemblage map of the Canadian Cordillera and adjacent parts of the United States of America: Geological Survey of Canada, Map 1712A.

CHAPTER 5:

U-PB GEOCHRONOLOGY AND RADIOGENIC ISOTOPIC SYSTEMATICS OF THE POLYMETALLIC TULSEQUAH CHIEF AND BIG BULL VMS DEPOSITS, NORTHWESTERN BRITISH COLUMBIA

Plate 5.1. Looking north to the Tulsequah River and Glacier, from Mount Eaton

Introduction

The Tulsequah Chief and Big Bull polymetallic volcanogenic massive sulphide (VMS) deposits are located on Mount Eaton, near the confluence of the Tulsequah and Taku Rivers in the Tulsequah map area (104K) of northwestern British Columbia (Figs. 5.1 and 5.2). The two deposits are separated by a distance of about 8.5 km. Massive sulphide mineralization was discovered at Tulsequah Chief in 1924, and at Big Bull in 1929. Mines at Tulsequah Chief and Big Bull were in production from 1951 to 1957, producing 0.58 Mt grading 1.8% Cu, 1.3% Pb, 6.7% Zn, 3.43 g/t Au and 108 g/t Ag at Tulsequah Chief and 0.36 Mt grading 1.2% Cu, 1.9% Pb, 7.3% Zn, 5.14 g/t Au and 154 g/t Ag at Big Bull (Carmichael and Curtis, 1994). The deposits, which are now owned by Redfern Resources Ltd., have geological reserves of 8.7 Mt grading 1.3% Cu, 1.2% Pb, 6.4% Zn, 2.4 g/t Au and 100 g/t Ag at the Tulsequah Chief deposit, and 0.58 Mt grading 1.1% Cu, 1.5% Pb, 5.6% Zn, 3.4 g/t Au and 154 g/t Ag at the Big Bull deposit (Carmichael et al. 1995; The Northern Miner, March 1996).

In this study, igneous rocks from the Tulsequah Chief and Big Bull deposit were sampled for analysis by U-Pb methods in an attempt to constrain the age(s) of VMS mineralization. Volcanic rocks from areas north and south of the deposit were also collected for dating, in an attempt correlate these rocks with those which host VMS mineralization at Tulsequah Chief, and therefore identify additional prospective stratigraphy for VMS exploration in the region. Igneous rocks from the Tulsequah Chief deposit were analyzed for their Nd isotopic signatures, and Pb isotopic compositions were determined for sulphides from both the Tulsequah Chief and Big Bull deposits, to determine the degree of evolution of these deposits and their host rocks.

Regional Geology

Regional mapping in the Tulsequah River and Glacier areas was begun by Kerr (1931), and was continued by Souther (1971), and more recently by Mihalynuk et al. (1994a and b).

Within the Tulsequah River and Glacier areas, the Llewellyn Fault separates Mesozoic and Paleozoic rocks of lower metamorphic grade to the east from rocks of higher metamorphic grade

to the west (Mihalynuk et al. 1994a and b) (Fig. 5.2). Rocks west of the faults are divided into three suites, the Whitewater and Boundary Ranges metamorphic suites, and the lower grade Mount Stapler Suite (Mihalynuk et al. 1994a; Mihalynuk and Rousse 1988). Mihalynuk et al. (1994a) has suggested that schistose rocks, quartzite, metabasite and ultramafite of the Whitewater Suite may be correlative with parts of the Yukon-Tanana terrane (in the sense of Mortensen 1992) (Fig. 5.1), and has mapped volcanic and sedimentary rocks of the Mount Stapler Suite as being gradational into rocks of the Whitewater Suite.

Rocks east of the Llewellyn fault were first correlated with the Upper Triassic Stuhini Group of the Stikine terrane by Souther (1971). However, subsequent biochronological data presented by Nelson and Payne (1984) indicated that rocks from the upper part of Mount Eaton are of late Paleozoic (Middle Pennsylvanian to Early Permian) age, and much of this area was reassigned to the Paleozoic Stikine Assemblage of the Stikine terrane (Fig. 5.1). In the Tulsequah River and Glacier areas, Nelson and Payne (1984) divided volcanic and sedimentary rocks of the Stikine Assemblage into three structural-stratigraphic blocks, separated by known or suspected faults. These are the weakly deformed Mount Eaton block and the more strongly deformed Mount Strong and Sittikanay blocks. The Tulsequah Chief and Big Bull deposit are hosted within arc-related bimodal volcanic rocks of the Mount Eaton block (Fig. 5.2).

The Stikine terrane is interpreted to be an allochthonous terrane of island arc affinity, whereas the Yukon-Tanana terrane is interpreted to have a continental arc affinity, possibly with links to ancestral North America (Monger et al. 1972; Samson et al. 1989; Mortensen 1992). However, based on several lines of evidence, Mihalynuk et al. (1994c) have suggested that early Mesozoic and Paleozoic arc assemblages of the Stikine terrane may have been built on the flanks of a continental margin represented by the Yukon-Tanana terrane. The radiogenic isotopic signatures of igneous rocks produced within island and continental arcs are distinctly different, with those from continental arcs being significantly more evolved (i.e., Samson et al. 1989). The radiogenic isotopic signatures determined in the current study are compared with published values for both the Stikine and Yukon-Tanana terranes, in order to test the hypothesis of Mihalynuk et al. (1994c).

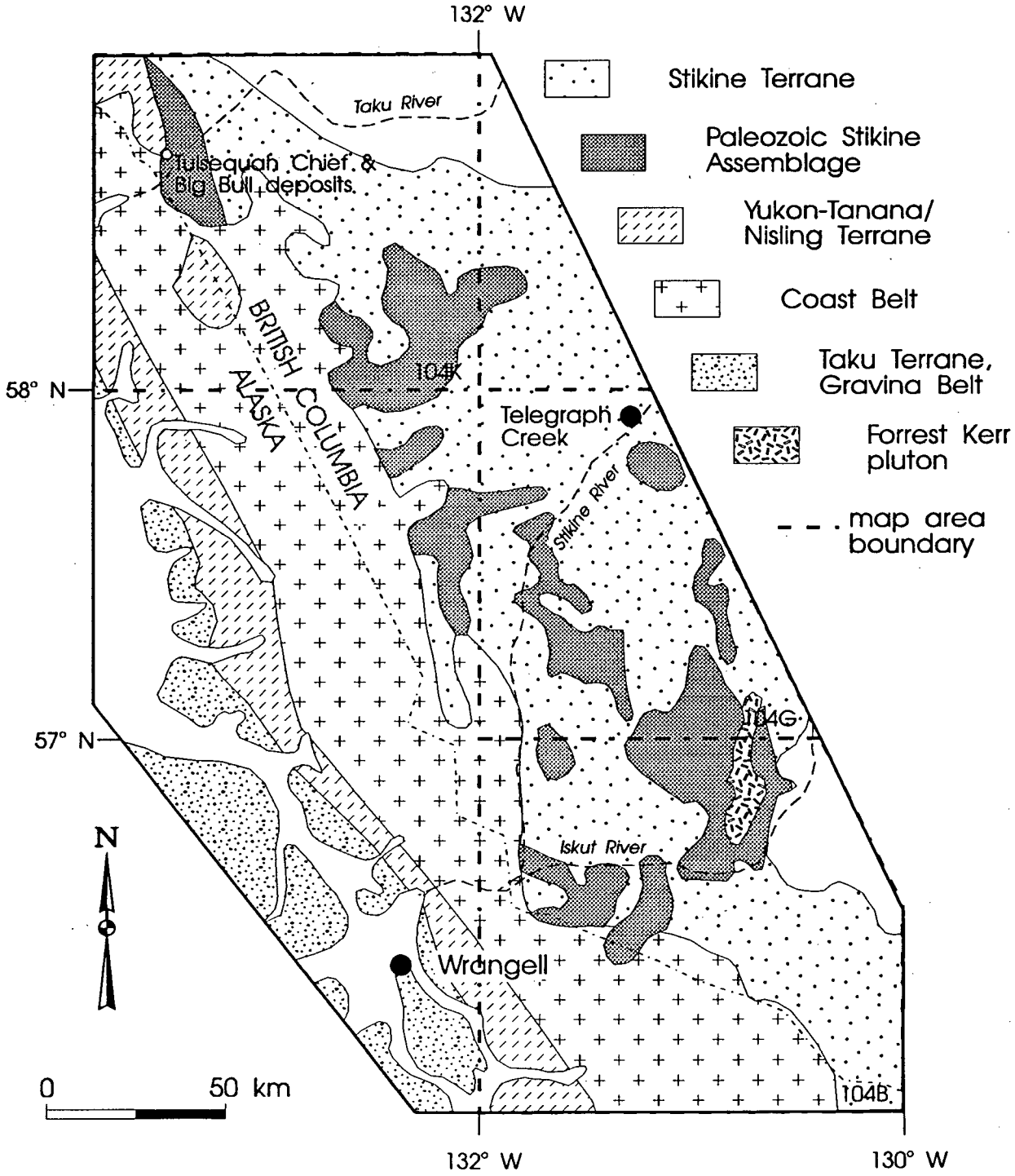

Figure 5. 1 Simplified tectonostratigraphic map showing the distribution of the Paleozoic Stikine Assemblage, the Tulsequah Chief and Big Bull deposits, and the Forrest Kerr pluton (104B = Iskut River map area; 104G = Telegraph Creek map area; 104K = Tulsequah map area) (after McClelland 1992).

Rocks of the Stikine Assemblage east of the Llewellyn fault are overlain by volcanic and sedimentary rocks of the Upper Triassic Stuhini Group of the Stikine terrane and sedimentary rocks of the Lower to Middle Jurassic Laberge Group. Paleozoic and Mesozoic rocks are cross cut by Cretaceous to Tertiary intrusions, including dykes of the Eocene Sloko Group (Mihalynuk et al. 1994a).

Geology of the Tulsequah Chief and Big Bull deposits

For a detailed description of the geology and mineralization of the Tulsequah Chief and Big Bull deposits, the reader is referred to papers by McGuigan et al. (1993), Sherlock et al. (1994), Carmichael and Curtis (1994), Carmichael et al. (1995), Sebert et al. (1995), and Sebert and Barrett (1996).

The Tulsequah Chief footwall, mine, and hangingwall series are a northward-younging bimodal volcanic sequence. The footwall series consists of mafic volcanic rocks; these rocks are conformably overlain by felsic tuffaceous rocks and feldspar- and quartz-porphyritic flows and breccias of the mine series, which are in turn overlain by mafic volcanic flows and volcaniclastic sedimentary rocks which comprise the hangingwall series (McGuigan et al. 1993; Sebert and Barrett 1996). Mineralization at Tulsequah Chief occurs within the hydrothermally altered lower portion of the felsic volcanic mine series as massive to semi-massive sulphide lenses, termed the AB_1, AB_2, F, G, H, and I lenses (McGuigan et al. 1993) (Plates 5.2, 5.3 and 5.4). Mineralization can be divided into three main facies: pyrite, zinc, and copper (McGuigan et al. 1993). The pyrite facies consists of predominantly of massive pyrite, with only minor base metals. The zinc facies comprises semi-massive pale yellow sphalerite, pyrite, galena, chalcopyrite, and tetrahedrite, in a matrix of barite, quartz and sericitically altered felsic volcaniclastic material. The copper facies consists mainly of massive pyrite, with up to several percent disseminated chalcopyrite. Felsic volcanic rocks of the mine series have been dilated by the intrusion of a semi-concordant sill of gabbroic composition. The sill is compositionally and mineralogically similar to the mafic volcanic rocks which comprise the hangingwall series of the deposit and may represent a sub-volcanic equivalent to the mafic flows (Sebert and Barrett 1996; Sherlock et al. 1996).

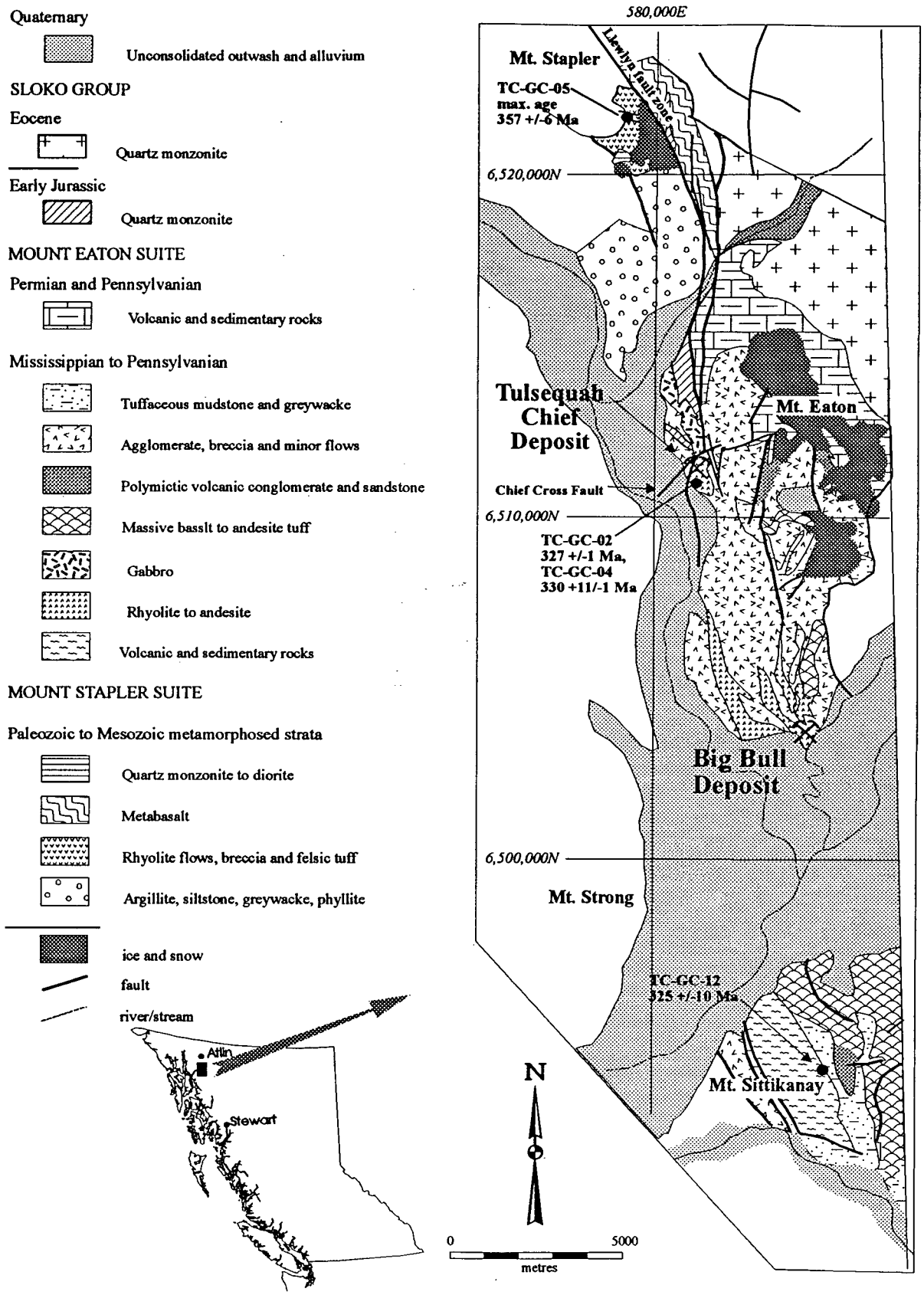

Figure 5. 2 Generalized geology of the Tulsequah Glacier area, showing locations of U-Pb geochronology samples (after Mihalynuk et al. 1994)

At the Big Bull deposit the oldest rocks exposed consist of mafic lapilli and ash tuffs with rare mafic flow rocks. These rocks are overlain by fine-grained felsic crystal to ash tuffs, which are in turn overlain by intermediate composition, fine- to coarse-grained fragmental and tuffaceous rocks with interbedded massive, black manganese oxides and silicates. The sequence is capped by mafic lapilli, ash and crystal tuffs characterized by streaks and patches of black hematite (Carmichael et al. 1995) (Plate 5.5). Massive to semi-massive sulphides consisting of pyrite, galena, sphalerite, chalcopyrite and tetrahedrite in a matrix of barite and sericitized lithic fragments are hosted within hydrothermally altered, fine-grained felsic crystal to ash tuffs of dacitic composition within this sequence. In contrast to the Tulsequah Chief mine series, felsic flow rocks are rare to absent around the Big Bull deposit. In addition, felsic tuffaceous rocks are finer grained than those at the Tulsequah Chief deposit. Carmichael et al. (1995) has suggested that these differences may indicate formation of Big Bull mineralization in a more distal environment than mineralization at Tulsequah Chief.

U-Pb Geochronology

In the current study samples were collected for analysis by U-Pb methods to address a number of specific problems. One of these was to attempt to verify and refine a preliminary latest Devonian to earliest Mississippian U-Pb zircon date of 351 +15/-6 Ma on a felsic volcaniclastic rock in the upper part of the Tulsequah Chief mine series (Sherlock et al. 1994). Sherlock et al. (1994) report a high degree of inheritance in zircon from the dated sample, a feature which is inconsistent with formation within the basal assemblage of a terrane that has been interpreted to be composed almost completely of juvenile, mantle-derived material (Samson et al. 1989). Samples of the sill of gabbroic composition which intrudes the Tulsequah Chief mine series were also collected, along with volcanic rocks from the Big Bull deposit, but none of these samples yielded suitable material for analysis by U-Pb methods. Volcaniclastic rocks were also collected from the Mount Stapler Suite on Mount Stapler, and the Sittikanay block on Mount Sittikanay, to determine the time of volcanism in these areas; the results are presented below.

The U-Pb results reported in this paper are based on analysis of zircons recovered from 20-30 kilogram samples collected from drill core, outcrop or underground workings; sample descriptions are given below. Heavy mineral extraction procedures and U-Pb analytical

procedures follow those of Mortensen et al. (1995). All zircon fractions were abraded prior to analysis (Krogh 1982). Isotopic ratios were measured using a modified single collector VG-54R thermal ionization mass spectrometer equipped with a Daly photomultiplier. Procedural blanks were 6-20 picograms for Pb and 1-2 picograms for U. Concordia intercept ages and associated errors were calculated using a modified York-II regression model (York 1969), and the algorithm of Ludwig (1980); ages were calculated using the decay constants recommended by Steiger and Jäger (1977). Age assignments follow the time scale of Harland et al. (1990). Analytical results are given in Table 5.1 and shown graphically in Figure 5.3.

Tulsequah Chief Mine Series

Two felsic volcanic rocks of rhyodacitic to rhyolitic composition, from the Tulsequah Chief mine series, were sampled for analysis for by U-Pb methods. Sample TC-GC-02 was a massive quartz+feldspar porphyritic flow of rhyodacitic composition from near the top of the felsic volcanic sequence. Sample TC-GC-04 was a massive to autobrecciated quartz+feldspar porphyritic flow of rhyolitic composition which directly overlay massive sulphide mineralization of the H zone mineralization, and occurred at a lower stratigraphic level than sample TC-GC-02. Both of these samples occur at a lower stratigraphic level than the sample dated by Sherlock et al. (1994).

Sample TC-GC-02 contained small equant to prismatic zircons, some of which were characterized by slightly turbid centers. In the hand-picking of zircon grains for analysis, only those with the best clarity and least turbidity were selected. Analysis of four fractions yielded $^{207}Pb/^{206}Pb$ ages of 325 to 340 Ma; two fractions, G and H, were overlapping and concordant (Table 5.1, Fig. 5.3a). A Late Mississippian age of 327 +/-1 Ma was calculated as the age of this rock, based on the $^{206}Pb/^{238}U$ ages and errors of concordant fractions G and H. Fractions A and B are slightly discordant (2 and 6%), probably as a result of post-crystallization lead-loss. Fraction A gives a slightly older $^{207}Pb/^{206}Pb$ age than the other fractions, but it is within error of the date determined from the two concordant fractions.

Zircons from sample TC-GC-04 were visually similar to those described above from sample TC-GC-02. Analysis of three fractions yielded $^{207}Pb/^{206}Pb$ ages of 325 to 330 Ma; error

ellipses of all three fractions had some overlap with concordia, but the degree of concordance is observed to increase with $^{206}Pb/^{238}U$ age (Table 5.1, Fig. 5.3b). A Late Mississippian age of 330 +11/-1 Ma was calculated as the age of this rock based on the $^{206}Pb/^{238}U$ age and $^{206}Pb/^{238}U$ and $^{207}Pb/^{206}Pb$ errors of fraction E, the fraction which has the most significant overlap with concordia.

Table 5. 1 U-Pb analytical data.

Fraction[1]	Wt.	U	Pb[2]	^{206}Pb[3]	Pb[4]	^{208}Pb[5]	Isotopic ratios(±1σ,%)[6]			Isotopic dates(Ma,±2σ)[6]		
	mg	ppm	ppm	^{204}Pb	pg	%	$^{206}Pb/^{238}U$	$^{207}Pb/^{235}U$	$^{207}Pb/^{206}Pb$	$^{206}Pb/^{238}U$	$^{207}Pb/^{235}U$	$^{207}Pb/^{206}Pb$
TULSEQUAH CHIEF												
Mine Series rhyodacite (TC-GC-02, underground via 5400 level portal)												
A,f,N2,p	0.052	293	16	976	51	13.6	0.05107±0.11	0.3751±0.36	0.05327±0.29	321.1±0.7	323.4±2.0	340.2±13.2
B,f,N2,p,s	0.112	235	12	1606	53	12.9	0.05071±0.20	0.3702±0.35	0.05294±0.24	318.9±1.2	319.8±1.9	326.2±10.7
G,f,M2,s	0.198	305	16	1019	198	12.2	0.5202±0.12	0.3795±0.21	0.05292±0.14	326.9±0.8	326.7±1.2	325.2±6.5
H,f,M2,s	0.054	366	20	1642	40	13.8	0.5207±0.16	0.3807±0.31	0.05302±0.21	327.2±1.0	327.5±1.7	329.7±9.6
Mine Series rhyolite (TC-GC-04, DDH TCU-91-32, 312.4-326.9 m)												
D,f,M1,p	0.028	197	10	647	26	12.6	0.04957±0.12	0.3616±0.43	0.05290±0.36	311.9±0.7	313.4±2.3	324.6±16.2
E,f,N1,p	0.033	241	13	908	29	12.5	0.05246±0.12	0.3835±0.33	0.05302±0.25	329.6±0.8	329.6±1.9	329.7±11.3
H,m,M2,p	0.024	318	17	768	33	13.6	0.05160±0.13	0.3771±0.41	0.05300±0.33	324.3±0.8	324.9±2.3	329.0±14.9
Mount Stapler rhyolite (TC-GC-05, surface)												
A,f,N1,s	0.189	530	31	612	563	14.2	0.05442±0.11	0.4039±0.30	0.05383±0.24	341.6±0.7	344.5±1.7	364.0±10.5
B,f,N1,p,s	0.079	420	24	519	200	13.9	0.05315±0.15	0.3933±0.37	0.05367±0.28	333.8±0.9	336.8±2.1	357.3±12.8
C,f,N1,p	0.040	189	11	1385	19	12.8	0.05594±0.11	0.4158±0.27	0.05392±0.19	350.9±0.7	353.1±1.6	367.6±8.3
D,f,N1,s	0.032	396	23	773	57	13.7	0.05490±0.13	0.4076±0.35	0.05385±0.25	344.5±0.9	347.1±2.1	364.6±11.4
E,f,M2,s	0.063	273	16	1005	59	13.7	0.05496±0.11	0.4071±0.30	0.05372±0.22	344.9±0.7	346.8±1.8	359.5±9.8
G,f,M2p,s	0.100	150	9	770	68	14.7	0.05465±0.13	0.4038±0.37	0.05358±0.29	343.0±0.8	344.4±2.2	353.5±13.0
Mount Sittikanay volcaniclastic (TC-GC-12, surface)												
A,m,N1,p	0.040	458	22	2595	21	11.9	0.04715±0.11	0.3450±0.22	0.05306±0.14	297.0±0.6	300.9±1.2	331.3±6.3
B,f,N1,p	0.063	317	16	3822	15	13.3	0.04810±0.10	0.3503±0.20	0.05282±0.12	302.9±0.6	305.0±1.1	321.0±5.2
D,f,M1,p	0.020	229	11	1903	7	7.7	0.04932±0.14	0.3630±0.29	0.05339±0.21	310.3±0.8	314.5±1.6	345.3±9.4

[1]All fractions are air abraded; Grain size, smallest dimension: c= +134μm, m=-134μm+74μm, f=-74μm; Magnetic codes
Franz magnetic separator sideslope at which grains are nonmagnetic; e.g., N1=nonmagnetic at 1°; Field strength for all fractions =1.8A; Front slope for all fractions=20°; Grain character codes: p=prismatic, s=subhedral.
[2]Radiogenic Pb
[3]Measured ratio corrected for spike and Pb fractionation of 0.0043/amu ±20% (Daly collector)
[4]Total common Pb in analysis based on blank isotopic composition
[5]Radiogenic Pb
[6]Corrected for blank Pb, U and common Pb (Stacey-Kramers model Pb composition at the $^{207}Pb/^{206}Pb$ date of fraction, or age of sample).

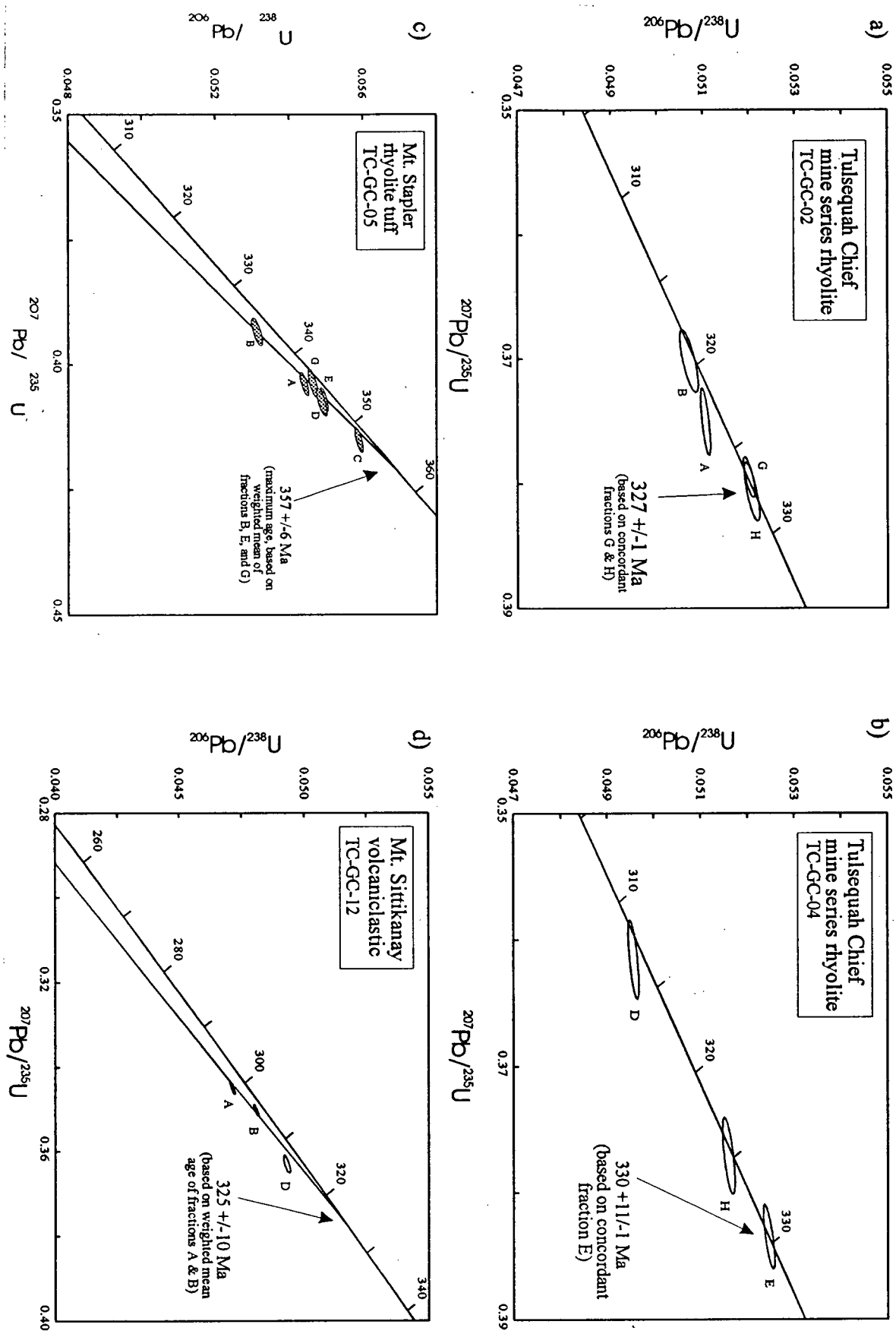

Figure 5. 3U-Pb concordia diagrams for a) rhyodacite from the Tulsequah Chief mine series, b) rhyolite from the Tulsequah Chief mine series, c) rhyolite from Mount Eaton, and d) volcaniclastic from Mount Sittikanay.

Mount Stapler

A sample of a strongly foliated rhyolite ash to lapilli tuff was sampled from Mount Stapler (TC-GC-05) and yielded a limited quantity of small, prismatic zircons (Plate 5.6). Analysis of six fractions yielded $^{207}Pb/^{206}Pb$ ages of 354 to 368 Ma. All fractions are slightly discordant and this feature is attributed mainly to post-crystallization Pb-loss (Fig. 5.3c). The range of $^{207}Pb/^{206}Pb$ ages may also reflect a minor degree of inheritance in some zircon fractions from this rock. A weighted mean $^{207}Pb/^{206}Pb$ age was calculated for the fractions which show the least degree of inheritance (Fractions B, E and G), and yielded an Earliest Mississippian date of 357 $\pm$6 Ma. Because of the interpreted inheritance, this age is considered to be an estimate of the maximum age of this rock.

A second sample, which consisted of an intrusion of quartz monzonitic composition, was collected by the author and M. Mihalynuk from Mount Stapler, west of the Llewlyn fault. Analytical results for this sample, which yielded an Early Jurassic crystallization age, are presented in Appendix 3.

Mount Sittikanay volcaniclastic

Two volcaniclastic rocks were sampled for U-Pb dating from Mount Sittikanay (TC-GC-11 and -12). The samples consisted of a strongly foliated, fine-grained medium green andesite (TC-GC-11) (Plate 5.7) and a strongly to moderately foliated, heterolithic volcaniclastic debris flow, with a strong to moderate deformational fabric (TC-GC-12) (Plate 5.8). Sample TC-GC-11 failed to yield minerals suitable for dating, but sample TC-GC-12 contained a small amount of zircon.

Zircons from sample TC-GC-12 were prismatic (l:w = 2:1 to 3:1) with good clarity and minor colourless bubble and rod-shaped inclusions. All of the zircon from this rock was picked and separated into three fractions. Analysis of the three fractions yielded $^{207}Pb/^{206}Pb$ ages of 321, 331, and 345 Ma. All three fractions were slightly discordant (6-10%), and this feature is attributed to post-crystallization Pb-loss (Table 5.1, Fig. 5.3d). A weighted mean age of 325 +/-

10 Ma was calculated for the two fractions with the lowest $^{207}Pb/^{206}Pb$ ages. As neither point is concordant, this age can be regarded as a maximum age for this rock. The $^{207}Pb/^{206}Pb$ age of fraction D is not within error of this age; this may result from either inheritance or incorporation of detrital material during deposition of this volcaniclastic rock.

Lithogeochemistry

Samples collected for analysis by U-Pb methods in the current study were also analyzed for their major and trace element concentrations (Table 5.2). Felsic volcanic rocks from the Tulsequah Chief deposit and Mount Stapler have rhyodacitic to rhyolitic compositions, and Zr/Y ratios of 4.9 to 6.7 indicate transitional magmatic affinities, based on the limits defined by Barrett and MacLean (1994) (Table 5.2 and Fig. 5.4). Felsic volcanic rocks from the Big Bull deposit have dacitic to rhyodacitic compositions, and tholeiitic to transitional magmatic affinities (Zr/Y = 2.9 to 5.7). Volcaniclastic rocks from Mount Sittikanay have basaltic to andesitic average compositions and tholeiitic magmatic affinities (Zr/Y = 3.7 to 4.0). Sills which intrude the Tulsequah Chief mine series have gabbroic compositions and tholeiitic magmatic affinities (Zr/Y = 2.6 to 3.6). Compositions determined here for rocks form the Tulsequah Chief deposit are consistent with results determined by Sebert and Barrett (1996).

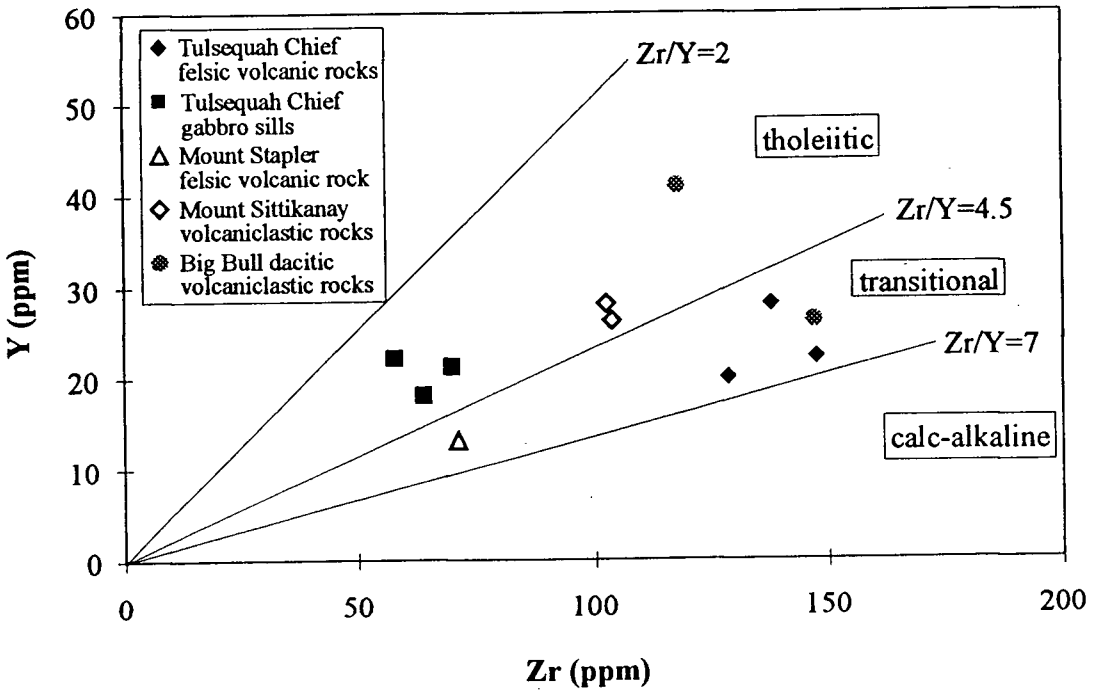

Figure 5. 4 Y *versus* Zr diagram for U-Pb samples from the Tulsequah Glacier area (data fields after Barrett and MacLean 1994).

Table 5.2 Major and trace element data for U-Pb samples from the Tulsequah River and Glacier areas.

sample number	lithology	SiO2 %	TiO2 %	Al2O3 %	Fe2O3 %	MnO %	MgO %	CaO %	Na2O %	K2O %	P2O5 %	LOI	Total	BaO ppm
TC-GC-01	mine series rhyodacite	78.42	0.22	12.23	2.04	0.01	0.01	0.27	4.01	1.62	0.03	0.89	99.75	488
TC-GC-02	mine series rhyodacite	70.95	0.27	14.14	3.52	0.08	2.08	3.20	1.23	2.15	0.03	2.16	99.81	1033
TC-GC-03	gabbro sill	48.74	0.83	18.00	8.76	0.14	7.97	9.69	2.49	1.84	0.15	1.67	100.28	749
TC-GC-04	mine series rhyodacite	74.59	0.26	12.61	2.48	0.05	0.29	1.51	6.28	0.33	0.07	1.41	99.88	1387
TC-GC-05	Mt. Stapler rhyodacite	73.30	0.21	14.72	1.58	0.02	0.43	0.98	3.58	2.71	0.04	2.06	99.63	1515
TC-GC-08	Big Bull dacite	73.69	0.28	13.77	2.82	0.03	0.30	0.96	4.51	2.42	0.06	1.17	100.15	1317
TC-GC-09	gabbro sill	53.08	0.89	19.79	6.31	0.11	6.32	6.11	5.24	1.33	0.16	1.28	100.78	482
TC-GC-10	gabbro sill	48.41	0.90	17.50	9.31	0.17	9.14	10.45	2.90	0.73	0.16	1.02	100.85	618
TC-GC-11	Mt. Sittikanay fragmental	65.43	0.79	13.81	7.73	0.14	3.31	1.82	4.77	0.08	0.18	2.91	101.01	79
TC-GC-12	Mt. Sittikanay fragmental	53.92	0.89	16.07	8.50	0.15	3.99	5.18	5.17	0.37	0.49	5.58	100.40	464
BB-GC-01	Big Bull dacite	68.44	0.56	14.13	5.91	0.13	1.35	2.06	5.25	0.64	0.24	1.28	99.99	480
Detection Limit (ppm):		60.00	35.00	120.00	30.00	30.00	95.00	15.00	75.00	25.00	35.00			17

sample number	Co ppm	Cr2O3 ppm	Cu ppm	Ni ppm	V ppm	Zn ppm	Ga ppm	Nb ppm	Pb ppm	Rb ppm	Sr ppm	U ppm	Y ppm	Zr ppm	Zr/Y
TC-GC-01	48	10	33	8	26	66	n/a	n/a	n/a	15	50	n/a	20	129	6.5
TC-GC-02	37	54	57	15	34	131	n/a	n/a	n/a	52	377	n/a	22	148	6.7
TC-GC-03	46	522	48	164	190	52	n/a	n/a	n/a	42	445	n/a	18	64	3.6
TC-GC-04	35	84	130	17	35	82	n/a	n/a	n/a	5	150	n/a	28	138	4.9
TC-GC-05	28	98	66	16	35	33	n/a	n/a	n/a	71	104	n/a	13	71	5.5
TC-GC-08	22	4	40	<d/l	21	64	14	9	2	42	137	3	26	147	5.7
TC-GC-09	32	566	31	176	216	89	18	5	3	24	221	1	22	58	2.6
TC-GC-10	26	487	77	164	244	97	18	1	2	9	774	<d/l	21	70	3.3
TC-GC-11	14	32	86	18	203	118	16	4	1	1	331	<d/l	26	104	4.0
TC-GC-12	19	32	60	4	196	113	16	4	<d/l	8	301	1	28	103	3.7
BB-GC-01	42	12	50	12	51	79	n/a	n/a	n/a	14	213	n/a	41	118	2.9
Detection Limit	10	2	15	3	10	2	1	1	1	1	1	1	1	1	

>d/l = below detection limit n/a = not available

Nd Isotopic data

Rhyolite from the Tulsequah Chief mine series and the mafic sill which intrudes the mine series were analyzed for their Nd isotopic compositions to determine the degree of evolution of these rocks and therefore better constrain potential magmatic sources. Although suitable material was not found in the mafic sill to permit determination of an age by U-Pb methods, the similarity in chemistry and mineralogy between this intrusive unit and mafic flows in the hangingwall of the deposit noted by Sebert and Barrett (1996) suggests that the sill may be an intrusive equivalent of the hangingwall mafic flows, and therefore was probably emplaced contemporaneously with mafic volcanic flows in the hangingwall to mineralization. The rhyolite flow and gabbro sill had ε_{Nd} (initial) values of +2.7 and +3.9, respectively (Table 5.2).

In Figure 5, ε_{Nd} (initial) values for these rocks are compared with the regional data set for the Stikine Assemblage, as well as for data from the Yukon-Tanana terrane (Samson et al. 1989; Mortensen 1992; Logan et al. 1993). The data set for the Stikine terrane consists of mafic to felsic volcanic rocks (n= 5, ε_{Nd} (initial) = 5.1-5.9) from the northern Iskut River and southern Telegraph Creek map areas, 150 to 200 km to the south, comparable data for the Stikine Assemblage in the Tulsequah Chief map area is not available. There is a minor, but detectable difference that exceeds analytical error in the ε_{Nd} (initial) values determined for rocks from the Tulsequah Chief deposit and the regional data set for the Stikine terrane; values determined here are isotopically somewhat less primitive than those of the regional data set. In contrast, igneous rocks from the Yukon-Tanana continental-arc terrane have significantly more evolved ε_{Nd} values than those determined here. The tectonic implications of these results are discussed below.

Sample	Sm (ppm)	Nd (ppm)	$^{147}Sm/^{144}Nd$	meas. $^{143}Nd/^{144}Nd$ (error x 10^{-6}, 2σ)	ε_{Nd}[2] (present day)	age[1] (Ma)	ε_{Nd}[2] (initial)
TULSEQUAH CHIEF DEPOSIT							
TC-GC-02 mine series rhyolite A	3.29	15.54	0.1280	0.512619 (11)	-0.4	327	+2.7
S-93-145 mine series gabbro sill	3.02	10.85	0.1681	0.512771 (4)	+2.6	327	+3.9

[1]used for the calculation of ε_{Nd} (initial).
[2]error = $\pm$0.5 ε_{Nd} units.

Table 5. 3 Nd isotopic data for rocks from the Tulsequah Chief deposit.

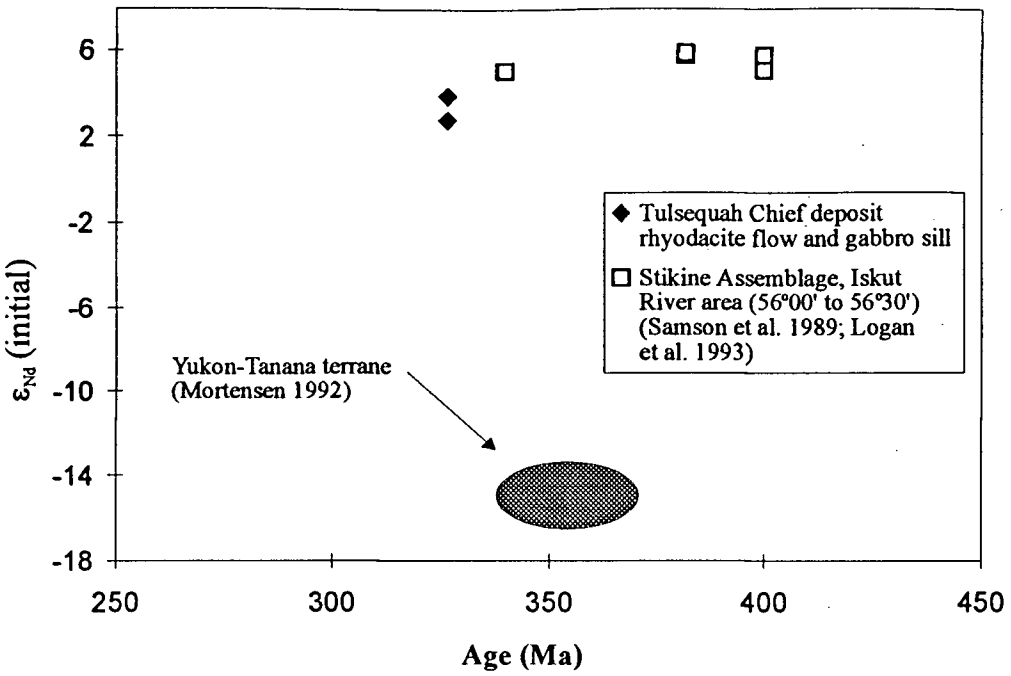

Figure 5. 5 ε_{Nd}(initial) *versus* age for volcanic rocks from the Stikine Assemblage (Iskut River area data from Samson et al. 1989; Logan et al. 1993)

Pb Isotopic Data

Sulphides from the Tulsequah Chief and Big Bull deposits were analyzed for their Pb isotopic compositions to assess the degree of evolution of metallogenic sources to mineralization. Sulphides from the AB_1, AB_2, H, and I zones of the Tulsequah Chief deposit yielded Pb isotopic ratios of $^{207}Pb/^{206}Pb$ = 0.8379-0.8387 and $^{208}Pb/^{206}Pb$ = 2.053-2.056, the Big Bull deposit yielded comparable ratios of $^{207}Pb/^{206}Pb$ = 0.8375-0.8380 and $^{208}Pb/^{206}Pb$ = 2.053-2.056 (Table 5.6).

In Figure 6 the Pb isotopic signature of sulphides from the Tulsequah Chief deposit are compared with those of Tertiary mineralization in the Stewart Mining Camp, Triassic and Jurassic VMS deposits, and the Late Devonian Forrest Kerr pluton, all of which comprise, or intrude the Stikine terrane in the Iskut River and southern Telegraph Creek map areas, and Devono-Mississippian VMS deposits in the Yukon-Tanana terrane in the Yukon and Alaska. Lead isotopic data from the Upper Triassic Granduc and Middle Jurassic Eskay Creek deposits, as well as Tertiary mineralization define an evolution from less to more evolved radiogenic lead compositions with time from the Mesozoic to the Cenozoic within the Stikine terrane; this evolution is best observed in the increasing $^{206}Pb/^{204}Pb$ values (Fig. 5.6) (Alldrick 1991; Childe *this volume*). With the addition of feldspar isotopic compositions from the Forrest Kerr pluton,

Table 5. 4 Pb isotopic data for sulphides from the Tulsequah Chief and Big Bull deposits.

SAMPLE NUMBER	SAMPLE LOCATION	MIN. [1]	$^{206}Pb/^{204}Pb$ (% error) [2,3]	$^{207}Pb/^{204}Pb$ (% error) [2,3]	$^{208}Pb/^{204}Pb$ (% error) [2,3]	$^{207}Pb/^{206}Pb$ (% error) [2,3]	$^{208}Pb/^{206}Pb$ (% error) [2,3]
TULSEQUAH CHIEF DEPOSIT							
T1a	I zone	gl	18.634 (0.011)	15.637 (0.014)	38.303 (0.018)	0.8387 (0.005)	2.056 (0.003)
T3a	AB2 zone	gl	18.654 (0.127)	15.637 (0.127)	38.298 (0.128)	0.8378 (0.013)	2.053 (0.009)
T4a	AB1 zone	gl	18.674 (0.033)	15.660 (0.033)	38.352 (0.036)	0.8381 (0.008)	2.054 (0.003)
T5a	H zone	gl	18.638 (0.013)	15.633 (0.015)	38.292 (0.020)	0.8383 (0.007)	2.055 (0.006)
T6a	H zone	gl	18.631 (0.031)	15.631 (0.032)	38.270 (0.034)	0.8385 (0.007)	2.054 (0.006)
T7a	sx clasts	gl	18.651 (0.014)	15.637 (0.016)	38.301 (0.019)	0.8380 (0.005)	2.054 (0.003)
T8a	H zone	gl	18.639 (0.040)	15.635 (0.041)	38.291 (0.043)	0.8384 (0.007)	2.054 (0.006)
T10a	AB1 zone	gl	18.642 (0.011)	15.635 (0.014)	38.296 (0.018)	0.8383 (0.005)	2.054 (0.002)
T11a	AB2 zone	gl	18.651 (0.017)	15.651 (0.016)	38.355 (0.023)	0.8387 (0.011)	2.056 (0.008)
T13a	AB1 zone	gl	18.630 (0.011)	15.629 (0.014)	38.275 (0.018)	0.8385 (0.005)	2.055 (0.003)
T14a	AB1 zone	gl	18.630 (0.011)	15.618 (0.014)	38.242 (0.018)	0.8379 (0.005)	2.053 (0.003)
T16a	H zone	gl	18.645 (0.043)	15.642 (0.044)	38.319 (0.045)	0.84385 (0.006)	2.055 (0.005)
T17a	H zone	gl	18.637 (0.018)	15.631 (0.019)	38.286 (0.023)	0.8383 (0.006)	2.054 (0.004)
	BIG BULL DEPOSIT						
B1a	Big Bull	gl	18.637 (0.030)	15.650 (0.030)	38.37 (0.033)	0.8398 (0.008)	2.059 (0.010)
B1b	Big Bull	gl	18.619 (0.020)	15.619 (0.021)	38.261 (0.025)	0.8389 (0.009)	2.055 (0.010)
B2a	Big Bull	gl	18.663 (0.024)	15.640 (0.021)	38.354 (0.030)	0.8380 (0.016)	2.055 (0.0015)
B3c	Big Bull	gl	18.674 (0.016)	15.656 (0.017)	38.398 (0.022)	0.8384 (0.008)	2.056 (0.010)
B4a	Big Bull	gl	18.775 (0.056)	15.758 (0.050)	38.697 (0.063)	0.8393 (0.028)	2.061 (0.025)
B4b	Big Bull	gl	18.671 (0.035)	15.644 (0.033)	38.368 (0.046)	0.8379 (0.014)	2.055 (0.027)
B5a	Big Bull	gl	18.654 (0.014)	15.627 (0.016)	38.309 (0.020)	0.8377 (0.005)	2.054 (0.008)
B5c	Big Bull	gl	18.681 (0.034)	15.652 (0.035)	38.381 (0.037)	0.8379 (0.007)	2.055 (0.009)
B5d	Big Bull	gl	18.664 (0.050)	15.632 (0.050)	38.314 (0.052)	0.8376 (0.011)	2.053 (0.011)

[1] mineral abbreviations: gl=galena

[2] errors are quoted at the 2σ (95% confidence) level.

[3] values are corrected for instrument fractionation by normalization based on replicate analyses of the NBS-981 standard.

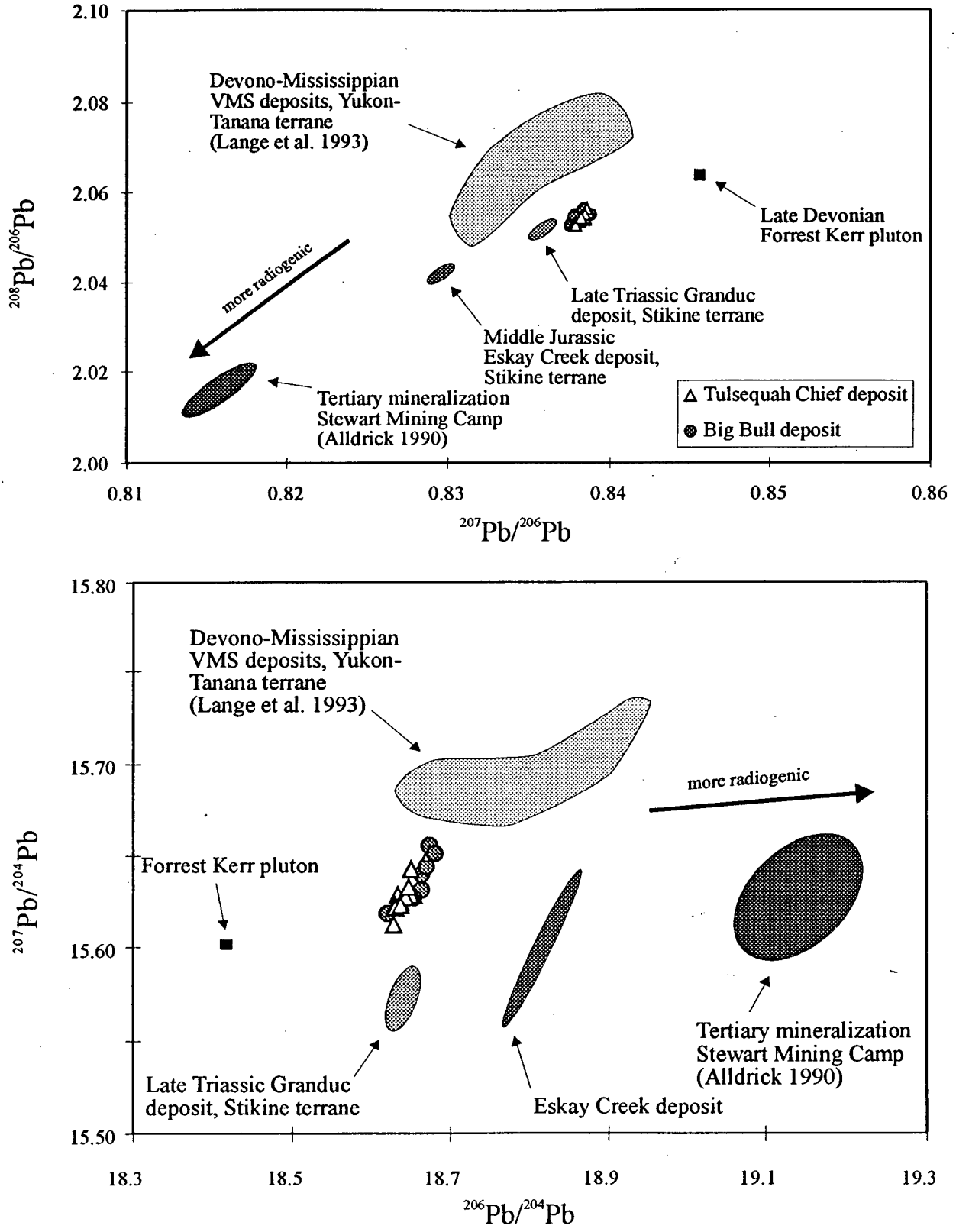

Figure 5. 6 Plots of a) $^{207}Pb/^{206}Pb$ *versus* $^{208}Pb/^{206}Pb$, and b) $^{207}Pb/^{204}Pb$ *versus* $^{206}Pb/^{204}Pb$ for sulphides from the Tulsequah Chief and Big Bull deposits, references for other data fields given in text.

this evolution can be extended back to the Late Devonian (Fig. 5.6). In comparison, Devono-Mississippian VMS mineralization in the Yukon-Tanana terrane has a wide range of $^{206}Pb/^{204}Pb$ values and significantly higher $^{207}Pb/^{204}Pb$ values than mineralization or magmatism of any age in the Stikine terrane. These elevated isotopic compositions in the Yukon-Tanana terrane, relative to younger mineralization and magmatism in the Stikine terrane, appear to reflect a continentally derived, more evolved source to mineralization. Early Mississippian Tulsequah Chief mineralization is more evolved than would be predicted by the evolution of lead in the Iskut River area of the Stikine terrane, with $^{206}Pb/^{204}Pb$ values comparable to the approximately 100 Ma younger Granduc deposit, and $^{207}Pb/^{204}Pb$ values intermediate between those of the island-arc Stikine terrane and continental-arc related mineralization.

Discussion

In the current study U-Pb dates of 327 +/-1 Ma and 330 +10/-1 Ma were determined from volcanic rocks of rhyodacitic to rhyolitic composition from the Tulsequah Chief mine series; these dates indicate a Late Mississippian age for VMS mineralization at Tulsequah Chief. The date determined for the felsic rock lower in the stratigraphy (330 +10/-1 Ma) is slightly older than the age determined for the rock which occurs at a higher level in the stratigraphy (327 +/-1 Ma), and may reflect an age difference between the upper and lower portions of the volcanic sequence which hosts mineralization.

The dates determined for felsic rocks in the Tulsequah Chief mine series are in good agreement with Middle Pennsylvanian to Early Permian dates determined on fossils in limestone units near the peak of Mount Eaton (Nelson and Payne 1984), and suggests that the time span between the eruption of felsic volcanic rock which hosts VMS mineralization at the base of Mount Eaton, and the deposition of limestone and andesite at the top of Mount Eaton may be as little as 10-20 m.y. However, the dates determined here are significantly younger than an Early Mississippian date of 351 +15/-6 Ma determined by Sherlock et al. (1994) on a felsic volcaniclastic rock near the top of the Tulsequah Chief mine series. Zircon from this rock were characterized by significantly older (up to 2040 Ma) $^{207}Pb/^{206}Pb$ ages, which was attributed to inherited cores or xenocrystic grains within the zircon population. In contrast, zircons analyzed from the same felsic volcanic sequence at Tulsequah Chief in this study did not exhibit any

evidence of inheritance (Figs. 5.3a and b). The question as to the source of the Precambrian zircon component in a volcaniclastic rock of the Stikine Assemblage, which is not present in underlying flow rocks, is an intriguing one. The source of this xenocrystic zircon could potentially be far-traveled continental detritus incorporated into the rock during deposition, or an assimilated component of older crustal material.

Although attempts to date felsic volcaniclastic rocks which host mineralization at Big Bull were unsuccessful, the similarity in the Pb isotopic signatures of sulphide from the Big Bull and Tulsequah Chief deposits suggests that the two deposits are of comparable age.

Nelson and Payne (1984) noted lithological similarities between volcanic and sedimentary rocks on Mount Eaton and those on Mount Sittikanay. Mihalynuk et al. (1994) suggested that volcanic and sedimentary rocks of the Mount Sittikanay block, about 20 km south of the Tulsequah Chief deposit, are the finer-grained, deformed distal equivalents of rocks of similar lithology which occur on Mount Eaton (Fig. 2). A maximum age of 325 +/-10 Ma determined for a volcaniclastic rock from Mount Sittikanay suggests that this correlation is valid and that the stratigraphic sequence which hosts mineralization at Tulsequah Chief may extend south of the deposit to Mount Sittikanay. An Early Mississippian age of 334 +5/-4 Ma determined by Brown and McLelland (1995) for felsic tuffaceous rocks of the Stikine Assemblage in the Golden Bear area, some 100 km south of Tulsequah Chief, further extends prospective stratigraphy for the exploration of Tulsequah Chief-equivalent VMS mineralization.

A maximum age of 357 +/-6 Ma determined for a felsic volcanic rock from the Mount Stapler block indicates that these rocks may be significantly older than those which host VMS mineralization at Tulsequah Chief. This unit lies west of the Llewlyn fault and has been correlated with rocks of the Whitewater Suite, which may be related to the Yukon-Tanana terrane (Mihalynuk et al. 1994a). Correlation of these rocks with Yukon-Tanana rather than Stikinia may account for the significant difference in age between these felsic volcanic rocks and those to the south on Mount Eaton and Mount Sittikanay. Neodymium isotopic analyses of rocks from Mount Stapler may assist in resolving this question.

Volcanic rocks which host VMS mineralization at the Tulsequah Chief and Big Bull deposits are interpreted to be part of the most northerly extreme of the Paleozoic Stikine Assemblage, the oldest recognized sequence within Stikinia, a terrane of island arc affinity (Monger 1977; Nelson and Payne 1984) (Fig. 5.1). However, Mihalynuk et al. (1994) have suggested that northern Stikinia may have been built in part on rocks of continental affinity, such as the Yukon-Tanana terrane. The Nd and Pb isotopic signatures from the Tulsequah Chief and Big Bull deposits are slightly more evolved than would be expected, based on data from the southern portions of Stikinia. However, these values are significantly less evolved than signatures from the Yukon Tanana terrane, and do not support these rocks being built directly on *bona fide* Yukon-Tanana rocks (Figs. 5.4 and 5.5). Available isotopic data are consistent with the basement at Tulsequah Chief and Big Bull being composed of one or more of the following: strongly attenuated continental arc components; continentally derived detritus directly overlying oceanic crust, or older, and more evolved island arc components than are present below rocks in more southerly parts of the Stikine Assemblage.

Plate 5. 2 Felsic fragmental unit, Tulsequah Chief mine series.

Plate 5. 3 Silicified felsic fragmental unit, Tulsequah Chief mine series.

Plate 5. 4 Baritic pyrite-rich sulphides, Tulsequah Chief Mine Series, I Zone (hammer for scale).

Plate 5. 5 Deformed dacitic tuffaceous rock, Big Bull deposit (hammer for scale).

Plate 5. 6 Flattened felsic fragmental unit, sample TC-GC-05, Mount Stapler (pen for scale).

Plate 5. 7 Deformed andesite tuffaceous rock, sample TC-GC-11, Mount Sittikanay.

Plate 5. 8 Deformed heterolithic fragmental unit, sample TC-GC-12, Mount Sittikanay (lens cap for scale).

Plate 5.2

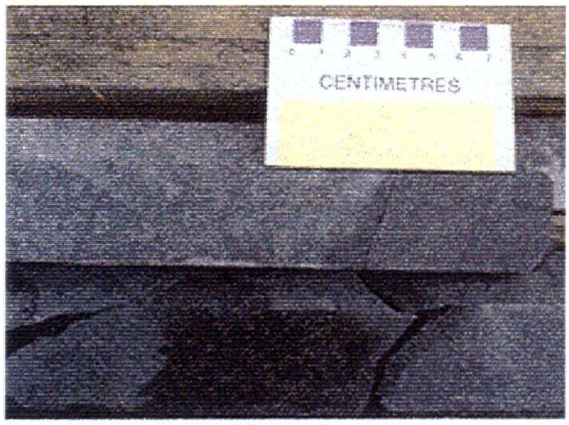

Plate 5.3

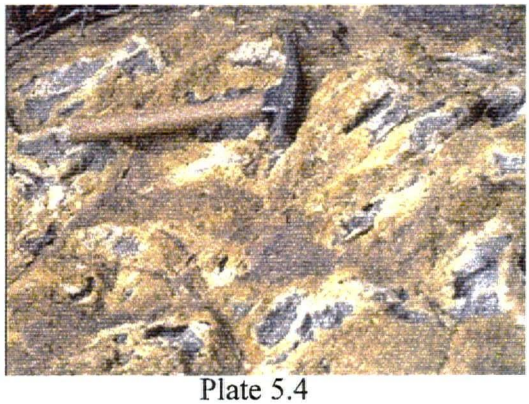

Plate 5.4

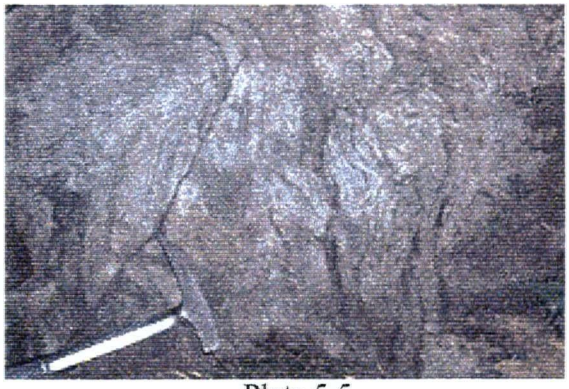

Plate 5.5

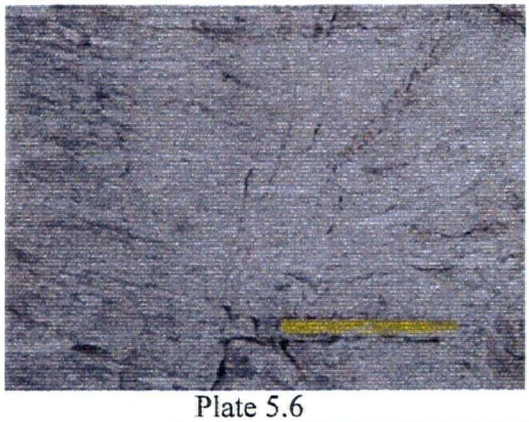

Plate 5.6

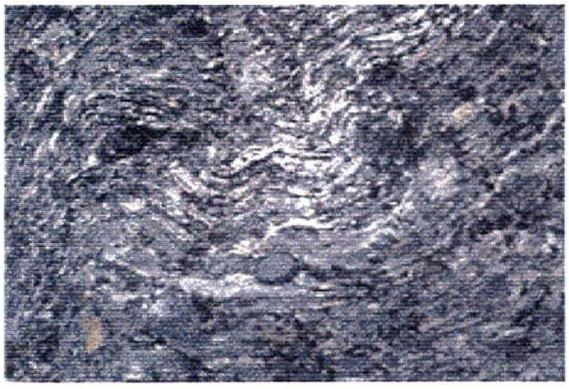

Plate 5.7

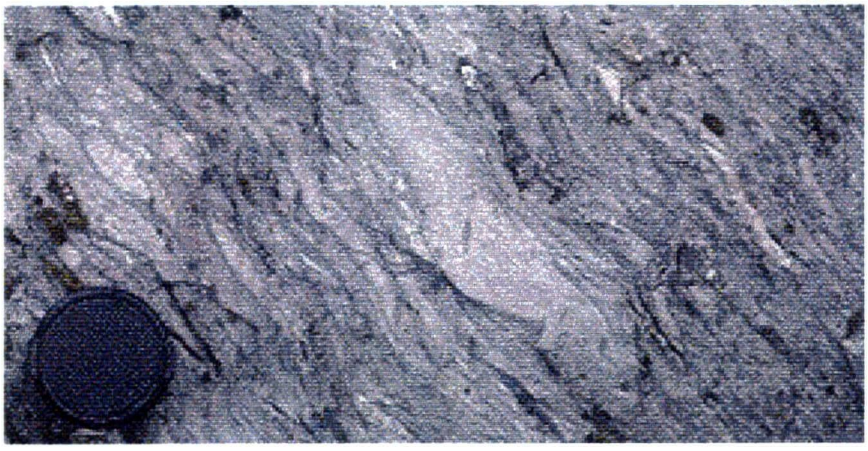

Plate 5.8

References

Alldrick, D.J. 1991. Geology and Ore Deposits of the Stewart Mining Camp. Ph.D. thesis, University of British Columbia, Vancouver, 417p.

Barrett, T.J. and MacLean, W.H. 1994. Chemostratigraphy and hydrothermal alteration in exploration for VHMS deposits in greenstones and younger volcanic rocks. *In* Alteration and Alteration Processes associated with Ore-Forming Systems. *Edited by* D.R. Lentz, Geological Association of Canada, Short Course Notes, pp. 433-467.

Brown, D.A., and McLelland, W.C. 1995. U-Pb dates for northern Stikinia: Tulsequah/Chutine areas (104F, K). Geological Association of Canada-Mineralogical Association of Canada Joint Annual Meeting, Program with Abstracts, Victoria, p. A-10.

Carmichael, R.G. and Curtis, K.M. 1994. 1993 Exploration Program: Geology, Geophysics and Diamond Drilling at the Big Bull Mine Area (NTS 104K/12E). Internal Report for Redfern Resources Ltd., 22p.

Carmichael, R.G. Sherlock, R.L., and Barrett, T.J. 1995. The geology of the Big Bull polymetallic volcanogenic massive sulphide deposit, northwestern British Columbia (104K/12). *In* British Columbia Ministry of Energy, Mines and Petroleum Resources, Geological Fieldwork 1994. *Edited by* B. Grant and J.M. Newell, p. 541-550.

Harland, W.B., Armstrong, R.L., Cox, A.V., Craig, L.E., Smith, A.G., and Smith, D.G. 1990. A Geological Time Scale, 1989. Cambridge University Press, Cambridge, 263 p.

Kerr, F.A. 1931. Explorations between the Stikine and Taku Rivers, B.C. Geological Survey of Canada, Summary Report 1930, Part A, pp. 41-55.

Krogh, T.E. 1982. Improved accuracy of U-Pb zircon ages by the creation of more concordant systems using an air abrasion technique. Geochemica and Cosmochemica Acta, **46**: 637-649.

Lange, I.M., Nockelburg, W.J., Newkirk, S.R., Aleinikoff, J.N., Church, S.E., and Krouse, H.R. 1993. Devonian volcanogenic massive sulphide deposits and occurrences, southern Yukon-Tanana terrane, eastern Alaska range, Alaska. Economic Geology, **88**: 344-376.

Logan, J.M., Drobe, R., McClelland, W.C., and Anderson, R.G. 1993. Devonian intraoceanic arc magmatism in northwestern Stikinia. Geological Association of Canada/Mineralogical Association of Canada Annual Meeting, Program with Abstracts, Edmonton, p. A-60.

Ludwig, K.R. 1980. Calculation of uncertainties of U-Pb isotope data. Earth and Planetary Science Letters, **46**: 212-220.

McClelland, W.C. 1992. Permian and older rocks of the southwestern Iskut River map area, northwestern British Columbia. *In* Current Research, Part A, Geological Survey of Canada, Paper 92-1A, pp. 303-307.

McGuigan, P., Melnyk, W., Dawson., G.L., and Harrison, D. 1993. Tulsequah Chief Mine, Northwestern B.C. 1992 Exploration Program: Diamond Drilling, Geology and Reserve Estimation. Unpublished Report by Cambria Geological Ltd., Vancouver, 3 volumes.

Mihalynuk, M.G., and Rousse, J.N. 1988. Preliminary geology of the Tutshi Lake area, northwestern British Columbia (104M/15). *In* Geological Fieldwork 1987, *Edited by* B. Grant and J.M. Newell, British Columbia Ministry of Energy, Mines and Petroleum Resources Paper 1988-1, p. 217-231.

Mihalynuk, M.G., Smith, M.T., Hancock, K.D., and Dudka, S. 1994a. Regional and economic geology of the Tulsequah River and Glacier areas (104K/12 &13). *In* Geological Fieldwork 1993, *Edited by* B. Grant and J.M. Newell, British Columbia Ministry of Energy, Mines and Petroleum Resources Paper 1994-1, p. 171-200.

Mihalynuk, M.G., Smith, M.T., Hancock, K.D., and Dudka, S. 1994b. Tulsequah River a map area geology (104K/12). British Columbia Ministry of Energy, Mines and Petroleum Resources, Open File 1994-3.

Mihalynuk, M.G., Nelson, J., and Diakow, L. 1994c. Cache Creek terrane entrapment: Oroclinal paradox within the Canadian Cordillera. Tectonics, **13**: 575-595.

Monger, J.W.H. 1977. Upper Paleozoic rocks of the western Canadian Cordillera and their bearing on Cordilleran evolution. Canadian Journal of Earth Sciences, **14**: 1832-1859.

Monger, J.W.H., Souther, J.G., and Gabrielse, H. 1972. Evolution of the Canadian Cordillera: A plate-tectonic model. American Journal of Science, **272**: 577-602.

Mortensen, J.K. 1992. Pre-mid-Mesozoic tectonic evolution of the Yukon-Tanana terrane, Yukon and Alaska. Tectonics, **11**: 836-853.

Mortensen, J.K., Ghosh, D.K., and Ferri, P. 1995. U-Pb geochronology of intrusive rocks associated with Cu-Au deposits in the Canadian Cordillera. *In* Porphyry Deposits in the Northwestern Cordillera of North America. *Edited by* T.G. Schroter. **G-2**: 491-531.

Nelson, J. and Payne, J.G. 1984. Paleozoic volcanic assemblages and volcanogenic massive sulphide deposits near Tulsequah, British Columbia. Canadian Journal of Earth Sciences, **21**: 379-381.

Samson, S.D., McClelland, W.C., Patchett, P.J., Gehrels, G.E., and Anderson, R.G. 1989. Evidence from neodymium isotopes for mantle contributions to Phanerozoic crustal genesis in the Canadian Cordillera, Nature, **337**: 705-709.

Sebert, C., Curtis, K.M., Barrett, T.J., and Sherlock, R.L. 1995. Geology of the Tulsequah Chief VMS deposit, Northwestern British Columbia (104K/12). *In* British Columbia Ministry of

Energy, Mines and Petroleum Resources Geological Fieldwork, *Edited by* B. Grant and J.M. Newell, pp. 529-540.

Sebert, C. and Barrett, T.J. *1996.* Stratigraphy, alteration and mineralization at the Tulsequah Chief massive sulphide deposit, Northwestern British Columbia. Exploration and Mining Geology.

Sherlock, R.L., Childe., F., Barrett., T.J., Mortensen, J.K., Lewis, P.D., Chandler, T., and Allen., R. 1994. Geological Investigations of the Tulsequah Chief Massive Sulphide Deposit, Northwestern British Columbia (104K/12). *In* British Columbia Ministry of Energy, Mines and Petroleum Resources Geological Fieldwork, *Edited by* B. Grant and J.M. Newell, p.373-379.

Souther, J.G. 1971. Geology and mineral deposits of the Tulsequah map-area, British Columbia. Geological Survey of Canada, Memoir 362.

Steiger, R.H., and Jäger, E. 1977. Subcommission on geochronology: Convention on the use of decay constants in geo- and cosmochronology. Earth and Planetary Science Letters, **14**: 359-362.

Thériault, R., J. 1990. Methods for Rb-Sr and Sm-Nd isotopic analyses at the geochronology laboratory, Geological Survey of Canada. *in* Radiogenic Age and Isotopic Studies: Report 2, Geological Survey of Canada, Paper 89-2, p. 3-6.

York, D. 1969. Least-squares fit of a straight line with correlated errors. Earth and Planetary Science Letters, **5**: 320-324.

CHAPTER 6:

U-PB GEOCHRONOLOGY AND RADIOGENIC ISOTOPIC SYSTEMATICS OF ROOF PENDANTS IN THE COAST PLUTONIC COMPLEX WHICH HOST VMS MINERALIZATION

Plate 6.1. Abandoned power plant at Anyox.

Part I:

U-Pb Geochronology and Pb Isotopic Systematics of the Anyox pendant, West-Central British Columbia

Introduction

The Anyox pendant lies within the Coast Plutonic Complex in the Nass River (103P/5) map area of west-central British Columbia (Figs. 6.1 and 6.2). Mafic volcanic and sedimentary rocks of uncertain, but probable Mesozoic age, on the eastern side of the pendant are host to the Anyox volcanogenic massive sulphide (VMS) deposits. These deposits were mined between 1914 and 1935, and the two largest orebodies, the Hidden Creek and Bonanza deposits produced 21.7 Mt grading 1.5% Cu, 9.25 g/t Ag, and 0.17 g/t Au, and 0.66 Mt grading 2.2% Cu, respectively (Höy 1991).

Both the age and terrane affiliation of the Anyox pendant have been topics of debate (e.g., Alldrick 1986a; Grove 1986; Smith 1993). Prior to this study there were no U-Pb ages and only limited biochronological data for rocks of the Anyox pendant. In the current study volcanic, intrusive, and sedimentary rocks were collected in an attempt to constrain the age of VMS mineralization in the Anyox pendant using U-Pb methods. In addition, sulphides from the Hidden Creek orebody, and base and precious metal-rich quartz veins from Granby Peninsula, in the easternmost portion of the pendant, were analyzed for their Pb isotopic compositions. Detrital zircon grains from turbiditic sedimentary rocks, also on Granby Peninsula, were dated by U-Pb methods to begin to constrain the provenance of this strata, and a diorite sill from Mount Clashmore was dated to begin to establish the age of some of the igneous rocks in the central to western portions of the pendant.

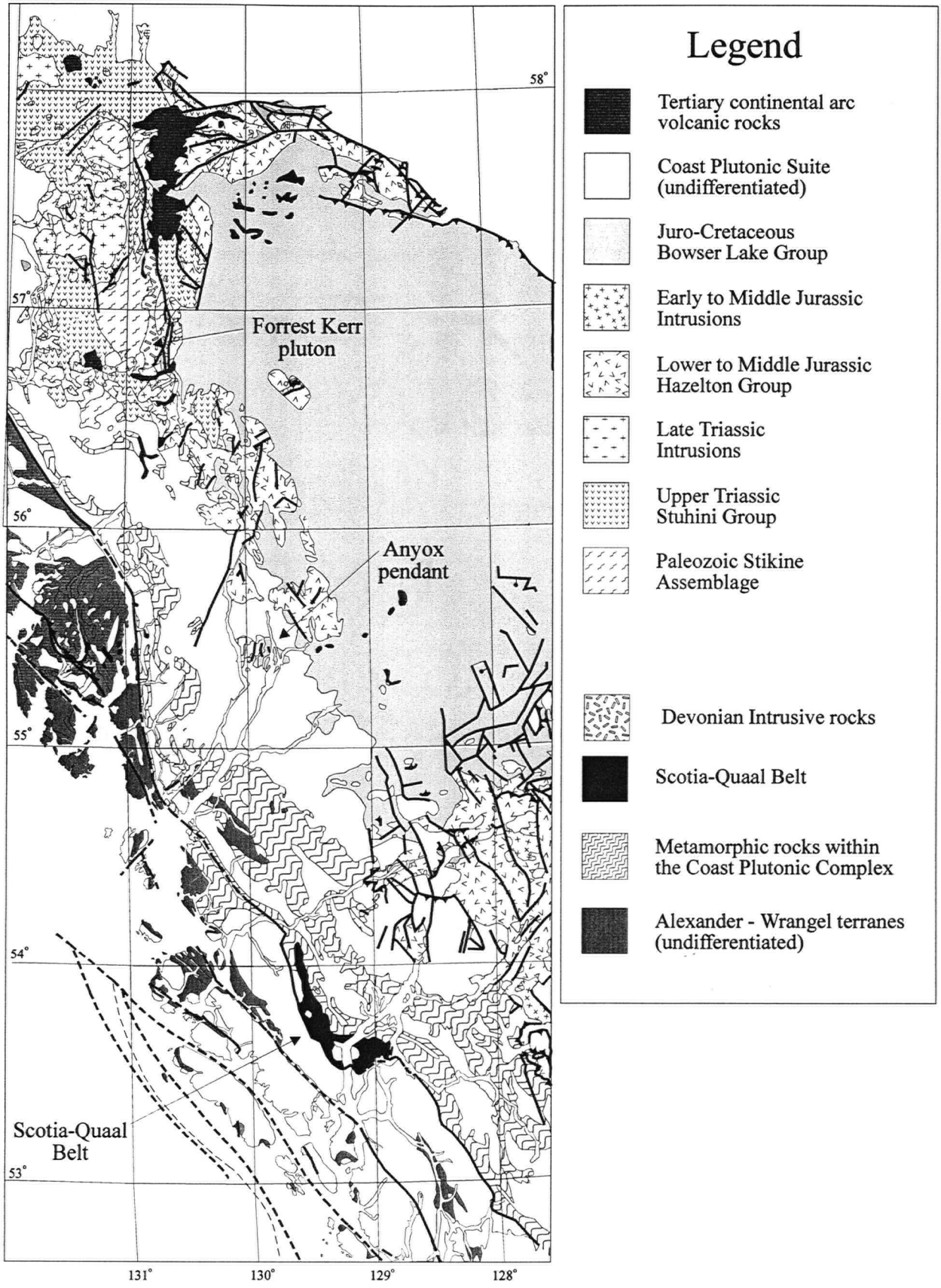

Figure 6. 1 Generalized geology of the Canadian Cordillera between 53° to 58°N, and 128° to 132°W (after Wheeler and McFeely, 1991).

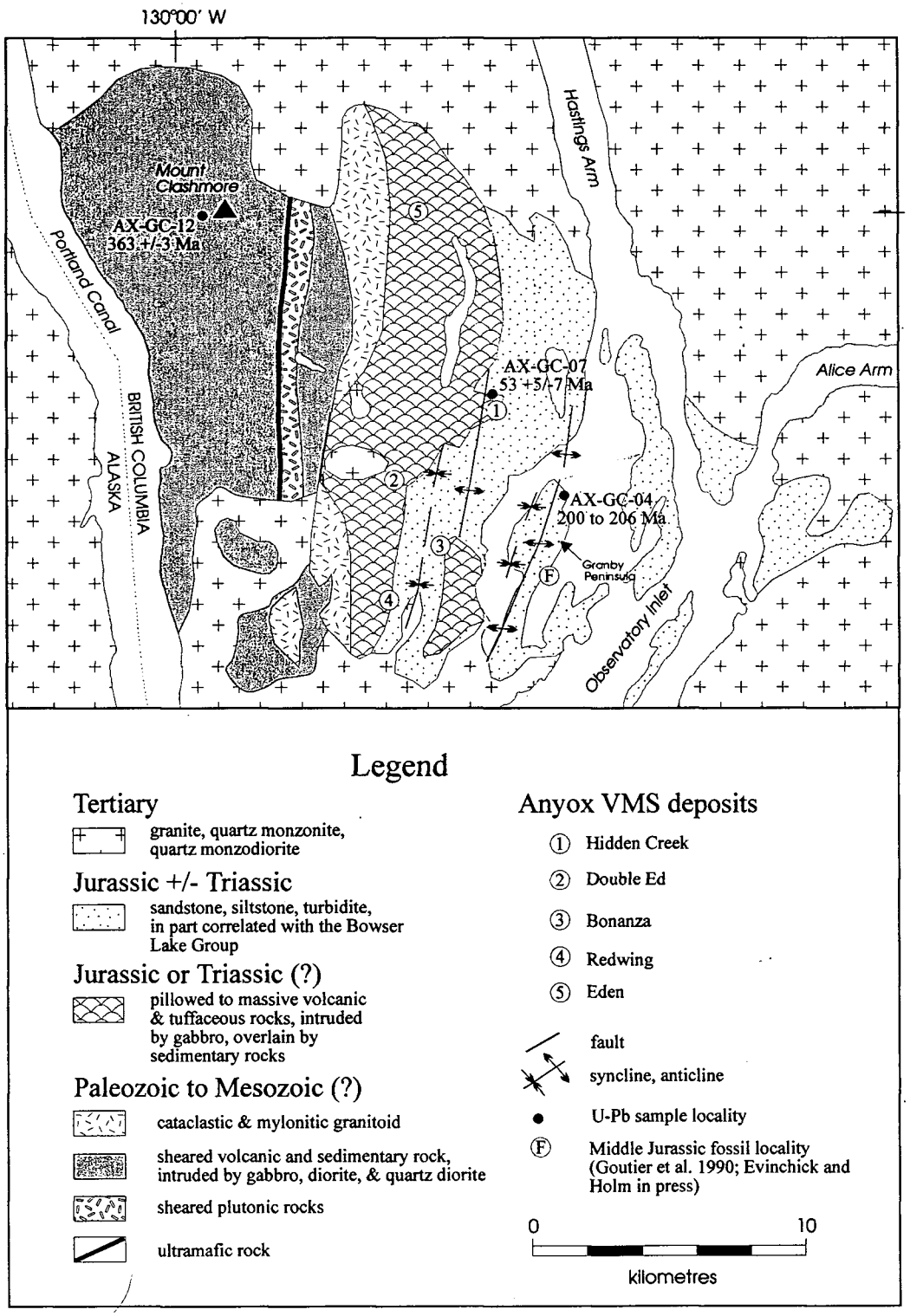

Figure 6. 2 Generalized geology of Anyox pendant, west-central British Columbia (after Alldrick 1986a; Grove 1986; Evinchick and Holm 1997).

Geology and mineral deposits of the Anyox pendant

The eastern portion of the Anyox pendant has been mapped, and its contained mineral deposits described by Sharp (1980), Alldrick (1986a and b), Grove (1986), and Macdonald et al. (1996). Geochemical studies of the tholeiitic mafic volcanic rocks that host VMS mineralization were conducted by Smith (1993) and Macdonald et al. (1995 and 1996). Until recently there has been no systematic mapping of the western portion of the pendant. Geological mapping of the entire Anyox pendant, as well as description of mineral deposits within the western portion of the pendant, is the focus of collaborative project by the Geological Survey of Canada and the British Columbia Geological Survey (Alldrick et al. 1996; Evenchick and Holm 1997; Evenchick et al. 1997).

The western two thirds of the Anyox pendant is composed of strongly to moderately deformed metavolcanic and metasedimentary rocks that have been intruded by gabbroic to quartz-dioritic composition sill-like bodies (Alldrick et al. 1996; Evinchick and Holm 1997). The Maple Bay quartz-Cu+/-precious metal vein systems occur along brittle fracture zones in the westernmost portion of the pendant (Alldrick et al. 1996).

The eastern third of the Anyox pendant contains pillowed to massive mafic volcanic and tuffaceous rocks that are locally overlain by chert and carbonate, and cross cut by intrusions of gabbroic composition (Sharp 1980; Alldrick 1986a and b). This sequence is overlain by turbiditic sedimentary rocks. Both the volcanic and overlying sedimentary rocks have been metamorphosed at up to lower greenschist facies and are moderately to weakly deformed (Sharp 1980; Alldrick 1986a; Macdonald et al. 1995). The volcano-sedimentary sequence is cross cut by a suite of undeformed diorite dykes, one of which was dated as part of the current study. Volcanic and sedimentary rocks which comprise the western portion of the pendant are separated from rocks of the western two thirds of the pendant by a 0.5 to 2 km wide zone of cataclastic to mylonitic granitic rocks (Evenchick and Holm 1997).

Copper-rich massive sulphide deposits in the Anyox pendant are hosted at, just below, and just above the contact between an underlying, mainly volcanic sequence that comprises predominantly pillowed tholeiitic basaltic to basaltic andesitic composition flow rocks, with lesser

tuffaceous rocks and an overlying sequence of chemical and clastic sedimentary rocks. Massive sulphide deposits within the Anyox camp include the Hidden Creek, Double Ed, Bonanza, Redwing, and Eden deposits (B.C. MINFILE numbers 103P-021, -203, -024, -025, and -026) (Alldrick 1986a; Macdonald et al. 1995, 1996) (Fig. 6.2). Chloritic alteration within the volcanic sequence and lower parts of the sedimentary sequence is attributed to hydrothermal processes associated with VMS mineralization (Alldrick 1986a). Sedimentary rocks which overlie mafic volcanic rocks in the easternmost part of the Anyox pendant consist of a sandstone-siltstone-mudstone turbiditic sequence. On Granby Peninsula these turbiditic sedimentary rocks are cross cut by quartz veins which contain base-metal sulphides +/- precious metals (Granby Point quartz and Goldleaf, B.C. MINFILE numbers 103P-022 and -028, respectively).

Age assignments and terrane correlations for the Anyox pendant

In addition to the Anyox deposits, there are two other significant mafic volcanic- and sediment-hosted Cu-rich VMS deposits in allochthonous terranes of the Cordillera, these are the Windy Craggy deposit, in the Alexander terrane, and the Granduc deposit, in Stikinia; both of these deposits are of Late Triassic age (Orchard 1986; Grove 1986; Peter 1992; Childe *this volume*). The presence of generally similar types of mineralization to Anyox has lead some workers (e.g. Höy 1991) to suggest that mafic volcanic and sedimentary rocks in the Anyox pendant could be of comparable age and formed in one of the terranes that hosts these deposits. However, VMS mineralization, albeit of a distinctly different style than that at Anyox, also occurs within Middle Jurassic rocks in Stikinia at Eskay Creek (Childe *this volume*).

There have been a number of previous age assignments and terrane correlations made for mafic volcanic and sedimentary rocks of the Anyox pendant and associated VMS mineralization, in part based on the presence of VMS mineralization within other terranes. A number of these correlations are summarized here. Sharp (1980) correlated pillowed mafic volcanic rocks and overlying sedimentary rocks which host VMS mineralization at Anyox with the Upper Triassic Kunga Group of the Alexander terrane. Grove (1986) suggested that rocks from the western portion of the pendant represent more strongly deformed and metamorphosed equivalents of mafic volcanic rocks in the eastern portion of the pendant, and concluded that these rocks were correlative with lithologically similar lavas and sedimentary rocks of the Jurassic Hazelton Group

of the Stikine terrane at Treaty Creek, and assigned a Middle Jurassic age to VMS mineralization. Alldrick (1986a) suggested that the mafic volcanic rocks and their contained VMS mineralization may be of Late Triassic age based on a similarity between the Pb isotopic signature of VMS mineralization at Anyox and that of whole rock samples and galenas from the Late Triassic Karmutsen Formation in Wrangellia. Höy (1991) assigns the Anyox deposit and its host rocks a Late Triassic age, and relates them to both Stikinia and the Karmutsen Group in Wrangellia. Smith (1993) argued that Anyox volcanic rocks were chemically and isotopically dissimilar to rocks of the Karmutsen and Nicoli Formations, and correlated these rocks with the Spider Peak Formation of the Methow terrane.

There is a general consensus that VMS mineralization at Anyox is of Mesozoic age, but the question as to whether it is Late Triassic, Early Jurassic or Middle Jurassic remains unresolved. Smith (1993) calculated Pb-Pb isochron ages for mafic volcanic rocks and sulphides from the Anyox pendant. Ages of 170 and 260 Ma (errors not given) were obtained for basaltic rocks from the Hidden Creek area. An age of 168 +/-37 Ma (Triassic-Jurassic boundary to Late Cretaceous) was determined from three galena samples. However, one of the samples used in this calculation, a 'late stage vein', has a Pb isotopic composition comparable to quartz-sulphide veins from Granby Peninsula, interpreted in this study to be of Tertiary age and unrelated to VMS mineralization. Therefore this age determination is not considered to be a valid estimate of the age of VMS mineralization in the Anyox pendant.

Goutier et al. (1990) determined a probable Middle Jurassic age for deformed ammonites hosted within turbiditic sedimentary rocks on Granby Peninsula (Fig. 6.2). Re-collection of less deformed ammonites from a nearby location within the same strata by Evinchick and Holm (1997) yielded a more precise late Middle Jurassic age. On the basis of lithology, these rocks have been correlated with the Middle to Upper Jurassic Bowser Lake Group (Wheeler and McFeely 1991; Evenchick and Holm 1997). Unfortunately, this portion of the sedimentary sequence overlies the Anyox deposits by an unknown stratigraphic interval and as such provides only a minimum estimate of the age of VMS mineralization in the Anyox pendant.

U-Pb Geochronology

The U-Pb results reported in this paper are based on analysis of zircons recovered from samples collected from drill core and outcrop; sample descriptions are given below. Heavy mineral extraction procedures and U-Pb analytical procedures follow those of Mortensen et al. (1995). Both single and multiple grain zircon fractions were abraded prior to analysis (Krogh 1982), unless otherwise indicated in the text. Isotopic ratios were measured using a modified single collector VG-54R thermal ionization mass spectrometer equipped with a Daly photomultiplier. Procedural blanks were 5-25 picograms for Pb and 1-5 picograms for U. Concordia intercept ages and associated errors were calculated using a modified York-II regression model (York 1969), and the algorithm of Ludwig (1980); ages were calculated using the decay constants recommended by Steiger and Jäger (1977). Age assignments follow the time scale of Harland et al. (1990). Analytical results are given in Table 6.1 and shown graphically in Figure 6.3.

Granby Peninsula turbiditic sedimentary rocks

The sandstone base of a turbiditic flow (sample AX-GC-04) from the northeast side of Granby Peninsula was collected for U-Pb detrital zircon dating, to assist in establishing the provenance of detrital zircon and possible source reservoirs for sedimentary rocks in this portion of the Anyox pendant (Plate 6.2). The sample contained abundant fine- to coarse-grained, predominantly euhedral zircon. Single grain analyses were obtained for five coarse-grained, colourless, prismatic zircon crystals which contained a minor amount of colourless inclusions. All zircon crystals were strongly abraded prior to analysis. Analysis of four of the five zircon crystals yielded concordant or near-concordant results (fractions C, E, F, and H), and are therefore interpreted to represent crystallization ages. The fifth fraction (fraction G) was 11% discordant (Fig. 6.3a). It is not possible to determine the geological significance of this latter analysis, as the discordance could be the result of inheritance, Pb loss, multiple stage growth of zircon, or some combination of these processes (c.f. Heaman and Parrish 1991; Gehrels et al. 1995). The concordant to near-concordant analyses yielded Early Jurassic $^{207}Pb/^{206}Pb$ ages of 201 to 206 Ma, with the analysis with the best precision having a $^{207}Pb/^{206}Pb$ age and associated error of 204 +/-7 Ma (Table 6.1).

Table 6. 1 U-Pb analytical data for samples from the Anyox pendant and Scotia-Quaal Belt.

Fraction[1]	Wt.	U	Pb[2]	$^{206}Pb/^{204}Pb$[3]	Pb[4]	^{208}Pb[5]	Isotopic ratios(±1σ,%)[6]			Isotopic dates(Ma,±2σ)[6]		
	mg	ppm	ppm		pg	%	$^{206}Pb/^{238}U$	$^{207}Pb/^{235}U$	$^{207}Pb/^{206}Pb$	$^{206}Pb/^{238}U$	$^{207}Pb/^{235}U$	$^{207}Pb/^{206}Pb$
ANYOX PENDANT												
Granby Peninsula turbiditic sediment (AX-GC-04)												
zircon												
C,c,N1,p*	0.010	1242	38.6	810	31	8.3	0.03158±0.13	0.2188±0.45	0.05024±0.38	200.4±0.5	200.9±1.6	206.2±17.5
E,c,N1,p*	0.020	382	11.7	2029	7	8.4	0.03088±0.11	0.2138±0.24	0.05020±0.16	196.1±0.4	196.7±0.9	204.2±7.3
F,c,N1,p*	0.015	184	5.9	384	14	9.9	0.03175±0.42	0.2194±1.45	0.05013±1.30	201.5±1.6	201.4±5.3	200.9±59.1
G,c,N1,p*	0.022	601	20.1	3225	8	7.00000	0.03436±0.11	0.2418±0.23	0.05105±0.15	217.8±0.5	219.9±0.9	243.1±7.0
H,c,N1,p*	0.030	124	3.9	557	14	7.9	0.03232±0.21	0.2240±0.51	0.05025±0.39	205.1±0.9	205.2±1.9	206.4±18.1
Hidden Creek area undeformed gabbro dyke (AX-GC-07)												
zircon												
A,m,N1,mf	0.238	1428	15.5	3894	60	8.2	0.01089±0.22	0.09658±0.23	0.06430±0.06	69.8±0.3	93.6±0.4	751.4±2.7
B,m,N1,mf-s	0.370	1052	11.3	3599	73	8.8	0.01065±0.11	0.09788±0.13	0.06669±0.05	68.3±0.2	94.8±0.2	828.0±2.2
C,m,M1,mf-s	0.275	1208	10.3	3672	50	7.5	0.008738±0.26	0.06285±0.28	0.05216±0.11	56.1±0.3	61.9±0.3	292.5±5.0
D,m,N1,mf	0.023	912	8.7	638	21	6.2	0.009750±0.11	0.08245±0.50	0.06134±0.43	62.5±0.1	80.4±0.8	651.0±18.4
Mount Clashmore quartz-diorite sill (AX-GC-12)												
zircon												
B,m,N1,mf	0.077	348	16.9	3258	24	7.5	0.04948±0.15	0.3673±0.27	0.05383±0.18	311.3±0.9	317.6±1.5	364.0±8.1
C,f,N1,mf	0.167	310	16.2	11950	14	7.4	0.05325±0.16	0.3950±0.22	0.05381±0.12	334.4±1.1	338.0±1.3	363.0±5.6
E,m,N1,mf	0.070	279	14.4	3709	17	8.3	0.05205±0.17	0.3864±0.25	0.05385±0.14	327.1±1.1	331.8±1.4	364.9±6.3
G,m,N1,s	0.024	286	14.3	1271	17	7.53	0.05100±0.10	0.3786±0.26	0.05383±0.17	320.7±0.6	326.0±1.4	364.1±7.8
Hidden Creek area gabbro sill (AX-GC-11)												
zircon												
A,fm,N1,s	0.019	468	8.9	261	44	7.2	0.01945±0.21	0.1327±0.72	0.04950±0.72	124.2±0.5	126.5±2.0	171.5±33.2
titanite												
C,c,N1,w	0.960	1.6	0.03	20	722	20.0						
D,c,M5,w	1.55	1.7	0.02	20	1020	11.6						
E,c,M5,wi	1.30	2.1	0.03	20	812	17.4						
F,c,M5,w	0.25	1.9	0.05	21	160	37.5						
Hidden Creek area gabbro sill (AX-GC-01)												
titanite												
A,c,M2,w	0.523	4.7	0.22	19	779	43.4						
B,c,M5,w	0.863	0.7	0.07	19	869	50.6						
D,c,M20,w	0.225	12.8	0.30	19	1150	14.1						
SCOTIA-QUAAL BELT												
Ecstall Property quartz diorite sill (EL-GC-01)												
zircon												
A,c,N1,p	0.315	393	22	20943	21	6.5	0.05803±0.25	0.4331±0.29	0.05413±0.10	363.6±1.8	365.4±1.8	376.6±4.4
B,c,N1,p	0.236	474	26	27192	14	6.9	0.05588±0.15	0.4165±0.21	0.05406±0.09	350.5±1.0	353.5±1.3	373.6±4.1
C,m,N1,p	0.275	438	25	40696	11	6.7	0.05786±0.63	0.4315±0.64	0.05409±0.10	362.6±4.4	364.2±3.9	374.6±4.4
D,f,N1,p	0.072	511	29	18076	7	7.2	0.05729±0.13	0.4272±0.20	0.05408±0.09	359.1±0.9	361.2±1.2	374.4±4.2
E,c,N1,p	0.042	579	33	9146	10	6.5	0.05858±0.11	0.4371±0.19	0.05411±0.10	367.0±0.8	368.2±1.2	375.8±4.3
F,c,M1,p	0.091	430	24	5766	24	6.8	0.05657±0.13	0.4215±0.21	0.05404±0.12	354.7±0.9	357.1±1.3	372.9±5.4
G,c,N1,p	0.045	493	28	7931	10	6.6	0.05773±0.21	0.4304±0.27	0.05407±0.11	361.8±1.5	363.4±1.6	373.9±4.7
H,m,N1,p	0.054	484	27	8154	12	6.7	0.05764±0.11	0.4298±0.20	0.05409±0.10	361.2±0.8	363.0±1.2	374.7±4.6

Table 6.1 (cont.)

[1]All fractions are air abraded; Grain size, smallest dimension: c= +134μm, m=-134μm+74μm, f=-74μm; Magnetic codes Franz magnetic separator sideslope at which grains are nonmagnetic; e.g., N1=nonmagnetic at 1°; Field strength for all fractions =1.8A; Front slope for all fractions=20°; Grain character codes: p=prismatic, s=subhedral, mf=prismatic multi-faceted, *=single grain, w=wedge-shaped titanite.

[2]Radiogenic Pb

[3]Measured ratio corrected for spike and Pb fractionation of 0.0043/amu ±20% (Daly collector)

[4]Total common Pb in analysis based on blank isotopic composition

[5]Radiogenic Pb

[6]Corrected for blank Pb, U and common Pb (Stacey-Kramers model Pb composition at the $^{207}Pb/^{206}Pb$ date of fraction, or age of sample)

Hidden Creek area undeformed dyke

A coarse-grained undeformed dyke of gabbroic composition that intrudes foliated and altered mafic volcanic and sedimentary rocks which host the Anyox VMS deposits was sampled from drill core (DDH D2, 79.2-79.6 m) for U-Pb analysis. The sample contained abundant euhedral zircons with excellent clarity and no visible cores. Four zircon fractions yielded highly discordant results, with $^{207}Pb/^{206}Pb$ ages of 293 to 828 Ma (Fig. 6.3b). The discordance exhibited by zircons from this rock is attributed to varying degrees of inheritance within "cryptic" cores or xenocrysts. Regression of the four points yielded a well constrained Early Eocene lower intercept age of 53 +5/-7 Ma, with a poorly constrained upper intercept age of 2095 +500/-405 Ma. The lower intercept age is considered a valid estimate of crystallization of the age of this rock.

Mount Clashmore quartz diorite sill

A fine- to medium-grained quartz diorite sill from Mount Clashmore, in the central part of the Anyox pendant was originally sampled by R. Macdonald for lithogeochemistry to compare with rocks from the eastern portion of the pendant (Plate 6.3). The sample was subsequently processed for U-Pb zircon analysis, and although the sample weighed <2 kg, heavy mineral extraction procedures yielded sufficient zircon for U-Pb analysis. Zircons from this rock were euhedral and multi-faceted with excellent clarity and few inclusions. Analysis of four fractions were between 8 and 15% discordant, with a restricted range of $^{207}Pb/^{206}Pb$ ages that varied from 363 to 365 Ma (Fig. 6.3c). A latest Devonian - earliest Mississippian $^{207}Pb/^{206}Pb$ weighted mean

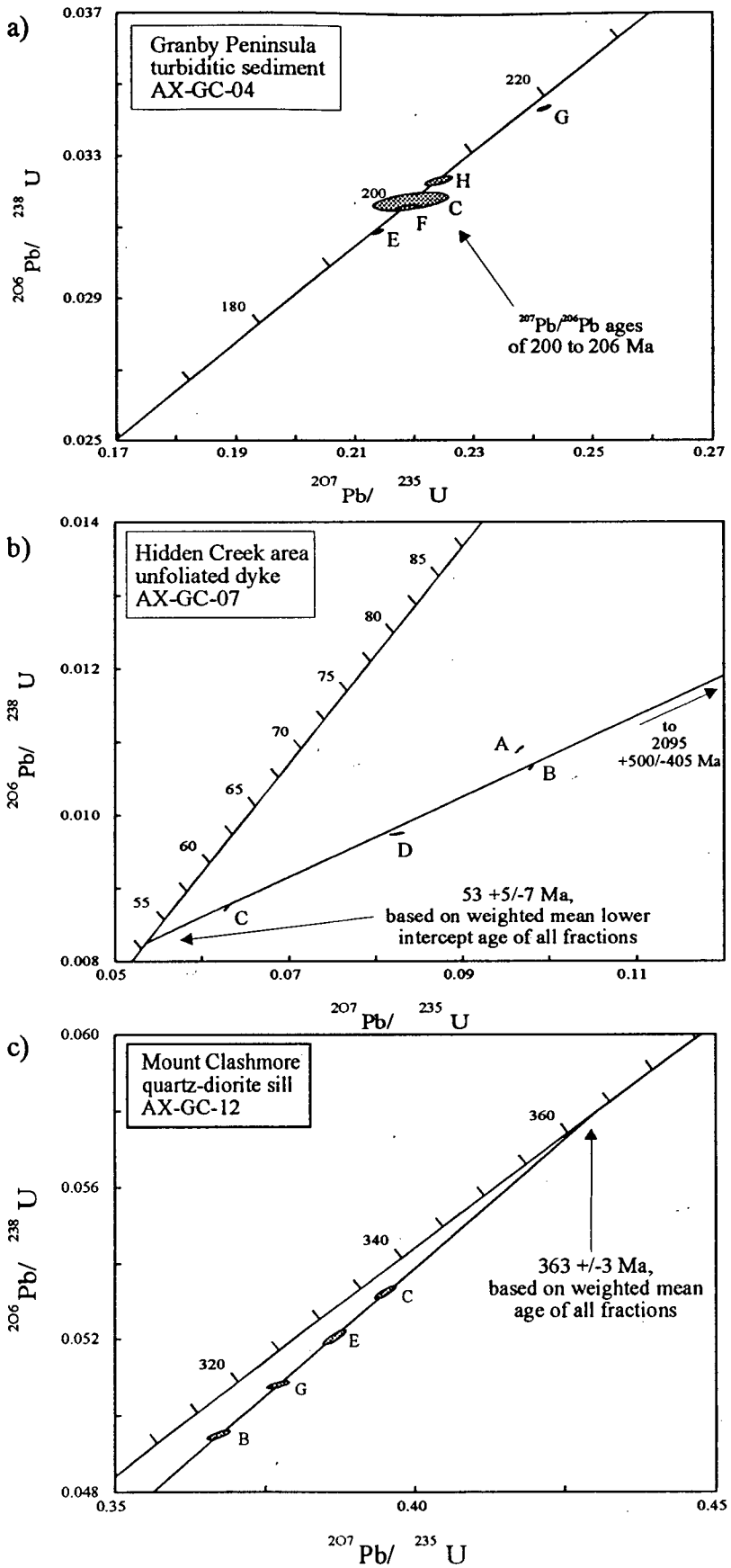

Figure 6. 3 U-Pb concordia diagrams for a) detrital zircon from turbiditic sedimentary rocks on Granby Peninsula (AX-GC-04); b) an unfoliated mafic dyke which cross cuts mafic volcanic rocks which host the Hidden Creek VMS deposit (AX-GC-07); and c) a quartz diorite sill from Mount Clashmore (AX-GC-12).

age of 363 +/-3 Ma, based on all four fractions, is considered to be the best estimate of the age of this rock.

Hidden Creek area gabbro sills

Two weakly to moderately foliated, fine- to medium-grained sills of gabbroic composition (AX-GC-01 and -11), which intrude mafic volcanic rocks in the area of VMS mineralization were sampled from surface for U-Pb analysis. Macdonald et al. (1995) determined that these foliated mafic sills are chemically similar to the mafic volcanic rocks they intrude. As such they may be comagmatic with the mafic volcanic rocks, and therefore of approximately the same age as VMS mineralization in the Anyox pendant. Both samples contained a moderate amount of colourless to pale orange wedge-shaped titanite. Attempts to date the titanite by U-Pb methods were unsuccessful due to extremely low U concentrations (0.7 to 12.8 ppm). An extremely small amount (16 grains) of colourless, ovoid zircon with good clarity, few colourless rod- and bubble-shaped inclusions, and resorption pits were recovered from sample AX-GC-11. All of these grains were analyzed as a single fraction; this fraction contained a high level of common Pb and yielded a strongly discordant (28%), very imprecise analysis with a $^{207}Pb/^{206}Pb$ age of 172 +/-33 Ma (Table 6.1). The poor quality of this analysis indicates that it should not be used in determining an age for this rock. Although this analysis does not provide useful age information for this rock, the presence of a minor amount of zircon, although apparently partially resorbed, suggests that the other samples of this unit may yield sufficient zircon to determine a U-Pb age.

Hidden Creek area basaltic flows and sedimentary rocks

A moderately foliated, fine-grained volcanic flow of basaltic composition (AX-GC-06) from the sequence which hosts the Hidden Creek orebody was sampled for U-Pb analysis (DDH E2, 78.0-82.6 m) but did not yield minerals suitable for analysis by U-Pb methods.

A fine-grained medium green to white weathering, pale green, siliceous, laminated sedimentary rock which directly overlies massive sulphide mineralization of the Hidden Creek orebody (#1 pit) was also sampled (Plate 6.4). The age(s) of detrital zircon from this unit would

have helped in constraining the minimum age of VMS mineralization at Hidden Creek. However, no zircon or other detrital minerals suitable for analysis by U-Pb methods were recovered.

Lithogeochemistry

Samples processed for U-Pb isotopic analysis were analyzed by X-ray fluorescence at McGill University using glass beads for major elements and pressed pellets for trace elements to determine the chemical composition and magmatic affinity of these rocks (Table 6.2 and Fig. 6.4).

Foliated mafic volcanic and intrusive rocks from the Hidden Creek area have basaltic and gabbroic compositions, respectively. Ratios of Zr/Y of 1.8 to 2.6 are consistent with tholeiitic magmatic affinities, using the limits defined by Barrett and MacLean (1994) (Fig. 6.4). Major and trace element concentrations determined for these samples are consistent with those determined for significantly larger numbers of samples of mafic volcanic and intrusive rocks from this area by Macdonald et al. (1996).

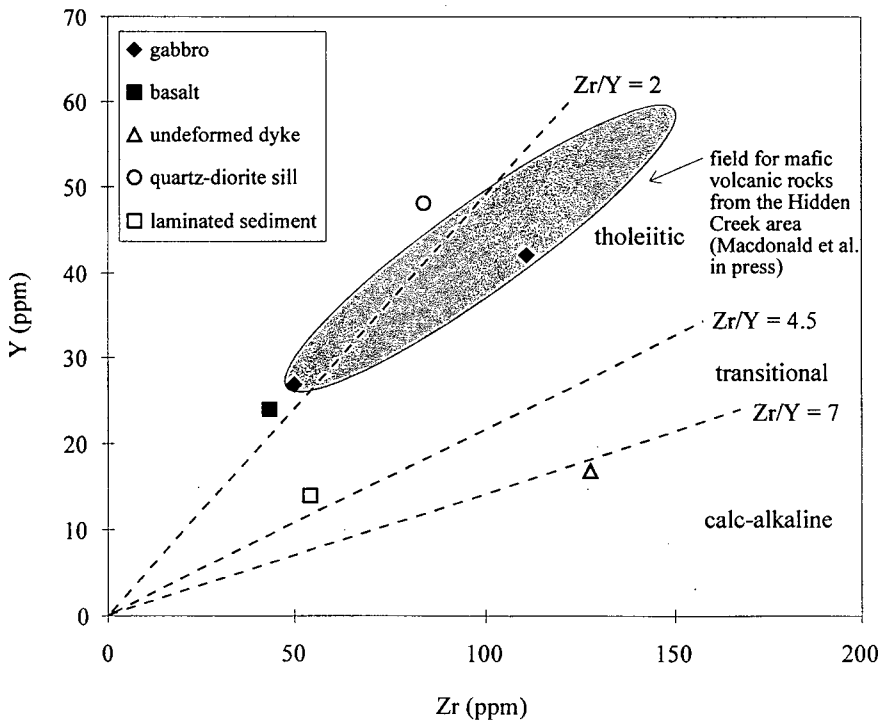

Figure 6. 4 Plot of Y *versus* Zr for rocks from the Anyox pendant (fields from Barrett and MacLean, 1994).

Table 6.2 Major and trace element data for U-Pb samples from the Anyox pendant.

sample number	lithology	SiO2 %	TiO2 %	Al2O3 %	Fe2O3 %	MnO %	MgO %	CaO %	Na2O %	K2O %	P2O5 %	LOI	Total	BaO ppm
AX-GC-01	micro-gabbro	49.17	1.83	16.11	10.74	0.19	5.75	10.01	3.59	0.29	0.19	1.77	99.78	537
AX-GC-05	laminated sediment	85.21	0.15	3.79	4.85	0.03	1.53	0.22	0.90	0.06	0.05	3.82	100.64	>d/l
AX-GC-06	basaltic flow	49.81	0.84	13.76	10.93	0.22	10.40	9.16	2.26	1.47	0.05	1.75	100.87	1112
AX-GC-07	undeformed diorite dyke	45.77	0.74	10.21	18.70	0.15	9.16	5.74	1.90	0.74	0.34	4.24	98.28	832
AX-GC-11	gabbro	46.41	0.94	17.54	10.50	0.19	10.49	10.93	1.78	0.19	0.05	1.72	100.86	10
AX-GC-12	quartz-diorite sill	69.95	0.25	15.01	3.22	0.37	1.93	2.21	2.63	2.58	0.05	1.98	100.32	1028
Detection Limits (ppm):		60.00	35.00	120.00	30.00	30.00	95.00	15.00	75.00	25.00	35.00			17

sample number	Co ppm	Cr2O3 ppm	Cu ppm	Ni ppm	V ppm	Zn ppm	Ga ppm	Nb ppm	Pb ppm	Rb ppm	Sr ppm	Th ppm	U ppm	Y ppm	Zr ppm	Zr/Y
AX-GC-01	63	195	79	58	349	115	15	10	3	2	160	>d/l	>d/l	42	111	2.6
AX-GC-05	>d/l	>d/l	129	>d/l	46	107	6	5	2	2	28	>d/l	7	14	54	3.9
AX-GC-06	50	569	34	152	256	127	12	3	3	46	97	>d/l	11	24	43	1.8
AX-GC-07	146	755	2832	1138	126	177	13	10	11	12	483	6	5	17	128	7.5
AX-GC-11	50	444	35	196	246	151	17	2	2	9	116	n/a	n/a	27	50	1.9
AX-GC-12	17	3	19	3	45	270	16	2	11	31	130	n/a	n/a	48	84	1.8
Detection Limits	10	2	15	3	10	2	1	1	1	1	1	1	1	1	1	

>d/l = below detection limit n/a = not available

The undeformed dyke (AX-GC-07) which cross cuts mafic volcanic rocks in the Hidden Creek area has a gabbroic composition. Although this rock has a lower SiO_2 concentration than the mafic volcanic rocks it intrudes, it is characterized by higher concentrations of high field strength elements (Th, U, Zr) and a Zr/Y ratio of 7.5, the later being consistent with a calc-alkaline magmatic affinity (Fig. 6.4). This more evolved chemical affinity may explain in part why this mafic rock contained abundant euhedral zircon, whereas the foliated mafic volcanic and intrusive rocks discussed above contained almost no recoverable zircon.

The sill of latest Devonian to earliest Mississippian age from Mount Clashmore has a quartz-dioritic composition and a Zr/Y ratio of 1.8, the latter being consistent with a tholeiitic magmatic affinity (Fig. 6.4).

Pb Isotopic Data

The Pb isotopic signature of mineralization can yield information on the degree of evolution of metallogenic sources to mineralization. It can also help constrain the age of mineralization, if suitable Pb isotopic model growth curves or Pb isotopic signatures of mineralization of known ages, which formed within the same tectonic regime, are available (e.g., Alldrick 1991; Childe *this volume*). In this study the Pb isotopic signatures of galena from the Hidden Creek VMS deposit and base $\pm$ precious metal-rich quartz veins form Granby Peninsula are compared with signatures for VMS deposits of known age in Stikinia and the Alexander terrane, as well as clusters defined by Alldrick et al. (1986) and Alldrick (1991) for Early Jurassic and Tertiary mineralization in the Stewart Mining Camp, which lies approximately 60 km north of the Anyox pendant. Analytical results are given in Table 6.3 and shown graphically in Figure 6.5.

Hidden Creek VMS deposit

Galena from the Cu-rich Hidden Creek VMS deposit was sampled for Pb isotopic analysis. Sample A1 contained massive fine- to coarse-grained pyrite cubes with 2% fine-grained galena in 1-2 cm quartz veins, hosted within altered mafic volcanic rocks. Sample A2 consisted of semi-massive fine-grained pyrite with minor (<1%) galena, sphalerite, and chalcopyrite, hosted within carbonate of possible exhalitive origin. Analysis of galena from these samples yielded Pb isotopic ratios of $^{207}Pb/^{206}Pb$ = 0.8310-0.8327, and $^{208}Pb/^{206}Pb$ = 2.042-2.047 (Table 6.3 and Fig.

Table 6. 3 Lead isotopic data for samples from the Anyox pendant, Scotia-Quaal Belt and Forrest Kerr pluton.

SAMPLE NUMBER	SAMPLE LOCATION	SAMPLE DESCRIPTION	MIN[1].	$^{206}Pb/^{204}Pb$ (% error)[2,3]	$^{207}Pb/^{204}Pb$ (% error)[2,3]	$^{208}Pb/^{204}Pb$ (% error)[2,3]	$^{207}Pb/^{206}Pb$ (% error)[2,3]	$^{208}Pb/^{206}Pb$ (% error)[2,3]
ANYOX PENDANT								
A1a	DDH D9 41.8 m. Hidden Creek	quartz-py-gl stringers	gl	18.72 (0.029)	15.58 (0.029)	38.29 (0.036)	0.8326 (0.011)	2.046 (0.017)
A1b	DDH D9 41.8 m. Hidden Creek	quartz-py-gl stringers	gl	18.68 (0.038)	15.55 (0.039)	38.19 (0.041)	0.8325 (0.007)	2.044 (0.009)
A1c	DDH D9 41.8 m. Hidden Creek	quartz-py-gl stringers	gl	18.70 (0.016)	15.57 (0.018)	38.27 (0.021)	0.8327 (0.005)	2.047 (0.008)
A2b	DDH D9 58.2 m. Hidden Creek	py-gl-sph-cp in carbonate	gl	18.78 (0.051)	15.61 (0.051)	38.36 (0.054)	0.8310 (0.011)	2.042 (0.011)
A4a	surface sample Granby Peninsula	quartz vein with sph-py-gl	gl	19.08 (0.011)	15.63 (0.012)	38.62 (0.018)	0.8193 (0.008)	2.024 (0.009)
A4b	surface sample Granby Peninsula	quartz vein with sph-py-gl	gl	19.06 (0.011)	15.62 (0.012)	38.58 (0.018)	0.8194 (0.008)	2.024 (0.009)
A5a	surface sample Granby Peninsula	quartz vein with sph-py-cp-gl	gl	19.04 (0.014)	15.61 (0.016)	38.54 (0.019)	0.8198 (0.005)	2.024 (0.008)
A5b	surface sample Granby Peninsula	quartz vein with sph-py-cp-gl	gl	19.04 (0.019)	15.61 (0.021)	38.54 (0.024)	0.8195 (0.006)	2.024 (0.008)
ECSTALL PROSPECT, SCOTIA-QUAAL BELT								
EL-1a	N lense	coarse gl vein	gl	18.34 (0.013)	15.60 (0.006)	37.93 (0.015)	0.8503 (0.011)	2.068 (0.008)
EL-1c	N lense	coarse gl vein	gl	18.34 (0.013)	15.59 (0.012)	37.92 (0.013)	0.8502 (0.004)	2.067 (0.002)
EL-2a	high Cu-Au float	massive py, trace cp	py	18.34 (0.039)	15.56 (0.026)	37.83 (0.056)	0.8481 (0.029)	2.062 (0.039)
EL-2b	high Cu-Au float	massive py, trace cp	py	18.36 (0.053)	15.58 (0.039)	37.87 (0.074)	0.8486 (0.036)	2.062 (0.051)
EL-3a	high Cu-Au float	massive py, trace cp	py	18.37 (0.013)	15.59 (0.012)	37.84 (0.016)	0.8491 (0.003)	2.066 (0.010)
EL-3b	high Cu-Au float	massive py, trace cp	py	18.36 (0.020)	15.59 (0.017)	37.92 (0.027)	0.8490 (0.010)	2.065 (0.018)
EL-5a	N lense	massive py	py	18.37 (0.030)	15.57 (0.019)	37.81 (0.035)	0.8475 (0.023)	2.058 (0.019)
EL-6a	N lense	massive py	py	18.35 (0.024)	15.60 (0.020)	37.94 (0.027)	0.8502 (0.012)	2.068 (0.013)
EL-6b	N lense	massive py	py	18.35 (0.061)	15.60 (0.056)	37.93 (0.073)	0.8499 (0.024)	2.067 (0.040)
EL-9a	S lense	massive py	py	18.36 (0.029)	15.59 (0.023)	37.92 (0.038)	0.8491 (0.018)	2.065 (0.024)
EL-9b	S lense	massive py	py	18.34 (0.088)	15.59 (0.073)	37.95 (0.117)	0.8502 (0.049)	2.070 (0.077)
EL-10a	S lense	massive py	py	18.35 (0.070)	15.57 (0.053)	37.84 (0.037)	0.8484 (0.047)	2.062 (0.024)
FORREST KERR PLUTON, STIKINE TERRANE								
90JLO-13-9a		diorite	kf	18.40 (0.030)	15.60 (0.030)	38.07 (0.031)	0.8477 (0.007)	2.069 (0.006)
90JLO-13-9b		diorite	kf+pf	18.45 (0.085)	15.60 (0.084)	37.84 (0.085)	0.8457 (0.011)	2.064 (0.006)

Table 6.3 (cont.)

[1] mineral abreviations: gl=galena, py=pyrite, kf=potassium feldspar, pf=plagioclase feldspar.

[2] errors are quoted at the 2ş (95% confidence) level.

[3] values are corrected for instrument fractionation by normalization based on replicate analyses of the NBS-981 standard.

6.5). These values are less evolved than data clusters for either Early Jurassic and Tertiary mineralization in the Stewart Mining Camp. They lie between values determined for the Middle Jurassic Eskay Creek and the Upper Triassic Granduc deposits in Stikinia, and are similar to values determined by Peter (1992) for sulphides from the Upper Triassic Windy Craggy deposit in the Alexander terrane (Fig. 6.5).

Granby Peninsula base +/- precious metal-rich quartz veins

Quartz veins which contain base metal sulphides +/- precious metals are observed to cross cut folded turbiditic sedimentary rocks on Granby Peninsula (Plate 6.5). Galena from two of these veins (samples A4 and A5) yielded Pb isotopic ratios of $^{207}Pb/^{206}Pb$ = 0.8193-0.8198, and $^{208}Pb/^{206}Pb$ = 2.024 (Table 6.3 and Fig. 6.5). These values are significantly more radiogenic than values for galena from the Hidden Creek deposit, and overlap within the cluster defined for Tertiary mineralization in the Stewart Mining Camp.

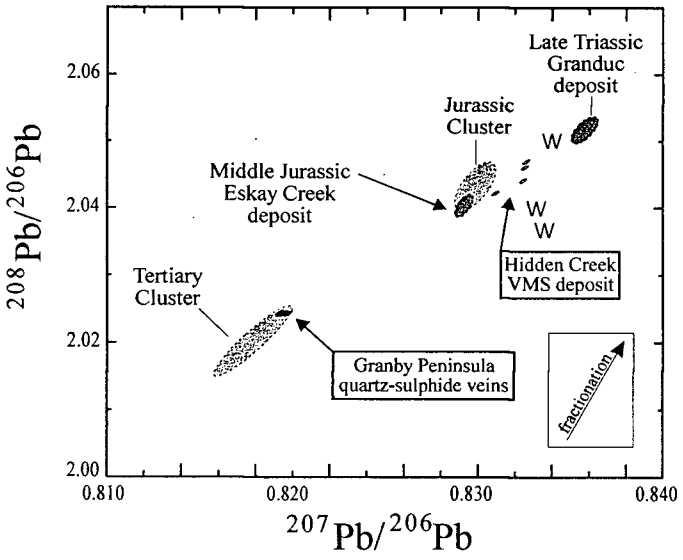

Figure 6. 5 Plot of $^{207}Pb/^{206}Pb$ *versus* $^{208}Pb/^{206}Pb$ for galena from the Anyox pendant, samples from the Hidden Creek VMS deposit are plotted as filled error ellipses, samples from Granby Peninsula quartz-sulphide veins are plotted as unfilled error ellipses. Plotted for comparison are clusters defined for Jurassic and Tertiary mineralization in the Stewart Mining Camp, the Late Triassic Granduc and Middle Jurassic Eskay Creek deposit in the Stikine terrane, and values for the Late Triassic Windy Craggy deposit (W) in the Alexander terrane (Alldrick 1991; Peter 1992; Childe *this volume*; UBC Geochronology Laboratory *unpublished data*).

Discussion

Ages of rocks from the Anyox pendant, east of the cataclasite zone

An undeformed mafic dyke which cross cuts foliated mafic volcanic rocks in the Hidden Creek area in the Anyox pendant yielded an Early Eocene date of 53 +5/-7 Ma. This is consistent with ages determined for rocks from the eastern margin of the Coast Plutonic Complex which surrounds the Anyox pendant, and this suite of unfoliated, calc-alkaline mafic dykes is therefore correlated with rocks of the of the Coast Plutonic Complex. As this age is younger than that determined for sedimentary rocks which overlie mineralization it does not assist in further constraining the age of VMS mineralization at Anyox.

Detrital zircon from turbiditic sedimentary rocks on Granby Peninsula analyzed in this study yielded Early Jurassic U-Pb ages which are approximately 40 Ma older than the sedimentary rocks they are contained within (Fig. 6.2). The large size of the zircons analyzed (length = 400 to 500μ) suggests that they are more likely to have been derived from plutonic, than volcanic sources. These zircons may therefore have been derived in part from rapidly (<40 Ma) uplifted and eroded Early Jurassic plutonic rocks, such as those found in the nearby Stikine terrane (e.g., Alldrick et al. 1986; Friedman and Ash 1997). However, plutons of this age are not unique to Stikinia and occur within other terranes in the Cordillera. Clast lithologies and paleocurrent indicators suggest that sedimentary rocks of the Bowser Lake Group are derived in large part from oceanic rocks of the Cache Creek Group, to the north to northeast (e.g., Eisbacher 1981; Currie 1984), although the presence of felsic volcanic clasts within these sedimentary rocks indicates that some component of the detritus shed into the Bowser Basin was derived from terranes of arc affinity (Ricketts and Parrish 1992).

Isotopic dating of mafic volcanic and chemically similar plutonic rocks at Anyox proved unsuccessful in this study. Ammonites contained within turbidites indicate a Middle Jurassic age for sedimentary rocks on Granby Peninsula (Evinchick and Holm 1997). However, folding, faulting and lack of exposure has hindered efforts to determine if the sedimentary rocks exposed at Granby peninsula represent a continuous sequence with sedimentary rocks which overlie and

host massive sulphide mineralization in the pendant. Such a relationship could support a Jurassic age for mineralization.

Age of rocks from the Anyox pendant, west of the cataclasite zone

A latest Devonian to earliest Mississippian date of 363 +/-3 Ma determined for a quartz diorite sill from Mount Clashmore represents the first radiometric age determination for rocks in the western and central parts of the Anyox pendant. This date indicates that rocks in this portion of the pendant, west of the cataclasite zone, are at least in part of Paleozoic age. Igneous activity of this age is common to the Wrangell, Stikine and Alexander terranes, as well as to the Ecstall pendant, which lies approximately 100 km south of the Anyox pendant (e.g., Gehrels and Saleeby 1987; Juras 1987; Logan et al. 1993; Childe *this volume*), therefore this date alone cannot be used to determine the terrane affiliation of this portion of the pendant. Additional geochronology and geochemistry, combined with mapping and radiogenic isotopic studies may assist in correlation of these rocks with others in the Cordillera.

Pb Isotopic Data

The Pb isotopic signature of galena from the Hidden Creek VMS deposit and quartz-sulphide veins from Granby Peninsula provide an indication of the age of each of these styles of mineralization.

Galena contained within base +/- precious metal-rich quartz veins on Granby Peninsula have a Pb isotopic signature which lies within the cluster defined for Tertiary vein-style and skarn mineralization in the Stewart Mining Camp, directly north of the Anyox pendant, and is significantly more radiogenic than values determined for VMS mineralization at Hidden Creek. These data suggest that these veins are of Tertiary age and are unrelated to, and younger than, VMS mineralization in the Anyox pendant.

The Pb isotopic signatures of galenas from the Hidden Creek deposit are significantly more radiogenic than those of the Late Triassic Granduc deposit, but less radiogenic than those of the Middle Jurassic Eskay Creek deposit, both of which formed within the Stikine terrane. These

data suggest that if VMS mineralization at Anyox formed within the Stikine terrane, it may be of Jurassic rather than Late Triassic age. However, the Pb signature of galena from the Hidden Creek deposit is also similar to that of sulphides from the Late Triassic Windy Craggy deposit in the Alexander terrane, and if the Anyox pendant is part of the Alexander terrane, a Late Triassic age cannot be ruled out for VMS mineralization at Anyox.

Conclusions

Volcanic and sedimentary rocks of the Anyox pendant are cross cut by Early Eocene calc-alkaline mafic dykes, which are correlated with intrusive rocks of the Coast Plutonic Complex. Middle Jurassic turbiditic sedimentary rocks on Granby Peninsula, which have been correlated by Evinchick and Holm (1997) with the Bowser Lake Group, contain 206 to 200 Ma detrital zircons of probable plutonic origin, suggesting that these sedimentary rocks were derived from rapidly uplifted and eroded Early Jurassic plutonic rocks, such as those found in the nearby Stikine terrane.

A latest Devonian to earliest Mississippian date for a quartz-dioritic composition intrusion on Mount Clashmore indicates that rocks in this portion of the pendant are at least in part of Paleozoic age, and therefore significantly older than previously recognized.

Lead isotopic analyses indicate that base +/- precious metal-rich quartz veins on Granby Peninsula, at the eastern edge of the Anyox pendant are of probable Tertiary age. Comparison of the Pb isotopic signature of VMS mineralization at Anyox with those of deposits of known age suggests that if the Anyox pendant is related to the Alexander terrane, mineralization is probably of Triassic age, whereas if the pendant is related to Stikinia, mineralization is more likely of Jurassic age. No single line of evidence conclusively supports a link between the Anyox pendant and Stikinia, but together the correlation of some of the sedimentary rocks in the pendant with the Bowser Lake Group by Wheeler and McFeely (1991), Greig (pers. comm., 1994), and Evinchick and Holm (1997), the presence of Early Jurassic detrital zircon within these sedimentary rocks, and intrusive rocks of comparable age to plutonic rocks in Stikinia in the western part of the pendant support a correlation with Stikinia, and therefore a Jurassic age for VMS mineralization.

Part 2:

U-Pb Geochronology and Pb Isotopic Systematics of the Ecstall prospect, Scotia-Quaal Belt, West-Central British Columbia

Geology of the Scotia-Quaal Belt

The Scotia-Quaal belt is a medium to high grade metamorphic belt which occurs in the Coast Plutonic Complex and is bounded by Late Cretaceous to Eocene plutonic rocks in the Prince Rupert and Douglas Channel map areas (103 J & H) of west-central British Columbia (Figs. 6.1 and 6.6). The belt occurs along the southern extension of the Work Channel lineament, which marks a major Late Paleocene to Early Eocene ductile shear zone in the Coast Plutonic Complex (Gareau, 1991a and b). Recent mapping of the Scotia-Quaal belt, complimented by U-Pb age determinations on the main metaintrusive lithologies by Gareau (1991a and b), has greatly increased the geological database for the Scotia-Quaal belt. However, the terrane affiliation of the belt remains in question.

Gareau (1991b) divided stratified rocks of the Scotia-Quaal belt into four principal units: metavolcanic rocks, metasedimentary rocks, quartzite and layered gneissic rocks. The metavolcanic unit consists of mafic to intermediate composition metavolcanic rocks, interlayered with lesser felsic metavolcanic and metasedimentary rocks (Gareau 1991b). Within the belt metavolcanic rocks are observed to grade into the Late Devonian Big Falls orthogneiss, the volumetrically most significant intrusive lithology in the belt. Gareau (1991b) has postulated that the intervening zone between identifiably plutonic and volcanic rock may mark a transition from cogenetic high-level intrusive to extrusive rock, implying that volcanic rocks in the belt are at least in part of Late Devonian age. In addition to Paleozoic intrusions, two plutonic bodies of Early Jurassic age, the Johnson Lake and the Foch Lake Orthogneisses, intrude the eastern part of the Scotia-Quaal belt (Gareau 1991b) (Fig. 6.6).

The Ecstall prospect, which occurs within the Scotia-Quaal belt, consists of two outcropping *en echelon* lenses of massive pyrite with lesser chalcopyrite and sphalerite, and minor pyrrhotite, marcasite and galena. The two lenses, termed the north and south lenses, have a combined geological reserve of 6.9 Mt, grading 0.6% Cu and 2.5% Zn, with minor Au and Ag (BC MINFILE number 103H/11). Mineralization is hosted within hydrothermally altered metavolcanic and metasedimentary rocks. The Fe-rich massive sulphide bodies are bounded by, and locally interbedded with quartz-sericite-pyrite altered felsic volcanic rocks on one sided, and locally conformable argillaceous metasedimentary rocks on the other (T. Barrett pers. comm. 1995). In proximity to mineralization, metasedimentary rocks are intruded by metamorphosed sills of quartz dioritic composition. In the current study one of these sills was dated by U-Pb methods to constrain a minimum age for VMS mineralization at Ecstall. In addition, the Pb isotopic signatures of sulphides from the Fe-rich north and south lenses, and Cu- and Au-rich boulders on the property were determined to assess the degree of evolution of Pb isotopic sources for mineralization.

Terrane affiliation of the Ecstall deposit

In attempting to relate rocks of the Scotia-Quaal belt with other Cordilleran terranes, Gareau (1991b) suggested that: 1) the belt was not related to either the Alexander or Wrangell terranes; 2) that correlation with rocks of the Stikine terrane could not be ruled out; and 3) that the strongest similarities were with the Nisling terrane. The Nisling terrane has been described as a continental margin assemblage, composed predominantly of quartz-rich metasedimentary rocks, metapelitic rocks and marble (Currie 1994). However, the abundance of metavolcanic rocks, and relative scarcity of quartzite and thick carbonate sequences within the Scotia-Quaal belt suggest an affiliation with the island arc Stikine terrane rather than the Nisling terrane (L. Currie, pers. comm., 1995). Early Jurassic intrusive rocks from the Scotia-Quaal belt are similar in age and composition to intrusive rocks in the Stikine terrane, and support a common tectonic history between the Scotia-Quaal belt and Stikine terrane from the Jurassic onwards (Gareau, 1991b).

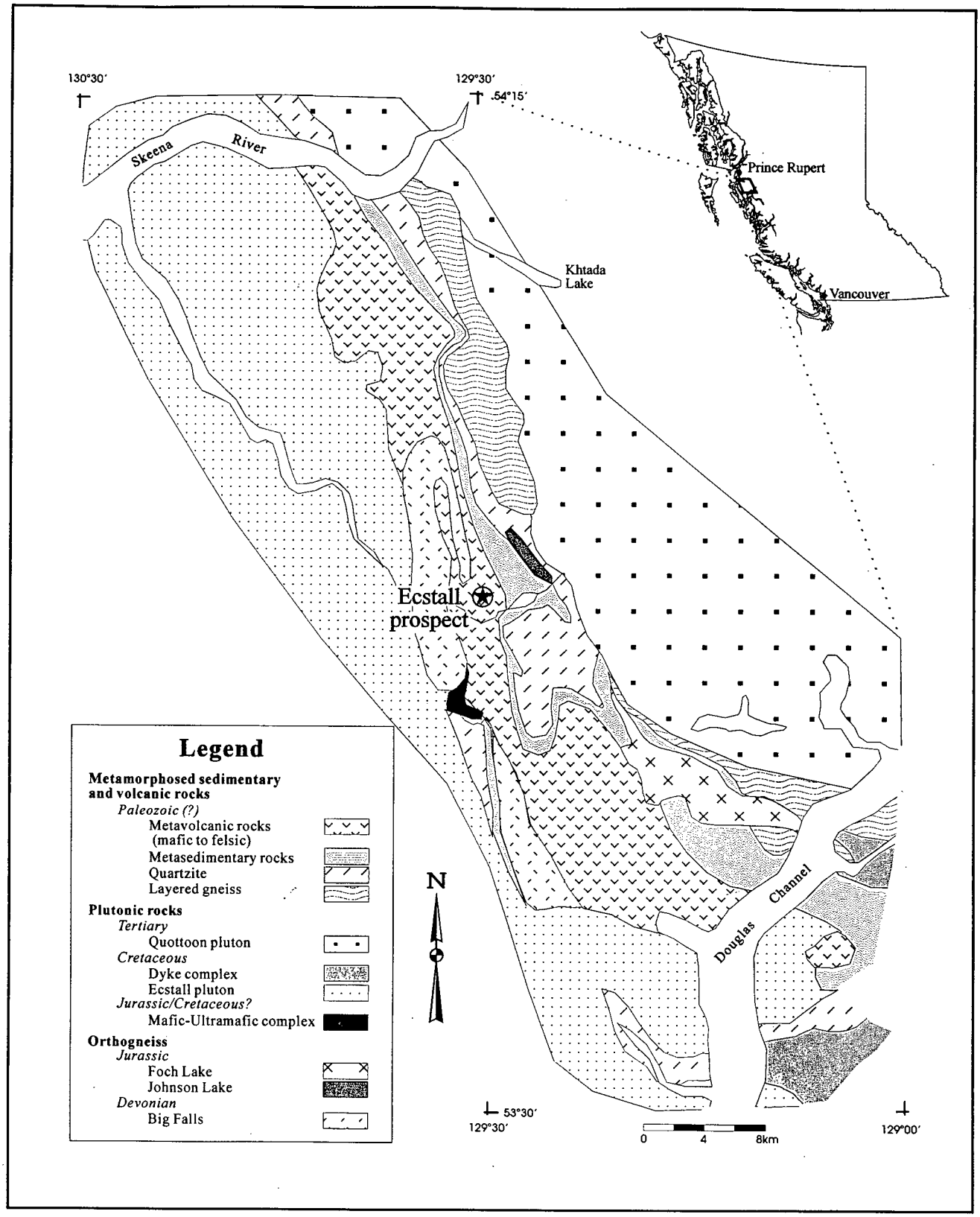

Figure 6. 6 Simplified geological map of the Scotia-Quaal belt (after Gareau 1991b).

U-Pb Geochronology

The U-Pb results reported here are based on the analysis of zircons recovered from a sample collected from outcrop by Drs. T. Barrett and R. Sherlock of the Mineral Deposit Research Unit; the sample description is given below. Analytical techniques are outline in Part I of this chapter; analytical results are given in Table 6.1 and shown graphically in Figure 6.7.

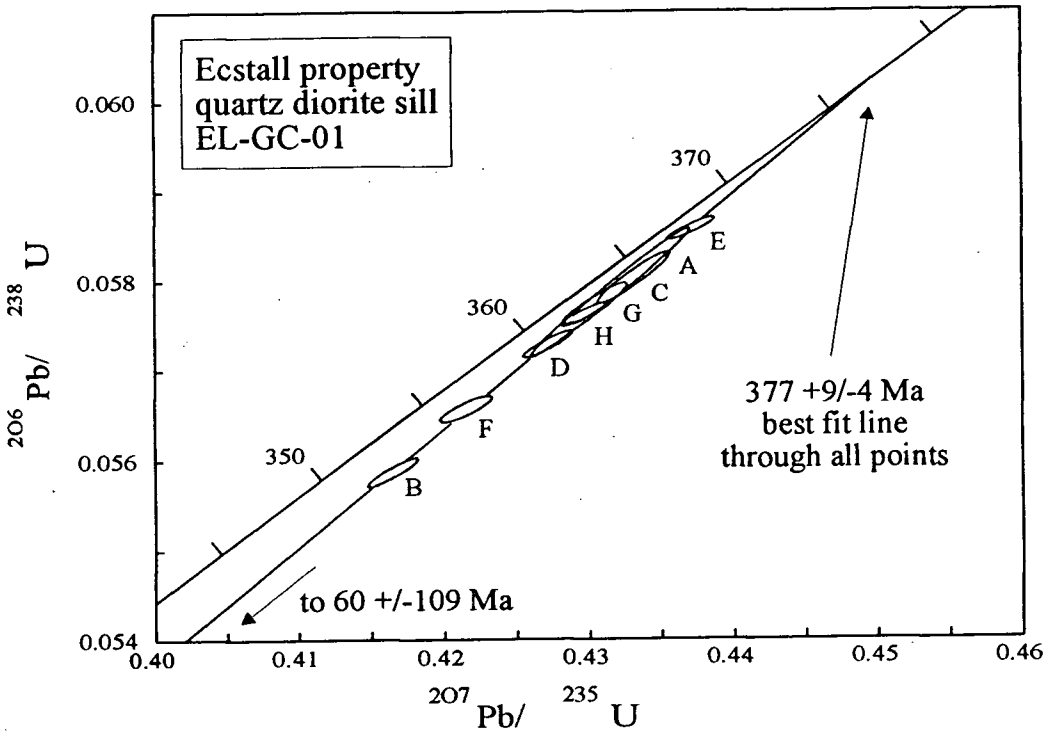

Figure 6. 7 U-Pb concordia diagram for a quartz diorite sill from the Ecstall prospect, Scotia-Quaal belt.

Ecstall prospect quart diorite sill

Abundant high-quality zircon was recovered by standard heavy mineral separation procedures from a coarse-grained metamorphosed sill of quartz dioritic composition in the structural footwall of the Ecstall deposit (EL-GC-01). Analysis of eight fractions of zircon from this rock yielded $^{207}Pb/^{206}Pb$ ages of 373 to 377 Ma (Table 6.1). Despite strong abrasion all zircon fractions were slightly discordant (2-6%), probably as a result of post-crystallization Pb-loss. The weighted mean of the $^{207}Pb/^{206}Pb$ ages of all eight fractions from this unit is 375 +/-1 Ma. However, a more conservative estimate of the age is obtained from a best fit line through the

eight points, which yields an upper intercept age of 377 +9/-4 Ma and a poorly constrained lower intercept age of 60 +/-109 Ma (Fig. 6.7); the 377 +9/-4 Ma age takes into account the possibility of a non-zero (up to 169 Ma) age perturbation of the zircon from this rock, as was suggested by Gareau (1991b) for Paleozoic rocks in the Scotia-Quaal belt.

Pb Isotopic Data

Sulphide samples collected by Drs. T. Barrett and R. Sherlock from the Ecstall prospect for Pb isotopic analysis consisted of: massive pyrite from various locations within the north and south lenses (EL-5, -6, -9, and -10); a zone of coarse, probably remobilized galena+chalcopyrite within the margin of the north lens (EL-1); and two samples from boulders which are enriched in Cu and Au, relative to the pyritiferous lenses on the property (EL-2, and -3). Sulphides from these samples yielded Pb isotopic ratios of $^{207}Pb/^{206}Pb$ = 0.8475-0.8503, and $^{208}Pb/^{206}Pb$ = 2.058-2.070 (Table 6.3 and Fig. 6.8), indicating a relatively homogeneous Pb isotopic signature for galena and pyrite from the samples.

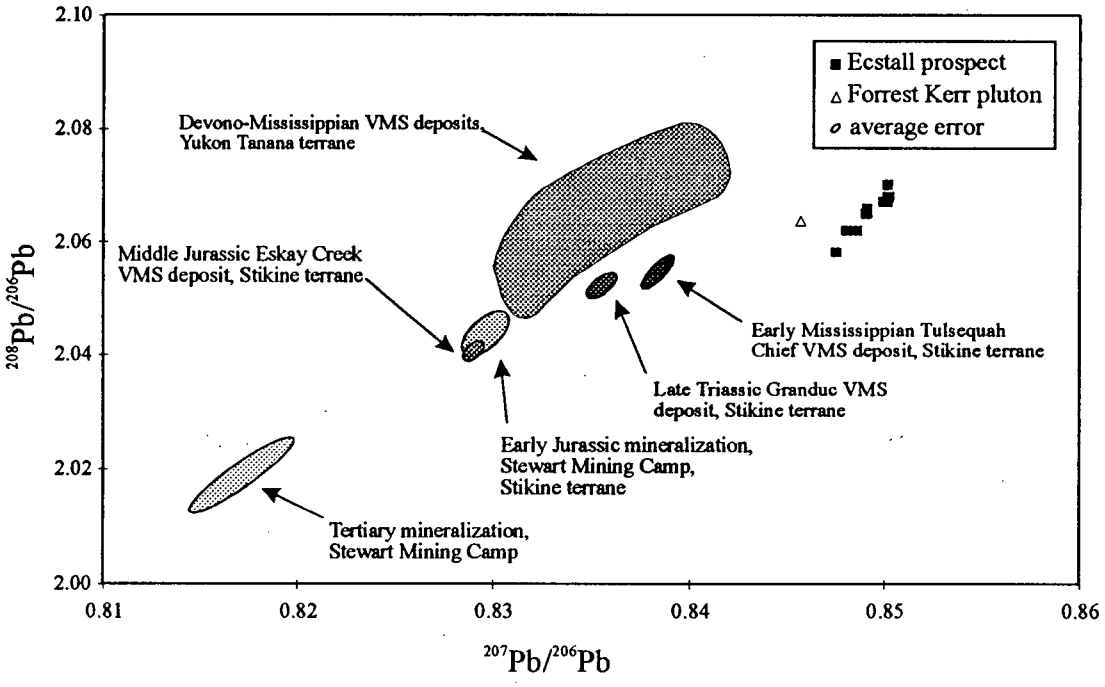

Figure 6. 8 Plot of $^{207}Pb/^{206}Pb$ *versus* $^{208}Pb/^{206}Pb$ for sulphides from the Ecstall prospect, Scotia-Quaal belt. Plotted for comparison are fields for Devono-Mississippian VMS deposits in the Yukon-Tanana terrane, Paleozoic to Mesozoic VMS deposits in the Stikine terrane and Early Jurassic and Tertiary mineralization in the Stewart Mining Camp (Alldrick 1990; Lange et al. 1993; Childe *this volume*)

The Pb isotopic signature of sulphides determined here are compared with those of other mineral occurrences and feldspar from selected intrusions in the Cordillera. These consist of: VMS deposits of known age within the island arc Stikine terrane, which are interpreted to have island arc affinities; the Late Devonian Forrest Kerr pluton, which intrudes stratified rocks of the Stikine Assemblage; and Devono-Mississippian VMS deposits in the Yukon-Tanana terrane, which are interpreted to have a continental arc affinities (Fig. 6.8) (Mortensen 1992; Lange et al. 1993). The Pb isotopic signature of sulphides from the Ecstall prospect is significantly less radiogenic than the signature of the Tulsequah Chief deposit, an Early Mississippian VMS deposit in the northern portion of the Stikine terrane, and the Devono-Mississippian VMS deposits of the Yukon-Tanana terrane. In contrast, the Pb isotopic signature of sulphides from the Ecstall prospect is only slightly more radiogenic than that of feldspars from the Late Devonian Forrest Kerr pluton.

Discussion and Conclusions

Age of VMS mineralization at the Ecstall prospect

In the current study a Late Devonian date of 377 +9/-4 Ma was obtained on a quartz diorite sill which occurs within the structural footwall to mineralization at the Ecstall prospect. This date is within error of a date of 385 +/-4 Ma determined by Gareau (1991b) for the Big Falls orthogneiss, a major lithology within the Scotia-Quaal belt (Fig. 6.6), suggesting a possible correlation between the two units. The date determined in the current study provides a Late Devonian minimum age for VMS mineralization at Ecstall.

Pb isotopic data

A restricted range of Pb isotopic compositions for sulphides from the north and south lenses of the Ecstall prospect and Cu- and Au-enriched boulders on the property suggests that the boulders could have been derived from one of the known sulphide lenses on the property, or an as-yet unidentified, higher grade lens with the same Pb isotopic composition as the known lenses. With this database it is possible to analyze known or newly discovered showings in the area to determine if they could be a potential source of the high Cu-Au boulders.

Implications for the terrane affiliation of the Scotia-Quaal Belt

Based in part on the presence of plutons of Early Jurassic age in the Scotia-Quaal belt, Gareau (1991b) has suggested that the Scotia-Quaal belt and the Stikine terrane share a common post-Early Jurassic history. However, recent mapping and U-Pb age determinations by Brown et al. (1991), Logan and Drobe (1993), and Logan et al. (1993) in the Iskut River and Telegraph Creek map areas (NTS 104B and G) indicates that lithologically similar rocks, of comparable age to those of the Scotia-Quaal belt occur in the Stikine terrane. The possibility of a correlation between Paleozoic rocks of the Stikine terrane and the Scotia-Quaal belt is investigated in the following section.

Part 3:

Tectonic and Metallogenic Implications of Paleozoic U-Pb dates from the Anyox Pendant and Scotia-Quaal Belt

Introduction

The Scotia-Quaal metamorphic belt contains metavolcanic and metasedimentary rocks of unknown age. The metavolcanic rocks are cross cut by, and may in part grade into metaintrusive rocks of Middle to Late Devonian age (385 +/-4 to 377 +9/-4 Ma) (Gareau 1991b; Childe *this volume*). The terrane affiliation of the belt has not been established, but Gareau (1991b) suggests that the Scotia-Quaal belt and Stikine terrane share a common post-Early Jurassic history.

The western portion of the Anyox pendant contains metavolcanic and metasedimentary rocks cross cut by intrusions of gabbroic to quartz-dioritic composition (Alldrick et al. 1996; Evinchick and Holm 1997). In the current study, it was determined that intrusive rocks from this region are at least in part of latest Devonian to earliest Mississippian age (363 +/-3 Ma). These rocks are separated from mafic volcanic rocks and sedimentary rocks by a zone of cataclastic to mylonitic granitic rocks (Evinchick and Holm 1997). The sedimentary rocks are in part of Middle Jurassic age and have been correlated with the Middle to Upper Jurassic Bowser Lake Group (Evinchick and Holm 1997). The terrane affiliation of the Anyox pendant has not been established, but correlation of sedimentary rocks in the pendant with the Bowser Lake Group suggests correlation of at least the underlying mafic volcanic rocks in the pendant with the Stikine terrane.

Paleozoic volcanic and sedimentary rocks of the Stikine Assemblage which are intruded by the Forrest Kerr pluton have been mapped in the Iskut River and Telegraph Creek map areas by Brown et al. (1991) and Logan and Drobe (1993). The Forrest Kerr pluton is a large (590 km^2) mafic to felsic Late Devonian (370 +/-3 Ma; U-Pb zircon) intrusive body within the Iskut River and Telegraph Creek map areas (104B & G) of northwestern British Columbia (Logan et al.

1993). The pluton and adjacent mafic and felsic volcanic rocks have been interpreted by Logan et al. (1993) to represent a Devonian volcano-plutonic complex within the Paleozoic Stikine Assemblage.

The Forrest Kerr pluton and surrounding volcanic strata, the western portion of the Anyox pendant and the Scotia-Quaal belt form a near-linear, north-northeast trending array of Paleozoic volcanic and intrusive rocks which stretches from the Stikine terrane at Forrest Kerr into the Coast Plutonic Complex (Fig. 6.1). There is a conspicuous similarity between the lithologies and ages of Paleozoic rocks of the Stikine terrane around Forrest Kerr, and those of the Scotia-Quaal belt. Rocks of the western Anyox pendant have yet to be mapped in detail, but it has been determined in this study that the area contains intrusive rocks of comparable age to the Forrest Kerr pluton and Scotia-Quaal belt. Metamorphic grade and degree of deformation increases from the Forrest Kerr pluton, to the western Anyox pendant, to the Scotia-Quaal belt, that is, metamorphism and deformation increase away from rocks known to be part of the Stikine terrane, to pendants or belts totally encompassed by the Coast Plutonic Complex.

To further investigate a possible correlation between the Scotia-Quaal belt and the Stikine terrane the Pb isotopic composition of feldspars from the Forrest Kerr pluton was determined to obtain an estimate of the Pb isotopic signature of magmatic rocks in this portion of the Stikine terrane during Devonian time.

Pb Isotopic Data

Forrest Kerr pluton

Two samples of feldspar from a granodioritic phase of the Forrest Kerr pluton were analyzed. Fraction A consisted of pure unaltered potassium feldspar, and fraction B of intergrown unaltered potassium and plagioclase feldspar. Analytical procedures are presented in Appendix 1; analytical results are given in Table 6.3 and shown graphically in Fig. 6.8.

The Pb isotopic values for the two fractions vary slightly (Table 6.3); as Pb in plagioclase feldspar is more susceptible than Pb in potassium feldspar to perturbation due to alteration or low

grade metamorphism, the result from fraction A is considered to be a more reliable estimate of the initial Pb isotopic composition of the Forrest Kerr pluton.

Discussion

Pb isotopic data

The Pb isotopic composition of potassium feldspar from the Forrest Kerr pluton is slightly more evolved than that of Ecstall mineralization. These data are permissive with formation of the Scotia-Quaal belt as part of the Stikine terrane, and mineralization at the Ecstall deposit being slightly older than the Forrest Kerr pluton.

Tectonic and metallogenic implications

The similarities in ages and lithologies of volcano-plutonic rocks of the Stikine terrane around the Forrest Kerr pluton, in the western portion of the Anyox Pendant, and in the Scotia-Quaal belt suggests that these three regions may represent a Paleozoic volcano-plutonic complex which formed as part of the Stikine terrane. The Scotia-Quaal belt contains Late Devonian or older VMS mineralization at the Ecstall prospect. A correlation between these rocks and those of the western Anyox pendant and Stikine terrane would suggest that Late Devonian or older volcanic strata in these regions have exploration potential for VMS mineralization.

The validity of this tentative correlation could be further investigated by obtaining trace and rare earth element data, and Nd and Pb isotopic data for rocks from the three regions, as well as by further mapping and U-Pb dating of rocks in the western Anyox pendant.

References

Alldrick, D.J. 1986a. Stratigraphy and structure in the Anyox area (103P/5), British Columbia Ministry of Energy, Mines and Petroleum Resources, Paper 1986-1, pp. 211-216.

Alldrick, D.J. 1986b. Geology of the Anyox area, British Columbia Ministry of Energy, Mines and Petroleum Resources, Property File Map, Scale 1:50,000.

Alldrick, D.J. Mortensen, J.K. and Armstrong, R.L. 1986. U-Pb age determinations in the Stewart area. *In* British Columbia Ministry of Energy, Mines and Petroleum Resources, Geological Fieldwork, *Edited by* B. Grant and M. Newell, Paper 1986-1, pp. 217-218.

Alldrick, D.J. 1991. Geology and Ore Deposits of the Stewart Mining Camp; Ph.D. thesis, University of British Columbia, Vancouver, 417p.

Alldrick, D.J., Gabites, J.E., and Godwin, C.I. 1987. Lead Isotope Data from the Stewart Mining Camp (104B/I). *In* Geological Fieldwork 1986, British Columbia Ministry of Energy, Mines and Petroleum Resources, Paper 1987-1, pp. 93-102.

Alldrick, D.J., Mawani, Z.M.S., Mortensen, J.K., and Childe, F. 1996. Mineral deposit studies in the Stewart district (NTS 103O/P and 104A/B). *In* Exploration in British Columbia, British Columbia Ministry of Employment and Investment.

Barrett, T.J., and MacLean, W.H. 1994. Chemostratigraphy and hydrothermal alteration in exploration for VHMS deposits in greenstones and younger volcanic rocks. *In* Alteration and Alteration Processes associated with Ore-forming Systems: Geological Association of Canada, Short Course Notes. *Edited by* D.R. Lentz, **11**: 433-467.

Brown, D.A., Logan , J.M., Gunning, M.H., Orchard, M.J., and Bamber, W.E. 1991. Stratigraphic evolution of the Paleozoic Stikine Assemblage in the Stikine and Iskut River area, Northwestern British Columbia. Canadian Journal of Earth Sciences, **28**: 958-972.

Currie, L.D. 1984. The provenance of chert clasts in the Ashman conglomerates of the northeastern Bowser Basin. B.Sc. thesis, Queens University, Kingston, 59 p.

Currie, L.D. 1994. The geology and mid-Jurassic amalgamation of Tracey Arm terrane and Stikinia of northwestern British Columbia. Ph.D. thesis, Carleton University, Ottawa, 385 p.

Eisbacher, G.H. 1981. Late Mesozoic-Paleogene Bowser Basin molasse and Cordilleran tectonics, western Canada. *In* Sedimentation and Tectonics in Alluvial Basins, *Edited by* A.D. Miall, Geological Association of Canada, Special Paper 23, p. 125-151.

Evinchick, C.A. and Holm, K. 1997. Bedrock geology of the Anyox pendant and surrounding areas, Observatory Inlet (103P/5) and parts of Hasting Arm (103P/12) and 103O/9 map areas, British Columbia. *In* Current Research 1997-A, Geological Survey of Canada, pp. 11-20.

Evinchick, C.A. Alldrick, D.J., Currie, L.D., Haggart, J.W., McCuaig, S., McNicoll, V., and Woodsworth, G.J. 1997. Status of research in the Nass River multidisiplinary geoscience project, British Columbia. *In* Current Research 1997-A, Geological Survey of Canada, pp.21-30.

Friedman, R.M. and Ash, C.H. 1997. U-Pb age of intrusions related to porphyry Cu-Au mineralization in the Tatoga Lake area, northwestern British Columbia. *In* British Columbia Ministry of Employment and Investment, Geological Fieldwork, B. Grant, Editor, Paper 1997-1.

Gareau, S.A. 1991a. Geology of the Scotia-Quaal Metamorphic Belt, Coast Plutonic Complex, British Columbia. Geological Survey of Canada, Open File 2337.

Gareau, S.A. 1991b. Geology of the Scotia-Quaal Metamorphic Belt, Coast Plutonic Complex, British Columbia. Ph.D. thesis, Carleton University, Ottawa, 380p.

Gehrels, G.E. and Saleeby, J.B. 1987. Geologic framework, tectonic evolution, and displacement history of the Alexander terrane. Tectonics, **6**: 151-173.

Gehrels, G.E., Dickinson, W.R., Ross, G.M., Stewart, J.H. and Howell, D.G. 1995. Detrital zircon reference for Cambrian to Triassic miogeoclinal strata of western North America. Geology, **23**: 831-834.

Goutier, J., Marcotte, C., and Wares, R. 1990. Deformation of the Anyox massive sulphide deposit, British Columbia. Geological Association of Canada, Program with Abstracts, p. A-50.

Grove, E.W. 1986. Geology and mineral deposits of the Unuk River-Salmon River-Anyox area; British Columbia Ministry of Energy, Mines and Petroleum Resources, Bulletin 63, 152 p.

Harland, W.B., Armstrong, R.L., Cox, A.V., Craig, L.E., Smith, A.G., and Smith, D.G. 1990. A Geological Time Scale, 1989, Cambridge University Press, Cambridge, 263 p.

Heaman, L. and Parrish, R. 1991. U-Pb geochronology of accessory minerals. *In* Mineralogical Association of Canada Short Course Handbook on Applications of Radiogenic Isotope Systems to Problems in Geology. *Edited by* L. Heaman and J.N. Ludden, pp. 59-102.

Höy, T. 1991. Volcanogenic Massive Sulphide Deposits in British Columbia: in Ore Deposits, Tectonics and metallogeny in the Canadian Cordillera. British Columbia Ministry of Mines and Petroleum Resources, Paper 1991-4, pp. 89-123.

Juras, S.J. 1987. Geology of the polymetallic volcanogenic Buttle Lake Camp, with emphasis on the Price Hillside, Central Vancouver Island, British Columbia, Canada; Ph.D. thesis, University of British Columbia, Vancouver, 279 p.

Krogh, T.E. 1982. Improved accuracy of U-Pb zircon ages by the creation of more concordant systems using an air abrasion technique. Geochemica and Cosmochemica Acta, **46**: 637-649.

Lange, I.M., Nockelburg, W.J., Newkirk, S.R., Aleinikoff, J.N., Church, S.E., and Krouse, H.R., 1993. Devonian volcanogenic massive sulphide deposits and occurrences, southern Yukon-Tanana terrane, eastern Alaska range, Alaska. Economic Geology, **88**: 344-376.

Logan, J.M., and Drobe, R. 1993. Geology and mineral occurrences of the Mess Lake area (104G/7W). *In* Geological Fieldwork 1992, *Edited by* B. Grant and J.M. Newell, British Columbia Ministry of Energy, Mines and Petroleum Resources, Paper 1993-1, pp. 135-148.

Logan, J.M., Drobe, R., McClelland, W.C., and Anderson, R.G. 1993. Devonian intraoceanic arc magmatism in northwestern Stikinia. Geological Association of Canada - Mineralogical Association of Canada Annual Meeting, Program with Abstracts, p. A-60.

Ludwig, K.R. 1980. Calculation of uncertainties of U-Pb isotope data. Earth and Planetary Science Letters, **46**: 212-220.

Macdonald, R.W.J., Barrett, T.J., and Sherlock, R.L. 1995. Geological investigations of the Hidden Creek deposit, Anyox, West-central British Columbia (103P/5). *In* Geological Fieldwork 1994, British Columbia Ministry of Energy, Mines and Petroleum Resources, Paper 1987-1, *Edited by* B. Grant and J.M. Newell, pages 93-102

Macdonald, R.W.J., Barrett, T.J., and Sherlock, R.L. 1996. Geochemistry and lithogeochemistry of the Hidden Creek deposit, Anyox, West-Central British Columbia. Exploration and Mining Geology.

Mortensen, J.K., 1992. Pre-mid-Mesozoic tectonic evolution of the Yukon-Tanana terrane, Yukon and Alaska, Tectonics, v. 11, p. 836-853.

Mortensen, J.K., Ghosh, D.K., and Ferri, P. 1995. U-Pb geochronology of intrusive rocks associated with Cu-Au deposits in the Canadian Cordillera. *In* Porphyry Deposits in the Northwestern Cordillera of North America. *Edited by* T.G. Schroter. **G-2**: 491-531.

Peter, J.M. 1992. Comparative Geochemical Studies of the Upper Triassic Windy Craggy and Modern Guaymas Basin Deposits: A contribution to the understanding of massive sulphide formation in volcano-sedimentary environments. Ph.D. thesis, University of Toronto, Toronto, 235 p.

Ricketts, B.D. and Parrish, R.R. 1992. Age and provenance of felsic clasts in Bowser Basin, northern British Columbia. *In* Radiogenic Age and Isotopic Studies: Report 6, Geological Survey of Canada, Paper 92-2, p. 141-144.

Sharp, R.J. 1980. The geology, geochemistry, and sulfur isotopes of the Anyox massive sulphide deposits, M.Sc. thesis, University of Alberta, Edmonton, 211 p.

Smith, A.D. 1993. Geochemistry and tectonic setting of volcanics from the Anyox mining camp, British Columbia. Canadian Journal of Earth Sciences, **30:** 48-59.

Steiger, R.H., and Jäger, E. 1977. Subcommission on geochronology: Convention on the use of decay constants in geo- and cosmochronology. Earth and Planetary Science Letters, **14**: 359-362.

Wheeler, J.O. and McFeely, P. 1991. Tectonic assemblage map of the Canadian Cordillera, and adjacent parts of the United States of America. Geological Survey of Canada Map 1712A.

York, D. 1969. Least-squares fit of a straight line with correlated errors. Earth and Planetary Science Letters, **5**: 320-324.

Plate 6. 2 Turbiditic sedimentary rocks on Granby Peninsula, fining upwards from fine sandstone bases to inter-turbidite mudstone tops (AX-GC-04 from sandstone base) .

Plate 6. 3 Pale green to white quartz diorite sill (AX-GC-12) cross-cut by dark green gabbro dykes, Mount Clashmore (photo by R. Macdonald) (hammer for scale).

Plate 6. 4 Pale green to white weathering, finely laminated, siliceous sedimentary rocks of possible partial exhalitive origin (AX-GC-05), directly above #1 pit, Hidden Creek Mine.

Plate 6. 5 Turbiditic sedimentary rocks on Granby Peninsula cross-cut by base ±precious metal-rich quartz veins (A4 and A5).

Plate 6.2

Plate 6.3

Plate 6.4

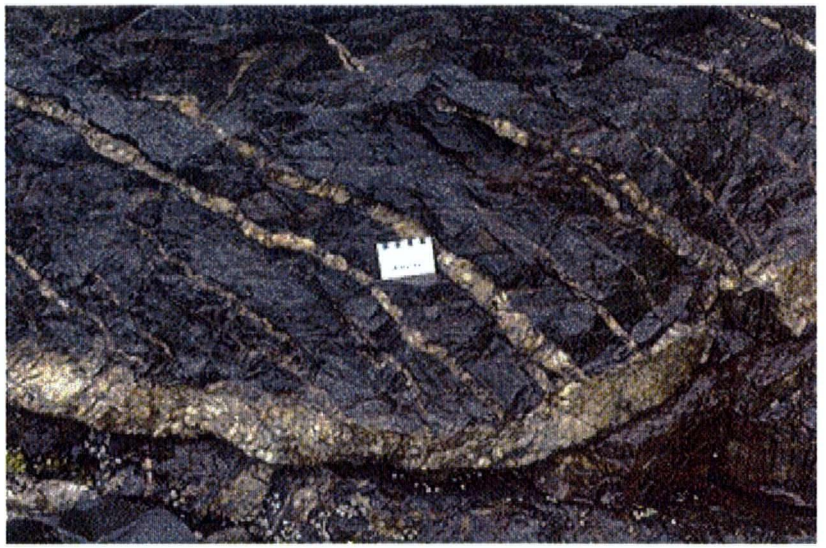

Plate 6.5

CHAPTER 7

AGE AND RADIOGENIC ISOTOPIC CHARACTERISTICS OF VMS MINERALIZATION IN ALLOCHTHONOUS TERRANES OF THE NORTH AMERICAN CORDILLERA IN BRITISH COLUMBIA

Introduction

Volcanogenic massive sulphide (VMS) deposits are an important source of base and precious metals in British Columbia, and elsewhere in Canada, producing copper, zinc, lead, silver, and gold, and at some deposits by-products such as cadmium and cobalt (Höy 1991; Franklin 1996). In 1988, 33% of the Cu, 56% of the Zn, 29% of the Pb, 3.6% of the Au, and 30% of the Ag produced in Canada was obtained through the mining of VMS deposits (Franklin 1996).

Volcanogenic massive sulphide deposits are part of a larger group of mineral deposits termed concordant massive sulphide deposits (Lydon 1988). Although VMS deposits include a range of ore mineralogies and host lithologies, these deposits share a number of features which distinguish them from other concordant massive sulphide deposits, including an association with subaqueous volcanic and/or sedimentary rocks and formation at plate boundaries (Franklin 1996). Other features which are commonly observed are the presence of discordant alteration pipes below the massive sulphide, which rarely extend for significant distances into the hangingwall to mineralization, as well as faults of interpreted syn-depositional origin which may have acted as fluid conduits, an association with chemical sedimentary rocks of interpreted exhalative origin, and intrusive bodies which may have acted as a heat source to drive the hydrothermal system (Lydon 1988; Franklin 1996).

Worldwide, VMS deposits span an age range from Archean to present (i.e., Lydon 1988; Franklin 1996). In the allochthonous terranes of British Columbia and adjacent parts of southeast Alaska the known age range of VMS mineralization coincides with the age range of subaqueous volcanism, and extends from latest Precambrian to Cretaceous (Table 7.1). However, this age

range can be extended to the present, if sub-seafloor magmatism and massive sulphide mineralization currently forming at Middle Valley on the Juan de Fuca Ridge is included.

This chapter discusses and presents:

- an overview of the regional tectonic setting of allochthonous terranes in the Cordillera which host VMS deposits,
- the classification scheme for VMS mineralization in the Cordillera used here,
- age, host lithologies, metal suite, and geochemical affinity of several significant VMS deposits in British Columbia, and their currently interpreted tectonic settings, and
- a comparison of the Pb and Nd isotopic signatures of mineralization and host rocks for the deposits discussed here, contrasted against each other and the age of mineralization, to assess the degree of evolution of magmatic and metallogenic sources associated with VMS mineralization.

Regional Tectonic Setting

Rocks within the Canadian portion of the North American Cordillera have been divided into five morphogeological belts. From east to west these are the Foreland, Omineca, Intermontane, Coast, and Insular Belts (Gabrielse et al. 1991). The Intermontane and Insular Belts consist largely of terranes of uncertain affinity to ancestral North America. These belts are separated from each other by the Coast Belt, which is composed mainly of Cretaceous to Tertiary age granitic and metamorphic rocks of the Coast Plutonic Complex. The Coast Plutonic Complex is interpreted to have formed in response to long lived subduction and/or accretion of rocks which comprise the Insular Belt (Gabrielse et al. 1991). However, the Coast Belt also contains belts and pendants of pre-Cretaceous age and undetermined terrane affiliation, some of which host VMS mineralization.

Stikinia represents the largest terrane in the Intermontane Belt. It comprises arc assemblages of the Paleozoic Stikine Assemblage, Upper Triassic Stuhini Group, and Lower to Middle Jurassic Hazelton Group, all of which host VMS mineralization (Höy 1991; Souther 1991; Childe *this volume*) (Table 7.1). Arc assemblages of similar age and character are found in the Insular belt; these consist of the Alexander terrane in the north and Wrangellia in the south (Fig.

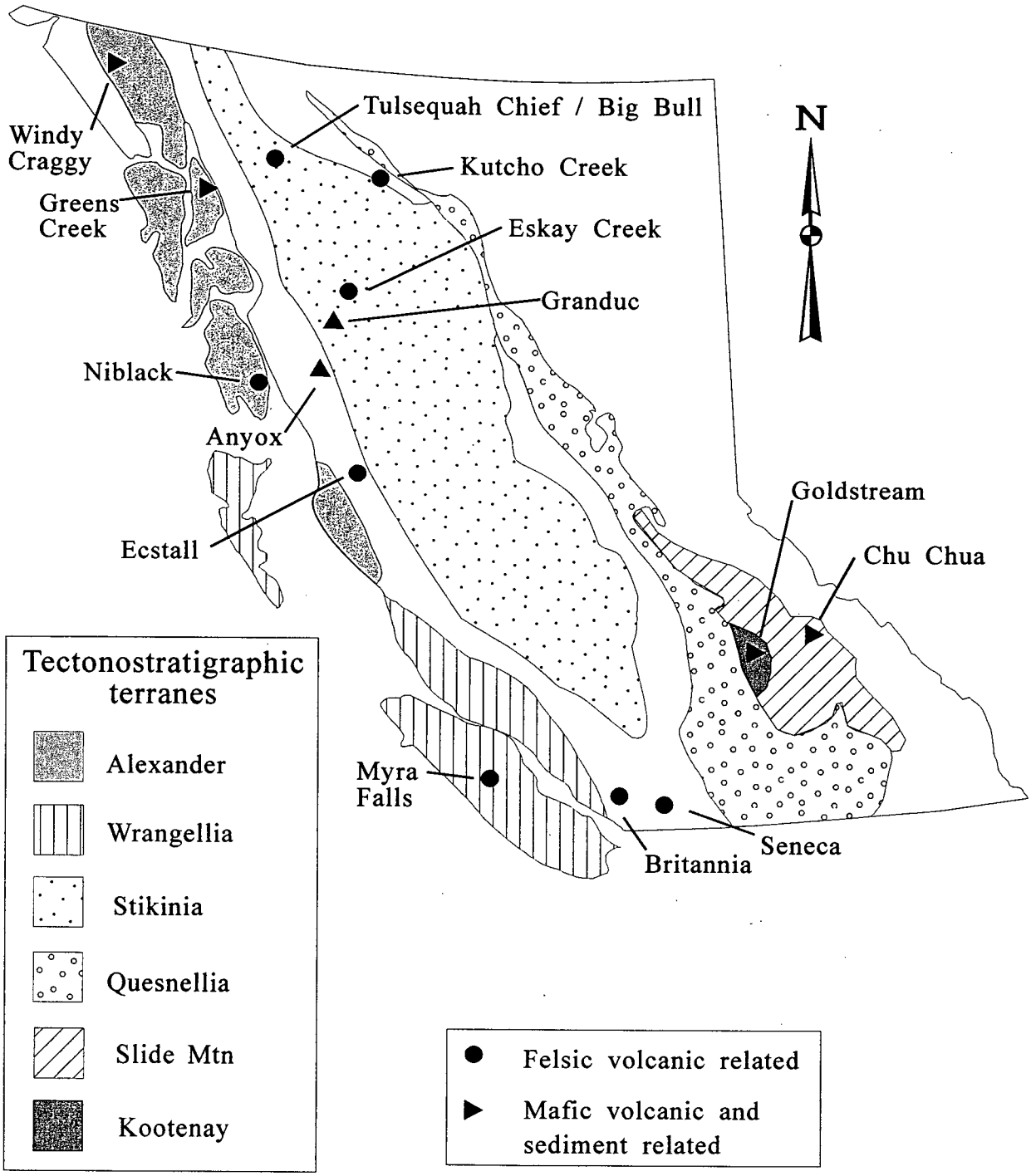

Figure 7. 1 Volcanogenic massive sulphide deposits and developed prospects in British Columbia and southeastern Alaska.

7.1). Both of these terranes, which are thought to share a common post-Pennsylvanian tectonic history, host VMS mineralization (Gardner et al. 1988; Höy 1991) (Table 7.1). This study examines and contrasts VMS deposits of different ages which occur in Stikinia, as well as deposits in other terranes, which were previously thought to be of similar age to deposits in Stikinia.

Classification

A number of different classification schemes have been proposed for grouping the wide range of styles of mineralization, host lithologies, and interpreted tectonic settings of VMS deposits. Sawkins (1976) suggested a threefold classification of such deposits based mainly on tectonic setting and host lithology; the three types proposed were Kuroko-, Besshi-, and Cyprus-type deposits. Franklin et al. (1981) subsequently proposed a classification scheme based on metal content, recognizing two groups: Cu-Zn and Zn-Pb-Cu. Höy (1991) refined these classification schemes for VMS deposits in British Columbia to include both tectonic and metal associations. Höy (1991) proposed three categories: Cu-Zn Cyprus-type, Cu-Zn Besshi-type, and Zn-Pb-Cu (+/-Au, Ag) Kuroko-type. However, based on either metal content or tectonic setting, a number of VMS deposits in British Columbia cannot clearly be assigned to any of these categories. Therefore a classification scheme based on those proposed by Thompson et al. (1994) and Sherlock et al. (1996) is adopted here. The twofold subdivision adopted here, in which deposits are grouped by host lithology, without reference to tectonic setting or metal content, are mafic volcanic and sediment-related, and felsic volcanic-related deposits (Table 7.1).

Mafic volcanic & sediment-related deposits

Deposits of this class in the Canadian Cordillera include Windy Craggy in the Alexander terrane, Granduc in Stikinia, and Anyox, which lies within a roof pendant in the Coast Plutonic Complex (Table 7.1 and Fig. 7.1). Host lithologies for these deposits consist of mafic volcanic rocks, typically cross cut by contemporaneous and probably comagmatic dykes and sills, and overlain or underlain by clastic +/- chemical sedimentary rocks, with lesser mafic volcanic rocks. The majority of these deposits have a simple sulphide mineralogy and metal suite, characterized by Cu+/-Zn. However, the world class Windy Craggy deposit also contains significant Co (MacIntyre 1986). The polymetallic Greens Creek deposit, in southeast Alaska may also belong

to this group, but the chemical composition of igneous host rocks has not been well established, and the deposit is unusually rich in precious metals compared to VMS deposits typically associated with mafic rocks (Newberry et al. 1990).

Deposit/Prospect	Primary Commodities	Terrane	Host Lithologies	Age	ε_{Nd} (initial)
Britannia	Zn-Pb-Cu	Harrison (?)[9]	felsic volcanic	Cretaceous[9]	
Seneca	Zn-Pb-Cu	Harrison[7] (Wrangellia)	felsic volcanic	Middle Jurassic[8]	
Eskay Creek	Au-Ag-Zn-Pb-Cu	Stikinia	felsic volcanic - sediment	Middle Jurassic	+5.5 to +6.9
Anyox	Cu	Stikinia (?)	mafic volcanic - sediment	Early or Middle Jurassic	+7.8 to +8.4[1]
Windy Craggy	Cu-Co	Alexander	mafic volcanic - sediment	Late Triassic[2]	+2.4 to +3.0[3]
Granduc	Cu-Zn	Stikinia	mafic volcanic - sediment	Late Triassic	+6.1 to +6.8
Greens Creek	Zn-Pb-Cu-Ag-Au	Alexander	mafic volcanic - sediment (?)	Late Triassic[4]	
Kutcho Creek	Cu-Zn	unnamed	felsic volcanic	Early Triassic	+7.6 to +7.8
Tulsequah Chief / Big Bull	Zn-Pb-Cu-Ag-Au	Stikinia	felsic volcanic	Late Mississippian	+2.7 to +3.9
Myra Falls	Zn-Pb-Cu-Ag-Au	Wrangellia	felsic volcanic	latest Devonian to earliest Mississippian[5]	
Ecstall	Cu-Zn	Stikinia (?)	felsic volcanic	Late Devonian or older	
Niblac	Zn-Pb-Cu-Ag-Au	Alexander	felsic volcanic	latest Proterozoic[6]	

Table 7. 1 Primary commodities, terrane affiliation, host lithologies, age and ε_{Nd} (initial) values for VMS deposits in allochthonous terranes of the North American Cordillera of British Columbia and southern Alaska ([1] Smith (1993) (calculated for 170 Ma); [2] Orchard (1986); [3] Smith and Fox (1989) (calculated for 220 Ma); [4] Newberry et al. (1990); [5] Juras (1987); [6] Gehrels et al. (1996); [7] Mahoney (1994); [8] Childe (unpublished data); [9] R. Friedman *pers. comm.*).

Granduc deposit

The Granduc deposit, which lies within Stikinia, contains massive to semi-massive Fe- and Cu-rich sulphides, hosted within a strongly deformed package of chemical and clastic sedimentary rocks with minor tuffaceous mafic volcanic rocks (Grove 1986) (Fig. 7.1). This sequence is structurally underlain by mafic volcanic flow rocks of basaltic to basaltic-andesitic composition, with weak hydrothermal alteration and base metal sulphide veining. Mafic volcanic strata are

cross cut by mafic intrusive rocks of dioritic composition, which have an identical isotopic age and similar chemistry to the rocks they intrude (Childe *this volume*). Late Triassic U-Pb isotopic dates for mafic volcanic and plutonic rocks from the volcanic- and sediment-dominated sequences, along with the Pb isotopic signature of mineralization, were used to constrain a Late Triassic age for VMS mineralization, and therefore support a correlation of the host strata with the Stuhini Group. Mafic volcanic rocks of the structural, and interpreted stratigraphic footwall to mineralization and the sediment-dominated sequence which hosts mineralization have predominantly tholeiitic magmatic affinities, but rare earth element (REE) patterns which are slightly enriched relative to normal mid-ocean ridge basalts (N-MORB); the trace and REE chemistry of these rocks is consistent with formation within an oceanic back arc basin or in the primitive, preliminary stages of island arc development (Childe *this volume*).

Anyox deposit

The Anyox deposit, which consists of several discrete massive sulphide deposits, is hosted by volcanic and sedimentary strata of probable Mesozoic age in the Anyox pendant (Alldrick 1986) (Fig. 7.1). The terrane affiliation of the pendant, which is contained within the Coast Plutonic Complex, is unconstrained (Childe *this volume*, and references therein). Copper-rich massive sulphide mineralization at Anyox occurs at, and immediately above and below, the contact between underlying mafic volcanic rocks of basaltic composition and overlying clastic sedimentary rocks (Alldrick 1986; Macdonald et al. 1996b). Chemical sedimentary rocks occur discontinuously along the contact between the overlying clastic sedimentary and underlying mafic volcanic rocks (Alldrick 1986).

Mafic volcanic rocks at Anyox are characterized by tholeiitic magmatic affinities and REE patterns which range from those of N-MORB to enriched mid-ocean ridge basalts (E-MORB); regional data suggest that N-MORB is the prevalent lava type, whereas E-MORB occurs locally and may have a spatial association with mineralization (Macdonald et al. 1996b, and references therein). A mid-ocean ridge setting similar to that found at Middle Valley on the Juan de Fuca Ridge, in which massive sulphide mineralization is forming during the waning stages of mafic volcanism, is proposed for VMS mineralization at Anyox (Macdonald et al. 1996b).

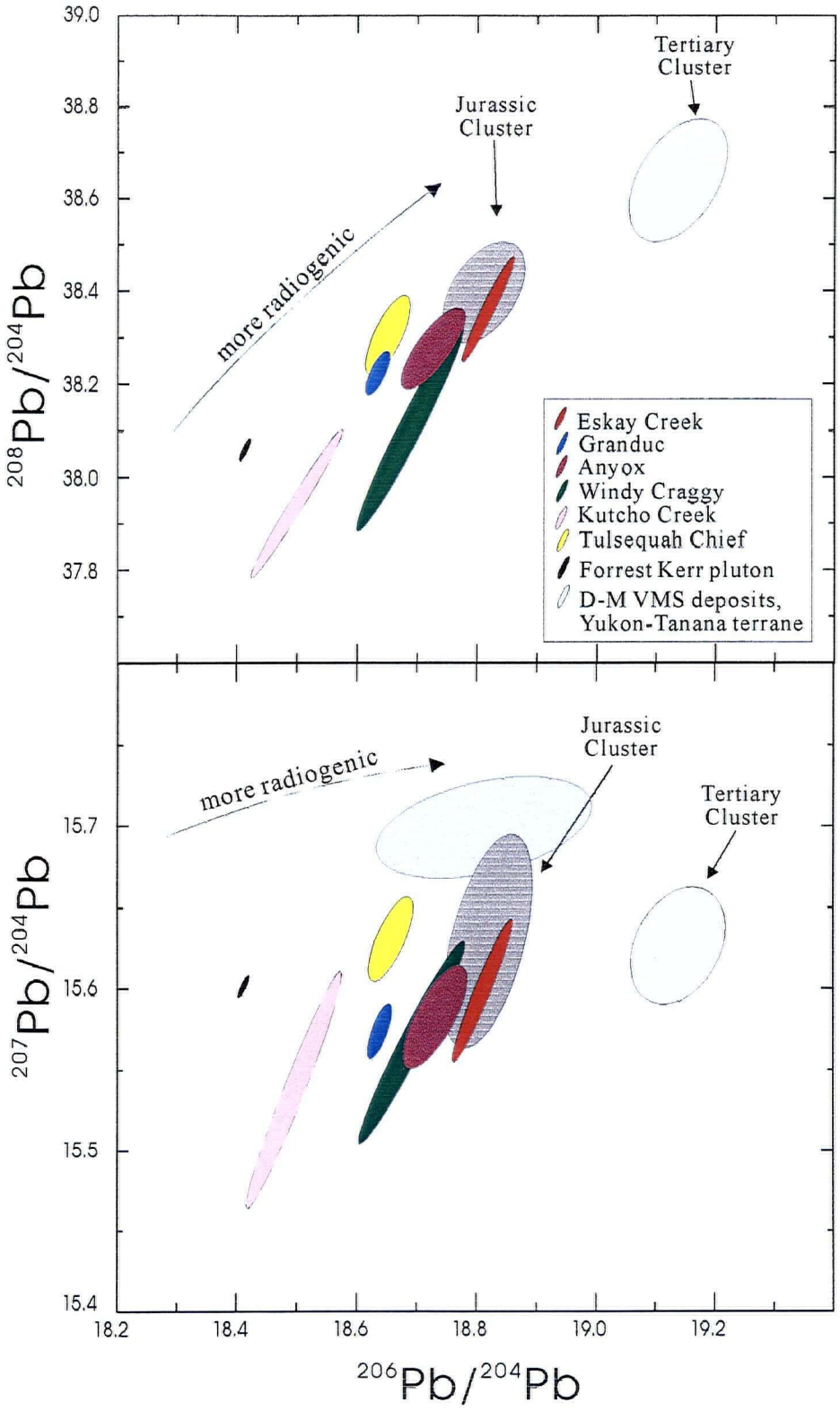

Figure 7.2 Pb-Pb diagrams showing fields for Tertiary and Jurassic mineralization in the Stewart Mining Camp, the Eskay Creek, Granduc, Anyox, Windy Craggy, and Tulsequah Chief deposits, the Forrest Kerr pluton, and Devono-Mississippian VMS deposits in the Yukon-Tanana terrane (data sources from Alldrick 1991; Peter 1992; Lange et al. 1993; Childe this volume).

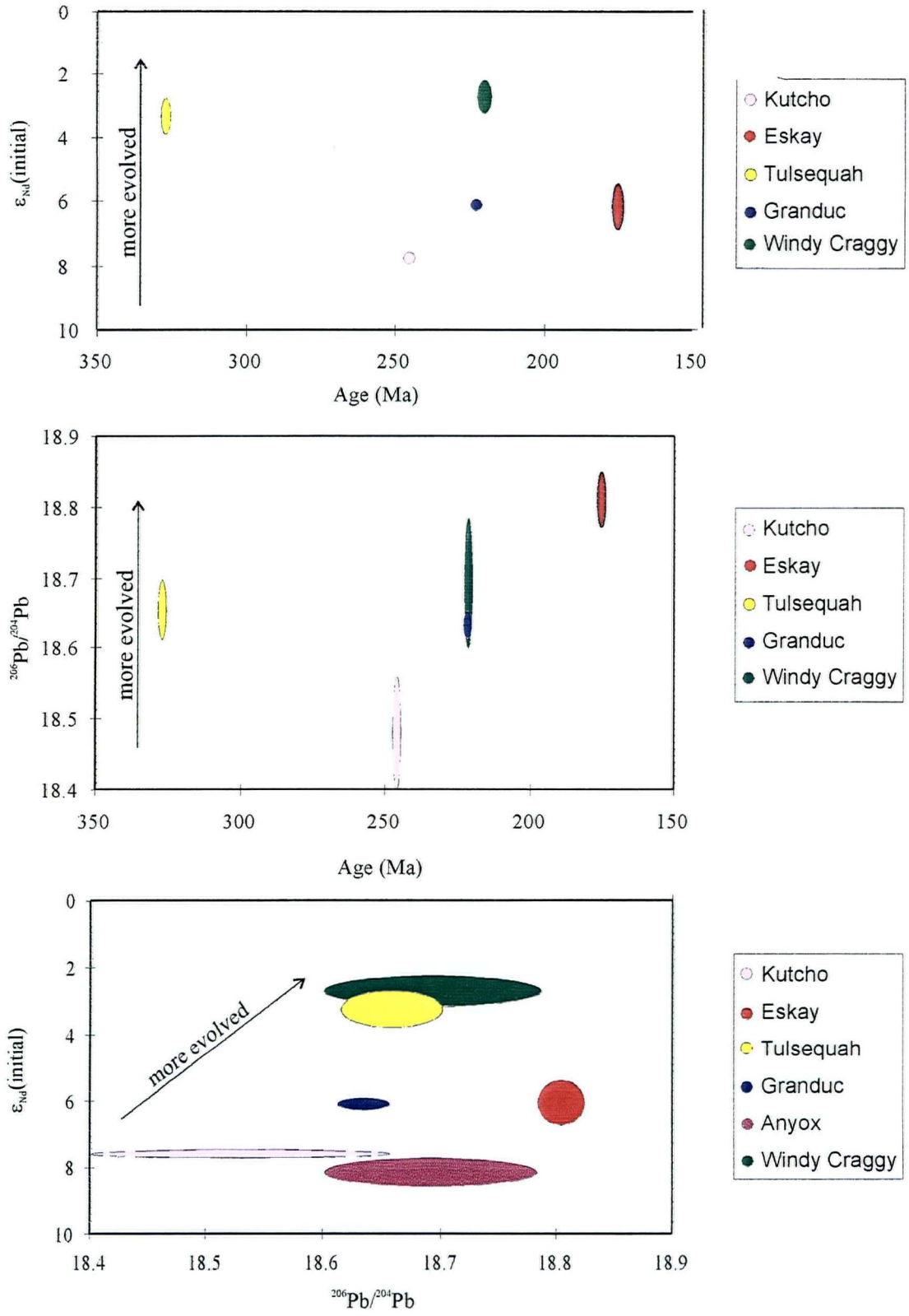

Figure 7.3 a) ε_{Nd}(initial) *versus* age, b) $^{206}Pb/^{204}Pb$ *versus* age, and c) ε_{Nd}(initial) *versus* $^{206}Pb/^{204}Pb$ for mineralization and host rocks of the Kutcho Creek, Eskay Creek, Tulsequah Chief, Granduc, Anyox, and Windy Craggy deposits (data from Childe this volume, except for Anyox Nd data from Smith (1993); Windy Craggy Nd and Pb data form Smith and Fox (1989) and Peter (1992), respectively.

Windy Craggy

The Cu-rich Windy Craggy deposit is hosted within volcano-sedimentary strata of Late Triassic age in the Alexander terrane (Mihalynuk et al. 1993; Orchard 1986) (Fig. 7.1). Strata at Windy Craggy consist of chemical to clastic sedimentary rocks, overlain by massive to pillowed mafic volcanic rocks, which are cross cut by sills and dykes of dioritic composition (MacIntyre 1986). Massive sulphide mineralization occurs near the contact between the sedimentary rocks and overlying mafic volcanic rocks (MacIntyre 1986). Mafic volcanic rocks at the Windy Craggy deposit have an alkaline to calc-alkaline affinity and REE patterns which exhibit strong light rare earth element (LREE) enrichments relative to N-MORB (MacIntyre 1986; Peter 1992). MacIntyre (1986) suggests that massive sulphide mineralization at Windy Craggy may have formed within a rift valley in a transform fault spreading center, adjacent to a continental margin, perhaps analogous to the tectonic setting of the presently forming Guaymas Basin in the Gulf of California.

Felsic volcanic-related deposits

This group of deposits is considerably more diverse than the previous, and includes Niblac in the Alexander terrane of southeast Alaska, Myra Falls in Wrangellia, Tulsequah Chief, Big Bull, and Eskay Creek in Stikinia, Kutcho Creek, which is associated with primitive rocks, possibly related to the Cache Creek terrane, and Ecstall in the Scotia-Quaal metamorphic belt of the Coast Plutonic Complex (Table 7.1 and Fig. 7.1). The single feature common to deposits in this group is a close spatial association between felsic volcanic rocks and massive sulphide mineralization. Generally the volcanic sequences which host mineralization are bimodal at the property scale, and in some cases also at the regional scale. Mafic and/or felsic intrusive rocks are locally present, and are of similar chemical composition and affinity to the volcanic rocks they intrude. The metal association of this group is diverse, ranging from polymetallic (Zn-Pb-Cu+/-Au+/-Ag) at deposits such as Tulsequah Chief and Myra Falls, to Cu-Zn-rich at Kutcho Creek, and strongly Au- and Ag-enriched at Eskay Creek (Table 7.1). The interpreted tectonic settings of these deposits are as diverse as their metal suites. The host lithologies, metal suites, and interpreted tectonic settings of three distinctly different deposits in this group are discussed below.

Tulsequah Chief deposit

The polymetallic (Pb-Zn-Cu-Au-Ag) Tulsequah Chief deposit occurs within bimodal volcanic rocks of Late Mississippian age that form part of the Stikine Assemblage (Childe *this volume*) (Fig. 7.1). Massive sulphide mineralization is hosted within felsic volcanic flows and tuffaceous rocks of rhyodacitic to rhyolitic composition, and is both underlain and overlain by mafic volcanic flows and breccias. The felsic volcanic strata which host mineralization are dilated by intrusion of a sill-like body of gabbroic composition, the geochemistry and mineralogy of which is similar to that of the mafic volcanic rocks overlying the ore-bearing felsic strata (Sebert and Barrett 1996). Trace and rare earth element chemistry suggests that felsic and mafic footwall rocks have transitional to mildly calc-alkaline magmatic affinities, and VMS mineralization and host rocks are interpreted to have formed in a mature island arc setting (Sebert and Barrett 1996).

Kutcho Creek deposit

Copper- and Zn-rich VMS mineralization at Kutcho Creek occurs within felsic volcanic rocks of earliest Triassic age, in the fault-bounded volcano-sedimentary King Salmon allochthon, between the Stikine, Cache Creek and Quesnel terranes (Thorstad and Gabrielse 1986; Childe *this volume*) (Fig. 7.1). Massive sulphide mineralization is hosted within quartz $\pm$ plagioclase porphyritic felsic mass and lapilli flows of rhyodacitic to rhyolitic composition. Compositionally bimodal rocks, consisting of mafic and felsic flow and tuffaceous rocks underlie, or occur distally to the felsic volcanic sequence which hosts mineralization. Felsic strata which host mineralization and overlying sedimentary strata are cross cut by sill-like bodies of gabbroic composition. The bimodal sequence is cross cut by felsic intrusions. Volcanic and felsic intrusive rocks have trace and rare earth element chemistries which suggest tholeiitic magmatic affinities (Childe *this volume*; Barrett et al. 1996). Mineralization at Kutcho Creek is interpreted to have formed within the fore arc portion of an intraoceanic island arc, perhaps built directly on oceanic crust (Thorstad and Gabrielse 1986; Childe *this volume*; Barrett et al. 1996). In contrast, the gabbroic intrusions have a chemistry which is distinct from other igneous rocks in the King Salmon Allochthon, and is similar to that of alkaline arc magmas. These intrusions may represent a change in the tectonic regime, immediately following the formation of massive sulphide mineralization at Kutcho Creek (Childe *this volume*).

Eskay Creek deposit

Eskay Creek is a precious and base metal-rich deposit which formed in a volcanic-dominated sequence of Middle Jurassic age in the Hazelton Group (Table 7.1) (Macdonald et al. 1996a; Childe *this volume*). The deposit is characterized by a mineralogy that is more typical of epithermal than VMS deposits (Macdonald et al. 1996a). Several different styles of stratiform and discordant mineralization occur within the deposit, but the bulk of the economic mineralization occurs as clastic sulphides and sulphosalts, hosted within an argillaceous sedimentary unit; this unit is underlain by felsic volcanic and intrusive rocks of rhyolitic composition and overlain by mafic volcanic massive to pillowed flows and sills of basaltic composition (Macdonald et al. 1996a). Felsic flows, sub-volcanic dykes and flow domes within the footwall to stratiform mineralization have been interpreted by Bartsch (1993) to represent a flow-dome complex. These felsic rocks, as well as mafic rocks in the hangingwall to mineralization, have trace and rare earth element chemistries consistent with tholeiitic magmatic affinities (Childe *this volume*; Barrett and Sherlock 1996). Bartsch (1993) suggested that the Eskay Creek deposit formed within a back arc or intra-arc basin.

Discussion of Nd and Pb isotopic systematics

The Tulsequah Chief, Granduc, and Eskay Creek deposits formed within the Paleozoic Stikine Assemblage, Upper Triassic Stuhini Group, and Lower to Middle Jurassic Hazelton Group of the Stikine terrane, respectively. An overall evolution from less to more radiogenic Pb isotopic compositions over time is observed in Stikinia, based on the Pb isotopic signatures of galenas from Tertiary and Jurassic mineralization in the Stewart Mining Camp, and feldspar from the Late Devonian Forrest Kerr pluton, which intrudes Stikinia (Alldrick 1991; Childe *this volume*). This evolution of Pb can be observed on plots of $^{207}Pb/^{204}Pb$ *versus* $^{206}Pb/^{204}Pb$ and $^{208}Pb/^{204}Pb$ *versus* $^{206}Pb/^{204}Pb$ (Figs. 7.2a and b). The Pb isotopic signatures of mineralization from the Late Triassic Granduc and Middle Jurassic Eskay Creek deposits are consistent with this evolution of Pb in Stikinia, whereas those of the Late Mississippian Tulsequah Chief deposit are slightly elevated in $^{206}Pb/^{204}Pb$, $^{207}Pb/^{204}Pb$, and $^{208}Pb/^{204}Pb$ (Fig. 7.2). This elevation in Pb isotopic ratios at Tulsequah Chief may be the result of a more evolved metallogenic source to this

deposit, approaching that of Devono-Mississippian VMS deposits in the Yukon-Tanana terrane (Lange et al. 1993) (Fig. 7.2b). Similarly, the ε_{Nd}(initial) signatures of igneous rocks at Tulsequah Chief are slightly more evolved than those of volcanic rocks of the Stikine Assemblage further to the south, and volcanic rocks of the younger Stuhini and Hazelton Groups, also to the south of Tulsequah Chief (Figs 3.8, 5.1 and 5.5, and Table 7.1). As with to the Pb isotopic data, the Nd data are consistent with magmatic rocks at Tulsequah Chief being derived from somewhat more evolved sources than those in more southern parts of Stikinia.

The Nd and Pb isotopic data for these three deposits are consistent with their interpreted tectonic settings, wherein the Granduc and Eskay Creek deposits formed in back arc settings, or early, tholeiitic portions of arc assemblages in Stikinia, and the Tulsequah Chief deposit, although part of an older portion of Stikinia, formed within a more mature island arc setting.

The Stikine and Alexander terranes represent allochthonous island arc assemblages which accreted onto the margin of ancestral North America in the Mesozoic (Monger et al. 1982; Monger et al. 1991). Based on Nd isotopic compositions, Samson et al. (1989) suggested that both the Stikine and Alexander terranes formed within probable intra-oceanic arc environments, with little to no assimilation of older, more evolved crustal material. The Granduc and Windy Craggy deposits represent VMS deposits which formed in the Stikine and Alexander terranes, respectively, in Late Triassic time (Table 7.1) (MacIntyre 1986; Orchard 1986; Childe *this volume*). Therefore a comparison of the Pb and Nd isotopic compositions of sulphides and host rocks at these two deposits provides a comparison of the degree of evolution of portions of these two terranes in Late Triassic (Early Norian) time. Sulphides from the Windy Craggy deposit have a wide range of Pb isotopic compositions, whereas those determined for the Granduc deposit have a more restricted range of values (Peter 1992; Childe *this volume*). However, when plotted on $^{207}Pb/^{204}Pb$ *versus* $^{206}Pb/^{204}Pb$ and $^{208}Pb/^{204}Pb$ *versus* $^{206}Pb/^{204}Pb$ diagrams, it is apparent that sulphides from Granduc are slightly less evolved than those from Windy Craggy (Figs. 7.2a and b). The range of Nd isotopic signatures of igneous rocks at Windy Craggy determined by Smith and Fox (1989) overlap the range of igneous rocks in the Stuhini Group, but are significantly more evolved than those from the Granduc deposit itself (Figs. 3.8 and 7.1b) (Childe *this volume*). The overlap of Nd isotopic compositions between the Windy Craggy deposit and the

Stuhini Group indicates that there is no significant difference in the degree of evolution of igneous rocks of Late Triassic age from the Stikine and Alexander terranes. The more evolved Nd and Pb isotopic signatures at Windy Craggy, relative to those at Granduc, suggests that mineralization and host rocks at Windy Craggy were derived from more evolved sources. The differences in the radiogenic isotopic signatures of the two deposits are consistent with the difference in interpreted tectonic setting, in that Granduc formed in an oceanic back arc or primitive island arc environment, and Windy Craggy in a rifted transform spreading center, perhaps in proximity to a continental margin (MacIntyre 1986; Childe *this volume*).

Both the age of the Anyox deposit, and the terrane affiliation of the pendant in which it is contained, remain unconstrained. It is therefore difficult to interpret the significance of the degree of evolution of radiogenic isotopes associated with mineralization and host rocks at Anyox. However, it can be observed that the Pb isotopic signature of mineralization at Anyox is similar to that at Windy Craggy, whereas the Nd isotopic signatures of mafic volcanic rocks that host mineralization at Anyox are more primitive than all other deposits considered here (Figs. 7.3a, b, and c). The isotopically primitive nature of the host rocks to the Anyox deposit is consistent with formation within a mid-ocean ridge setting as proposed by Macdonald et al. (1996b).

Massive sulphide mineralization at Kutcho Creek occurs within volcanic rocks of rhyodacitic to rhyolitic composition which, prior to this study, were assigned a Late Triassic age; this age designation implied a temporal association with deposits of known or inferred Late Triassic age in the Cordillera (Thorstad and Gabrielse 1986). However, U-Pb dating of volcanic rocks at Kutcho Creek indicates that the contained VMS mineralization formed in the earliest Triassic, some 20 to 25 m.y. prior to formation of the Late Triassic deposits. A tholeiitic magmatic affinity has been established for volcanic rocks at Kutcho Creek, and the deposit is interpreted to have formed in a primitive arc or fore-arc setting, built on a juvenile basement such as the oceanic Cache Creek terrane (Thorstad and Gabrielse 1986; Barrett et al. 1996; Childe *this volume*). The Nd isotopic signature of host rocks and the Pb isotopic signature of mineralization at Kutcho Creek are both extremely primitive and consistent with the interpreted environment of formation (Figs. 7.2 and 7.3a, b, and c).

Discussion

Paleozoic to Mesozoic VMS deposits which occur in allochthonous terranes of the North American Cordillera have a wide range of base and precious metal contents and host lithologies, reflecting in part formation in a wide range of interpreted tectonic settings. This range of tectonic settings can be compared to that of convergent and divergent plate margins at which massive sulphide mineralization is currently forming on the seafloor, which includes:

- the Jade hydrothermal field in the Okinawa Trough, where mineralization is forming in a back arc basins floored by continental crust (Halbach et al. 1993);
- the Valu Fa Ridge in the Lau Basin, where mineralization is forming in a back arc spreading center built on remnant arc crust (Herzig et al. 1993; Fouquet et al. 1993), and
- Middle Valley on the Juan de Fuca Ridge, where mineralization is forming in a mid-ocean ridge setting in the eastern Pacific (Goodfellow and Peter 1994).

Within both modern and ancient settings, VMS mineralization commonly forms during, or close to, a change in the overall tectonic regime (Urabe, 1987). For example, at Granduc and Anyox, mineralization formed during the waning stages of mafic volcanism, whereas at Kutcho Creek mineralization formed during the waning stages of tholeiitic felsic volcanism, and just prior to the intrusion of chemically distinct alkaline magmas. These changes in the tectonic regime are commonly accompanied by a hiatus in magmatism, and VMS mineralization occurs within periods of quiescence.

Volcanogenic massive sulphide deposits in allochthonous terranes of the North American Cordillera are grouped here using a broad classification scheme based on host lithology, without reference to tectonic setting or metallogenic affiliation, to accommodate the wide range of styles of deposits found in this region. Using this method of classification, most VMS deposits in British Columbia can be grouped into one of two categories: mafic volcanic and sediment-related, or felsic-volcanic-related.

References

Alldrick, D.J. 1986. Stratigraphy and structure in the Anyox area (103P/5). *In* Geological Fieldwork, British Columbia Ministry of Energy, Mines and Petroleum Resources, Paper 1986-1, pp. 211-216.

Alldrick, D.J. 1991. Geology and Ore Deposits of the Stewart Mining Camp; Ph.D. thesis, University of British Columbia, Vancouver, 417p.

Barrett, T.J., Sherlock, R.L., and Thompson, J.F.H. 1996. Geology and geochemistry of the Kutcho Creek deposit, Northern British Columbia. Exploration and Mining Geology.

Barrett, T.J. and Sherlock, R.L. 1996. Geology and geochemistry of the Eskay Creek deposit, Northwestern British Columbia. Exploration and Mining Geology.

Bartsch, R.D. 1993. Volcanic stratigraphy and lithogeochemistry of the Lower Jurassic Hazelton Group, host to the Eskay Creek precious and base metal volcanogenic deposit. M.Sc. thesis, The University of British Columbia, Vancouver, 178 p.

Binns, R.A., Parr, J.M., Scott, S.D., Gemmell, J.B., and Hertzig, P.M. 1995. PACMANUS: An active seafloor hydrothermal field on siliceous volcanic rocks in the eastern Manus Basin, Papua New Guinea. Proceedings of the 1995 PACRIM Congress, pp. 49-54.

Fouquet, Y., von Stackelberg, U., Charlou, J.L., Erzinger, J., Herzig, P.M., Muhe, R., and Wiedecke, M. 1993. Metallogenesis in back-arc environments: The Lau Basin example, Economic Geology, **88**: 2154-2181.

Franklin, J.M. 1996. Volcanic-associated massive sulphide base metals. *In* Geology of Canadian Mineral Deposit Types, *Edited by* O.R Eckstrand, W.D. Sinclair, and R.I. Thorpe, Geological Survey of Canada, Geology of Canada no. 8, pp. 158-183.

Franklin, J.M., Lydon, J.M., and Sangster, D.F. 1981. Volcanic-associated massive sulphide deposits. Economic Geology, 75th Anniversary Volume, pp. 485-627.

Gabrielse, H., Monger, J.W.H., Wheeler, J.O., and Yorath, C.J. 1991. Morphological belts, tectonic assemblages and terranes. *In* Upper Devonian to Middle Jurassic Assemblages, Part A of Chapter 1 of Geology of the Cordilleran Orogen in Canada, *Edited by* H. Gabrielse, and C.J. Yorath, Geological Survey of Canada, Geology of Canada, no. 4, pp. 15-28.

Gardner, M.C., Bergman, S.C., Cushing, S.C., MacKevett, E.M., Plafker, G., Campbell, R.B., McClelland, W.C., Mueller, P.A. 1988. Pennsylvanian pluton stitching of Wrangellia and the Alexander terrane, Wrangel Mountains, Alaska. Geology, **16**: 967-970.

Gehrels, G.E., Butler, R.F., Buzard, D.R. 1996. Detrital zircon geochronology of the Alexander terrane, southeast Alaska. Geological Society of America Bulletin, **108**: 722-734.

Goodfellow, W.D., and Peter, J.M. 1994. Geochemistry of hydrothermally altered sediments, Middle Valley, northern Juan de Fuca Ridge. *In* Proceedings of the Ocean Drilling Program. *Edited by* M.J. Mottl, E.E. Davis, A.T. Fisher, and J.F. Slack, **139**: 207-289.

Grove, E.W. 1986. Geology and mineral deposits of the Unuk River-Salmon River-Anyox area. British Columbia Ministry of Energy, Mines and Petroleum Resources Bulletin 63, 152 p.

Halbach, P., Pracejus, B., and Marten, A. 1993. Geology and mineralogy of massive sulphide ores from the central Okinawa trough, Japan. Economic Geology, **88**: 2210-2225.

Herzig, P.M., Hannington, M.D., Fouquet, Y., von Stackelberg, U., and Peterson, S. 1993. Gold-rich polymetallic sulphides from the Lau Back Arc and implications for the geochemistry of gold in sea-floor hydrothermal systems of the southwest Pacific. Economic Geology, **88**: 2182-2209.

Höy, T. 1991. Volcanogenic massive sulphide deposits in British Columbia. *In* Ore deposits, tectonics and metallogeny in the Canadian Cordillera, British Columbia Ministry of Energy, Mines and Petroleum Resources, Paper 1991-4, 276 pages.

Lange, I.M., Nockelburg, W.J., Newkirk, S.R., Aleinikoff, J.N., Church, S.E., and Krouse, H.R., 1993. Devonian volcanogenic massive sulphide deposits and occurrences, southern Yukon-Tanana terrane, eastern Alaska range, Alaska. Economic Geology, **88**: 344-376.

Lydon, J.M. 1988. Volcanogenic massive sulphide deposits, Part 1: A descriptive model. *In* Ore Deposit Models, *Edited by* R.G. Roberts and P.A. Sheahan, Geoscience Canada Reprint Series 3, pp. 145-154.

Macdonald, A.J., Lewis, P.D., Thompson, J.F.H., Nadaraju, G., Bartsch, R.D., Bridge, D.J., Rhys, D.A., Roth, T., Kaip, A., Godwin, C.I., and Sinclair, A.J. 1996a. Metallogeny of an Early to Middle Jurassic arc, Iskut River area, Northwestern British Columbia. Economic Geology, **91**: 1098-1114.

Macdonald, R.W.J., Barrett, T.J., and Sherlock, R.L. 1996b. Geochemistry and alteration of the Hidden Creek deposit, Anyox, West-central British Columbia. Exploration and Mining Geology.

MacIntyre, D.G. 1986. The geochemistry of basalts hosting massive sulphide deposits, Alexander terrane northwest British Columbia (114P). *In* British Columbia Ministry of Mines and Petroleum Resources, Paper 1996-1. *Edited by* W.J. McMillan, pp. 89-123.

Mihalynuk, M.I., Smith, M.T., and MacIntyre, D.G. 1993. Tatshenshini project, northwestern British Columbia (114P/11, 12, 13, 14; 114O/9, 10, 14, 15, and 16). *In* Geological Fieldwork, British Columbia Ministry of Energy, Mines and Petroleum Resources, Paper 1993-1, pp. 185-229.

Monger, J.W.H., Price, R.A., and Templeman-Kluit, D.J. 1982. Tectonic accretion and the origin of the two major metamorphic and plutonic welts in the Canadian Cordillera. Geology, **10**: 70-75.

Monger, J.W.H., Wheeler, J.O., Tipper, H.W., Gabrielse, H., Harms, T., Struik, L.C., Campbell, R.B., Dodds, C.J., Gehrels, G.E., and O'Brian, J. 1991. Cordilleran terranes. *In* Upper Devonian to Middle Jurassic Assemblages, Chapter 8 of Geology of the Cordilleran Orogen in Canada, *Edited by* H. Gabrielse, and C.J. Yorath, Geological Survey of Canada, Geology of Canada, no. 4, pp. 281-327.

Newberry, R.J., Brew, D.A., and Crafford, T.C. 1990. Genesis of the Greens Creek (GC) volcanogenic massive sulphide (VMS) deposit, S.E. Alaska: A geochemical study. Geological Association of Canada Annual Meeting Program with Abstracts, pp. A-96.

Orchard, M.J., 1986: Conodonts from western Canadian chert: Their nature, distribution and stratigraphic application, in Investigative Techniques and Applications, *Ellis Horwood Ltd.*, Chichester, p. 94-119.

Peter, J.M. 1992. Comparative geochemical studies of the Upper Triassic Windy Craggy and modern Guaymus Basin deposits: A contribution to the understanding of massive sulfide formation in volcano-sedimentary environments. Ph.D. thesis, University of Toronto, Toronto.

Samson, S.D., McClelland, W.C., Patchett, P.J., Gehrels, G.E., and Anderson, R.G., 1989, Evidence from neodymium isotopes for mantle contributions to Phanerozoic crustal genesis in the Canadian Cordillera: Nature, v.337, p. 705-709.

Sawkins, F.J. 1976. Massive sulphide deposits in relation to geotectonics. Geological Association of Canada, Special Paper **14**: 221-240.

Sebert, C. and Barrett, T.J. 1996. Stratigraphy, alteration and mineralization at the Tulsequah Chief massive sulphide deposit, Northwestern British Columbia. Exploration and Mining Geology.

Sharp, R.J. 1980. The geology, geochemistry and sulphur isotopes of the Anyox massive sulphide deposits. M.Sc. thesis, University of Alberta, Edmonton.

Sherlock, R.L., Barrett, T.J., Thompson, J.F.H., Macdonald, R.W., McKinley, S.D., Roth, T., Sebert, C., Childe, F. 1996. Geology of volcanogenic massive sulfide deposits in the Cordillera of British Columbia, Canada. *In* Geology and ore deposits of the American Cordillera, *Edited by* A.R. Coyner, and P.L. Fabey, Geological Society of Nevada Symposium Proceedings, Reno, Nevada, pp. 1253-1280.

Smith, A.D., and Fox, J.S. 1989. Geochemistry of basalts from the Windy Craggy and Anyox volcanogenic massive sulphide deposits, British Columbia. Geological Association of Canada, Mineralogical Association of Canada, Program with Abstracts, **14**: A22.

Souther, J.G. 1991. Volcanic Regimes, *In* Chapter 14, Geology of the Cordilleran Orogen in Canada, *Edited by* H. Gabrielse, and C.J. Yorath, Geological Survey of Canada, Geology of Canada, no. 4, pp. 457-490.

Thompson, J.F.H., Barrett, T.J., Childe, F.C., and Sherlock, R.L., 1994. Volcanogenic massive sulphide deposits of the Canadian Cordillera. Geological Society of America Annual Meeting, Abstracts with Programs, p. A-27.

Thorstad, L., and Gabrielse, H. 1986. The Upper Triassic Kutcho Formation Cassiar Mountains, North-Central British Columbia. Geological Survey of Canada Paper 86-16, 53 pages.

Urabe, T. 1987. Kuroko deposit modeling based on magmatic hydrothermal theory. Mining Geology, **37**: 159-176.

APPENDIX 1

PROCEDURES FOR ISOTOPIC ANALYSES

U-Pb Procedures

Samples were collected for U-Pb geochronology from drill core, surface, and underground workings, sample weights ranged from 2 to 30 kg. All samples were selected by the author, with the exception of samples EC-GC-03 (Eskay Creek east limb rhyolite), which was selected and collected by Andrew Kaip, sample AX-GC-11 (Anyox pendant, Mt. Clashmore quartz diorite), which was selected and collected by Rob Macdonald, and sample EL-GC-01 (Ecstall property quartz diorite), which was selected and collected by Tim Barrett and Ross Sherlock.

All U-Pb sample preparation and analyses were conducted in the Geochronology Laboratory of the University of British Columbia. Heavy mineral extraction procedures and U-Pb zircon analytical procedures follow those described by Mortensen et al. (1995). Isotopic ratios were measured using a modified single collector VG-54R thermal ionization mass spectrometer equipped with a Daly photomultiplier. Uranium and Pb analytical blanks for all samples analyzed during the course of this study were 1-5 and 5-25 picograms, respectively. Uranium fractionation was determined directly on individual runs using a $^{233-235}U$ spike; Pb isotopic ratios were corrected for a fractionation of 0.12%/amu and 0.43%/amu for Faraday and Daly runs, respectively, based on replicate analyses of the NBS-981 Pb standard (UBC Geochronology Laboratory *unpublished data*) and the values recommended by Todt et al. (1984). Concordia intercept ages and associated errors were calculated using a modified York-II regression model (York 1969), and the algorithm of Ludwig (1980); ages were calculated using the decay constants recommended by Steiger and Jäger (1977). All age assignments in this volume follow the time scale of Harland et al. (1990), with the exception of the Permo-Triassic boundary, which follows the designation of Renne et al. (1995).

Pb Procedures

Pb-rich sulphides and sulphosalts

Analytical procedures for the analysis of galena (PbS) and boulangerite ($Pb_5Sb_4S_{11}$) follow those of Cameron et al. (1969), in which a small grain of galena or boulangerite is hand picked using a binocular microscope, washed, and dissolved in dilute hydrochloric acid. Lead is then loaded in chloride form on to a rhenium filament and isotopic ratios were determined using a modified single collector VG-54R thermal ionization mass spectrometer at the Geochronology Laboratory of the University of British Columbia. Samples were analyzed using the Faraday detector and measured ratios were normalized for instrument mass fractionation of 0.12%/amu based on replicate analyses of the NBS-981 Pb standard following the procedures outlined by Godwin et al (1988) (UBC Geochronology Laboratory *unpublished data*). Errors were obtained by propagation of all mass fractionation and analytical errors as described by Godwin et al. (1988).

Trace Pb

Analytical procedures used for the Pb isotopic analysis of pyrite (FeS_2), chalcopyrite ($CuFeS_2$), sphalerite (ZnS), bornite (Cu_5FeS_4) and alkali ($KAlSi_3O_8$) and potassium feldspar ($NaAlSi_3O_8$ to $CaAlSi_3O_8$), based on those developed at the Geochronology Laboratory of the Geological Survey of Canada in Ottawa, are given below. Total procedural blanks for these analyses ranged from 80 to 130 picograms of Pb.

Picking and cleaning - feldspar

1 - <u>To coarse pick sample</u>: Chip out feldspar fragments from the hand sample using a rock hammer or rock saw. Crush the fragments in a plastic rock sample bag and separate out the cleanest pieces into a plastic watch glass.

- <u>To fine pick</u>: Re-crush the cleaner portion in another plastic bag and pour contents into the second half of the plastic watch glass. Separate out cleanest grains with clean tweezers. Pick in ethanol under a binocular microscope. If the feldspars being picked are clean enough (i.e. no other mineral grains present) these pieces can be placed directly into the *clean** agate mortar.

Otherwise, keep picking until you have the cleanest faction possible. Once the sample has been ground and sieved the non-feldspars will be more difficult to distinguish and remove.

2 - Grinding & sieving to 100-200μ: Grind sample in ethanol to minimize sample loss. Do not over grind. Decant off excess ethanol and wash sample through cleaned nested sieves using ethanol. Repeat grinding and sieving until the +100 micron fraction is between 100 and 300 milligrams. Place in a plastic picking container and remove contaminants. This is best done by allowing the sample to dry and removing particles with a metal pick and finger/forehead oil. Static will remove these particles easily. Transfer to Pyrex beaker. Sample is ready for acid leaching.

3 cleaning: In a laminar flow hood transfer dry sample from Pyrex to a cleaned and rinsed 7 ml savillex beaker.

To remove surface particulate from sample add 1ml distilled acetone to each sample, cap and ultrasonic for 10 minutes. Wipe savillex with MQ water and kimwipe before putting back in laminar flow hood. Open savillex in hood, decant off acetone and let sit until evaporated to dryness.

4 acid leaching:

- Add 1-2ml 2 bottle 6N HCl and cap. Reflux for 1 hour at 80°C.

- Pour off HCl. Rinse with MQ water twice, adding a few drops of 2 bottle acetone each time. For the third rinse, add 1 ml of the 2 bottle acetone and pour off. Evaporate to dryness in hood.

- Add 0.5 ml dilute HF-HBr and a few drops of 2 bottle acetone to the sample. Cap beaker and place in ultrasonic for 1 minute. Wipe down savillex with MQ water and kimwipe before placing in hood. Pour off solution and rinse with MQ water, plus a few drops of 2 bottle acetone, and repeat twice. Repeat entire step. The final third rinse should be done with 2 bottle acetone only.

- Let sit until evaporated to dryness, samples are now ready for dissolution.

5 dissolution:

- Add 1ml HF + 0.05 ml conc. HNO_3 (i.e. 1 drop) to each savillex (15 samples + 1 blank); cap and reflux on hot plate in laminar flow hood for 12 hours (overnight) at 80°C.

Picking and cleaning - trace Pb sulphides

1 - To coarse pick sample: Chip out sulphide fragments from the hand sample. Crush the fragments in a plastic rock sample bag and separate out the cleanest pieces into a plastic watch glass.

- To fine pick: Re-crush the cleaner portion in another plastic bag and pour contents into the second half of the plastic watch glass. Separate out cleanest grains with clean tweezers. Pick in ethanol under a binocular microscope.

2 In a laminar flow hood transfer dry sample from Pyrex or petri dish to a cleaned and rinsed 7 ml savillex beaker.

3 cleaning: add 1ml distilled acetone to each sample, cap and ultrasonic for 10 minutes. Wipe savillex with MQ water and kimwipe before putting back in laminar flow hood. Open savillex in hood, decant off acetone, rinse three times in acetone and let sit until evaporated to dryness.

4 acid cleaning

- Add 1-2ml 2 bottle 3N HNO_3 and cap. Reflux for 5-10 minutes on low heat .
- Pour off HNO_3. Rinse with acetone three times. Evaporate to dryness in hood.
- Add 1-2ml 2 bottle 6N HCl and cap. Reflux for 10 minutes on low heat .
- Pour off HCl. Rinse with acetone three times. Evaporate to dryness in hood.
- Samples are now clean and ready for dissolution.

5 dissolution

- Add 1-2 ml 3N HNO_3 to each savillex (15 samples + 1 blank); cap and reflux on hot plate in laminar flow hood for 12 hours (overnight) at 80°C.

- Dry down samples on hot plate in laminar hood, repeat above HNO_3 dissolution for another 12 hours (overnight).

loading blank preparation, trace Pb sulphides and feldspar

- Weigh ^{205}Pb spike and record value, add 1 drop ^{205}Pb spike into a clean savillex beaker. Re-weigh spike and record.

Dissolution and Pb extraction - trace Pb sulphides and feldspar

1 Uncap beakers and evaporate to dryness on hot plate, maximize separation of beakers. Rinse caps in 2 bottle water and store in hood.

2 Handle carefully, sample may be very staticy!!!! Add 0.5 ml MQ water to wash inside surface of beakers. Take to dryness. (Addition of water may be left out of procedures if there is no particulate on sides of beaker.)

3 Add 0.5 ml 2N HCl and evaporate to moist paste. DO NOT DRY OUT! This step takes anywhere from 1/2 to 1+ hours and should be monitored carefully.

4 Dissolve paste in 1 ml 1N HBr on hot plate for 3 days.

5 Remove Bio-Rad columns from storage container, rinse with MQ water and place on rack. Load columns with 1 ml clean Dow 100-200 mesh anionic resin in 6 N HCl, let stand 30 minutes to allow resin to settle. Follow the check list below for the two day chemical extraction and purification of Pb:

		1st day	2nd day
Clean resin:	add 3-4 ml 6N HCl	_____	_____
	add 2 ml 2B H_2O	_____	_____
Equilibrate Columns:	add 2 ml 1N HBr	_____	_____
	add 2 ml 1N HBr	_____	_____
Load sample onto columns in 1N HBr		_____	_____
Wash columns:	add 2 ml 1N HBr	_____	_____
	add 2 ml 1N HBr	_____	_____
Remove HBr:	add 2 ml 2N HCl	_____	_____
	add 2 ml 2N HCl	_____	_____
	Place *clean* savillex beaker under column		
Elute Pb from columns:	add 2 ml 6N HCl	_____	_____
DAY 2 ONLY:	Add 2-3 drops 0.3N H_3PO_4		_____
Dry on hot plate (3 to 4 hours)		_____	_____
DAY 1 ONLY:	Add 2-3 drops 2N HCl,		(finished!!)
	dry slightly	_____	
DAY 3 ONLY:	Re-dissolve in 1ml 1N HBr,		
	2-3 hours, capped	_____	

At the end of day 2 remove columns from stand, rinse under MQ water to dislodge resin from columns. Return to correct storage container and ultrasonic for 30 minutes. Samples are now ready for isotopic analysis following the procedures outlined for Pb-rich sulphides and sulphosalts.

References

Cameron, A.E., Smith, D.H., and Walker, R.L. 1969. Mass spectrometry of nanogram-size samples of lead. Analytical Chemistry, **41**:525-526.

Godwin, C.I., Gabites, J.E., and Andrews, A. 1988. Leadtable: A galena lead isotope data base for the Canadian Cordillera, with a guide to its use by explorationists. British Columbia Geological Survey Branch Paper 1988-4, 188 p.

Harland, W.B., Armstrong, R.L., Cox, A.V., Craig, L.E., Smith, A., G. 1990. A Geologic Time Scale, 1989. 263 pages.

Ludwig, K.R. 1980. Calculation of uncertainties of U-Pb isotope data. Earth and Planetary Science Letters, **46**: 212-220.

Mortensen, J.K., Ghosh, D.K., and Ferri, P. 1995. U-Pb geochronology of intrusive rocks associated with Cu-Au deposits in the Canadian Cordillera. *In* Porphyry Deposits in the Northwestern Cordillera of North America. *Edited by* T.G. Schroter. **G-2**: 491-531.

Renne, P.R. 1995. Synchrony and Causal Relations Between Permian-Triassic Boundary Crises and Siberian Flood Volcanism. Science, **269**: 1413-1416.

Steiger, R.H., and Jäger, E. 1977. Subcommission on geochronology: Convention on the use of decay constants in geo- and cosmochronology. Earth and Planetary Science Letters, **14**: 359-362.

Todt, W., Cliff, R., Hanser, A., and Hoffman, A.W. 1984. $^{202}Pb + {}^{205}Pb$ double spike for lead isotopic analyses. Terra Cognita, **4**: 209.

York, D. 1969. Least-squares fit of a straight line with correlated errors. Earth and Planetary Science Letters, **5**: 320-324.

APPENDIX 2

ANALYTICAL PRECISION

Lithogeochemical Data

Samples were collected for lithogeochemical analysis from drill core, surface, and underground mine workings. All samples were selected by the author, with the exception of those samples mentioned in Appendix 1. In the selection of samples collected for lithogeochemical analysis care was taken to avoid sampling vein material in the rocks. All lithogeochemistry samples were analyzed using X-ray fluorescence at the Geochemical Laboratory, at McGill University, Montreal, Quebec. All major elements and Cu, Zn, Ni, Cr, V, Sc were analyzed using glass beads. The trace elements Zr, Y, Nb, Rb, Sr, Ga and Pb were analyzed using pressed pellets. All rare earth elements were analyzed by induced neutron activation analysis at Activation Laboratories, Ancaster, Ontario. Geochemical data are presented in table format in chapters two to six, and detection limits are given in these tables.

Three Mineral Deposit Research Unit in-house standards were submitted with batches of samples analyzed, to examine the accuracy of the analytical data. The standards used were ALB-1, P-1, and QGRM-100. The MDRU-compiled data from previous analyses of these standards was taken from Fraser (1994). The mean values of the data were used as the accepted values reported in Table 8.1. It should be noted that these previous analyses were carried out at a different laboratory (X-RAL, Don Mills, Ontario) than that used in this study. As such, these standards only provide an approximate guide to the accuracy of analyses of the samples in this study. These standards were submitted at various times, with various batches of samples.

There was little analytical variation in the values of the standards, the percent errors were <5 %, and often < 1.5 % for the major elements. The trace elements exhibit a larger range of values, although the elements most commonly used in this study, such as Zr and Y, typically showed relatively low degrees of error (<10 % error for Zr, 7 to 13 % error for Y). The samples

Table 8.1 Analyses of in-house standards.

	ALB-1 Accepted				ALB-1 Measured				P-1 Accepted				P-1 Measured			
Element	**Mean**	**1 St. Dev**	**% Error**	**n**	**Mean**	**1 St. Dev**	**% Error**	**n**	**Mean**	**1 St. Dev**	**% Error**	**n**	**Mean**	**1 St. Dev**	**% Error**	**n**
SiO_2	55.02	0.25	0.45	14	55.51	0.19	0.34	8	69.65	0.35	0.50	15	70.91	0.37	0.52	8
TiO_2	0.61	0.28	1.50	14	0.61	0.01	0.88	8	0.41	0.02	4.19	15	0.38	0.01	1.35	8
Al_2O_3	18.92	0.01	1.63	14	19.00	0.17	0.90	8	14.42	0.17	1.21	15	14.54	0.16	1.07	8
Fe_2O_3	1.62	0.12	7.14	14	1.63	0.02	1.49	8	3.79	0.07	1.88	15	3.90	0.05	1.26	8
MnO	0.04	0.00	8.77	14	0.04	0.01	13.36	8	0.09	0.00	4.73	15	0.08	0.00	4.35	8
MgO	2.83	0.04	1.42	14	2.75	0.04	1.36	8	1.10	0.02	2.04	15	1.00	0.01	0.75	8
CaO	10.42	0.13	1.20	14	10.23	0.05	0.47	8	3.59	0.08	2.09	15	3.48	0.03	0.76	8
Na_2O	5.77	0.08	1.41	14	5.96	0.13	2.13	8	4.03	0.09	2.25	15	3.86	0.17	4.37	8
K_2O	0.83	0.06	6.88	14	0.81	0.01	0.91	8	2.05	0.07	3.31	15	2.09	0.02	0.84	8
P_2O_5	0.30	0.00	1.22	14	0.30	0.01	1.81	8	0.09	0.00	2.71	15	0.08	0.00	0.00	8
SUM	99.53	0.58	0.58	14	97.27	1.23	1.26	8	99.84	0.56	0.56	15	100.90	0.49	0.48	8
LOI	2.99	0.21	6.90	14	3.36	0.03	0.95	8	0.47	0.09	18.56	15	0.41	0.00	0.86	8
Cr	30.18	12.75	42.24	14	34.14	7.97	23.33	7	133.77	9.65	7.22	15	200.50	7.91	3.95	8
Ni	n/a	n/a	n/a	0	51.86	19.80	38.19	7	n/a	n/a	n/a	0	7.00	1.93	27.53	8
Co	12.14	1.17	9.61	14	9.57	4.12	43.02	7	8.73	0.96	11.01	15	5.25	2.12	40.41	8
V	183.23	12.22	6.67	14	177.57	4.43	2.49	7	58.27	5.01	8.59	15	63.88	3.48	5.45	8
Cu	1293.6	29.77	2.30	14	1402.00	86.69	6.18	7	2.35	2.40	101.85	15	23.63	12.39	52.43	8
Pb	1.29	0.83	64.20	14	1.15	1.80	156.88	6	5.41	2.27	41.86	15	7.87	1.73	22.04	6
Zn	26.79	14.36	53.61	14	21.86	10.73	49.09	7	71.33	56.93	79.81	15	43.63	14.96	34.28	8
Ba	292.86	47.46	16.21	14	269.29	13.35	4.96	7	853.33	83.38	9.77	15	795.50	22.26	2.80	8
Rb	27.31	9.72	35.58	14	15.47	2.56	16.53	6	53.87	8.43	15.66	15	44.90	2.63	5.86	6
Sr	990.38	38.04	3.84	14	762.55	15.93	2.09	6	250.00	0.00	0.00	15	216.72	2.99	1.38	6
Ga	n/a	n/a	n/a	14	18.07	0.35	1.94	6	n/a	n/a	n/a	15	14.87	0.45	3.00	6
Nb	10.77	6.80	63.11	14	0.77	1.08	141.13	6	11.07	5.64	50.94	15	5.32	1.33	25.08	6
Zr	60.00	12.33	20.55	14	78.98	6.12	7.75	6	137.47	11.66	8.48	15	114.62	5.89	5.14	6
Y	18.08	8.25	45.64	14	21.07	2.72	12.92	6	21.53	7.41	34.39	15	21.68	2.75	12.70	6
Th	1.16	0.18	15.66	14	n/a	n/a	n/a	0	3.99	0.34	8.42	15	n/a	n/a	n/a	0
U	1.04	0.22	21.51	14	n/a	n/a	n/a	0	1.53	0.20	12.98	15	1.70	1.74	102.43	6

	QGRM-100 Accepted				QGRM-100 Measured			
Element	**Mean**	**1 St. Dev**	**% Error**	**n**	**Mean**	**1 St. Dev**	**% Error**	**n**
SiO_2	48.63	0.26	0.53	11	49.11	0.15	0.31	7
TiO_2	1.98	0.03	1.33	11	2.02	0.02	0.80	7
Al_2O_3	15.51	0.23	1.47	11	16.10	0.06	0.39	7
Fe_2O_3	15.04	0.22	1.46	11	15.04	0.10	0.69	7
MnO	0.19	0.00	2.35	11	0.19	0.00	0.00	7
MgO	5.60	0.14	2.58	11	5.73	0.05	0.88	7
CaO	8.51	0.10	1.14	11	8.60	0.04	0.52	7
Na_2O	2.83	0.07	2.58	11	3.15	0.20	6.33	7
K_2O	1.07	0.05	4.42	11	1.07	0.01	0.76	7
P_2O_5	0.20	0.00	2.29	11	0.19	0.00	0.00	7
SUM	99.72	0.53	0.53	11	101.34	0.37	0.37	7
LOI	0.11	0.06	58.36	11	0.05	0.00	0.00	7
Cr	82.80	14.09	17.01	11	102.14	19.74	19.32	7
Ni	43.33	2.50	5.77	11	49.43	3.78	7.65	7
Co	56.91	2.84	5.00	11	42.43	5.35	12.61	7
V	235.55	25.90	11.00	11	258.29	11.97	4.63	7
Cu	91.50	8.03	8.77	11	139.71	7.99	5.72	7
Pb	2.33	2.10	90.15	11	6.50	0.42	6.41	4
Zn	107.67	5.82	5.41	11	116.00	3.06	2.63	7
Ba	225.27	41.66	18.49	11	245.57	53.67	21.86	7
Rb	35.55	10.57	29.73	11	27.03	1.37	5.08	4
Sr	232.18	8.86	3.82	11	273.70	9.80	3.58	4
Ga	n/a	n/a	n/a	0	22.48	1.27	5.64	4
Nb	17.36	8.83	50.88	11	4.93	2.12	43.02	4
Zr	153.18	10.45	6.82	11	139.95	5.89	4.21	4
Y	25.91	8.46	32.63	11	36.88	2.02	5.48	4
Th	1.94	0.20	10.14	11	2.65	3.07	115.84	4
U	0.86	0.29	33.67	11	7.80	6.07	77.80	4

analyzed at McGill University usually have smaller associated errors than those analyzed at XRAL. Different analytical techniques (e.g. XRF using glass beads versus pressed pellets) may account for some of the difference in trace element concentrations between data from the two labs.

Pb Isotopic Data

To test the reproducibility of samples analyzed for their Pb isotopic composition a sample of bornite from the Kutcho Creek deposit (K1e) was hand picked and dissolved following the procedures outlined in Appendix 1. Subsequent to dissolution, but prior to chemical purification of the Pb (*column chemistry*), the sample was split into two aliquots, K1e-1, which consisted of one third of the solution, and K1e-2, which consisted of two thirds of the solution. After chemical purification of the Pb, aliquot K1e-1 was loaded onto a rhenium filament for isotopic analysis, aliquot K1e-2 was split into two further aliquots, K1e-2 and K1e-3, which were then loaded onto separate rhenium filaments. These three aliquots of a single dissolved sample were subsequently analyzed, the normalized Pb isotopic compositions of these analyses are presented in Table 8.2, and plotted in Figure 8.1. These data show good reproducibility, with overlap of the 2σ (95% confidence) error ellipses for the three aliquots.

Table 8. 2 Reproducibility test for sample K1e.

SAMPLE NUMBER	SAMPLE LOCATION	MIN[1].	$^{206}Pb/^{204}Pb$ (% error)[2,3]	$^{207}Pb/^{204}Pb$ (% error)[2,3]	$^{208}Pb/^{204}Pb$ (% error)[2,3]	$^{207}Pb/^{206}Pb$ (% error)[2,3]	$^{208}Pb/^{206}Pb$ (% error)[2,3]
K1e-1	Kutcho Creek	bn	18.492 (0.054)	15.554 (0.037)	37.990 (0.060)	0.84117 (0.039)	2.0545 (0.026)
K1e-2	Kutcho Creek	bn	18.476 (0.0135)	15.538 (0.073)	37.958 (0.163)	0.84098 (0.113)	2.0545 (0.091)
K1e-3	Kutcho Creek	bn	18.495 (0.116)	15.548 (0.082)	37.995 (0.137)	0.84069 (0.082)	2.0544 (0.072)

[1] mineral abreviations: bn = bornite.
[2] errors are quoted at the 2σ (95% confidence) level.
[3] values are corrected for instrument fractionation by normalization based on replicate analyses of the NBS-981 standard.

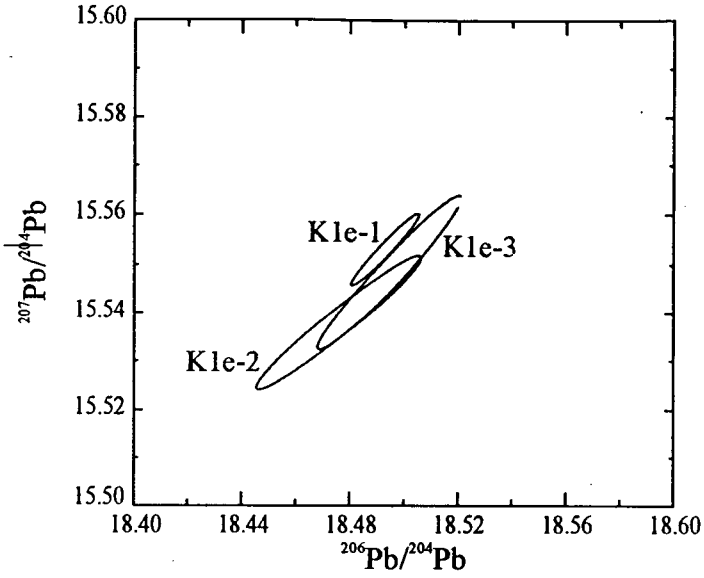
15.60
15.58
15.56
15.54
15.52
15.50
18.40
18.44
18.48
18.52
18.56
18.60
$^{207}Pb/^{204}Pb$
$^{206}Pb/^{204}Pb$
Kle-1
Kle-3
Kle-2

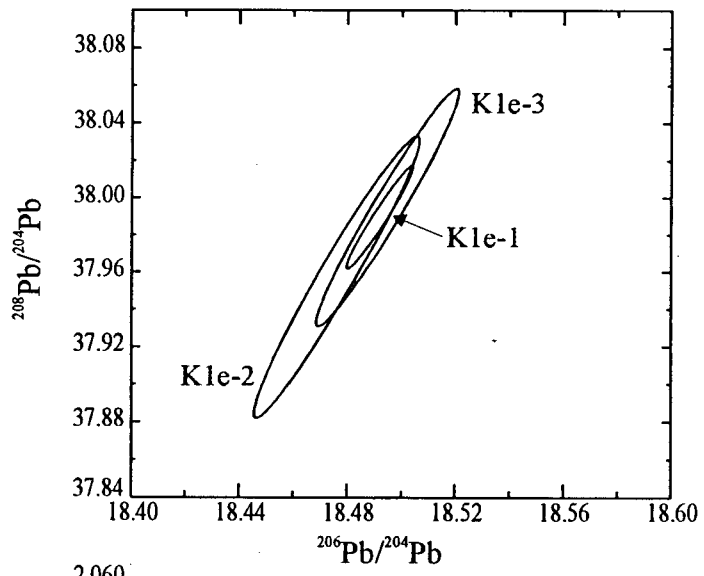
38.08
38.04
38.00
37.96
37.92
37.88
37.84
18.40
18.44
18.48
18.52
18.56
18.60
$^{208}Pb/^{204}Pb$
$^{206}Pb/^{204}Pb$
Kle-3
Kle-1
Kle-2

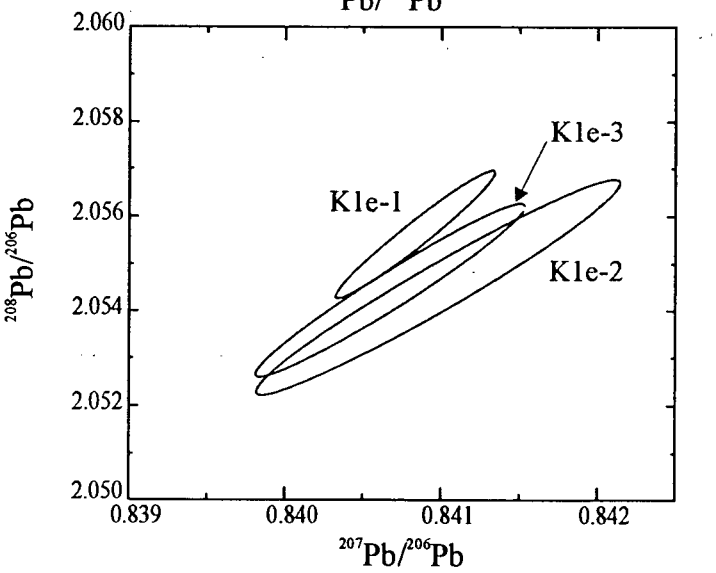
2.060
2.058
2.056
2.054
2.052
2.050
0.839
0.840
0.841
0.842
$^{208}Pb/^{206}Pb$
$^{207}Pb/^{206}Pb$
Kle-3
Kle-1
Kle-2

Figure 8. 1Pb-Pb diagrams for reproducibility test of sample K1e, showing 2σ (95% confidence) error ellipses.

References

Fraser, T.M. 1994. Geology, alteration and origin of hydrothermal breccias at the Mount Polley alkalic porphyry copper-gold deposit, South-central British Columbia. M.Sc. thesis, University of British Columbia, Vancouver, Canada, 261 p.

APPENDIX 3

GEOLOGICAL FIELDWORK PUBLICATIONS

U-Pb GEOCHRONOLOGY OF THE MOUNT STAPLER QUARTZ MONZONITE: EVIDENCE FOR EARLY JURASSIC MAGMATISM IN THE TULSEQUAH GLACIER AREA, NORTHWEST BRITISH COLUMBIA (104K/13)

F. Childe, Mineral Deposit Research Unit, UBC and
M.G. Mihalynuk, B.C. Geological Survey Branch

(M.D.R.U. Contribution P-058; Contribution to the Canada - British Columbia Mineral Development Agreement 1991-1995)

KEYWORDS: geochronology, Early Jurassic, Tulsequah Glacier, Mount Stapler suite, monzonite, age, Stikine assemblage

INTRODUCTION

The Tulsequah Glacier area is within the rugged Coast Mountains of northwestern British Columbia (Figure 1) at the westernmost edge of northern Stikine Terrane. Fieldwork in 1993 consisted of property-scale sampling and relogging of core from the Tulsequah Chief and Big Bull volcanogenic massive sulphide deposits by F.C. (Sherlock *et al.*, 1994) and 1:50 000-scale mapping of NTS map sheets 104K/12 and 13 by M.M. (Mihalynuk *et al.*, 1994a, b). Mapping on Mount Stapler revealed a tabular quartz monzonite stock with associated dissected dikes and (?)apophyses. The intrusive body dated in this study is truncated by splays of the Llewellyn fault, a long-lived crustal-scale north-northwest-trending fault with both sinistral and dextral motion.

GEOLOGICAL SETTING

Four tectonic elements constitute the gross geology between the Tulsequah Glacier area and the Yukon border. Two basement elements have been recognized: a regionally metamorphosed suite (here included with the Yukon-Tanana Terrane, *sensu* Mortensen, 1992) to the west, and late Paleozoic arc strata of the Stikine assemblage (Monger, 1977) to the east. They are overlapped by a succession of Jurassic and perhaps Upper Triassic rocks of mainly arc-derived marine sediment. All are cut by the Llewellyn fault. In northwestern British Columbia, these geologic elements have been mapped for 180 kilometres within the eastern Coast Ranges (Mihalynuk and Rouse, 1988b; Doherty and Hart, 1988; Mihalynuk *et al.*, 1989, 1990, 1994b, 1995, this volume; Currie, 1990). To the north, in southern Yukon Territory, the Llewellyn fault has been interpreted to converge with the Tally-Ho shear zone (Doherty and Hart, 1988).

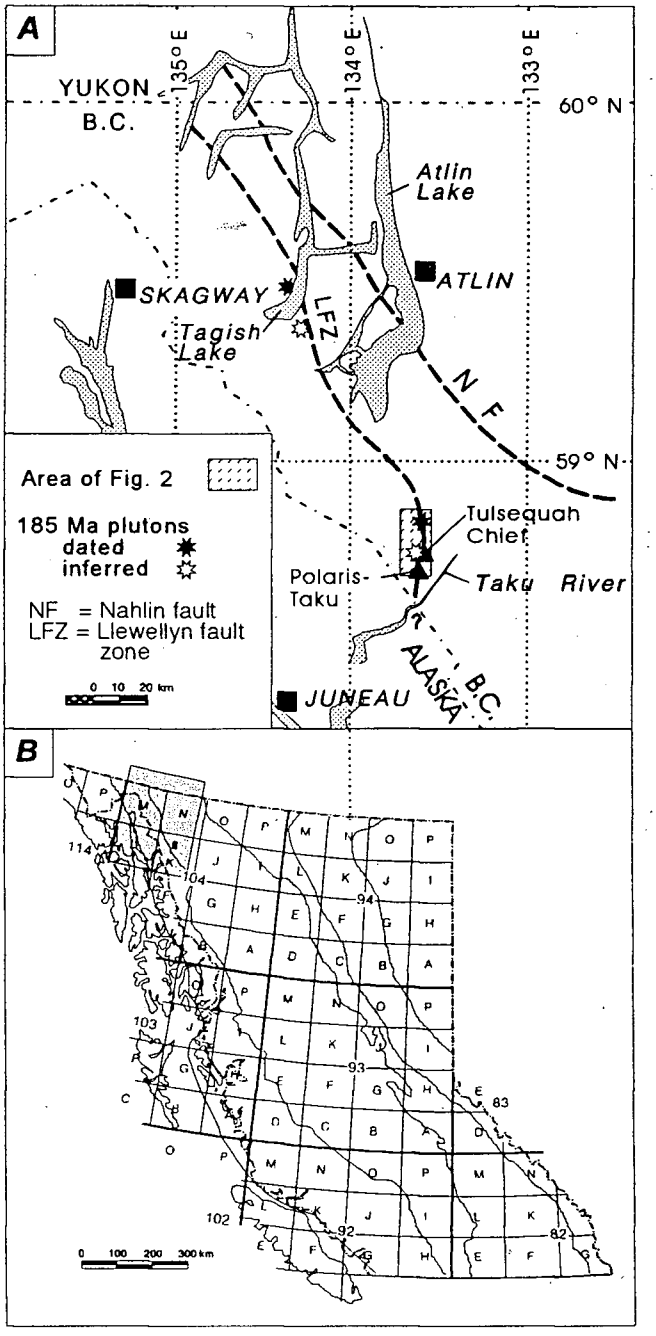

Figure 1. General location of the study area with respect to (a) geographic and cultural features and (b) the National Topographic System.

Original mapping in the Tulsequah area by Souther (1971) correlated most of the unmetamorphosed volcanic arc rocks with the Upper Triassic Stuhini Group. Recent biochronology (Nelson and Payne, 1984; Mihalynuk *et al.*, 1994b, 1995) and U-Pb geochronology (Sherlock *et al.*, 1994) have shown these rocks to be at least Early Permian to early Mississippian in age.

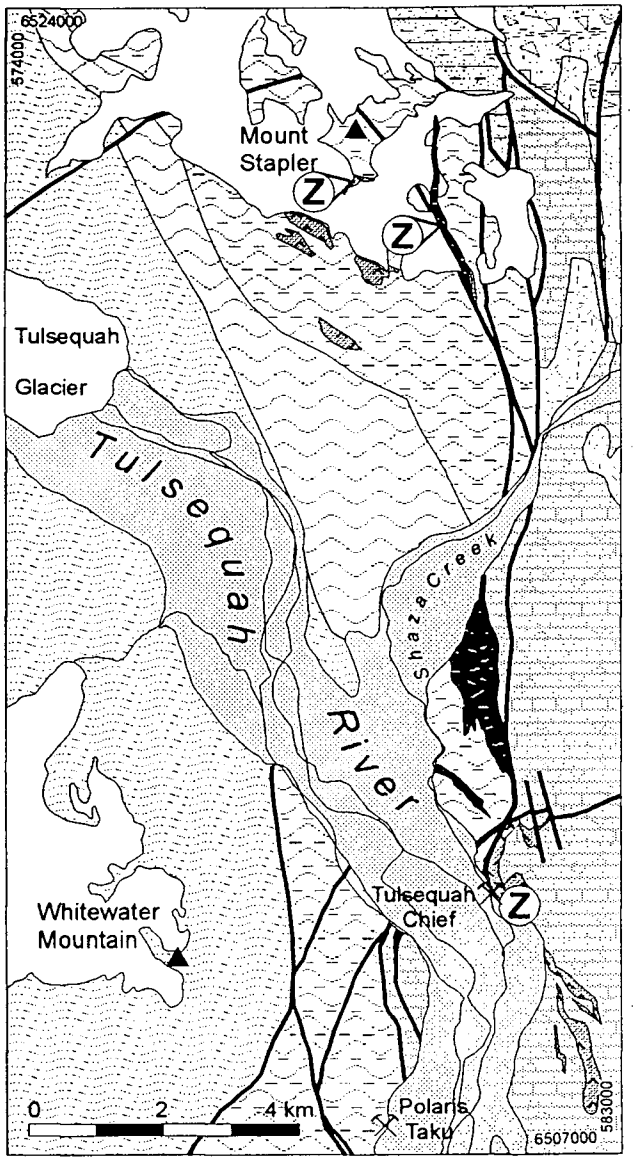

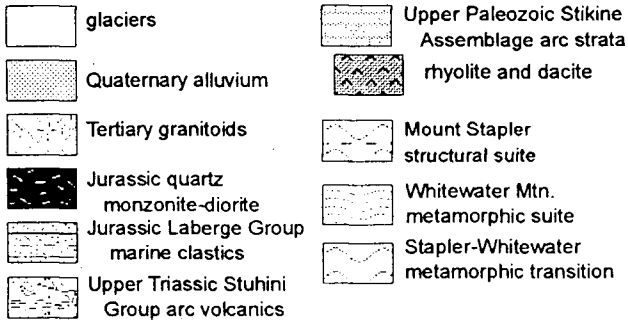

Figure 2. Distribution of metamorphic and structural suites, and Early Jurassic intrusive rocks near Tulsequah (simplified from Mihalynuk *et al.*, 1994b). 'Z' indicates sites of U-Pb zircon age date samples discussed.

Regionally metamorphosed rocks form a narrow (5 to 50 km), southward-broadening belt. For most of its northern length the metamorphic belt is composed of deformed volcanic rocks of arc derivation. These have been metamorphosed to transitional greenschist-amphibolite grade and are known as the Boundary Ranges Metamorphic Suite (Mihalynuk and Rouse, 1988a). Currie (1992) suggested that the Boundary Ranges suite is partially coeval with the Stikine assemblage; a contention which is supported by the data presented here.

Metamorphic grade in the belt culminates near the south end of Atlin Lake where sillimanite overprints kyanite. Protoliths there are thick carbonates, semipelites and quartzites of probable continental margin derivation. This package is known as the Florence Ranges Metamorphic Suite (Currie, 1990). Between Atlin Lake and the Tulsequah River area, several abrupt changes in structural style and/or protolith are recognized as separate metamorphic or structural suites. These include the Whitewater Metamorphic Suite that consists of quartz-rich graphitic schist, lesser metabasite and quartzite, and sparse carbonate and ultramafic rocks, and the Mount Stapler structural suite that consists of volcanic arc derived strata with relict protolith textures (Mihalynuk *et al.*, 1994a, b). The Mount Stapler suite is divided into upper and lower divisions, dominated by volcanic and sedimentary rocks, respectively. Rocks of the volcanic-dominated succession include pyroxene-phyric basaltic breccia and tuff (Photo 1), rhyolite tuff (Photo 2), tuffaceous sediment, and carbonate (Photo 3). Rocks of the lower division are primarily clastic sediments that change, structurally down-section, with decreasing tuffaceous component and increasing quartz content. At lowest structural levels, isoclinally refolded graphitic quartz siltstone gives way to graphitic schist of the Whitewater suite. The contact is interpreted to have originally been stratigraphic.

MOUNT STAPLER QUARTZ MONZONITE

The Mount Stapler suite is cut by one or more irregular, dissected intrusions of pink quartz monzonite cut by the Llewellyn fault (Figure 2). Quartz monzonitic rocks are most common near the contact between basaltic breccia dominated strata and siltstone-limestone dominated strata, and clearly intrude both.

The intrusion ranges in composition from leucogabbro to quartz monzonite. Foliation is variably developed; moderately strong foliation is typical but original igneous fabrics are locally preserved. The original texture is sparsely potassium feldspar porphyritic (<5%, up to 2 cm, pink) in a hypidomorphic matrix of plagioclase, quartz, altered hornblende and biotite. The monzonite is cut by aplite and pegmatitic dikelets that, in turn, are cut by minor brittle faults with apparent dextral

Photo 1a. Deformed basaltic tuff of the Mount Stapler suite. Note preservation of original breccia fragments, now flattened in the foliation. (1b) More intensely deformed, finer grained and less competent mafic ash tuff.

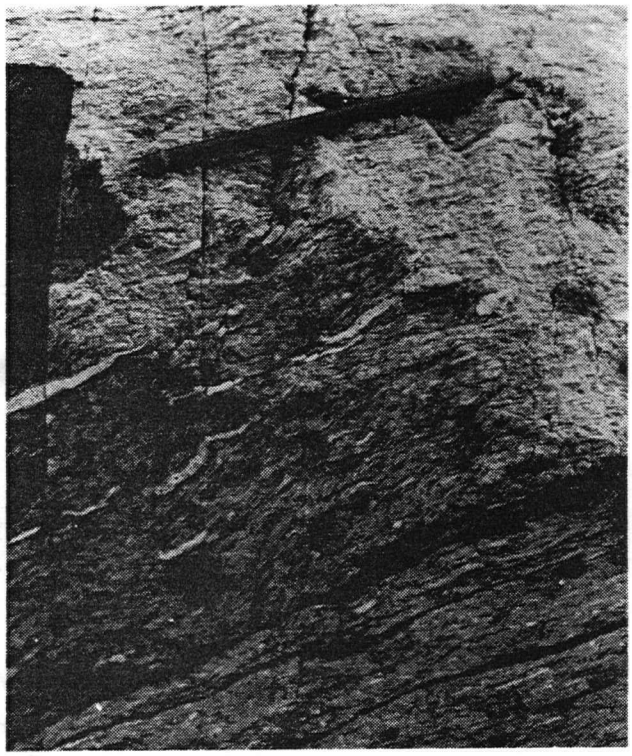

Photo 2. Deformed early Mississippian rhyolite of the Mount Stapler suite. Wavy white streaks are flattened and deformed lapilli.

Photo 3. Intensely folded, foliated, rusty carbonate of the Mount Stapler suite.

offset (Photo 4). No clear indication of shear sense is apparent within the ductile fabric; however, rotation of monzonite blocks is consistent with an overall sinistral shear sense (Photo 5). In places, brittle shears offset and isolate segments of monzonite dike (Photo 6).

GEOCHRONOLOGY

A sample was collected for U-Pb geochronology from the largest pink quartz monzonite body, a tabular stock 1.75 kilometres southeast of Mount Stapler (Figure 2). An effort was made to select the freshest, coarsest and most quartz-rich portion of the body. Approximately 40 kilograms, devoid of crosscutting dikelets, was collected. The results are presented below.

ANALYTICAL TECHNIQUES

The sample was processed and zircon was separated using conventional crushing, grinding, Wilfley table and heavy liquid techniques. All fractions were air abraded prior to analysis, to reduce the effects of surface-correlated lead loss (Krogh, 1982).

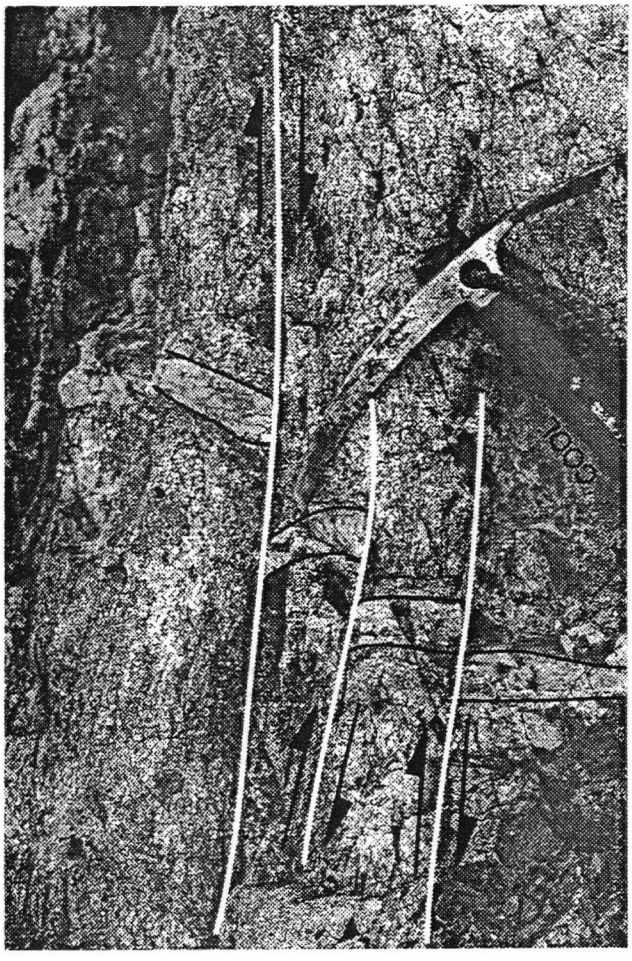

Photo 4. Pink quartz monzonite displays a weak to moderately developed foliation that is cut by late-phase(?) aplite and pegmatitic dikes. Dikes are cut by brittle faults with apparent dextral offset.

Photo 5. An apophysis of light-weathering pink quartz monzonite intrudes coarse basaltic tuff. It has been subjected to cataclasis, but the original eastern (left) contact is preserved (striking 170°, view to the north). Discrete shears offset the eastern contact in a consistently dextral sense, but do not offset the western contact, which is a ductile shear zone within chlorite schist. Counterclockwise rotation of the blocks is consistent with an overall sinistral shear sense.

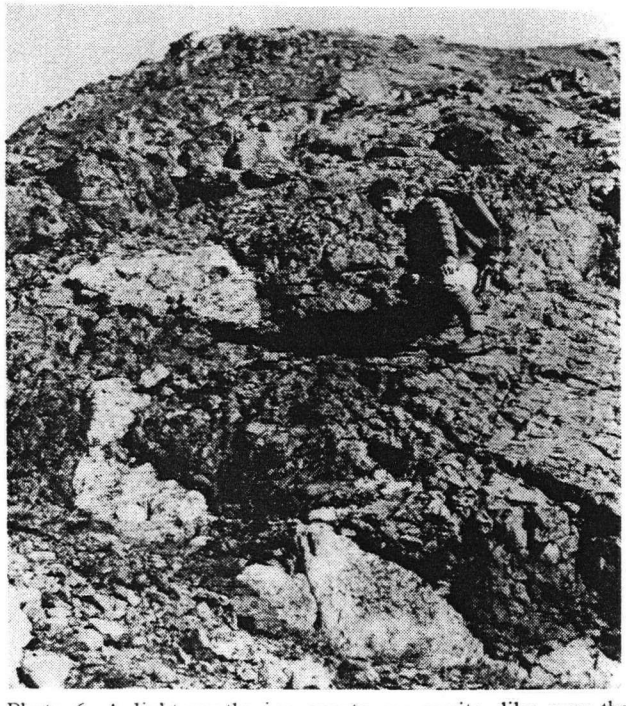

Photo 6. A light-weathering quartz monzonite dike near the Llewellyn fault zone is dissected by late brittle shears. In this photo, structurally isolated blocks float in matrix of chlorite schist with relict basaltic breccia fragments.

Sample preparation and U-Pb analyses were carried out at the Geochronology Laboratory of the University of British Columbia. Zircon grains were selected based on criteria such as magnetic susceptibility, clarity, morphology and size. Procedures for dissolution of zircon and extraction and purification of uranium and lead follow those of Parrish *et al.* (1987). Uranium and lead were loaded onto single, degassed refined rhenium filaments using the silica gel and phosphoric acid emitter technique. Procedural blanks were 9 and 6 picograms for lead and uranium, respectively. Errors assigned to individual analyses were calculated using the numerical error propagation method of Roddick (1987) and all errors are quoted at the 2σ level. Ages were calculated using the decay constants recommended by Steiger and Jäger (1977). Common lead corrections were made using the two-stage growth model of Stacey and Kramers (1975). Discordia lines were regressed using a modified York-II model (York, 1969; Parrish *et al.*, 1987). Uranium-lead analytical results are presented in Table 1.

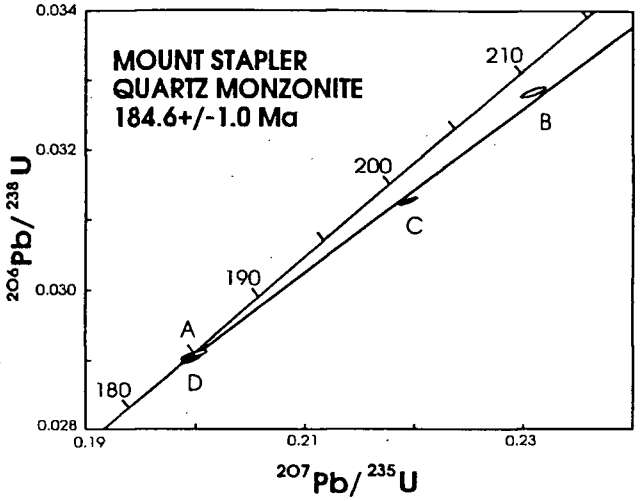

Figure 3. $^{206}Pb/^{238}U$ versus $^{207}Pb/^{238}U$ concordia diagram for the Mount Stapler quartz monzonite.

ANALYTICAL RESULTS

Zircons from this rock were high-quality prisms, with a length:width ratio of ~3:1. The grains had good clarity and contained minor colourless rod and bubble-shaped inclusions. Minimal material was found in the nonmagnetic separate therefore all fractions were picked from the 2°M separate. Initially three multi-grain fractions (A to C) of euhedral prisms, none with visible cores, were picked and separated on the basis of size. These three fractions yield $^{207}Pb/^{206}Pb$ ages which range from 185.2±10.4 to 240.2±7.8 Ma, for one concordant and two discordant analyses (Figure 3; Table 1). These results indicate an Early Jurassic crystallization age and the presence of an older, inherited zircon component, either as "cryptic" cores or xenocrysts. To confirm the age of the concordant fraction A, a fourth fraction was analyzed. Fraction D consisted of a single grain, broken in half and abraded to physically remove material which may have been present as an inherited component in the core of the grain. Fraction D is also concordant and is in good agreement with fraction A. Regression of the four fractions yields a loosely constrained lower Paleozoic upper intercept of $482\ ^{+161}/_{-145}$ Ma. This is consistent with the region being underlain by the Paleozoic Stikine assemblage. The best estimate of the age of crystallization of the quartz monzonite is given by the overlapping $^{206}Pb/^{238}U$ ages of fractions A and D, at 184.6 ±1.0 Ma.

CORRELATION AND IMPLICATIONS

Pink quartz monzonite within the Mount Stapler suite shares many lithological characteristics with coeval pink quartz monzonite of the Long Lakes Plutonic Suite in the Yukon (*sensu* Hart, 1994; Mortensen *et al.*, 1994). In southwest Yukon, these upper crustal level plutons intrude strongly foliated mid-crustal level quartz diorite bodies of the Aishihik Plutonic Suite (Hart, 1994; Johnston and Erdmer, in press), but both yield

TABLE 1. U-Pb ZIRCON ANALYTICAL DATA MOUNT STAPLER QUARTZ MONZONITE

Fraction[1]	Wt.	U	Pb^2	$^{206}Pb^3$	Pb^4	$^{208}Pb^5$	Isotopic ratios(±1σ,%)[6]			Isotopic dates(Ma,±2σ)[6]		
	mg	ppm	ppm	^{204}Pb	pg	%	$^{206}Pb/^{238}U$	$^{207}Pb/^{235}U$	$^{207}Pb/^{206}Pb$	$^{206}Pb/^{238}U$	$^{207}Pb/^{235}U$	$^{207}Pb/^{206}Pb$
A,m,M2,p(13)	0.072	241	7.2	1005	31	8.1	0.02909±0.11	0.1997±0.31	0.04979±0.23	184.8±0.4	184.8±1.0	185.2±10.4
B,f,M2,p(20)	0.072	263	8.7	1881	20	8.9	0.03284±0.12	0.2309±0.25	0.05099±0.17	208.3±0.5	210.9±0.9	240.2±7.8
C,f,M2,p(100)	0.144	508	15.8	4145	34	8.4	0.03126±0.10	0.2193±0.20	0.05088±0.11	198.5±0.4	201.3±0.7	235.3±5.1
D,c,M2,p(1)	0.012	2685	71.4	3562	16	8.6	0.02902±0.11	0.1993±0.23	0.04981±0.14	184.4±0.4	184.5±0.8	186.1±6.6

[1]All fractions are air abraded. Grain size, smallest dimension: c = +134μm, m = -134 μm + 74 μm, f = -74 μm;
Magnetic codes: Franz magnetic separator sideslope at which grains are magnetic; e.g., M2=magnetic at 1°; Field strength for all fractions =1.8A; Front slope for all fractions=20°; Grain character codes: p=prismatic; number in brackets refers to number of grains in analysis.
[2]Radiogenic Pb
[3]Measured ratio corrected for spike and Pb fractionation of 0.0043/amu ±20% (Daly collector)
[4]Total common Pb in analysis based on blank isotopic composition
[5]Radiogenic Pb
[6]Corrected for blank Pb, U and common Pb (Stacey-Kramers model Pb composition at the $^{207}Pb/^{206}Pb$ date of fraction, or age of sample)

crystallization ages that are the same within error. Near the south end of Tagish Lake, hornblende granodiorite orthogneiss is interleaved with metamorphosed volcanic arc rocks of the Boundary Ranges suite (Mihalynuk *et al.*, 1990; Currie, 1990). This unit yielded a U-Pb age of 185±1 Ma (Currie, 1992), similar to the lithologically identical Aishihik batholith (187 $^{+9.7}/_{-1.0}$ Ma; Johnston, 1993).

Plutons of identical age and similar composition are also present within the Stikine Terrane to the south, in the Iskut River area. These include 186±1 Ma plagioclase porphyry in the Brucejack Lake area (Davies *et al.*, 1994) and the 185±5 Ma Eskay porphyry (Macdonald *et al.*, 1992).

The Mount Stapler suite is interpreted to be metamorphosed Stikine assemblage. This correlation is supported by similarities between the Stikine assemblage and Mount Stapler lithologies (where relict protolith textures are preserved) and the proportion of similar lithologies within Stikine assemblage in the Tulsequah area. The correlation is further supported by a preliminary early Mississippian U-Pb age from a metarhyolite from Mount Stapler (F. Childe, preliminary data, not presented in this paper). Zircons from this unit have similar morphology and degree of inheritance to zircon from the early Mississippian Stikine assemblage rhyolite that hosts massive sulphide mineralization at the Tulsequah Chief mine (Sherlock *et al.*, 1994).

DISCUSSION

The Early Jurassic U-Pb age of 184.6±1.0 Ma from pink quartz monzonite intruding the Mount Stapler suite is significant as it strengthens correlations between upper units of the northern Stikine Terrane with those in the Yukon-Tanana Terrane to the north. If correlations between the Mount Stapler structural suite and the Stikine assemblage are correct, then many of the metavolcanic rocks to the north may be prospective for volcanogenic massive sulphide accumulations, similar to those at the Tulsequah Chief deposit.

ACKNOWLEDGMENTS

The authors thank Redfern Resources Limited for the generous use of its camp during the 1993 field season. Research by F.C. in the Tulsequah area forms part of a Mineral Deposit Research Unit project on Volcanogenic Massive Sulphide Deposits of the Canadian Cordillera, funded by the Natural Science and Engineering Research Council of Canada, Science Council of British Columbia and mining and exploration member companies.

REFERENCES

Currie, L.D. (1990): Metamorphic Rocks in the Florence Range, Coast Mountains, Northwestern British Columbia (104M/8); *in* Geological Fieldwork 1989, *B.C. Ministry of Energy, Mines and Petroleum Resources*, Paper 1990-1, pages 197-203.

Currie, L.D. (1992): Metamorphic Rocks in the Tagish Lake Area, Northern Coast Mountains, British Columbia: A Possible Link Between Stikinia and parts of the Yukon-Tanana Terrane; *in* Current Research, Part A, *Geological Survey of Canada*, Paper 92-1A, pages 199-208.

Davies, A. G. S., Lewis, P. D. and Macdonald, A. J. (1994): Stratigraphic and Structural Setting of Mineral Deposits in the Brucejack Lake Area, Northwestern British Columbia; *Geological Association of Canada*, Program with Abstracts, page A26.

Doherty, R. A. and Hart, C. R. J. (1988): Preliminary Geology of the Fenwick Creek (105D/3) and Alligator Lake (105D/6) Map Areas; *Indian and Northern Affairs Canada*, Open File 1988-2, 87 pages.

Hart, C.J.R. (1994): Magmatic and Tectonic Evolution of the Intermontane Superterrane and Coast Plutonic Complex in Southern Yukon Territory; unpublished M.Sc. thesis, *University of British Columbia*.

Johnston, S.T. (1993): The Geologic Evolution of Nisling Assemblage and Stikine Terrane in the Aishihik Lake Area, Southwest Yukon; unpublished Ph.D. thesis, *University of Alberta*, Edmonton, 270 pages.

Johnston, S.T. and Erdmer, P. (in press): Magmatic Flow and Emplacement Foliations in the Early Jurassic Aishihik Batholith, Southwest Yukon: Implications for Northern Stikinia; *in* Jurassic Magmatism and Tectonics of the North American Cordillera, Miller, D. and Ruby, C., Editors, *Geological Society of America*, Special Paper 299.

Krogh, T. (1982): Improved Accuracy of U-Pb Zircon Ages by the Creation of More Concordant Systems Using Air Abrasion Technique; *Geochemica et Cosmochemica Acta*, Volume 46, pages 637-649.

Macdonald, A. J., van der Heyden, P., Lefebure, D. V. and Alldrick, D. J. (1992): Geochronometry of the Iskut River Area - An Update (104A and B); *in* Geological Fieldwork 1991, Grant, B. and Newell, J. M., Editors, *B.C. Ministry of Energy, Mines and Petroleum Resources*, Paper 1992-1, pages 495-502.

Mihalynuk, M.G. and Rouse, J.N. (1988a): Preliminary Geology of the Tutshi Lake Area, Northwestern British Columbia (104M/15); *in* Geological Fieldwork 1987, *B.C. Ministry of Energy, Mines and Petroleum Resources*, Paper 1988-1, pages 217-231.

Mihalynuk, M.G. and Rouse, J.N. (1988b): Geology of the Tutshi Lake Area (104M/15); *B.C. Ministry of Energy, Mines and Petroleum Resources*, Open File 1988-5.

Mihalynuk, M.G., Currie, L.D., Mountjoy, K. and Wallace, C. (1989): Geology of the Fantail Lake (West) and Warm Creek (East) Map Area (NTS 104M/9W and 10E); *B.C. Ministry of Energy, Mines and Petroleum Resources*, Open File 1989-13.

Mihalynuk, M.G., Mountjoy, K.J., Currie, L.D., Lofthouse, D.L. and Winder, N. (1990): Geology and Geochemistry of the Edgar Lake and Fantail Lake Map Area, (NTS 104M/8, 9E); *B.C. Ministry of Energy, Mines and Petroleum Resources*, Open File 1990-4.

Mihalynuk, M.G., Smith, M.T. Hancock, K.D. and Dudka, S. (1994a): Regional and Economic Geology of the Tulsequah River and Glacier Areas (104K/12 & 13); *in* Geological Fieldwork 1993, Grant, B. and Newell, J.M., Editors, *B.C. Ministry of Energy, Mines and Petroleum Resources*, Paper 1994-1, pages 171-197.

Mihalynuk, M.G., Smith, M.T. Hancock, K.D., Dudka, S. and Payne, J. (1994b): Tulsequah River and Glacier Areas (104K/12 & 13); *B.C. Ministry of Energy, Mines and Petroleum Resources*, Open File 1994-3.

Mihalynuk, M.G., Meldrum, D., Sears, S. and Johannson, G. (1995): Geology and Mineralization of the Stuhini Creek Area (104K/11); *in* Geological Fieldwork 1994, Grant, B. and Newell, J.M., Editors, *B.C. Ministry of Energy,*

Mines and Petroleum Resources, Paper 1995-1, this volume.

Monger, J.W.H. (1977): Upper Paleozoic Rocks of the Western Canadian Cordillera and their Bearing on Cordilleran Evolution; *Canadian Journal of Earth Sciences*, Volume 14, pages 1832-1859.

Mortensen, J.K. (1992): Pre-mid-Mesozoic Evolution of the Yukon-Tanana Terrane, Yukon and Alaska; *Tectonics*, Volume 11, pages 836-854.

Mortensen, J.K., Johnston, S.T., Murphy, D.C. and Bremner, T.J. (1994): Age and Metallogeny of Mesozoic and Tertiary Plutonic Suites in the Yukon; Abstract, *Canadian Institute of Mining, Metallurgy and Petroleum*, 16th District 6 Annual General Meeting, Vancouver.

Nelson , J. and Payne, J. G. (1984): Paleozoic Volcanic Assemblages and Volcanogenic Massive Sulphide Deposits near Tulsequah, British Columbia; *Canadian Journal of Earth Sciences*, Volume 21, pages 379-381.

Parrish, R. R., Roddick, J. C., Loveridge, W. D. and Sullivan, R. W. (1987): Uranium-Lead Analytical Techniques at the Geochronological Laboratory, Geological Survey of Canada; *in* Radiogenic Age and Isotopic Studies, Report 1, *Geological Survey of Canada*, Paper 87-2, pages 3-7.

Roddick, J, C. (1987): Generalized Numerical Error Analysis with Applications to Geochronology and Thermodynamics; *Geochimica et Cosmochimica Acta*, Volume 51, pages 2129-2135.

Sherlock, R., Childe, F., Barrett, T.J., Mortensen, J.K., Chandler, T., Lewis, P., McGuigan, P., Dawson, G.L. and Allen, R. (1994): Geological Investigations of the Tulsequah Chief Massive Sulphide Deposit, Northwestern British Columbia; *in* Geological Fieldwork 1993, Grant, B. and Newell, J.M., Editors, *B.C. Ministry of Energy, Mines and Petroleum Resources*, Paper 1994-1, pages 373-379.

Souther, J. G. (1971): Geology and Mineral Deposits of the Tulsequah Map-area, British Columbia; *Geological Survey of Canada*, Memoir 362, 84 pages.

Stacey, S. J. and Kramers, J. D. (1975): Approximation of Terrestrial Lead Isotope Evolution by a Two-stage Model; *Earth and Planetary Science Letters*, Volume 26, pages 207-221.

Steiger, R. H. and Jäger, E. (1977): Subcommission on Geochronology: Convention on the Use of Decay Constants in Geo- and Cosmochronology; *Earth and Planetary Science Letters*, Volume 36, pages 359-362.

York, D. (1969): Least-squares Fitting of a Straight Line with Correlated Errors; *Earth and Planetary Science Letters*, Volume 5, pages 320-324.

GEOLOGICAL INVESTIGATIONS OF THE TULSEQUAH CHIEF MASSIVE SULPHIDE DEPOSIT, NORTHWESTERN BRITISH COLUMBIA (104K/12)

By R.L. Sherlock, F. Childe, T.J. Barrett, J.K. Mortensen, P.D. Lewis
Mineral Deposit Research Unit, U.B.C.
T. Chandler
Redfern Resources Limited
P. McGuigan, G.L. Dawson
Cambria Geological Limited
R. Allen
Volcanic Resources

(MDRU Contribution 045)

KEYWORDS: economic geology, Tulsequah Chief, Big Bull, massive sulphides, volcanogenic, Mount Eaton Group

INTRODUCTION

The Tulsequah Chief volcanogenic massive sulphide deposit (58° 30'N, 133° 35'W) is located along the east bank of the Tulsequah River, 100 kilometres south of Atlin, British Columbia and 70 kilometres northeast of Juneau, Alaska (Figure 1). At present, access to the site is limited to small aircraft via two nearby airstrips. The Tulsequah Chief deposit is accessible by adits at several levels on the west side of Mount Eaton. The Big Bull deposit is located along strike 10 kilometres south of Tulsequah Chief on the southern flank of Mount Manville at the confluence of the Tulsequah and Taku rivers (Figure 1).

Fieldwork in 1993 involved relogging and sampling of selected drill-core through sections of the Tulsequah Chief mine stratigraphy, as well as underground sampling on the 5400 level and surface sampling around both the Tulsequah Chief and Big Bull deposits. Samples are being analyzed for lithogeochemistry, geochronology, mineralogy and fluid inclusions. This contribution describes the preliminary results and interpretations of the volcanic stratigraphy at the Tulsequah Chief deposit.

The objectives of the overall study are: to define the main stratigraphic units at Tulsequah Chief on the basis of detailed lithogeochemistry and petrography; to determine if this stratigraphy can be correlated across the 4400E and 5300E faults, which divide the property into western, central and eastern blocks; to identify the different levels and styles of mineralization and their origins; to date both the host volcanic rocks and the associated intrusive rocks; and to determine the distribution and intensity of alteration associated with mineralization.

For a detailed discussion of the regional geology the reader is referred to Kerr (1948), Souther (1971), Nelson and Payne (1984) and Mihalynuk *et al.* (1994).

EXPLORATION AND PRODUCTION HISTORY

The Tulsequah Chief deposit was discovered in 1923 by W. Kirkham of Juneau. Subsequent activity in this area led to the discovery in 1929 of both the associated Big Bull massive sulphide deposit and the Polaris-Taku gold deposit. The Tulsequah Chief and Big Bull deposits were acquired by the Consolidated Mining and Smelting Company of Canada, Limited (Cominco) in 1946 and brought into production in 1951. The mines closed in 1957 due to depressed metal prices. Total production from the two orebodies was 933 520 tonnes with an average grade of 1.59% copper, 1.54% lead, 7.0% zinc, 3.84 grams per tonne gold and 126.5 grams per tonne silver. Of this ore, 622 136 tonnes were from the Tulsequah Chief orebody and the remaining 311 384 tonnes from the Big Bull deposit (McGuigan *et al.*, 1993).

A joint venture between Cominco and Redfern Resources Limited from 1987 to 1991 led to extensive exploration including over 21 000 metres of surface and underground diamond drilling (Casselman, 1988, 1989, 1990). In June 1992, Redfern Resources purchased Cominco's interest (60%) in the property and consequently now owns 100% of the Tulsequah Chief and Big Bull orebodies and adjacent ground. In 1992 an additional 4 579 metres of underground diamond-drilling was completed; in addition, surface mapping and relogging of drill core were carried out by Cambria Geological Limited. Reserve estimates made by Cambria Geological at the end of the 1992 program for all ore horizons and classes were 8 500 592 tonnes grading 1.48% copper, 1.17% lead, 6.86% zinc, 2.56 grams per tonne gold and 103.4 grams per tonne silver (McGuigan *et al.*, 1993).

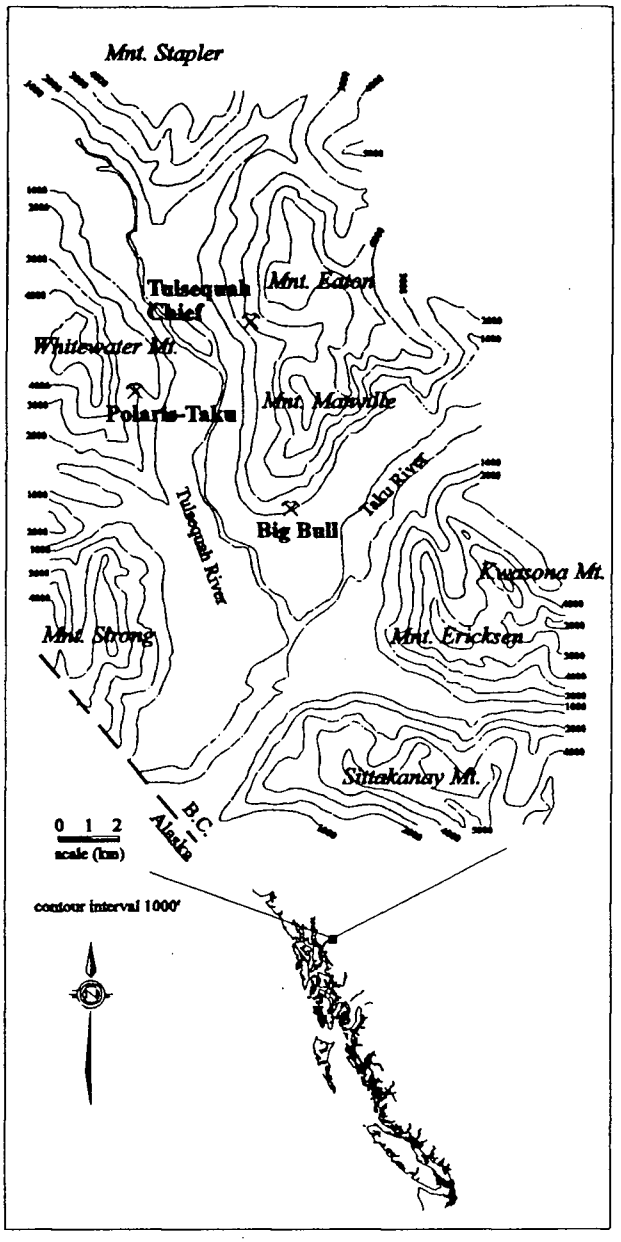

Figure 1. Location map for the Tulsequah Chief, Big Bull and Polaris-Taku deposits, from Nelson and Payne (1984).

Current exploration on the property, by Redfern Resources Limited, consists of geological mapping, geophysical surveys, underground and surface diamond-drilling at both the Tulsequah Chief and Big Bull orebodies. Diamond drilling in 1993 includes 8 060 metres from the surface and underground at Tulsequah Chief, and 3 700 metres from the surface at Big Bull.

MINE SEQUENCE STRATIGRAPHY

The stratigraphy at the Tulsequah Chief deposit is composed of a series of northward-younging mafic and felsic volcanic rocks (Figure 2). The stratigraphically lowest unit (unit 1) is composed of mafic volcanic rocks forming the footwall to mineralization. This unit is directly overlain by a series of dacitic flows, sills and volcaniclastic material (units 2 and 4). On the basis of contact relationships, units 2 and 4 are interpreted to have originally been a single felsic (dacitic) package which was subsequently intruded by a large mafic sill (unit 3). The upper felsic unit (unit 4) is overlain by a series of mafic flows or sills and volcaniclastic sediments (unit 5). All of these units are intruded by Tertiary Sloko dikes, mainly of felsic composition. The lithological units are based on field descriptions and limited petrology and may be modified as a result of future lithogeochemical results.

UNIT 1

Unit 1 forms the stratigraphic footwall to the massive sulphide deposits and comprises mainly massive to flow-brecciated mafic volcanics with minor volcanic sediment. Alteration and metamorphism have modified the primary mineralogy to an assemblage of quartz, sericite, chlorite, biotite, pyrite and hematite. The top of the unit is strongly amygdaloidal and commonly contains hyaloclastic textured material. The amygdules are typically filled by quartz, pyrite and chalcopyrite. Cordierite porphyroblasts are variably developed in areas immediately underlying the sulphide mineralization.

UNIT 2

Unit 2 is the principle host to sulphide mineralization in the lower mine stratigraphy, and comprises massive, flow-brecciated and volcaniclastic dacite. Several massive sulphide lenses, collectively termed the H-AB horizon, are hosted by dacite mass-flow material containing variable amounts of sulphide and cherty clasts. Intrusive into the mass-flow unit are dacite sills that locally dilate and split the package. This process, and subsequent fault dislocations, has separated the mineralized horizon into discrete sulphide lenses termed the F, AB_1, AB_2, H, I and G zones (Figure 2). Unit 2 thickens to the west, which may indicate a dacitic source in this direction. The dacite consists of plagioclase and quartz phenocrysts in a groundmass of quartz, sericite and epidote.

UNIT 3

A thick massive mafic sill (unit 3) with chilled margins and intercalations of dacitic material at either margin separates the upper and lower felsic packages. Unit 3 is up to 50 metres thick and is slightly discordant to stratigraphy; it probably represents a low-angle sill that has intruded the dacitic (fragmental-rich) package. The margins of unit 3 are finer-grained then the interior which has a diabasic texture. The primary mineralogy of the sill comprises augite, plagioclase and olivine phenocrysts in a fine-grained plagioclase groundmass. This assemblage is overprinted by coarse-grained randomly oriented chlorite and amphibole of possible metamorphic origin. The unit appears to be relatively unaltered compared to units 1, 2 and 4, suggesting it was emplaced after the mineralizing event. Unit 3 may be the subvolcanic equivalent of unit 5.

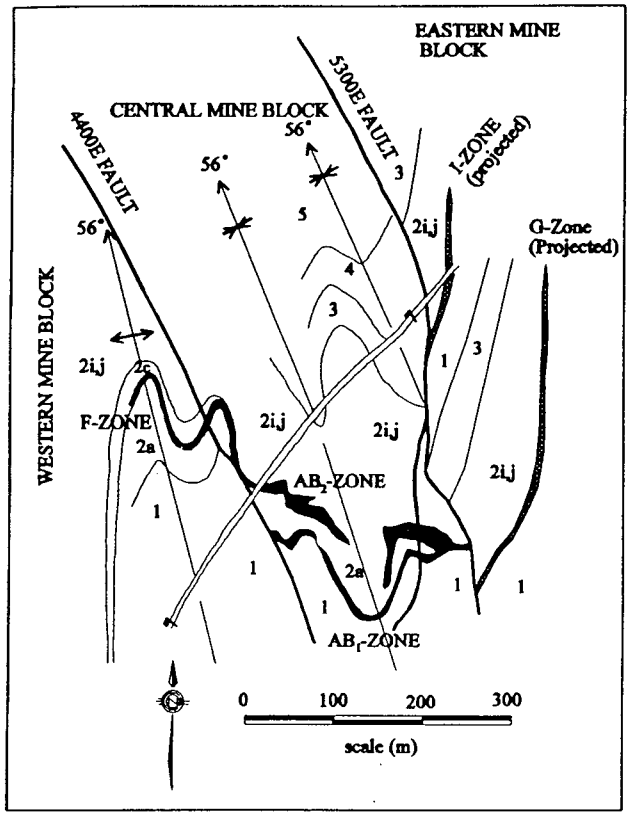

Figure 2. Tulsequah Chief 5400 level geology map: 1, undifferentiated basalt; 2a, mixed felsic fragmental rock; 2c, banded to massive chert; 2i,j, dacite flow, flow breccia and lapilli tuff; 3, undifferentiated mafic sill; 4, undifferentiated upper felsic horizon; 5, undifferentiated mafic flows and epiclastic rocks; 7, Sloko dike. Black areas are sulphide mineralization. Mapping from McGuigan *et al.*, 1993.

UNIT 4

The upper felsic package (unit 4) is very similar to unit 2 but may contain a greater proportion of volcaniclastic material. Unit 4 is composed mainly of dacitic mass-flows with pumice, lithic, chert and barite fragments. The preservation of angular pumice fragments suggests that the volcaniclastic material has not been highly reworked. East of the 5300E fault felsic rocks, previously assigned to unit 4, are host to the I zone sulphide lens which was the main focus of early mining activity. Recent mapping and drill-hole interpretation suggest that the I zone may be a structural offset of the G zone and may correlate with the lower felsic stratigraphy of unit 2.

UNIT 5

The upper mafic package (unit 5) is primarily massive mafic flows or sills, and intercalated sediments composed mainly of argillite, siltstone, ash tuff and minor chert. The unit is typically unaltered and lies above all known mineralization.

STRUCTURE

Stratigraphic units at Tulsequah Chief outline a series of north to northwest-plunging folds which are divided into three discrete structural blocks by the 5300E and 4400E faults (Figure 2). These faults are exposed in several locations in the 5400 level mine workings. The 5300E fault is the most significant and probably has the largest displacement of the faults on this level. Kinematic indicators record an early period of dextral motion with a gently northward-plunging slip vector, followed by movement along a southerly plunging slip vector of unknown sense. The dextral motion is probably the most important in terms of displacement, but determination of absolute displacements requires a detailed analysis of stratigraphy in the central and eastern mine blocks. The 4400E and minor unnamed faults of variable orientation cause no large-scale displacement of stratigraphic contacts.

MINERALIZATION

The sulphide deposits described here occur primarily within volcaniclastic mass-flows of unit 2. Several sulphide facies have been defined by Cambria Geological Limited and Redfern Resources. The pyrite facies consists mainly of massive pyrite with little base metal content. The zinc facies is composed primarily of semimassive pale yellow sphalerite, pyrite, galena, chalcopyrite and tetrahedrite, with barite, quartz and sericitically altered lithic fragments. The copper facies is mainly massive pyrite with up to several percent disseminated chalcopyrite. Stringer mineralization is quite common in the footwall and is composed of thin, anastomosing quartz veins with dark red sphalerite and minor chalcopyrite.

The sulphides in unit 2 felsic volcaniclastics may have formed from hydrothermal fluids that precipitated metals within the highly permeable felsic mass-flow, close to the seafloor. Also present in unit 2 are near-massive sulphide beds that may represent precipitates directly onto the seafloor, where barite and chert also accumulated episodically. Finally, the presence of detrital massive sulphide fragments and chert and barite clasts in unit 2 indicates that some reworking has occurred. The different styles of mineralization are currently under study in terms of stratigraphic level and facies variations, mineralogical and isotopic variations, and temperature and composition of mineralizing fluids.

Although the overall mine stratigraphy is relatively consistent, the composition of the sulphide mineralization and its relationships to extrusive and intrusive rocks are quite variable. This is best demonstrated by drill holes TCU 90-22 (Figure 3) and TCU 92-36 (Figure 4). Although these two holes are located less than 200 metres apart, TCU 90-22 intersects an interval of uninterrupted sulphide mineralization, in contrast to TCU 92-36 which intersects two significant intervals of mineralization separated by about 24 metres of dacite sill and 7 metres of mafic sill.

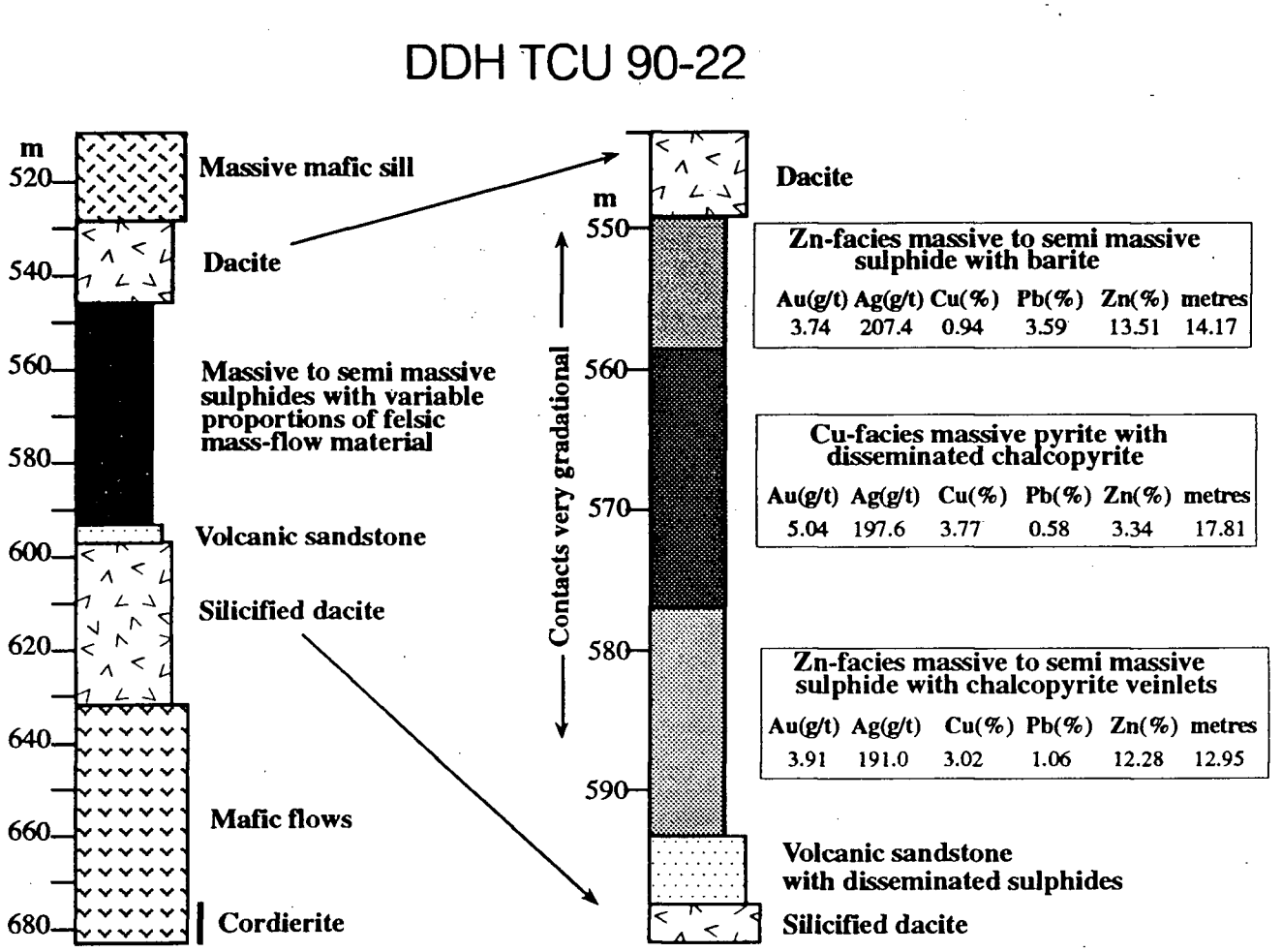

Figure 3. Stratigraphic section for diamond-drill hole TCU 90-22.

GEOCHRONOLOGY

On the basis of mapping and biochronology by Nelson and Payne (1984), the Tulsequah Chief deposit was considered to be mid-Pennsylvanian to Early Permian in age. The fossil locality described by Nelson and Payne is about 2 kilometres northeast of the Tulsequah deposit, making its stratigraphic position with respect to the ore horizon uncertain. In order to help date the volcanic stratigraphy, a coarse-grained volcaniclastic rock from unit 4, near the 6400 portal, was analyzed by J. Mortensen. Results for this sample are presented below.

ANALYTICAL TECHNIQUES

Approximately 50 kilograms of dacite from unit 4, the upper felsic volcanic unit, was collected by M. Casselman of Cominco for U-Pb dating. Zircons were separated using conventional Wilfley table and heavy liquid techniques. Most zircon fractions were abraded prior to analysis (Krogh, 1982) to minimize the effects of surface-correlated lead loss. Uranium-lead analyses were done at the geochronology laboratory at the Geological Survey of Canada (Ottawa). Criteria for selection of grains for analysis, and procedures used for dissolution, chemical extraction and purification of uranium and lead, and mass spectrometry are described in detail by Parrish *et al.* (1987). Procedural blanks were 20 to 7 picograms for lead and less than 1 picogram for uranium. Uranium-lead analytical data are given in Table 1. Errors assigned to individual analyses were calculated using the numerical error propagation method of Roddick (1987). Age calculations employed the decay constants recommended by Steiger and Jäger (1975), and initial common lead compositions from the model of Stacey and Kramers (1975). Concordia intercept ages were calculated using a modified York-II regression model as described by Parrish *et al.* (1987), and the algorithm of Ludwig (1980). All errors in ages are given at the 2σ level.

ANALYTICAL RESULTS

About one-half of the original dacite sample was processed initially. Only a small amount of zircon was recovered. The zircons form a relatively homogeneous population of mainly fine, very pale pink, clear grains with rare to abundant clear, bubble- and rod-shaped inclusions. Igneous zoning was faint to absent, and no cores were observed. The grains range from equant to

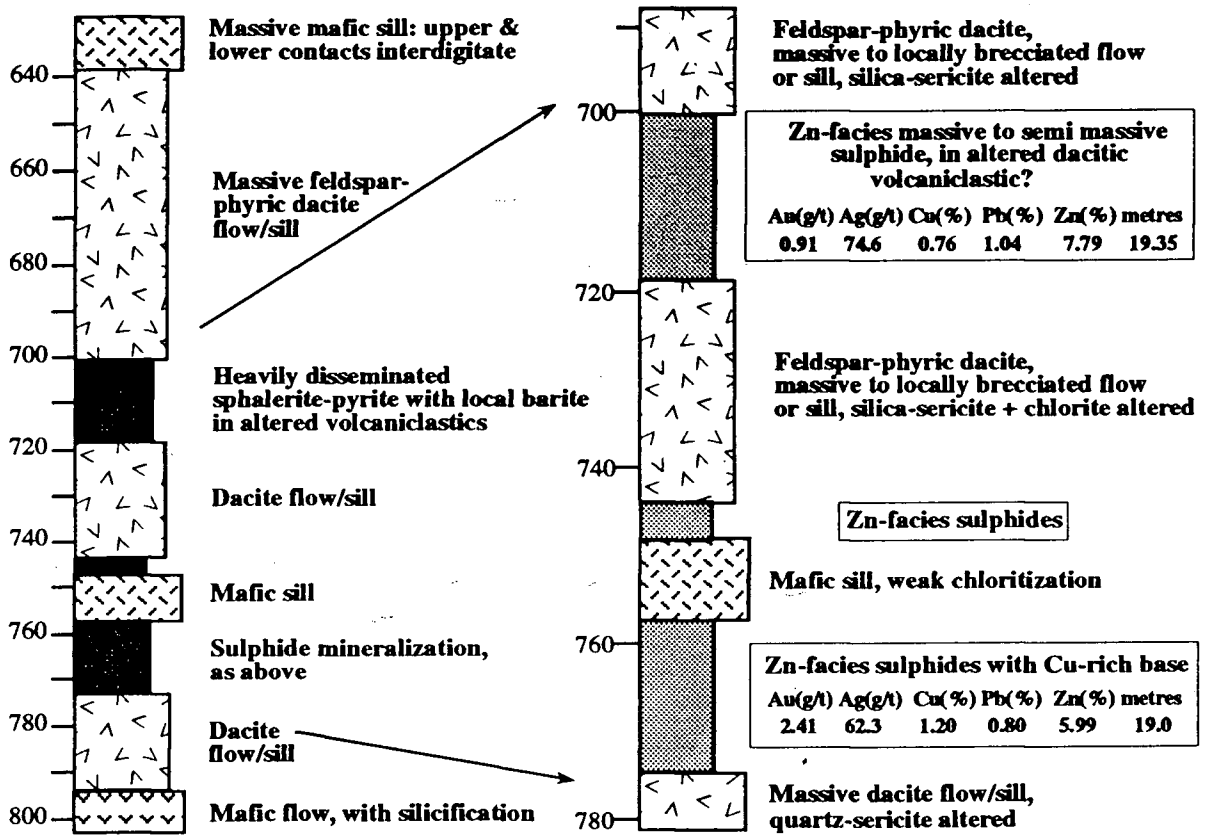

Figure 4. Stratigraphic section for diamond-drill hole TCU 92-36

TABLE 1
URANIUM-LEAD ANALYTICAL DATA FOR TULSEQUAH CHIEF UNIT 4 DACITE

Sample Description	Wt. (mg)	U (ppm)	Pb^2 (ppm)	$^{206}Pb/^{204}Pb$ (meas.)[3]	% ^{208}Pb[2]	$^{206}Pb/^{238}U$[4] (± % 1s)	$^{207}Pb/^{235}U$[4] (± % 1s)	$^{207}Pb/^{206}Pb$[4] (± % 1s)	$^{207}Pb/^{206}Pb$[4] (Ma; ± % 2s)
A: N,+74,a	0.039	198	61.6	4291	20.0	0.26286(0.09)	3.6394(0.10)	0.10042(0.04)	1631.8(1.4)
B: N,+74,a	0.057	269	84.9	6950	12.4	0.28528(0.09)	4.9473(0.10)	0.12577(0.03)	2039.7(1.1)
C: N,-44	0.079	275	55.5	5519	8.8	0.19475(0.08)	2.6157(0.10)	0.09741(0.03)	1575.1(1.3)
D: N,-44	0.063	390	64.8	2876	8.3	0.16325(0.09)	1.9072(0.11)	0.08473(0.05)	1309.4(1.8)
EA: bulk,a	0.011	193	11.3	737	12.6	0.05633(0.14)	0.4162(0.40)	0.05358(0.35)	353.4(15.8)
EB: bulk,single,a	0.003	292	15.1	318	15.8	0.04805(0.21)	0.3566(0.89)	0.05383(0.79)	363.9(35.4)
F: bulk,best prisms,a	0.015	213	12.0	1237	11.6	0.05478(0.10)	0.4042(0.23)	0.05352(0.19)	350.7(8.7)

[1] +74, -74 refers to grain size in diameter (μ); N, nonmagnetic on Frantz magnetic separator; a, abraded

[2] radiogenic Pb; corrected for blank, spike and initial common Pb

[3] corrected for spike and fractionation

[4] corrected for blank Pb and U, and common Pb. Errors are 1 standard error of mean for isotopic ratios and 1σ for derived ages

stubby prismatic (l:w = 2-3) subhedral forms to irregular, anhedral, commonly broken grains showing smoothly corroded surfaces suggestive of magmatic corrosion. Four fractions were selected for analysis. Two of these were relatively coarse (>74μ diameter) equant to prismatic grains, and were strongly abraded prior to dissolution. Two other fractions of finer unabraded grains were also analyzed. The four analyses are all moderately to highly discordant (Figure 5) and yield surprisingly old $^{207}Pb/^{206}Pb$ ages (up to 2040 Ma). In view of the probable mid-Paleozoic crystallization age inferred for the volcanic rocks in the Tulsequah region, the data were taken to indicate the presence of a major component of older zircon in the sample, either as inherited cores or, more likely, as xenocrysts that did not differ greatly in appearance from the igneous grains. Zircon was subsequently separated from the remaining sample of dacite, and three fractions were selected and abraded. One fraction (F) was of the clearest, most euhedral prismatic grains in the sample, a second fraction (EA) consisted of very clear fragments with at least one well-preserved euhedral facet, and the third fraction was a single, faintly zoned, subhedral, stubby prismatic grain with a slightly more inclusion-rich core. These three fractions yield much younger $^{207}Pb/^{206}Pb$ ages, and define a linear array (Figure 5) with calculated upper and lower intercept ages of 350.6 +14.7/-6.2 and -72 ± 267 Ma, respectively. One of the fractions (EA) is concordant with a $^{207}Pb/^{206}Pb$ age of 353.8 ± 15.8 Ma. The similarity of the $^{207}Pb/^{206}Pb$ ages of the three fractions suggests that they were all free of inheritance (despite the slightly cloudy core visible in single grain EB). We consider the best estimate of the crystallization age of the dacite sample to be given by the $^{207}Pb/^{206}Pb$ and $^{206}Pb/^{238}U$ ages of fraction EA, and therefore assign a latest Devonian to earliest Mississippian age of 353.4 +15.8/-0.9 Ma to the sample.

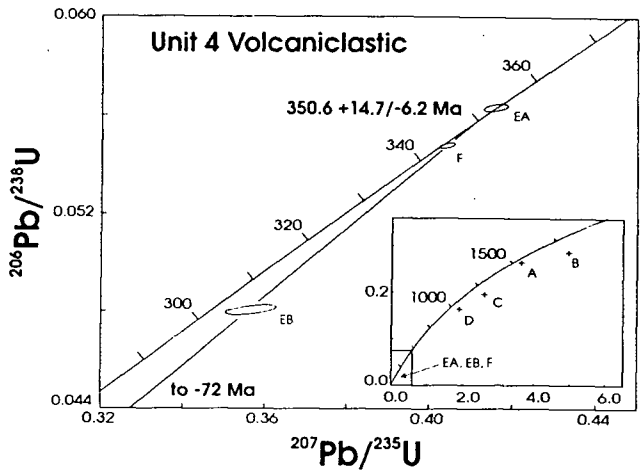

Figure 5. $^{206}Pb/^{238}U$ vs. $^{207}Pb/^{235}U$ concordia diagram for unit 4 (upper felsic horizon)

DISCUSSION

A preliminary interpretation of the early geological history of the mine area is:

1) accumulation of a widespread mafic volcanic basement composed of basaltic flows and sills and minor tuffaceous sediments;
2) accumulation of massive dacitic volcanic flows and flow breccias;
3) mass flows of dacitic to heterolithic volcaniclastic debris with local baritic to cherty intervals;
4) emplacement of sulphide mineralization at a number of stratigraphic levels associated with the dacitic volcaniclastic package; sulphides infilled porous unconsolidated debris flows and accumulated as exhalative units together with barite and chert between debris flows;
5) intrusion of the dacitic volcaniclastic package by one or more dacite sills which acted to dilate the original mineralized intervals;
6) intrusion of the unit 3 mafic sill, further dilating the felsic package to produce felsic units 2 and 4;
7) accumulation of the unit 5 mafic volcanic rocks. It is possible that unit 5 is coeval with, and genetically related to the unit 3 sill.

FURTHER WORK

Further work will involve: examination of primary volcanic textures and facies relationships to determine the physical environment of ore formation; lithogeochemical and petrographic analysis of all units to determine the stratigraphic relationships and the effect of alteration throughout the camp; uranium-lead geochronology on newly collected samples from, the upper and lower felsic volcanic packages within the central mine block, unit 3 mafic intrusion, a felsic volcanic sample from the Big Bull deposit and two regional felsic units.

Galena samples were collected from all mineralized horizons for lead isotope analysis. On a regional scale a detailed analysis of the lead isotopic signature may yield information on the tectonic setting and evolution of the Tulsequah Chief and Big Bull deposits. Locally, minor variations in the lead isotopic composition of the different ore lenses may assist in correlating mineralized horizons between the major fault blocks.

Mineralized intervals have been sampled for fluid inclusion and stable isotope analysis to determine the physical and chemical conditions of the ore-forming fluids and how they may have varied both temporally and spatially.

ACKNOWLEDGMENTS

We are indebted to Redfern Resources Limited and Cambria Geological Limited for permission to publish information on the Tulsequah Chief deposit. We have benefited from discussions with Don Harrison, Bob Carmichael and Kerry Curtis of Redfern Resources on the geology of the Tulsequah Chief and Big Bull properties. We thank Mike Casselman of Cominco Ltd., previous owner of the property, for supplying the dacite

sample for U-Pb dating.

JKM thanks the staff of the Geochronology Section at the Geological Survey of Canada in Ottawa for assistance in producing the U-Pb analytical data, and R.W. Kirkham for arranging for collection of the geochronology sample and for many useful discussions regarding Tulsequah and other volcanogenic massive sulphide deposits in the Cordillera.

Research at the Tulsequah Chief - Big Bull properties forms part of a Mineral Deposit Research Unit project on Volcanogenic Massive Sulphide Deposits of the Cordillera funded by the Natural Sciences and Engineering Research Council of Canada, Science Council of British Columbia and ten mining and exploration member companies.

REFERENCES

Casselman, M.J. (1988): Tulsequah Chief Property; *Cominco Ltd.*, 1987 Year End Internal Report.

Casselman, M.J. (1989): Tulsequah Chief Property; *Cominco Ltd.*, 1988 Year End Internal Report.

Casselman, M.J. (1990): Tulsequah Chief Property; *Cominco Ltd.*, 1989 Year End Internal Report.

Kerr, F.A. (1948):Taku River Map Area, British Columbia; *Geological Survey of Canada* Memoir 248, 84 pages.

Krogh, T. (1982): Improved Accuracy of U-Pb Zircon Ages by the Creation of More Concordant Systems Using Air Abrasion Technique; *Geochimica et Cosmochimica Acta*, Volume. 46, pages 637-649.

Ludwig, K. R. (1980): Calculation of Uncertainties of U-Pb Isotope Data; *Earth and Planetary Science Letters*, Volume 46, pages 212-220.

McGuigan, P., Melnyk, W., Dawson, G.L. and Harrison, D. (1993): Tulsequah Chief Mine, Northwestern B.C. 1992 Exploration Program: Diamond Drilling, Geology and Reserve Estimation; *Cambria Geological Limited*, Vancouver, B.C. unpublished report in three volumes.

Mihalynuk, M.G., Smith, M.T., Hancock, K.D. and Dudka, S. (1994): Regional and Economic Geology of the Tulsequah River and Tulsequah Glacier Areas. (NTS 104K-12 and 13); *in* Geological Fieldwork 1993, Grant, B., and Newell, J.M. Editors, *B.C. Ministry of Energy, Mines and Petroleum Resources*, Paper 1994-1, this volume.

Nelson, J. and Payne, J.G., (1984): Paleozoic Volcanic Assemblages and Volcanogenic Massive Sulphide Deposits near Tulsequah, British Columbia; *Canadian Journal of Earth Sciences*, Volume 21, pages 379-381.

Parrish, R.R., Roddick, J.C., Loveridge, W.D. and Sullivan, R.W. (1987): Uranium-Lead Analytical Techniques at the Geochronology Laboratory, Geological Survey of Canada. *in* Radiogenic Age and Isotopic Studies, Report 1, *Geological Survey of Canada*, Paper 87-2, pages 3-7.

Roddick, J.C. (1987): Generalized Numerical Error Analysis with Applications to Geochronology and Thermodynamics; *Geochimica et Cosmochimica Acta*, Volume 51, pages 2129-2135.

Stacey, J.S. and Kramers, J.D. (1975): Approximation of Terrestrial Lead Isotope Evolution by a Two-stage Model; *Earth and Planetary Science Letters*, Volume 26, pages 207-221.

Steiger, R.H. and Jäger, E. (1977): Subcommission on Geochronology: Convention on the Use of Decay Constants in Geo- and Cosmochronology; *Earth and Planetary Science Letters*, Volume 36, pages 359-362.

Souther, J.G., (1971): Geology and Mineral Deposits of the Tulsequah Map-area, British Columbia; *Geological Survey of Canada*, Memoir 362, 84 pages.

GEOLOGICAL INVESTIGATIONS OF THE 21B DEPOSIT, ESKAY CREEK, NORTHWESTERN BRITISH COLUMBIA (104B/9W)

By R.L. Sherlock, T.J. Barrett, T. Roth, F. Childe, J.F.H. Thompson
Mineral Deposit Research Unit, U.B.C.
D. Kuran, H. Marsden
Homestake Canada Inc.
R. Allen
Volcanic Resources

(MDRU Contribution 044)

KEYWORDS: economic geology, Eskay Creek, 21 zone, gold, silver, massive sulphides, Hazelton Group

INTRODUCTION

The Eskay Creek property (56° 38'N, 130° 27'W) is located in the Iskut River area, about 80 kilometres north of Stewart, British Columbia. It is underlain by Triassic Stuhini Group and Jurassic Hazelton Group sediments and volcanic rocks described by Alldrick *et al.* (1989); Britton (1991), Lewis (1992); and Lewis *et al.* (1992). The mineral deposits of the 21 zone are hosted by a sequence of mainly bimodal volcanic rocks of Lower to Middle Jurassic Hazelton Group. The 21A and 21B zones occur within fine-grained sedimentary rocks that are underlain by rhyolite and intermediate volcanic rocks, and overlain by basalts. Studies by company geologists (Blackwell, 1990; Rye, 1992; Edmunds and Kuran 1992) have outlined the main stratigraphic, lithogeochemical and alteration characteristics at Eskay Creek, and documented the nature of the mineral deposits. Regional geological relations on the property have been described by Bartsch (1992a, 1992b, 1993a, 1993b); Roth (1992) and Roth and Godwin (1992).

The 21A and 21B zones are distinguished by their mineralogy and geochemical characteristics. For a more detailed account of the 21A deposit the reader is referred to Roth and Godwin (1992) and Roth (1992). Field work in 1993 by the Mineral Deposit Research Unit involved relogging and sampling of selected drill-holes through various styles of mineralization in the 21B zone. This report concentrates on the stratigraphy, sedimentology and mineralization of the 21B orebody. The currently defined mineable reserves in the 21B zone are 1.08 million tonnes grading 65.5 grams per tonne gold, 2930 grams per tonne silver, 5.6 % zinc, and 0.77 % copper (Homestake Canada Inc. Feasibility Report August, 1993).

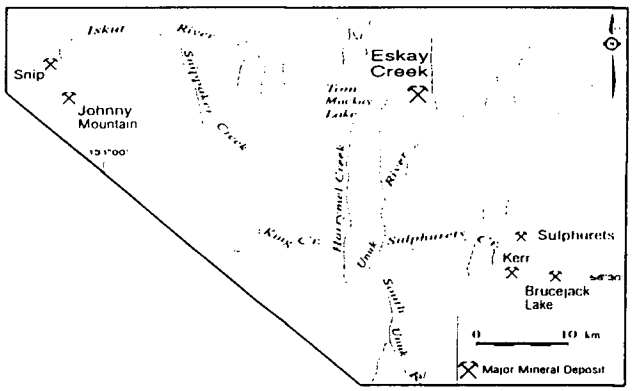

Figure 1. Location map of the Eskay Creek deposit, Iskut River Area

MINE SEQUENCE STRATIGRAPHY

FOOTWALL VOLCANIC UNIT

The footwall volcanic unit has in the past been referred to as the footwall dacite unit. It overlies marine sediments and volcaniclastic rocks, of Hettangian through late Pliensbachian age, of the lower Hazelton Group, and underlies the footwall rhyolite.

The unit comprises aphanitic flows, sills and primary to reworked volcaniclastic material. Geochemically it is quite variable, ranging from dacite to basalt (Rye, 1992). The unit is generally altered to a characteristic pink-beige colour and is cut locally by a series of quartz-pyrite ± sphalerite-galena-chalcopyrite veinlets with grey, sericitic envelopes. A distinctive marker horizon is the dacite datum which commonly contains quartz-filled or locally chlorite-filled amygdules. The footwall volcanic unit is regionally in excess of 100 metres thickness (Britton *et al.*, 1990).

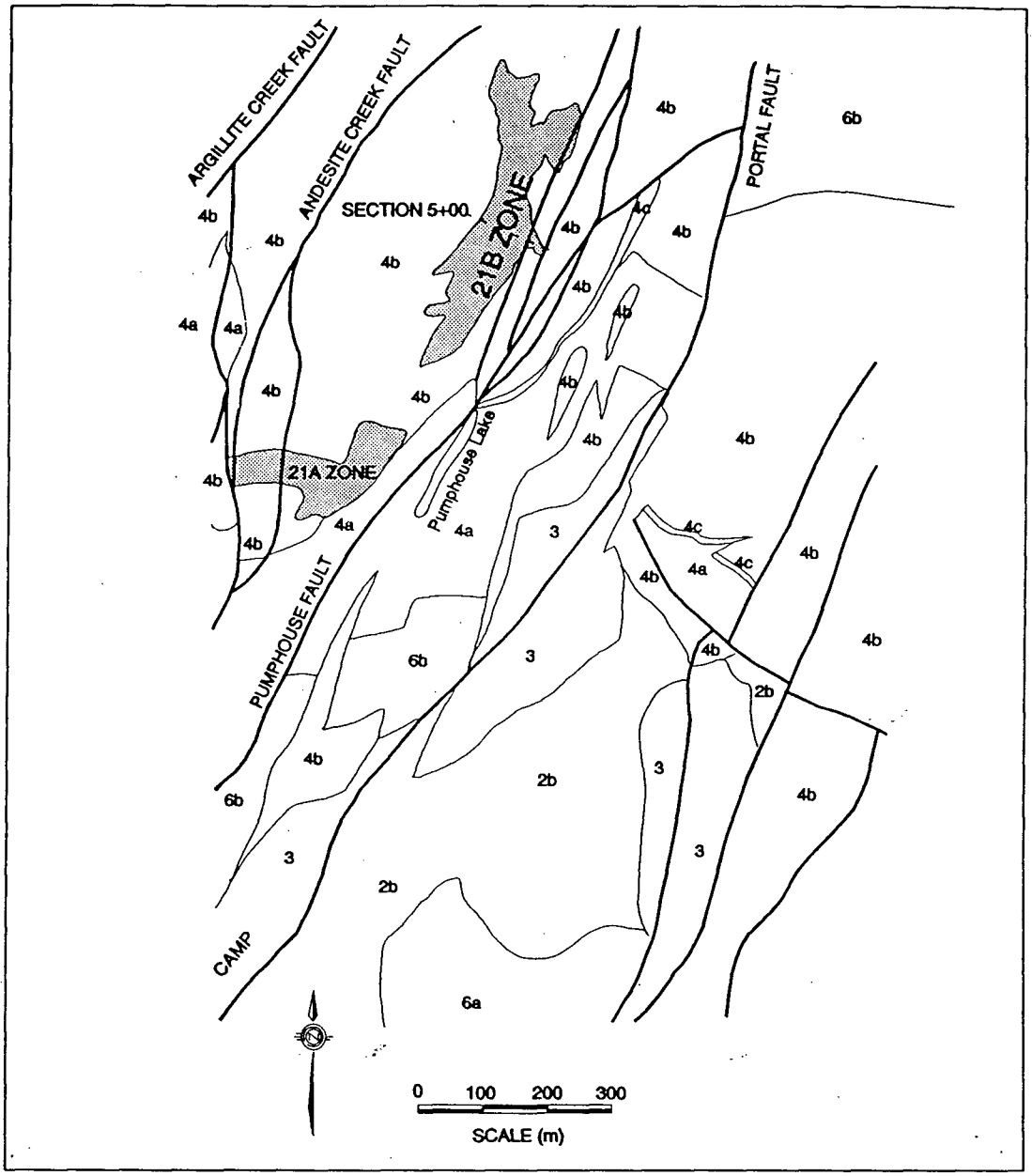

Figure 2. Geology of the Eskay Creek property. 2b, intermediate, coarse epiclastics with minor mudstone, limestone and andesite-derived conglomerates; 3, heterolithic felsic volcanic fragmentals, air fall welded tuffs, vesicular dacite fragmentals, and massive to perlitic dacite (lower volcanic unit); 4a, massive to flow-banded and autobrecciated rhyolite, with tuffs and fragmental units (footwall rhyolite); 4b, pillow basalts, hyaloclastites, debris flows, flow breccias, autobreccia with intercalated sediments, and unaltered mafic dikes (hangingwall basalt); 4c, argillite (contact zone argillite); 6a, monzodiorite; 6b, feldspar-phyric siliceous, pyritic dikes/sills (felsite). Geology based on company reports.

The footwall volcanic unit is commonly separated from the overlying footwall rhyolite by a narrow (less than 1 to 3 metres thick) black mudstone horizon, which may contain low-grade gold, silver and base metal mineralization.

FOOTWALL RHYOLITE

Rhyolite forms the immediate footwall to the 21B stratiform deposit and is the host to stringer-style discordant mineralization. This unit consists of massive to flow-banded rhyolite, flow and hydrothermal breccias, and pyroclastic deposits. Hyaloclastite and perlitic textures occur locally. Primary textures are commonly obscured by pervasive alteration. Within the mineralized zones, this unit is altered to an assemblage of quartz, potassium-feldspar, chlorite and sericite. The upper contact of the rhyolite with the argillite is commonly marked by a black-matrix breccia, consisting of matrix-supported white rhyolite fragments in a siliceous black matrix (Rye, 1992; Bartsch, 1993b; Roth, 1992). The footwall rhyolite ranges from 30 to 110 metres thick (Britton *et al.*, 1990).

CONTACT ARGILLITE (TRANSITION ZONE)

The contact argillite occurs between the rhyolite and the overlying basalt, and is the host to the stratiform sulphide-sulphosalt mineralization of the 21B zone. The unit consists of a laterally extensive, well-laminated, carbonaceous mudstone that is variably calcareous and siliceous. Radiolaria, dinoflagellates, rare belemnites and corals have been identified within it, indicating deposition in a marine environment (Roth, 1992; Nadaraju, 1993). Prehnite porphyroblasts are locally abundant in the argillite; these have been referred to as crystallites in exploration drill logs.

The basal member of the contact argillite is termed the transition zone, which comprises fine sericitic flakes in mudstone. The flakes tend to decrease in abundance away from the rhyolite. The sericite material are similar in appearance to some of the underlying altered rhyolite and were probably derived from this unit. The contact argillite ranges from less than 1 metre to more than 60 metres in thickness (Rye, 1992; Britton *et al.*, 1990).

HANGINGWALL BASALT

The hangingwall basalt occurs as both extrusive and intrusive phases, and ranges from aphanitic to medium grained with local feldspar phenocrysts. In places, basaltic sills and dikes are intrusive into the contact argillite. Elsewhere, well-preserved pillows and pillow breccias overlie the argillite. Chlorite and quartz-filled amygdules are common and tend to be concentrated at the upper contacts of flows (Rye , 1992). Thin argillite intervals are interbedded within the basalt. The unit exceeds 150 metres in thickness (Britton *et al.*, 1990).

INTRUSIVE ROCKS

Several intrusions are exposed on the property including monzodiorite (Eskay porphyry, 185 ± 5 Ma, Macdonald *et al.*, 1992), mafic intrusives (Salmon River equivalents) and the "felsite". The felsite is chemically equivalent to the Eskay rhyolite and is strongly altered to an assemblage of silica, pyrite and minor sericite forming the gossanous bluffs prominent at the Eskay camp. The felsites crosscut stratigraphy and reach their highest stratigraphic level directly below the 21 zone deposits (Edmunds and Kuran, 1992; Bartsch, 1993b).

STRUCTURE

The stratigraphy at Eskay Creek is folded about a gently plunging upright fold trending at 035°, called the Eskay anticline. The 21A and B deposits occur on the gently west-dipping, northeast-striking western limb of this fold. Faults striking north-northeast, notably the Andesite Creek, Pumphouse, Portal and East Break faults, crosscut and offset the stratigraphy (Edmunds and Kuran, 1992).

ALTERATION

Footwall alteration is dominated by pervasive silicification of the rhyolite. In the immediate footwall to the 21 zone, the alteration is marked by the development of a chlorite-sericite (± potassium-feldspar) assemblage that increases in intensity towards the rhyolite-argillite contact. The metasomatic effects are depletion of sodium, and enrichment of potassium, magnesium and commonly silica.

MINERALIZATION

Two main styles of mineralization are recognized in the 21B zone, stratiform and discordant. The relationship between the various styles of mineralization is poorly understood and is presently under investigation.

Stratiform mineralization in the 21B zone is dominated by detrital sulphide-sulphosalt beds. The stratiform segment of the zone is about 900 metres long, 60 to 200 metres wide and locally in excess of 40 metres thickness (Britton *et al.*, 1990). Individual clastic ore beds range from less than 1 centimetre to 50 centimetres in thickness and are composed dominantly of coarse-grained clasts of zoned sphalerite, with finer grained tetrahedrite, boulangerite, bournonite and minor galena and pyrite; also present are sericitized to chloritized rhyolite fragments. Gold and silver occur as electrum and in sulphosalts. In some holes, the stratigraphically lower clastic ore beds are rich in sulphide-sulphosalt cobbles and pebbles, and pass upwards into argillite containing

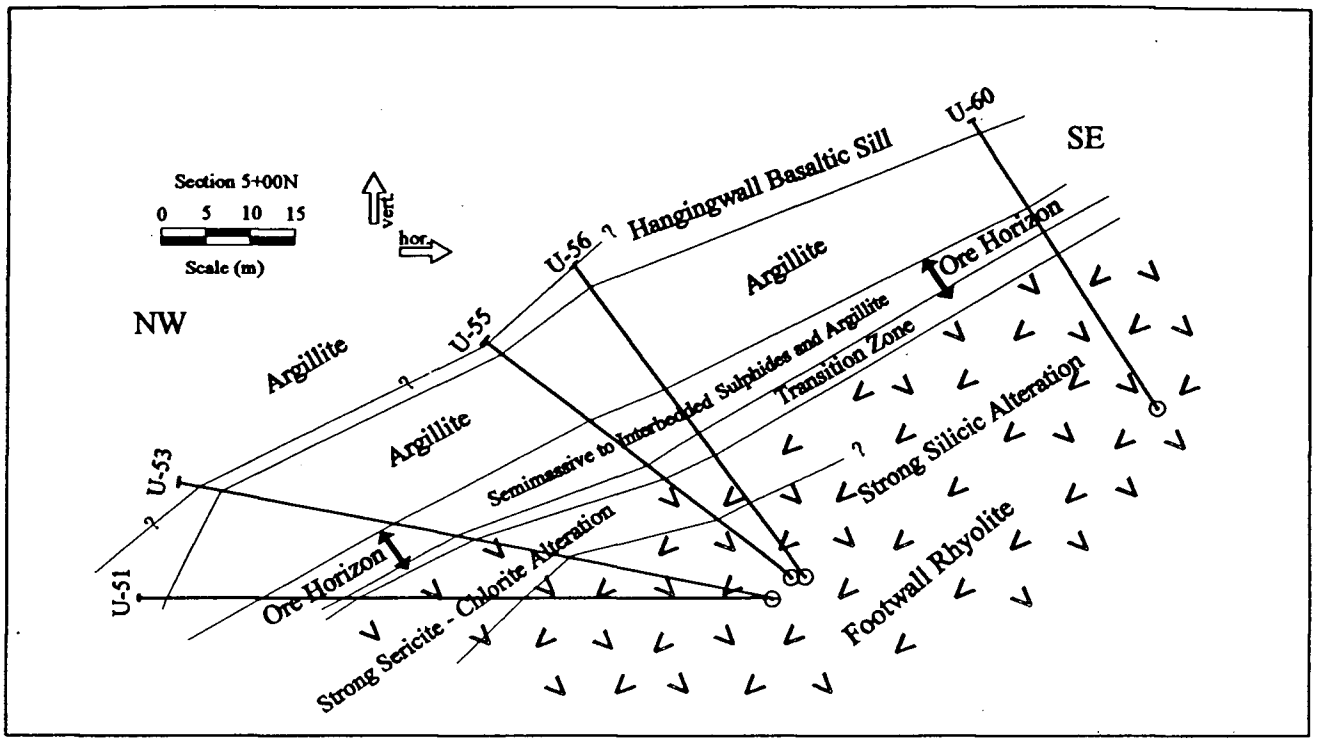

Figure 3. Cross-section through the 21B zone at section 5+00N. Based on company maps.

thinner rhythmically bedded and graded clastic ore beds. Thin, ungraded sulphide-sulphosalt beds and laminations are also present. Mineralization may have been localized in small synvolcanic seafloor depressions. The southernmost 600 metres of the 21B zone contains the highest grades and has the greatest lateral continuity; the northern 300 metres is mineralized at several stratigraphic intervals (Blackwell, 1990).

In the northern part of the 21B zone, a second interval of stratiform mineralization, termed the HW zone, is present within the contact argillite stratigraphically above the main zone of 21B stratiform mineralization. This interval is present as semimassive to massive sphalerite, galena, chalcopyrite and pyrite. The HW zone contains a much higher copper content than does the clastic ore in the lower part of the 21B zone.

Discordant mineralization occurs in the rhyolite-hosted 109 zone, which plunges down at a high angle to the rhyolite-argillite contact. The 109 zone is characterized by crustiform quartz veins and coarse-grained, zoned sphalerite, galena, minor pyrite and chalcopyrite and contains abundant carbonaceous material (Blackwell, 1990). Gold and silver occur as electrum and sulphosalts.

SECTIONS 5+00N & 5+25N

Although the gross stratigraphic relationships of the 21B zone are well constrained, in detail they are complex. Geological relations in the 21B zone are perhaps best examined in section 5+00N (Figure 3). Underground drilling on this section has provided high definition coverage allowing the geologic relationships to be investigated in detail. A total of eleven underground drill-holes and five surface holes penetrated the mineralized interval, although only five underground holes are shown, for clarity, in Figure 3.

In section 5+00N, the stratigraphy begins with silicified footwall rhyolite that becomes increasingly more sericitized and chloritized towards the argillite contact. The transition zone between the footwall rhyolite and the contact argillite is well developed with a variable thickness that increases to the east. The mineralized horizon comprises disseminated sulphides within the transition zone, and semimassive to thinly interbedded sulphides in the contact argillite. The contact between mineralized and overlying unmineralized argillite occurs over an interval of tens of centimetres, through a decreasing number of sulphide-sulphosalt beds. The overlying argillite is well laminated and composed of black mudstones with thin interbeds of brown ashy siltstone and grey calcareous sandstone. In section 5+00N, a basaltic sill, several metres thick, intrudes the contact argillite above the mineralized horizon.

Underground drill-hole U39, on section 5+25N, shows the stratigraphy in greater detail (Figure 4). The footwall rhyolite is divisible into several units beginning with *in situ* brecciated (hyaloclastite) and perlitically cracked rhyolite, overlain by an immature rhyolite sandstone. This is overlain by *in situ* rhyolite breccia of angular flow-banded fragments, which is probably an autoclastic flow breccia. The *in situ* breccia grades sharply into a zone of massive, waxy

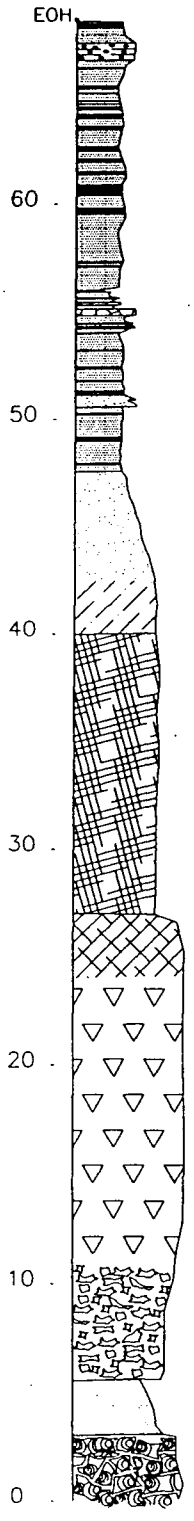

U39

Mudstone, dark grey tuffaceous silt, and very fine to *fine-grained sandstone*

- silty to sandy laminae and beds range up to 5 cm thick within bedded intervals from 5 to 50 cm.
- fine-grained beds are khaki coloured
- 1 m sandstone interval near the end of the hole contains round to irregular calcareous concretions.

Mudstone and clastic sulphide beds

Laminated mudstone

- black mudstone containing <5% folded to crenulated, 1 to 5 cm, graded pyrite laminae and minor medium to coarse-grained volcanic sandstone beds, up to 5 cm thick, with normal grading.
- 2-3% irregular, anastomosing, fine-grained stibnite veinlets.

Rhyolitic sandstone and pebbly sandstone - volcaniclastic

- sandstone is locally recognizeable through strong sericitic alteration
- moderately sorted, overall normal grading
- white sericite streaks and spots occur throughout
- up to 1% disseminated pyrite and minor sphalerite.

Sericite-chlorite altered rhyolite

- primary textures are obscured; dark grey with white patches of sericite

"Massive chlorite"

- pale green to grey, massive to mottled, waxy chlorite rock
- contains batchy cream coloured quartz-carbonate blebs up to 3 cm across, through the central 6 m of the interval. Minor to 2% pyrite and sphalerite occur disseminated and in veinlets and streaks.
- primary textures are not preserved.
- lower contact is sharp; upper contact is gradational, but changes rapidly to dark grey sericite-chlorite alteration.

In situ rhyolite breccia - autoclastic breccia

- clast-supported breccia of angular, flow-banded clasts of aphyric rhyolite.
- variation from preferred alignment to locally disorganized, rotated flow-banded clasts
- lower 5 m contains abundant chloritic cuspate clasts or patches suggesting possible altered glassy hyaloclastic margin.
- alteration is mainly grey, pervasive to mottled quartz-sericite, partly controlled by flow bands and clast boundaries. Few thin chlorite veins occur locally.
- minor disseminated pyrite occurs throughout. Minor sphalerite and tetrahedrite occur locally in thin (<2cm) veinlets with sericite or quartz-sericite.

Well sorted rhyolitic sandstone - pyroclastic deposit

- diffusely stratified; angular clasts range from 1 to 15 mm

In situ rhyolite breccia - hyaloclastite

- clast-supported breccia of broadly curved fragments containing arcuate to concentric perlitic fractures.

Figure 4. Detailed log of underground drill-hole U39, on section 5+25N.

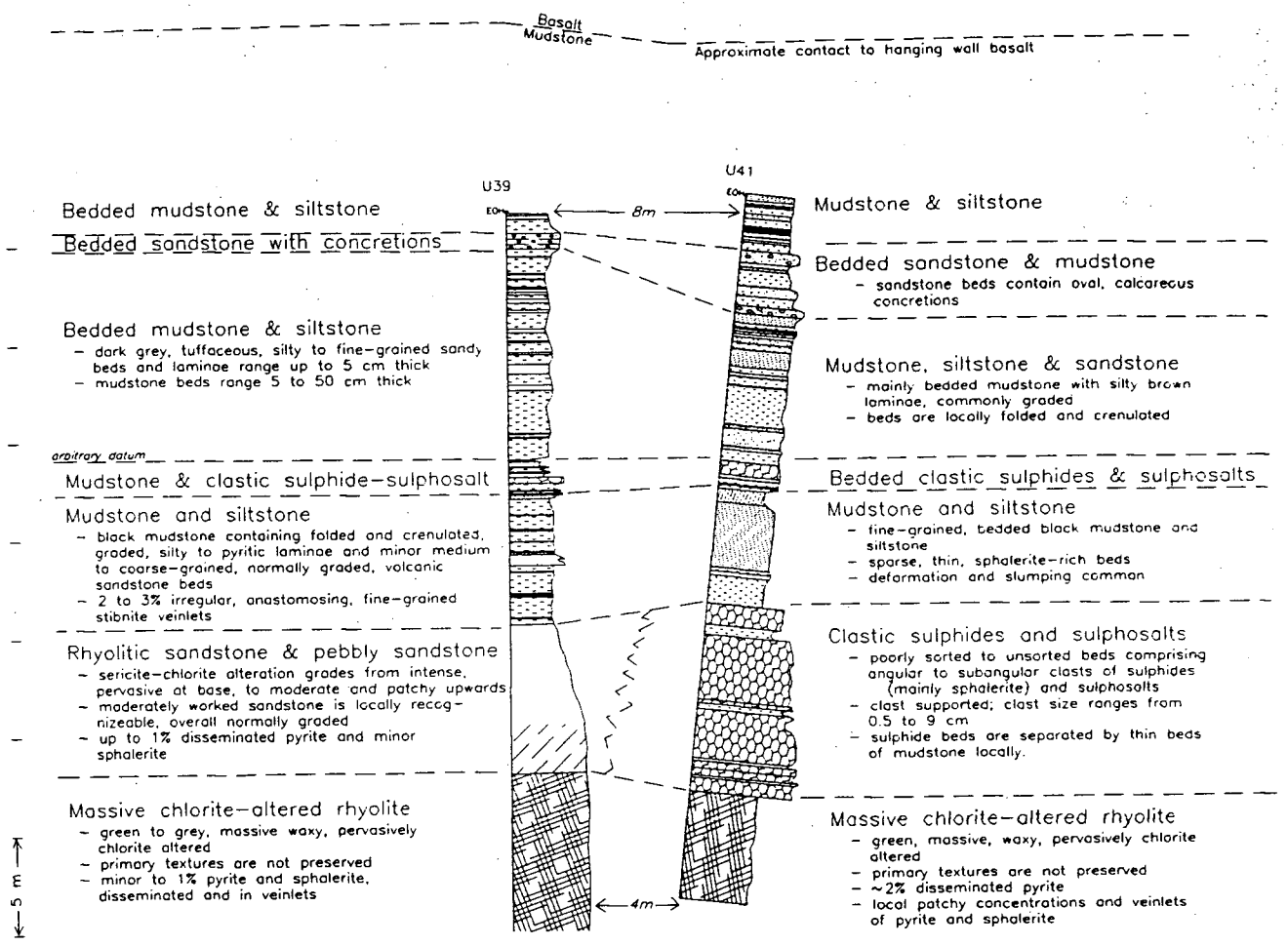

Figure 5. Detailed stratigraphy of underground drill holes U39 and U41, both from section 5+25N. Possible correlations are shown. Note the close spacing of the drill holes (4-8 metres).

green chlorite which is in turn overlain by a dark grey sericitized and chloritized rock. The actual field distinction between sericite-chlorite-altered rock and chlorite-altered rock is based on the physical appearance of the rock, not on chemical composition. This distinction may be misleading as some phases of the chlorite alteration are a pale brown colour and are often mistaken for sericite (R. Britten, personal communication, 1993). In U39, this intensely altered rock contains minor (3%) pyrite and sphalerite, disseminated and in thin veinlets. Intense sericite-chlorite alteration decreases gradually upward. Volcaniclastic rhyolitic sandstone is recognized locally at the top of the footwall. The footwall rhyolite is overlain by laminated mudstone with pyrite laminations and minor medium to coarse-grained, graded, volcanic sandstone beds. Within this interval are irregular anastomosing stibnite veinlets. The stratiform mineralized 21B horizon in hole U39 is entirely within the argillite unit, approximately 5 metres above the rhyolite-argillite contact. This mineralized horizon consists of eight clastic sulphide beds ranging between 0.5 and 25 centimetres thick; separated by mudstone beds; the total thickness of this package is 1.7 metres. Angular to subrounded clasts in the ore range from less than 1 millimetre to 3 centimetres in diameter and are generally poorly sorted to unsorted; normal grading is locally weakly developed in the thinner beds. The clasts are mainly sphalerite, tetrahedrite and fine-grained sulphosalts; specks of electrum are visible locally within the clasts. Clasts include sericite and chlorite-altered rhyolite, and local rip-up clasts of argillite with pyritic or silty laminae. These lithic clasts comprise less than 5% of the ore beds and commonly increase in abundance toward the tops of the graded sulphide-sulphosalt beds. The mineralized horizon is overlain by a variably calcareous mudstone with thin interbeds of grey tuffaceous siltstone and sandstone.

Rapid thickness variations of individual units are exhibited between U39 and U41, two closely spaced drillholes in section 5+25N (Figure 5). The drill intersections of the mineralized intervals are only 4 to 8 metres apart but are markedly different in character, even though the stratigraphy above and below the mineralized intervals is correlatable. The datum used

in Figure 5 was the uppermost clastic sulphide-sulphosalt bed. This datum is preferred as it also brings into alignment the main igneous-sedimentary contacts. However, different geological interpretations are possible using a different datum. Mineralization in drill hole U41 is dominated by 8 metres of almost continuous, massive, thickly bedded, unsorted, coarse-grained, heterolithic, clastic sulphide-sulphosalt fragments which occur immediately above the pervasively chloritized interval. Minor mudstone interbeds within this sequence are less than 10 centimetres thick. Barite fragments are common near the base of the ore sequence, but decrease upward. Lithic fragments are minor. Clasts are angular to subangular and range from 0.1 to 10 centimetres across. Colloform banding of sulphides and sulphosalts observed in one large clast is sharply truncated at the clast margins.

This thick sequence of clastic ore is overlain by a sequence of mudstone and siltstone which contains thin beds and laminae of clastic sulphides and sulphosalts over another 8.5 metres; the latter beds become most prominent in the uppermost 1 metre which may correlate with bedded mineralization in hole U39. Notably, a thin zone of gouge underlies this upper zone of bedded mineralization in both drill holes, and may reflect a shallow-dipping fault which has displaced beds at this locality.

The lateral variations between individual mineralized beds in U41 and U39 probably reflect cross-strike variations in the deposition of the mineralized beds. The beds were probably deposited rapidly, perhaps as chaotic mass-flows that infilled local depressions, or as sheets of debris that paralleled the elongation of the 21B zone. Thickness variations presumably were influenced by basement topography as well as distance from source. In section 5+25N, the thick sulphide-sulphosalt sequence can be traced for at least 25 metres in other drill holes to the east of U41.

DISCUSSION

Eskay Creek represents a precious metal enriched sea-floor deposit, with well-preserved stratiform mineralization as well as footwall stringer mineralization in areas such as the 109 zone. The overall geological relationships in the Eskay Creek camp have been documented by Rye (1992) and Edmunds and Kuran (1992). The present study is part of a detailed investigation into the physical nature of the volcanic and sedimentary environments during mineralization, and the mechanisms of emplacement of the mineralized beds. Many of these beds probably represent localized debris flows derived from *in situ* accumulation of sulphide-sulphosalt material but it is not yet understood if these beds are the product of seafloor mass wasting or fragmentation during volcanic activity.

Future work by the Mineral Deposit Research Unit will focus on measuring the composition of the fluids that formed the stratiform *versus* stringer mineralization, and quantifying footwall alteration using recent lithogeochemical and X-ray diffraction methods to assess chemical and mineralogical changes. Continuing efforts are being made to constrain the age of the volcanic rocks and the lead isotopic composition of the various mineralized zones using radiogenic isotopes.

The 21B zone is a small but very attractive exploration target. Understanding the relations between footwall and stratiform mineralization through studies of fluid evolution, footwall alteration, metal-precipitating mechanisms, and ore redistribution on the seafloor may aid future exploration for these unique mineral deposits.

ACKNOWLEDGMENTS

We are indebted to Homestake Canada Inc. for permission to publish information on the Eskay Creek property. We have benefited from discussion with Ron Britten of Homestake Canada Inc. and the previous work of Ken Rye and Carl Edmunds (now of Homestake Mineral Development Company) and Roland Bartsch (formerly of MDRU). Research at the Eskay Creek property forms part of a Mineral Deposit Research Unit project on Volcanogenic Massive Sulphide Deposits of the Cordillera, funded by the Natural Sciences and Engineering Research Council of Canada, the Science Council of British Columbia and ten mining and exploration companies.

REFERENCES

Alldrick, D.J., Britton, J.M., Webster, I.C.L. and Russell, C.W.P. (1989): Geology and Mineral Deposits of the Unuk Area (104B/7E, 8W, 9W, 10E); *B.C. Ministry of Energy, Mines and Petroleum Resources*, Open File 1989-10.

Bartsch, R.D. (1992a): Eskay Creek Area, Stratigraphy Update (104B/9, 10; *in* Geological Fieldwork 1991, Grant, B. and Newell, J.M., Editors, *B.C. Ministry of Energy, Mines and Petroleum Resources*, Paper 1991-1, pages 517-520.

Bartsch, R. D. (1992b): Lithostratigraphy - Prout Plateau; *in* Metallogenesis of the Iskut River Area, Northwestern B.C.; *Mineral Deposits Research Unit, The University of British Columbia*. Annual Technical Report for the period June 1991 to May 1992.

Bartsch, R.D. (1993a): A Rhyolite Flow Dome in the Upper Hazelton Group, Eskay Creek Area (104B/9, 10); *in* Geological Fieldwork 1992, Grant , B. and Newell, J.M., Editors, *B.C. Ministry of Energy, Mines and Petroleum Resources*, Paper 1993-1, pages 331-334.

Bartsch, R.D. (1993b): Volcanic Stratigraphy and Lithogeochemistry of the Lower Jurassic Hazelton Group, Host to the Eskay Creek Precious and Base Metal Volcanogenic Deposit; unpublished M.Sc. thesis, *The University of British Columbia*, 173 pages.

Blackwell, J.D. (1990): Geology of the Eskay Creek #21 Deposits; *Mineral Deposits Division, Geological Association of Canada Newsletter*, The Gangue, Number 31, April, 1990, pages 1-4.

Britton, J.M. (1991): Stratigraphic Notes from the Iskut-Sulphurets Area: *in* Geological Fieldwork 1990, *B.C. Ministry of Energy, Mines and Petroleum Resources*, Paper 1991-1, pages 331-334.

Britton, J.M., Blackwell, J.D. and Schroeter, T.G. (1990) #21 Zone Deposits, Eskay Creek, Northwestern British Columbia: *in* Exploration in British Columbia 1989, *B.C. Ministry of Energy, Mines and Petroleum Resources*, pages 197-223.

Edmunds, F.C. and Kuran, D.L. (1992): TOK-KAY and GNC 1991 Exploration Program, Geological and Diamond Drilling Program, *Prime Resources Group Inc.*, internal report.

Lewis, P.D. (1992): Structural Geology of the Prout Plateau Region, Iskut River Map Area, British Columbia; *in* Geological Fieldwork 1991, Grant, B. and Newell, J.M., Editors, *B.C. Ministry of Energy, Mines and Petroleum Resources*, Paper 1992-1, pages 521-527.

Lewis, P.D., Macdonald, A.J. and Bartsch, R.D. (1992): Hazelton Group / Bowser Lake Group Stratigraphy in the Iskut River Area: Progress and Problems; *in* Metallogenesis of the Iskut River Area, Northwestern B.C.; *Mineral Deposits Research Unit, The University of British Columbia*, Annual Technical Report for the period June 1991 to May 1992.

Macdonald, A.J., van der Heyden, P. Lefebure, D.V. and Alldrick, D.J. (1992): Geochronometry of the Iskut River Area - An Update (104A and B); *in* Geological Fieldwork 1991, Grant , B. and Newell, J.M., Editors, *B.C. Ministry of Energy, Mines and Petroleum Resources*, Paper 1992-1, pages 495-502.

Nadaraju, G.D. (1993): Triassic-Jurassic Biochronology of the Iskut River Map Areas, Northwestern British Columbia; unpublished M.Sc. thesis, *The University of British Columbia*, 268 pages.

Roth, T. (1992): Geology of the 21A Zone-An Update; *in* Metallogenesis of the Iskut River Area, Northwestern B.C.; *Mineral Deposits Research Unit, The University of British Columbia*. Annual Technical Report-for the period June 1991 to May 1992.

Roth, T. and Godwin, C.I. (1992): Preliminary Geology of the 21A Zone, Eskay Creek, British Columbia; *in* Geological Fieldwork 1991, Grant, B. and Newell, J.M., Editors, *B.C. Ministry of Energy, Mines and Petroleum Resources*, Paper 1992-1, pages 529-533.

Rye, K. (1992): Geological and Geochemical Report on the 1991 Eskay Creek Diamond Drill Relog Program; internal report, *Prime Resources Group Inc.*

AGE OF HOST STRATA VERSUS MINERALIZATION AT ERICKSEN-ASHBY: A SKARN DEPOSIT

By Mitchell G. Mihalynuk, and W. (Bill) J. McMillan, B.C. Geological Survey Branch, James K. Mortensen and Fiona C. Childe, University of British Columbia and Michael, J. Orchard, Geological Survey of Canada

KEYWORDS: Ericksen-Ashby, skarn, Tulsequah, massive sulphide, zinc, lead, radiogenic isotopes, uranium, geochronology, conodont, biochronology

INTRODUCTION

The Ericksen-Ashby deposit is located on the sharp northern ridge of Mount Ericksen, about 64 kilometres east of Juneau, Alaska and 130 kilometres south of Atlin in northwestern British Columbia (Figure 1). It is part of a mineralized belt that contains the Tulsequah Chief and Big Bull volcanogenic massive sulphide deposits within 12 kilometres along strike to the north, and was previously interpreted as this type of deposit (e.g. Payne, 1979). Originally discovered in 1929, it has received sporadic assessment work, including surface and underground drilling programs.

Strata hosting the deposit are different from those at both the Tulsequah Chief and Big Bull deposits. However, the Ericksen-Ashby deposit has generally been thought of as correlative, with stratigraphic differences accounted for by rapid facies changes, typical in volcanic arc environments. Most of these strata were originally considered to be Late Triassic in age (Souther, 1971). Late Carboniferous (Moscovian) fossils collected by Nelson and Payne (1984) from a structural high in the Tulsequah camp were the first clear indication that rocks at the Tulsequah Chief must be Paleozoic and not Triassic. It was not until a decade later that the first definitive age of the Tulsequah Chief deposit was obtained by U-Pb dating of zircons in the coarse rhyolite breccia that is included within the orebodies (353 +14 -7 Ma, Sherlock *et al.*, 1994).

In contrast, there were no age data for hostrocks or mineralization at the Ericksen-Ashby deposit prior to this study. Some lead isotope data are reported for the deposit (Godwin *et al.*, 1988), but are interpreted based on a Jurassic age for the host strata, and no description of the sample site or material analyzed is available. Lead isotope data needed to be reevaluated and augmented in light of new age constraints.

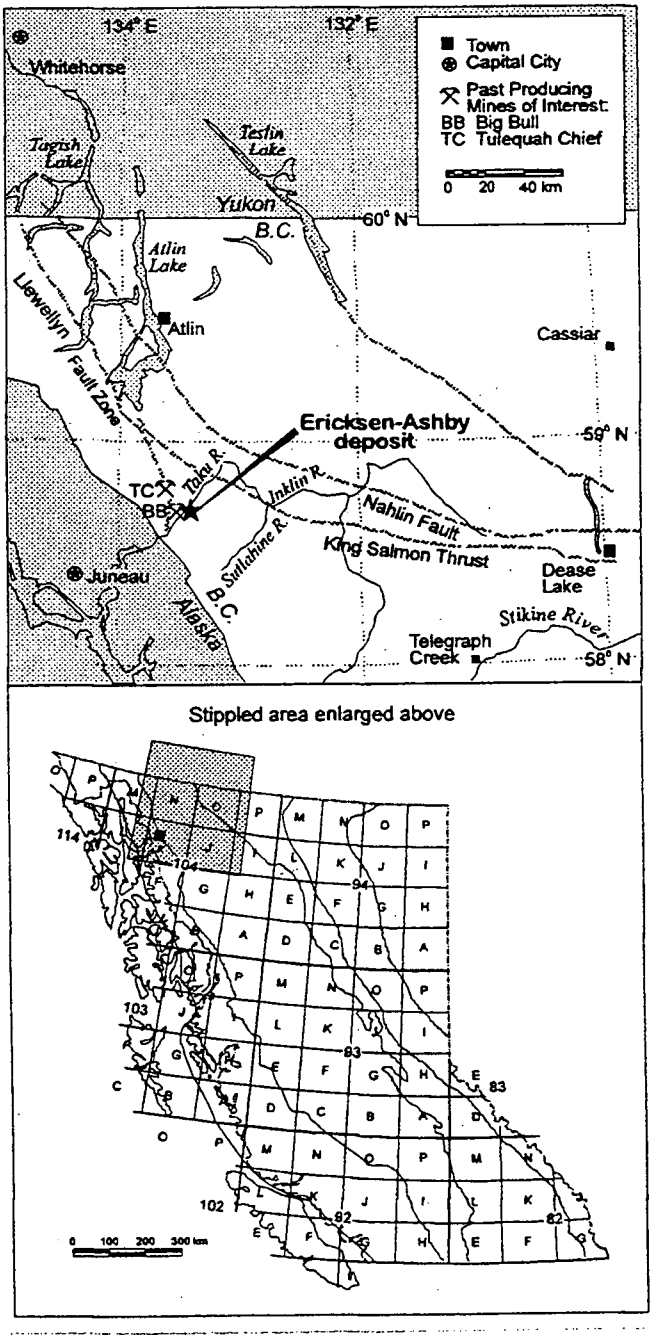

Figure 1. Location of the Ericksen-Ashby deposit in northwestern British Columbia.

ERICKSEN-ASHBY GEOLOGY

Payne (1979) produced excellent detailed geology

and descriptions of mineralization textures at the Ericksen-Ashby deposit during his evaluation of the property. The generalized geology that follows is based primarily on his work as well as brief visits (six man-days in the immediate area, two at the deposit) as part of a BCGS regional mapping program in 1994 (Mihalynuk *et al.*, 1994a, b, 1995a, b).

Strata on Mount Ericksen are dominated by pyroxene-phyric andesite or basaltic andesite and gabbro. Near the north end of the ridge, the volcanic strata are interrupted by two interlayers comprised of chert and carbonate (Figure 2). They are each approximately 100 metres thick, but strong internal deformation by close to isoclinal folds does not permit estimates of original stratigraphic thickness. The structurally highest sedimentary unit bifurcates northward to envelop andesite of approximately the same thickness. It also includes a thin layer of rhyolite. A subjacent, tabular, porphyritic quartz monzonite, 50 to 100 metres thick (but in at least one place up to 350 m thick), known as the Ericksen sill, thermally metamorphoses the entire section on Mount Ericksen.

All massive sulphide mineralization of economic interest occurs in the upper sedimentary division (SED-2 of Payne, 1979). Within SED-2, sulphide layers with high zinc, lead and silver contents occur above a thin, discontinuous rhyolite layer. Some sulphide pods and lenses are discordant, clearly related to late skarn alteration and/or remobilization of the stratiform sulphides.

Field evidence predominantly points to a volcanogenic origin for the deposit. Like the volcanogenic massive sulphides to the immediate north, it is closely associated with a felsic tuff horizon. Mineralization is dominantly stratiform and mainly restricted to the single SED-2 interval (Payne, 1979). Futhermore, a lithologically similar calcareous layer between SED-2 and the Ericksen sill is unmineralized although, given its closer proximity to the intrusion, it would seem a more likely host for skarn mineralization. Thus, Payne interpreted the Ericksen-Ashby as primarily a volcanogenic massive sulphide deposit with partial late remobilization due to the Ericksen sill. While our field observations are consistent with those of Payne and his interpretation, laboratory analytical data from galena from the massive sulphide lenses are incompatible with a volcanogenic origin of the galena

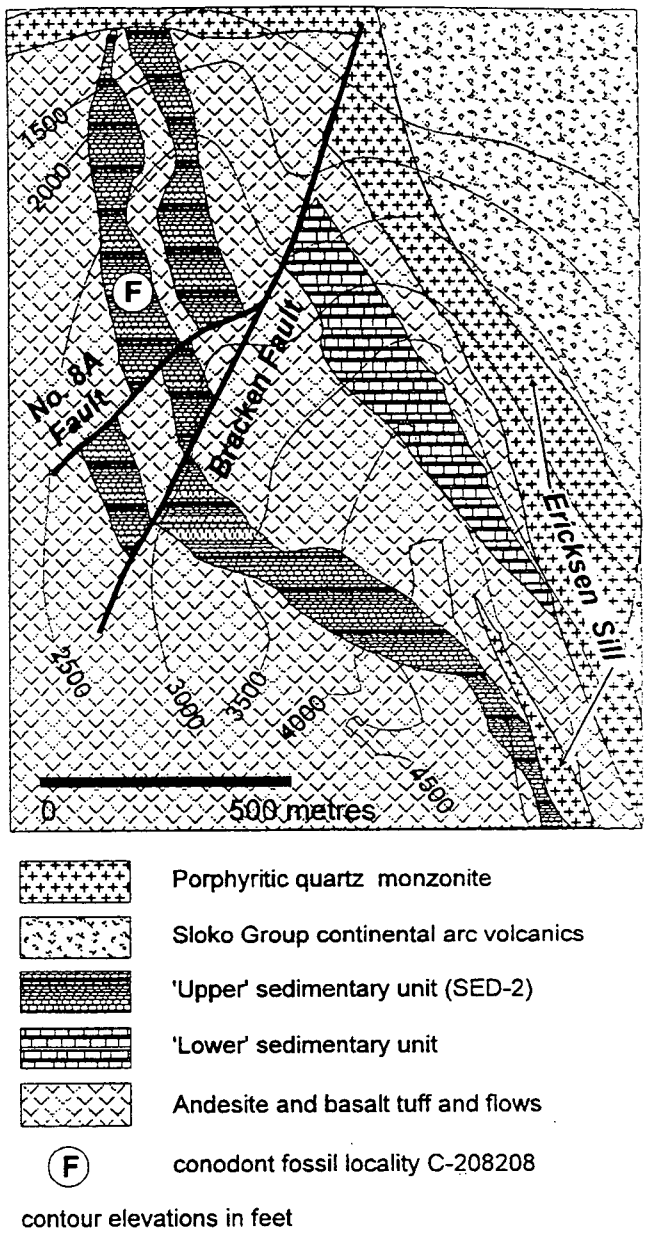

Figure 2. Stylized geology of the Ericksen-Ashby deposit, modified after Payne (1979) and Mihalynuk *et al.* (1995). For more detailed deposit geology see Figure 4 of Payne (1979). The U-Pb isotopic age determination sample site is 1.5 kilometres south of the southeast corner of the figure.

BIOCHRONOLOGY

Samples were collected for microfossil determination to help clarify the question of correlation between Ericksen-Ashby and massive sulphide stratigraphy of the Tulsequah Chief and Big Bull deposits. Only one sample was productive. It was from a 12-metre section of SED-2, comprised of fine-grained grey limestone with interlayered chert (sample C-208208, see location F, Figure 2). It yielded two deformed conodont fragments with a colour alteration index of 6. These suggest a Late Carboniferous to Permian age, although precise age remains elusive due to poor preservation of the conodonts and intense structural disruption. Nevertheless, the strata are definitely Paleozoic, not Triassic.

GEOCHRONOLOGY

A sample of pink, blocky to platy weathering, quartz

(15%) - feldspar (20%) porphyry was collected from near the base of the Ericksen sill for U-Pb geochronology (Figure 2). In hand sample the feldspars are zoned, displaying both twinned plagioclase (polysynthetic and simple) as well as untwinned crystals, possibly intergrowths of orthoclase and plagioclase. Mafic phenocrysts include biotite booklets (5%) and hornblende prisms (0.5%). The sample is very fresh and yields good quality zircons.

ANALYTICAL TECHNIQUES AND RESULTS

Sample preparation and U-Pb analyses were carried out at the Geochronology Laboratory of the University of British Columbia. The sample was processed using techniques as described in Mortensen *et al.* (1995). Analytical results are presented in Table 1. Two multigrain zircon fractions were analysed. Both yield concordant analyses (Figure 3), with the best estimate for the crystallization age for the unit given by the total overlap of the two error ellipses with concordia, at 53.5±0.7 Ma. This age is nearly identical to U-Pb age determinations from Sloko Group volcanic strata (Mihalynuk and Friedman, unpublished) which crop out in fault contact with older parts of the succession hosting the Ericksen-Ashby deposit.

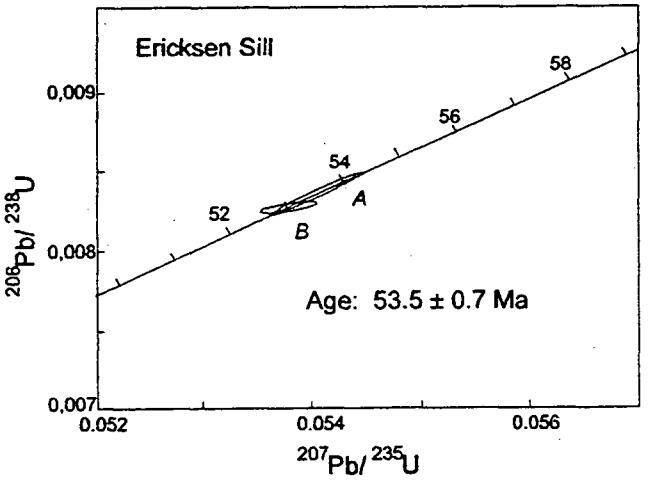

Figure 3. Concordia diagram showing the results of two zircon fractions from the Ericksen sill.

LEAD ISOTOPE SYSTEMATICS

A sample of mineralized material was collected from SED-2 about 60 metres above the fossil locality. It is fine to medium-grained, massive sphalerite (60%) and galena (20%) with unidentified, fine-grained gangue minerals comprising the remainder of the sample. Galena from this sample was analyzed for its lead isotopic composition. Analytical results of two fractions of galena

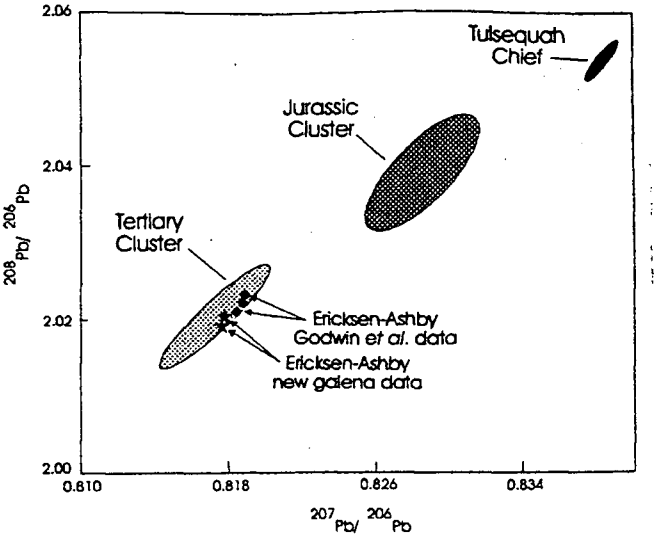

Figure 4. $^{207}Pb/^{206}Pb$ *vs.* $^{208}Pb/^{206}Pb$ diagram for galena from the Erickson-Ashby deposit, references to sources for Tertiary, Jurassic and Tulsequah Chief clusters are given in the text.

from the sample are presented in Table 2, and in a $^{207}Pb/^{206}Pb$ *versus* $^{208}Pb/^{206}Pb$ diagram in Figure 4. The lead isotopic signature of Ericksen-Ashby is compared with the signatures of Jurassic and Tertiary mineralizing epochs in the Stikine Terrane (Alldrick *et al.*, 1987; and UBC Geochronology Laboratory, unpublished data), as well as mineralization at the Devono-Mississippian Tulsequah Chief volcanogenic massive sulphide deposit (Childe, 1994). These data clusters show an increasingly more radiogenic lead signature with time in the Stikine Terrane. Late Carboniferous to Permian syngenetic mineralization in the Stikine Terrane would be expected to have a lead signature intermediate to that of Devono-Mississippian and Jurassic mineralization. However, the lead isotopic signature of galena from the Ericksen-Ashby deposit plots near the centre of the cluster defined by Tertiary mineralization.

DISCUSSION

Remobilization, metamorphism or skarn alteration of a pre-existing Paleozoic massive sulphide deposit (for example, Höy and Godwin, 1986) would not reset the lead isotopic signature of the galena within this lead-rich deposit. The lead signature is unequivocally Tertiary. In consideration of the 53.5±0.7 Ma age of the Ericksen sill which is responsible for skarn alteration at the deposit, it must be concluded that most or all of the lead was deposited during a Tertiary mineralizing event. Thus, Pb-Zn-Ag mineralization at the Ericksen-Ashby deposit is primarily a Tertiary skarn hosted by Late Carboniferous to Permian volcanosedimentary strata. Despite some field evidence to the contrary, it is apparently not a syngenetic deposit.

TABLE 1. U-PB ANALYTICAL RESULTS FOR SAMPLE MMI-94-18-9

Fraction[1]	Wt. mg	U ppm	Pb[2] ppm	$^{206}Pb/^{204}Pb$ measured	Pb[3] pg	%^{208}Pb	$^{206}Pb/^{238}U$[4]	$^{207}Pb/^{235}U$[4]	$^{207}Pb/^{206}Pb$[4]	$^{207}Pb/^{206}Pb$ age[5] (Ma)
A: n5, +134, a	0.313	810	7	2009	66	10.3	0.008339±0.73	0.05414±0.77 (0.9701)	0.04709±0.19	53.7 ±8.9
B: n5, 74-134, u	0.246	858	7	537	211	10.8	0.008260±0.18	0.05362±0.49 (0.7152)	0.04708±0.38	53.2 ±18.0

[1] n5 = non-magnetic at 5 degrees side tilt on Frantz isodynamic separator, grain size given in microns; u = unabraded; a = abraded

[2] radiogenic Pb; corrected for blank, initial common Pb, and spike

[3] common lead corrected for spike and fractionation

[4] corrected for blank Pb and U, and common Pb; errors are in percent at a 1σ level; correlation coefficient in parentheses

[5] errors are in Ma at a 2σ level

TABLE 2. COMMON LEAD DATA FOR THE ERICKSEN-ASHBY DEPOSIT

Sample	Mineral	$^{206}Pb/^{204}Pb$ (% error)[1]	$^{207}Pb/^{204}Pb$ (% error)[1]	$^{208}Pb/^{204}Pb$ (% error)[1]	$^{207}Pb/^{206}Pb$ (% error)[1]	$^{208}Pb/^{206}Pb$ (% error)[1]
EA a	galena	19.073 (0.010)	15.594 (0.009)	38.515 (0.011)	0.81761 (0.004)	2.0194 (0.004)
EA b	galena	19.111 (0.007)	15.627 (0.006)	38.618 (0.007)	0.81770 (0.003)	2.0208 (0.002)

[1] Errors are quoted at the 2σ (95% confidence) level, values are corrected for instrument fractionation by normalization based on replicate analyses of the NBS-981 standard.

ACKNOWLEDGMENTS

Sandy Sears helped in mapping and sample collection at the Ericksen-Ashby deposit. Dani Alldrick kindly provided an unsolicited and helpful review of the paper.

REFERENCES

Alldrick, D.J., Gabites, J.E., and Godwin, C.I. (1987): Lead Isotope Data from the Stewart Mining Camp (104B/I); *in* Geological Fieldwork 1986, *B.C. Ministry of Energy, Mines and Petroleum Resources,* Paper 1987-1, pages 93-102.

Childe, F. (1994): Chronology and Radiogenic Isotope Studies of the Kutcho, Granduc, Anyox and Tulsequah Chief Volcanogenic Massive Sulphide Deposits; *in* Volcanogenic Massive Sulphide Deposits of the Cordillera Project, Second Annual Report, *Mineral Deposit Research Unit,* The University of British Columbia.

Godwin, C.I., Gabites, J.E. and Andrew, A. (1988): Leadtable: A Galena Lead Isotope Data Base for the Canadian Cordillera, with a Guide to its Use by Explorationists; *B.C. Ministry of Energy, Mines and Petroleum Resources*, Paper 1988-4, 188 pages.

Höy, T. and Godwin, C.I. (1986): Significance of a Cambrian Date from Galena Lead-isotope Data for the Stratiform Cottonbelt Deposit in the Monashee Complex, Southeastern British Columbia; *Canadian Journal of Earth Sciences*, Volume 25, pages 1534-1541.

Mihalynuk, M.G., Smith, M.T. Hancock, K.D. and Dudka, S. (1994a): Regional and Economic Geology of the Tulsequah River and Glacier Areas (104K/12 & 13); *in* Geological Fieldwork 1993, Grant, B. and Newell, J.M., Editors, *B.C. Ministry of Energy, Mines and Petroleum Resources*, Paper 1994-1, pages 171-197.

Mihalynuk, M.G., Smith, M.T. Hancock, K.D., Dudka, S. and Payne, J. (1994b): Tulsequah River and Glacier Areas

(104K/12 & 13); *B.C. Ministry of Energy, Mines and Petroleum Resources*, Open File 1994-3.

Mihalynuk, M.G., Meldrum, D., Sears, S. and Johannson, G. (1995a): Geology and Mineralization of the Stuhini Creek Area (104K/11); *in* Geological Fieldwork 1994, Grant, B. and Newell, J.M., Editors, *B.C. Ministry of Energy, Mines and Petroleum Resources*, Paper 1995-1, pages 321-342.

Mihalynuk, M.G., Meldrum, D.G., Sears, W.A., Johannson, G.G., Madu, B.E., Vance, S., Tipper, H.W. and Monger, J.W.H. (1995b): Geology and Lithogeochemistry of the Stuhini Creek Map Area (104K/11); *B.C. Ministry of Energy, Mines and Petroleum Resources*, Open File 1995-1.

Mortensen, J.K., Gosh, D. and Ferri, F. (1995):.U-Pb Geochronology of Intrusions Associated with Cu-Au Porphyry Deposits in the Canadian Cordillera; *in* Canadian Institute of Mining and Metallurgy, Special Volume 46, in press.

Nelson J. and Payne, J.G. (1984): Paleozoic Volcanic Assemblages and Volcanogenic Massive Sulphide Deposits near Tulsequah, British Columbia; *Canadian Journal of Earth Sciences*, Volume 21, pages 379-381.

Payne, J.G. (1979): Geology Report for Semco Mining Corporation on the Ericksen-Ashby Claims; *B.C. Ministry of Energy, Mines and Petroleum Resources*, Assessment Report 7707.

Sherlock, R., Childe, F., Barrett, T.J., Mortensen, J.K., Chandler, T., Lewis, P., McGuigan, P., Dawson, G.L. and Allen, R. (1994): Geological Investigations of the Tulsequah Chief Massive Sulphide Deposit, Northwestern British Columbia; *in* Geological Fieldwork 1993, Grant, B. and Newell, J.M., Editors, *B.C. Ministry of Energy, Mines and Petroleum Resources*, Paper 1994-1, pages 373-379.

Souther, J. G. (1971): Geology and Mineral Deposits of the Tulsequah Map-area, British Columbia; *Geological Survey of Canada*, Memoir 362, 84 pages.